THE UNIVERSITY
of EDINBURGH

The Eye as a Window to the Brain: investigating the clinical utility of retinal imaging derived biomarkers in the phenotyping of neurodegenerative disease.

James R. Cameron

A thesis submitted in fulfilment of requirements for the degree of Doctor of Philosophy

University of Edinburgh

2018

I declare that this thesis, and the research described within, is my own work, unless otherwise stated in the thesis where appropriate.

The work described in this thesis has not been submitted for any other degree or professional qualification.

Where content has been submitted, or published in peer-review journals, this is clearly stated in the thesis in the relevant section.

_____

James R. Cameron

_____

February 2018

for Alice

Acknowledgements

Thanks to:

The Anne Rowling Regenerative Neurology Clinic at the University of Edinburgh – for awarding me a prestigious Rowling Scholarship, as well as being the setting for my research, with clinic patients, and equipment

Prof. Siddharthan Chandran and Prof. Baljean Dhillon – my PhD supervisors

Clinical colleagues: Suvankar Pal, Belinda Weller, Anna Williams, Katy Murray, Richard Davenport, Andrew Tatham, Shuna Colville, Dawn Lyle, Nicola MacLeod, Matt Justin

Image analysis software group: Tom MacGillivray and the 'VAMPIRE' programming team (Lucia Ballerini, Enrico Pellegrini, Roberto Annunziata, and Emanuele Trucco)

The many patients and volunteers who kindly and enthusiastically agreed to participate in my research

Abstract

Background

Neurodegenerative diseases, like multiple sclerosis, dementia and motor neurone disease, represent one of the major public health threats of our time. There is a clear persistent need for novel, affordable, and patient-acceptable biomarkers of these diseases, to assist with diagnosis, prognosis and impact of interventions. And these biomarkers need to be sensitive, specific and precise.

The retina is an attractive site for exploring this potential, as it is easily accessible to non-invasive imaging. Remarkable technology revolutions in retinal imaging are enabling us to see the retina in microscopic level detail, and measure neuronal and vascular integrity.

Aims and objectives

I therefore propose that retinal imaging could provide reliable and accurate markers of these neurological diseases.

In this project, I aimed to explore the clinical utility of retinal imaging derived measures of retinal neuronal and vessel size and morphology, and determine their candidacy for being reliable biomarkers in these diseases.

I also aimed to detail the methods of retinal imaging acquisition, and processing, and the principles underlying all these stages, in relation to understanding of retinal structure and function. This provides an essential foundation to the application of retinal imaging analysis, highlighting both the strengths and potential weaknesses of retinal biomarkers and how they are interpreted.

Methods

After performing detailed systematic reviews and meta-analyses of the existing work on retinal biomarkers of neurodegenerative disease, I carried out a prospective, controlled, cross-sectional study of retinal image analysis, in patients with MS, dementia, and ALS. This involved developing new software for vessel analysis, to add value and maximise the data available from patient imaging episodes.

Results

From the systematic reviews, I identified key unanswered questions relating to the detailed analysis and utility of neuroretinal markers, and diseases with no studies yet performed of retinal biomarkers, such as non-AD dementias.

I recruited and imaged 961 participants over a two-year period, and found clear patterns of significance in the phenotyping of MS, dementia and ALS.

Detailed analysis has provided new insights into how the retina may yield important disease information for the individual patient, and also generate new hypotheses with relation to the disease pathophysiology itself.

Conclusions

Overall, the results show that retinal imaging derived biomarkers have an important and specific role in the phenotyping of neurodegenerative diseases, and support the hypothesis that the eye is an important window to neurological brain disease.

Lay Summary

Neurological diseases, like multiple sclerosis, dementia and motor neurone disease, are complicated conditions to understand. In the search for new treatments for these devastating diseases, we need reliable ways of assessing people who have these diseases, so we can accurately measure what treatments are best.

At present, we use a combination of tests to assess people, such as brain scans and genetic blood tests. In this study, I wanted to see if we can look inside the eye at the retina at the back of the eye, and detect and measure these diseases in the retina, in a way that could also be useful. The retina is connected very closely with the brain, but has the huge advantage of being much more accessible for us to study, thanks to new eye scanning equipment.

I have found that the retina is indeed a valuable source of information to monitor these neurological conditions, and may even help us predict which patients need more aggressive treatment, as well as helping us understand more about these diseases.

Contents

List of Figures

List of Tables

List of Abbreviations

Aβ	amyloid β
ACE	Addenbrooke's cognitive examination
AD	Alzheimer's disease
AF	asymmetry factor
ALS	amyotrophic lateral sclerosis
ALSFRS-R	amyotrophic lateral sclerosis functional rating scale - revised
AN	arterio-venous nipping
ANA	antinuclear antibody
anti-TPO	anti-thyroid peroxidase antibody
AO-OCT	adaptive optics – optical coherence tomography
APOE	apolipoprotein E
APP	amyloid precursor protein
AQP4	aquaporin-4
AREDS	age-related eye disease study
ARMD	age-related macular degeneration
ARR	annualised relapse rate
ARRNC	Anne Rowling regenerative neurology clinic
aTort	arteriolar tortuosity
AUC	area under (the ROC) curve
AVR	arterio-venous ratio
BA	branching angle
BBB	blood-brain barrier
BC	branching coefficient
BRB	blood-retinal barrier
BSTD	zone B standard deviation
bvFTD	behavioural variant frontotemporal dementia
C/D	cup to disc ratio
CBD	corticobasal degeneration
CHD	coronary heart disease
CI	confidence interval
CIS	clinically isolated syndrome
CJD	Creutzfeldt-Jakob disease
CNS	central nervous system
CRAE	central retinal arteriolar equivalent
CRVE	central retinal venular equivalent
CSCR	central serious chorioretinopathy
CSF	cerebrospinal fluid
CT	choroidal thickness
CV	coefficient of variation
CVD	cardiovascular disease

DFA	disc fovea angle
DM	diabetes mellitus
DR	diabetic retinopathy
DTI	diffusion tensor imaging
EAE	experimental autoimmune encephalomyelitis
EDI	enhanced depth imaging
EDSS	expanded disability status scale
ELISA	enzyme-linked immunosorbent assay
ETDRS	early treatment diabetic retinopathy study
FA	fluorescein angiography/angiogram
FAN	focal arteriolar narrowing
fMRI	functional magnetic resonance imaging
FoDi	foveal disc alignment
FS	functional system
FTD	frontotemporal dementia
GCL	ganglion cell (body) layer
HDD	hard disk drive
HR	hazard ratio
HT	hypertension
ICG	indocyanine green
IgG	immunoglobulin G
IOP	intraocular pressure
IQR	interquartile range
IRMA	intra-retinal microvascular abnormalities
JE	junctional exponent deviation
LBD	Lewy body dementia
LCVA	low contrast visual acuity
LDR	length diameter ratio
LGN	lateral geniculate nucleus
LMN	lower motor neuron
LogMAR	logarithm of the minimum angle of resolution
LP	lumbar puncture
MCI	mild cognitive impairment
MD	mean difference
MMSE	mini-mental state examination
MND	motor neurone disease
MRI	magnetic resonance imaging
MS	multiple sclerosis
MTR	magnetisation transfer ratio
MV	macular volume
NfL	neurofilament light chain
NMO	neuromyelitis optica
Num1stB	number of first branching vessels in Zone C
OCT	optical coherence tomography
OCT-A	optical coherence tomography angiography

OD	optic disc
OR	odds ratio
PCA	posterior cortical atrophy
PET	positron emission tomography
POAG	primary open angle glaucoma
PPA	primary progressive aphasia
PPMS	primary progressive multiple sclerosis
ppRNFL	peripapillary retinal nerve fibre layer
PRMS	progressive-relapsing multiple sclerosis
PS-OCT	polarisation sensitive – optical coherence tomography
PSP	progressive supranuclear palsy
p-tau	phosphorylated tau protein
RGC	retinal ganglion cell
RNFL	retinal nerve fibre layer
ROC	receiver operating characteristic
RORA	retinoic acid receptor-related orphan receptor alpha
RRMS	relapsing-remitting multiple sclerosis
RT-QuIC	real-time quaking induced conversion
SC	superior colliculus
SCT	stromal choroidal thickness
SD	standard deviation
SD-OCT	spectral domain – optical coherence tomography
sfCT	sub-foveal choroidal thickness
SIVA	Singapore I vessel assessment
SPECT	single-photon emission computer tomography
SPMS	secondary progressive multiple sclerosis
TCT	total choroidal thickness
TD-OCT	time domain – optical coherence tomography
t-tau	total tau protein
UMN	upper motor neuron
VA	visual acuity
VaD	vascular dementia
VAMPIRE	vascular assessment and measurement platform for images of the retina
VCT	vascular choroidal thickness
VISTA	variable interscan time analysis
vTort	venular tortuosity
WMD	weighted mean difference

List of Publications and Presentations from this work

Publications

Lateral thinking - symmetry and asymmetry in neurovascular patterning, in health and disease.

JR Cameron, RD Megaw, AJ Tatham, S McGrory, TJ MacGillivray, F Doubal, JM Wardlaw, E Trucco, S Chandran, B Dhillon

Progress in Retinal and Eye Research 2017; 59: 131-157

Retinal imaging in early Alzheimer's disease.

TJ MacGillivray, S McGrory, T Pearson, JR Cameron

Book chapter in 'Biomarkers for Preclinical Alzheimer's Disease': NeuroMethods Vol. 137, Robert Perneczky (Ed.), Humana Press. (2018)

The application of retinal fundus imaging in dementia: a systematic review.

S McGrory, JR Cameron, C Warren, F Doubal, IJ Deary, B Dhillon, J Wardlaw, E Trucco, TJ MacGillivray

Alzheimer's & Dementia (Amst) 2017; 6(1): 91-107

OCT update: Beyond the nerve fibre layer.

JR Cameron

View on Glaucoma 2017; 12(1): 9-13

Chorioretinal thinning in chronic kidney disease links to inflammation & endothelial dysfunction.

C Balmforth, J van Bragt, T Ruijs, JR Cameron, R Kimmitt, R Moorhouse, A Czopek, M Hu, P Gallacher, J Dear, S Borooah, I MacIntyre, T Pearson, L Willox, D Talwar, M Tafflet, C Roubeix, F Sennlaub, S Chandran, B Dhillon, D Webb, N Dhaun

JCI Insight 2016; 1(20): e89173

Modulation of retinal image vasculature analysis to extend utility and provide secondary value from optical coherence tomography imaging.

JR Cameron, L Ballerini, C Langan, C Warren, N Denholm, K Smart, TJ MacGillivray

Journal of Medical Imaging 2016 May; 3(2): 020501

A Window to Beyond the Orbit: the value of optical coherence tomography in non-ocular disease.

JR Cameron, AJ Tatham

Acta Ophthalmologica 2016; 94: 533-539

The APOSTEL recommendations for reporting quantitative optical coherence studies.

JR Cameron

Neurology 2016; 87(18): 1960

Suitability of UK Biobank retinal images for automatic analysis of morphometric properties of the vasculature.

TJ MacGillivray, JR Cameron, Q Zhang, AYM El-Medany, C Mulholland, Z Sheng, B Dhillon, FN Doubal, PJ Foster, E Trucco, C Sudlow for the UK Biobank Eye and Vision Consortium

PLoS ONE 2015; 10(5): e0127914

Systematic review & meta-analysis of optical coherence tomography in dementia.

KL Thomson, JM Yeo, B Waddell, JR Cameron, S Pal

Alzheimer's & Dementia (Amst) 2015; 1(2): 136-143

Retinal imaging as a source of biomarkers for diagnosis, characterisation and prognosis of chronic illness or long-term conditions.

TJ MacGillivray, E Trucco, JR Cameron, B Dhillon, JG Houston, EJR van Beek

British Journal of Radiology 2014; 87: 20130832

Oral Presentations

'OCT for neurologists - what you need to know'

Edinburgh Clinical Neurology Course – Edinburgh, 4 October 2016

'Optical coherence tomography of the retina, providing new insights into neurodegenerative disease'

SINAPSE Annual Scientific Meeting – Stirling, 17 June 2016

'Losing your nerve? Keep an eye on it - Optical coherence tomography in neurological disease'

Stroke Research Group meeting – Edinburgh, 18 May 2016

'Retinal Imaging in Neurodegenerative Disease'

Centre for Clinical Brain Sciences - Away Day – Edinburgh, 20 January 2016

'A Window to the Brain: OCT-measured Neuroretinal Biomarkers Yield New Insights into Multiple Sclerosis'

Scottish Ophthalmological Club meeting – Stirling, 20 February 2015

'Losing Your Nerve? Keep an eye on it…'

Imaging Sciences Seminar – Edinburgh, 23 February 2015

'An overview of optical coherence tomography in neurodegenerative diseases'

Edinburgh Dept of Clinical Neuroscience: Academic Half Day – DCN, Edinburgh, 5 December 2013

Poster Presentations

Neuroretinal involvement of ALS, assessed with optical coherence tomography (OCT)

JR Cameron, S Pal, R Davenport, B Dhillon, S Chandran

27th International Symposium on ALS/MND – Dublin, December 2016

Optical coherence tomography in secondary progressive multiple sclerosis: a baseline data report from the MS-SMART trial.

F De Angelis, JR Cameron, P Connick, D Miller, S Pavitt, G Giovannoni, C Wheeler-Kingshott, D Plantone, A Doshi, C Weir, R Parker, N Stallard, C Hawkins, B Sharrack, G Cranswick, S Chandran, J Chataway

European Committee for Treatment and Research in MS (ECTRIMS) meeting – London, September 2016

Modulation of VAMPIRE retinal vasculature analysis software to extend utility and provide secondary value from optical coherence tomography imaging.

JR Cameron, L Ballerini, C Langan, C Warren, N Denholm, K Smart, TJ MacGillivray

ARVO annual meeting – Seattle, May 2016

Clinical utility of retinal and choroidal OCT in the assessment of chronic kidney disease.

JR Cameron, S Borooah, C Balmforth, T Ruijs, T MacGillivray, B Dhillon, DJ Webb, N Dhaun

ARVO annual meeting – Denver, May 2015

List of Awards and Prizes from this work

Journal of Medical Imaging 3(2) 'Cover Image' – June 2016

Retinal image from my published paper in this issue of the journal chosen as the front cover image for the print copy of the journal.

(http://spie.org/publications/journals/journal-of-medical-imaging)

SINAPSE 'Image of the Month' - April 2016

Animated image of OCT macula 3D scan awarded 'Image of the Month' by SINAPSE group.

(www.sinapse.ac.uk/news/sinapse-image-of-the-month-oct-retinal-layers)

Institute of Physics & SINAPSE 'Year of Light 2015' Video Competition: Winner

Winner of the three-minute video competition, for submitted video entitled 'Window to the Brain', describing the methods and impact of my research.

Competition organised to promote research involving light.

(www.sinapse.ac.uk/news/winning-entry-from-sinapse-in-iop-international-year-of-light-video-competition
& www.iopblog.org/video-blog-how-light-is-used-in-research)

Ut imago est animi voltus sic indices oculi

The face is a picture of the mind as the eyes are its interpreter

- MARCUS TULLIUS CICERO
Roman orator and philosopher
106-43 B.C.

1 INTRODUCTION

Neurodegenerative disease

Neurodegenerative diseases, like multiple sclerosis, dementia and motor neurone disease, represent one of the major public health threats of our time, with around 35 million people worldwide currently living with one of these brain diseases, and an estimated annual cost burden of $700 billion, greater than 1% of global GDP.[1]

Patients with these devastating diseases have complex needs, and with an ageing population, the problem is on the rise. The absence of effective treatments for many of these conditions reflects the complexity of the diseases and our inadequate understanding of their causes.

There is geographical variation in incidence of these conditions across the world, reflecting the interplay between socio-economic, environmental and genetic factors, all of which play some role in these multi-factorial conditions. For example, there is a particularly high incidence of multiple sclerosis in Scotland, though the reason for this is uncertain.

Epidemiology in Scotland

Multiple sclerosis

Multiple sclerosis is a chronic disease of the central nervous system, characterised by inflammatory demyelination and subsequent neurodegeneration with permanent functional disability. The prevalence of MS in the UK is around 126,000, with an incidence of 6000 new cases per year, making it relatively common.[2] The Orkney Isles of Scotland endure the highest incidence of MS in the world, with one woman in every 170 having the disease.[3]

With a frequent onset in young adult aged people, the initial presentations are often similar, however the longer-term natural history of the disease is difficult to predict. The functional impact of MS is variable, but frequently affects patients' ability to perform household and social tasks, as well as employment functions. The

psychological impact of MS is also increasingly recognised, with depression and apathy compounding the symptoms and affecting quality of life.[4]

The symptoms of MS manifest in almost all body systems, and so require a complex and multi-disciplinary approach to management. There is increasing focus on a stratified and person-centred approach to care, reflecting the heterogeneity of the disease and the differing needs of patients. Simultaneously, research into the pathophysiology of the disease process is enabling a greater understanding of the factors that conspire to cause this debilitating disease.

Dementia

The dementias are a group of diseases, characterised by symptoms of memory loss, personality change, impaired reasoning and language, and resulting in difficulties in performing everyday activities, including maintaining safety. Dementia as a broad term describes this collection of symptoms and implies a chronic and progressive course. However, within this umbrella term, many diseases, pathologies and syndromes exist, with some or all the above symptoms.

Around 90,000 people in Scotland have dementia, with 3200 of these aged under 65.[5] There are challenges associated with diagnosing these conditions, with an increasing pressure on early diagnosis, utilising multi-modal assessments, including brain imaging and psychological assessments, to enable better stratification of disease subtype, prognosis and potential for intervention.

Whilst more cases of early-onset dementia are being seen, recent reports show that the rates of dementia in the elderly are actually falling, both in Europe and the US.[6, 7] The reason for this fall is unknown, and is in contrast to the increasing prevalence of other major health challenges such as diabetes and obesity. But despite this falling rate, dementia became the leading cause of mortality in England and Wales in 2015, accounting for 11.6% of all deaths, and overtaking heart disease for the first time.[8] In Scotland, 8% of deaths in the same year were attributed to mental disorders including dementia, still below heart disease (12%).[9]

Importantly, with a rapidly rising elderly population, the number of people with dementia will continue to rise, despite a slowing rate. A population growth model has predicted that by 2080, Europe will have a population of 520 million, of which 13.7

million will have dementia.[10] This is a staggering number and represents an enormous burden in both social and economic terms.

Dozens of ongoing clinical trials are in progress, across all phases from pre-clinical to phase IV, and encompassing all domains of pathological intervention: β amyloid, tau, cholinergics and others.

It is therefore essential to have reliable tools to accurately identify disease, particularly early or pre-symptomatic disease. And in addition, to monitor the impact of these new treatments as they emerge. As with MS, detailed and deep phenotyping of patients with dementia will be central to advancing personalised medicine in this heterogenous and complex spectrum of disease

Amyotrophic lateral sclerosis (Motor neurone disease)

Amyotrophic lateral sclerosis (ALS) - often referred to as motor neurone disease (MND) in the UK - is a rapidly progressing degenerative disease affecting the upper and lower motor neurones.

A recent report on the worldwide variation in incidence of ALS showed a pooled worldwide standardised incidence of 1.68 (1.50-1.85)/100,000) but with variation from 0.83 (0.42-1.24)/100,000 in Eastern Asia to 1.89 (1.46-2.32)/100,000 in Northern Europe; supporting the hypothesis that genetic factors as well as environmental factors are as important in the occurrence of ALS.[11] This challenged previous assumptions that there would be a similar incidence of ALS across all European-origin populations.[12] In addition, disparate mortality rates for ALS between seemingly similar populations support the complex interaction of genetic factors in this disease.[11]

In Scotland, we benefit from the epidemiological data provided by the Scottish MND Register, introduced in 1989.[13] In 1989, the Scottish (standardised) incidence of MND was 2.32 (2.26-2.37)/100,000. A 2015 update reported it to have increased to 3.34 (3.27-3.40)/100,000 - again standardised to the US Census population data (2010) to align with the epidemiological data from the worldwide study discussed above.[14]

This is a reported 44% increase in Scottish incidence, over a 25-year period, and is now one of the highest incidences of the disease in the world. The reasons behind the increase are unclear, but certainly a wider recognition of the disease and earlier access to a neurologist to make the diagnosis are at least partly responsible - i.e. better data.

Mean Scottish survival from onset is currently 28 months (95% CI [24.88, 30.55]) but with significant differences noted for sex, and age of onset. Site of onset does not however confer any prognostic difference in this population study.[14]

Presently, riluzole is the only available drug treatment, though with only a modest effect in prolonging life by 3 months.

Range of pathology

One of the things that links these conditions is the wide spectrum of disease seen in patients, both phenotypically, but also in potential pathological mechanisms. They are particularly heterogeneous conditions, with a wide range of severity and disease impact, and a similar variability in prognosis. This means it is difficult to give a person at diagnosis a prognosis for their personal disease course. Mean estimates are provided, based on clinical experience and epidemiological evidence, but with such wide variation, this is generally unhelpful to the individual patient, and doesn't reflect any personal disease attributes or features.

Of course, what patients and healthcare providers alike really want are new treatments that maintain health and prolong life. In the absence of treatments, what patients want is a reliable prediction of disease trajectory, highlighting important physical and mental deteriorations, in order to aid planning and support. Therefore, an important goal in the management of these complex diseases is to find useful markers of disease that allow us to subtype the conditions more usefully, as well as provide patients with more relevant information and personalised care.

Diagnosis and monitoring

Diagnostic criteria for MS

The McDonald criteria, most recently revised in 2010, are the standard criteria by which neurologists diagnose MS. The criteria are based on a patient's presentation with typical symptoms and signs of demyelinating disease, usually accompanied by imaging that is consistent with MS, disseminated in both space and time - that is two areas of the CNS, and at different time-points.[15] Cerebrospinal fluid (CSF) analysis is not a requirement for diagnosis, but remains a useful investigation to support the diagnosis,

particularly in difficult cases. Pragmatically, many diagnoses of MS are made by neurologists based upon clinical experience, with a recent audit suggesting adherence to the McDonald criteria is not high.[16]

The category of clinically-isolated syndrome (CIS) is an interesting one. This refers to someone's first episode of neurological symptoms. Not everyone with CIS will go on to be diagnosed with MS. For others, it marks the first attack of what will later be revealed as MS. If an MRI is performed, and shows brain lesions typical of MS, then we know there is greater risk of having further episodes which would lead to a diagnosis of MS.[15]

There are four subtype labels of MS, reflecting the disease trajectory types.

Relapsing-remitting MS (RRMS) is the commonest type, in around 80% MS patients, and represents the typical clinical course of symptomatic flare-ups occurring at variable rates - relapses - with intervening periods of good or complete recovery - remissions. In secondary-progressive MS (SPMS) patients previously labelled as RRMS find that the pattern of their relapse-remission changes, with less fluctuation in the severity of their disease, but the disability gradually and steadily increases. In primary-progressive MS (PPMS), the level of disability increases from the outset, with very few or no relapses. This is less common, affecting 10% of MS patients, but is frequently associated with a more rapid and debilitating course. Finally, progressive-relapsing MS (PRMS) represents the few patients with a progressive disabling course, but who continue to have relapses and then periods of partial remission.[4]

Disease status in MS

The 2013 revisions to the definitions recommended supplementing these subtype categories with modifiers to indicate degree of activity and progression, for example, progressive disease may be active in terms of clinical relapses or MRI enhancing lesions, but clinical evaluation suggests progression is currently static.[17]

Regardless of the subtype label attributed to the patient and their apparent clinical course, there is a typical natural history of the disease that sees them accrue disability over time, reflecting damage to the brain, as result of the repeated inflammatory demyelinating insults. (Fig. 1.1) The complex interplay between inflammation, damage and repair in the brain is beyond the scope of this thesis, but is at the forefront of much MS research, and will ultimately explain the variance in gradient of the disease trajectory between patients, and guide individualised treatment plans.

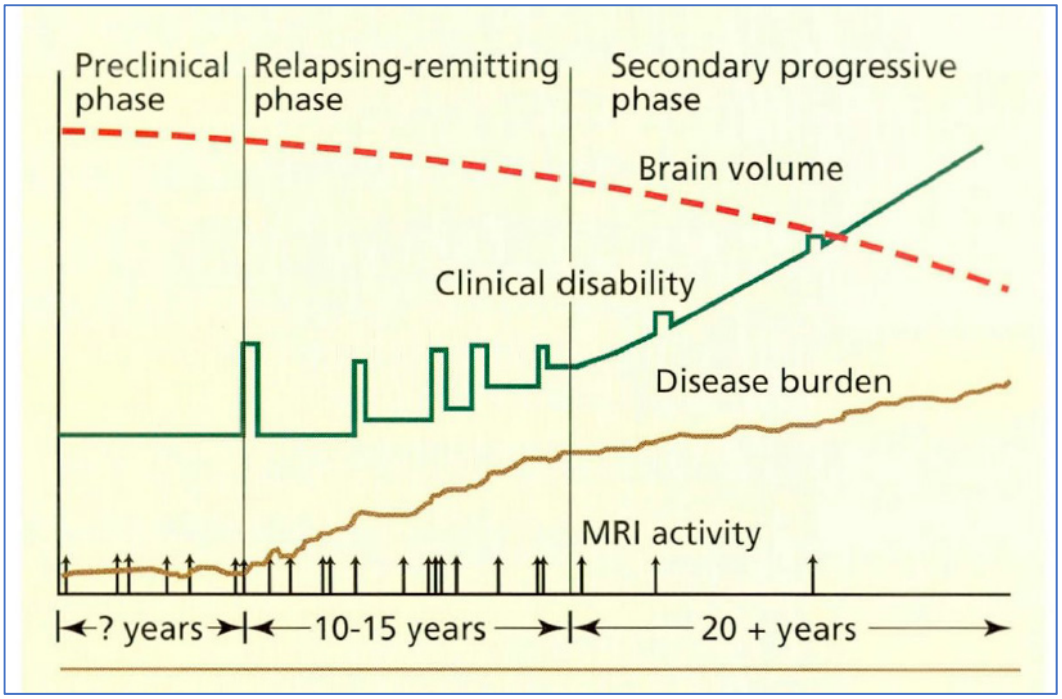

Figure 1.1: Typical clinical and MRI course in multiple sclerosis. MRI activity (vertical arrows) indicates an inflammatory process as measured on brain MRI by gadolinium enhancement or new T2 hyperintense brain lesions. MRI activity typically is more frequent than clinical relapses (spikes in clinical disability), which indicates that more disease activity is taking place than is clinically apparent. Loss of brain volume and increase in disease burden (total volume of lesions), both measured on MRI, indicate permanent tissue damage, which is present early in the disease and gradually progresses over time.

[Image from Fox and Cohen. Cleveland Clinic Journal of Medicine 2001 [18]]

Treatments in MS

Several disease-modifying treatments are now available for MS, but only for specific groups of patients, or with certain disease patterns. At present, that is generally manageable with current clinical labelling to define patient phenotypes, but in the future, more complex targeting of treatments is likely in line with the concepts of stratified or personalised medicine. This means detailed and deep phenotyping of patients will be necessary to not only understand and inform our patients, but guide the most appropriate treatments.

In parallel, trials of new treatments require real-world outcome measures that are practical, meaningful, and as objective as possible and appropriate.

Dementia syndromes

Dementia can be defined in terms of intellectual or cognitive decline, but is more of a description than a diagnosis, and represents a group of conditions with heterogenous presentations, courses and pathologies. Traditional diagnoses are therefore syndromic in nature, reflecting the clinical presentation, but subject to modification in light of new features or symptoms emerging.

As the pathology becomes better understood, there is modification of diagnosis nomenclature to reflect new or common pathological mechanisms, but there remains an unmet need for more precision in dementia diagnosis.

Some classifications separate dementia types into cortical or sub-cortical in brain location, which topographically link the clinical neuropsychological syndrome to the pathological location. The severity of the symptoms can sometimes indicate the diagnosis, and also carry prognostic value. However, there is overlap between many of the dementia syndromes, considerable variation in severity, and so diagnostics is perhaps of limited utility.

In addition, whilst a vascular component is an important contributor in some dementia syndromes, it is not in itself a diagnostic subtype. And indeed, co-morbid vascular cognitive impairment is possible in all dementia syndromes. Therefore, it is perhaps better to accept the limitations of diagnosis in dementia, but instead search for markers that identify important parameters such as cognitive decline or systemic symptoms.

Diagnosis of ALS

The diagnosis of ALS can be clinically difficult, and may require observation time before a certain diagnosis is made. The El Escorial criteria were a consensus attempt to provide guidance on diagnosing this devastating condition, recognising the extreme importance of avoiding both false positive and false negative diagnoses.[19]

The criteria require the presence of:

1. Signs of lower motor neuron (LMN) degeneration by clinical, electrophysiological or neuropathologic examination,

2. Signs of upper motor neuron (UMN) degeneration by clinical examination, and

3. Progressive spread of signs within a region or to other regions, together with the absence of:

- Electrophysiological evidence of other disease processes that might explain the signs of LMN and/or UMN degenerations; and
- Neuroimaging evidence of other disease processes that might explain the observed clinical and electrophysiological signs.

Strengths and weaknesses of these diagnostic criteria have been extensively discussed.[20] Unsurprisingly, neurologists will seek to exclude other differential diagnoses and be sure of the diagnosis before confirming it to the patient, despite extending the diagnostic latency period.

Like MS and dementia, subtypes of ALS are descriptive, relating to clinical symptoms rather than to any pathological identifier. Therefore, their utility is in assessing current clinical need, with little prognostic information, or personal stratified trajectory of disease.

Typically, ALS is sub-divided into bulbar or limb onset, based simply on the first clinical presentation. Whilst the patient's immediate clinical needs are easily identified from this subtyping, it is insufficient in predicting the disease trajectory, and requires improvement. This may well come from recent advances in genetic profiling in ALS, and so it may be that a molecular taxonomy is the next format of ALS subtyping, with a more useful and personal diagnosis modifier to inform on their disease.

The need for reliable biomarkers

The term "biomarker" was defined by the National Institutes of Health Biomarkers Definitions Working Group in 1998 as *"a characteristic that is objectively measured and evaluated as an indicator of normal biological processes, pathogenic processes, or pharmacologic responses to a therapeutic intervention".*[21]

A portmanteau of "biological" and "marker", some broader definitions of the term exist, referring to almost any interaction with a biological system, including chemical and physical, as a biomarker. Nevertheless, all definitions agree with the need for a biomarker to be an objective, quantifiable measurement, that is relevant and valid.[22]

The use of biomarkers in research is not always desirable, with surrogate endpoints in trials of new therapeutics frequently amplified in pharmaceutical advertising to the detriment of revealing the true impact of a treatment upon the patient experience. Therefore, it is imperative that potential biomarkers are subjected to repeated and rigorous evaluation.

Uses of biomarkers

Biomarkers can inform on many facets of a disease. (Fig. 1.2)

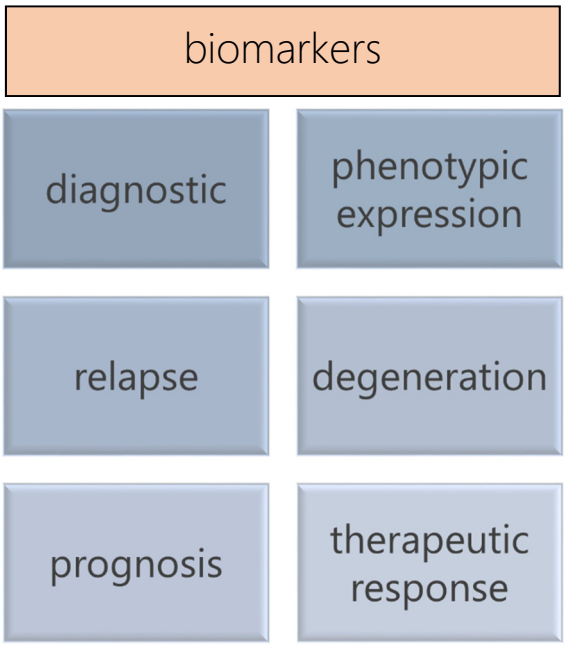

Figure 1.2: Biomarkers can report on a range of disease characteristics

- Diagnostic: can aid accurate or early diagnosis, rule out differential diagnoses, and be used for screening
- Relapse: objective characterisation of disease relapse, trajectory change, subtype classification, or aid treatment decision-making
- Prognosis: predictive biomarkers may aid treatment planning as well as informing on disease trajectory and likely course
- Phenotypic expression: can reflect underlying biological mechanisms
- Degeneration: identifying pathological process
- Therapeutic response: monitoring impact of interventions, screening for adverse events, clinical trials

Characteristics of a good biomarker

Several scientific writers have lately commented on the proliferation of published work on "potential biomarkers" for every medical condition known, and frequently these works describe something that will have no ability in the 'real world' to fulfil the requirements of a clinical biomarker, or represents an area of research in its infancy, where such big claims are out of proportion to the status of development and understanding.

In fact, the term "biomarker" is so frequently inappropriately used, perhaps with poor understanding of its definition, that it can act as a 'red flag' to reviewers who may see it as a sign of inadequate exploration of the topic being investigated.

It seems logical then to maintain an agreed set of criteria to which new tests, metrics, assays or scores should be compared against, in order to provide more useful and precise information about the potential of a marker of disease, rather than the descriptor "biomarker". For each mode of use of a biomarker, key statistical analyses can aid evaluation against those criteria.[23] (Table 1.1)

Table 1.1: Domains for assessing utility of a biomarker

Character	Method of assessment
Detection method should be precise, reliable and transferrable	size, strength, repeatability
Distinguish between healthy and disease; and pre-clinical screening test	sensitivity and specificity, positive and negative predictive value
Differentiate between diseases that are clinical similar	discrimination (ROC curve, C-statistic), likelihood ratio
Value as a prognostic marker	association (relative risk, odds ratio)
Use in monitoring disease progression	correlation, association, interaction

For the retinal metrics explored within this study, this evaluation is an essential step to understand how they perform in the 'real world' of clinical neurology, and yet is omitted - either partially or wholly - in much of the published work on the subject. In fairness, this does represent the infancy of the research area, and indeed in this thesis I have been unable to fully answer some of the criteria to determine the utility of some retinal metrics, nevertheless a qualitative description of the findings is more valuable than a binary comment on a measure being a "potential biomarker".

Biomarkers in neurodegenerative disease

The last few years have seen an increasing number of genetic mutations responsible for the phenotypes seen in neurodegeneration - particularly in the dementias, and ALS - being found, and some have started to be used as part of a diagnostic workup for newly presenting patients.[24]

However, less patient-specific tests and measures have been developed and used in the assessment of neurological diseases for some time, with varying degrees of precision and specificity. For example, in MS, multiple biomarkers have been suggested for each of the characteristic domains of the disease described above. (Fig. 1.3) These reflect new developments in biochemical analysis of CSF, as well as more traditional scoring methods from brain imaging, and clinical presentation.

This is also true in the dementias, where our incomplete understanding of the pathophysiology limits us to syndromic phentotypic descriptions as diagnoses.

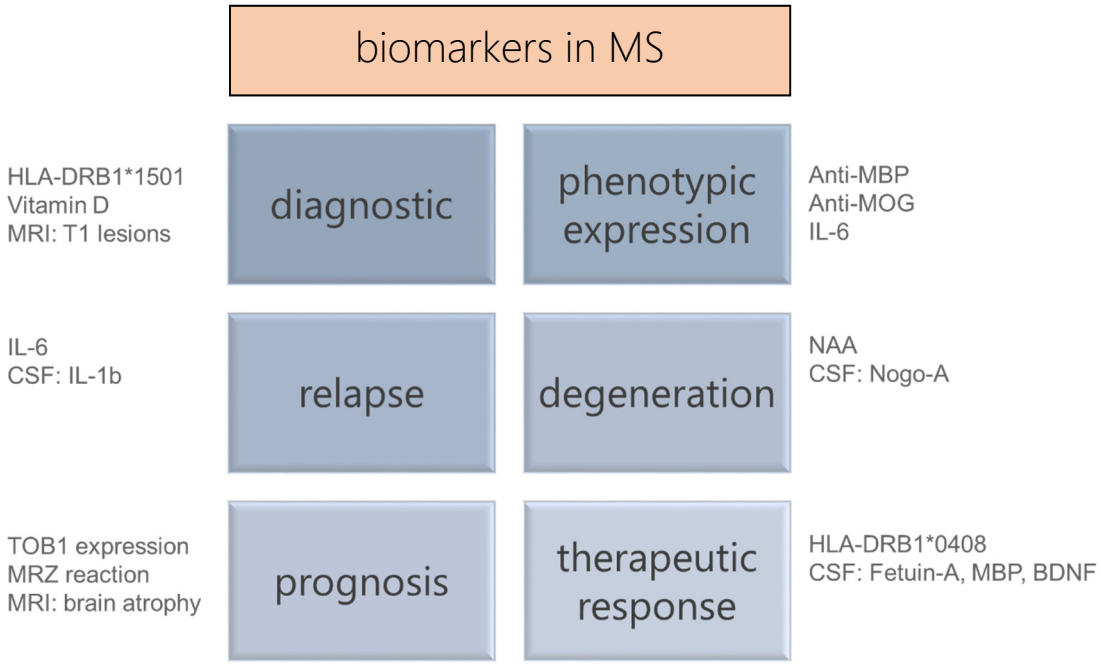

Figure 1.3: Examples of biomarkers in multiple sclerosis, across domains

Clinical measures

In clinical neurology, it is generally clinical measures - in both history and physical examination - that have determined diagnosis, subtyping and disease status. This reflects the syndromic nature of many neurological diseases, but also the relative paucity of biochemical or similar diagnostic 'tests' for neurological disease that are more common in diseases of other body systems.

MS

A key question in MS has been the prognosis of disease based upon clinical measures or prognostic indicators at diagnosis. Several natural history studies have followed newly diagnosed patients through their journey, and attempted to match up risk factors with their disease-related morbidity or accumulation of disability.

A poorer prognosis has been associated with male gender, older age at onset of disease, motor, cerebellar, and sphincter involvement at onset, and a higher number of attacks early in the disease with only short periods of remission.[25] Positive indicators include

age < 35 years, monosymptomatic onset (particularly if single sensory such as optic neuritis), and initial remission within 1 month.[26]

For 85% of patients with MS, their first episode was a clinically isolated syndrome (CIS), with uncertain prognosis given.[27] With an uncertain number of patients progressing from CIS to MS, prognostic markers are needed. Observationally, MRI lesions are regarded as an important indicator. More recent studies have looked specifically at the conversion from a single clinical episode to confirmed MS, with an attempt to stratify these prognostic factors into the level of risk or impact they confer. One study concluded that *"...demographic and topographic characteristics are low-impact prognostic factors, the presence of oligoclonal bands is a medium-impact prognostic factor, and the number of lesions on brain magnetic resonance is a high-impact prognostic factor".*[28]

Therefore, clinical measures of the phenotypic pattern of disease onset maybe less helpful in determining the disease trajectory in a patient with MS, and that it is in neuroimaging where this important information resides.

Dementia

The diagnosis of the different dementia subtypes relies upon a detailed history of the patient's symptoms and behaviour, as well as family history, and an examination that includes psychological testing. The essential criteria for diagnosing dementia (as per the Diagnostic and Statistical Manual of Mental Disorders [DSM-V][29]) are loss in 2 or more of the following domains: memory, language, calculation, orientation, or judgment.[30] Whilst the Mini-Mental State Examination (MMSE) is the most well-known 'bedside test' for cognitive assessment, it is the Addenbrooke's Cognitive Examination (ACE-III) that is a superior tool in the diagnosis of early-onset dementia, with a high discrimination of disease from healthy controls.[31]

However, in the identification of dementia type, neurologists rely on history and examination to identify non-AD dementia types, for example frontotemporal dementia (FTD), or Lewy body dementia (LBD). Whilst clear dementia syndromes are seen and characterised, it is not uncommon for a diagnosis to change over time, as new symptoms or signs emerge.

For predicting the trajectory of dementia, recent studies have suggested that some clinical measures can indeed be used as indicators for clinically significant progression

of disease. A large multi-centre Canadian study found that poorer cognition, greater dependence, and more neuropsychiatric symptoms at baseline, were predictive of greater decline over the following 12 months.[32]

Perhaps more relevant for the future are factors that may predict decline early in the disease, in particular the conversion from MCI to AD, as this may be the best time to attempt treatment to slow or prevent that deterioration. As with progression of more advanced dementia, lower educational attainment and lower baseline cognitive scores appear to be predictors of conversion from MCI to AD.[33] In addition, specific behaviours - resisting help, forgetting appointments, difficulty shopping alone - are also associated with a higher risk of progression.[34]

ALS

Whilst the diagnosis of ALS may be suspected in clinical presentation of upper and lower motor neurone signs, confirmation with nerve conduction studies is important.

In bulbar-onset ALS, patients present with difficulty speaking or swallowing. This may mean that these patients present earlier than those with limb-onset symptoms, that may be attributed to less serious musculoskeletal disease in the early stage. Clinical examination of the tongue, swallowing and jaw movements will reveal the pattern of paresis associated with ALS, as well as assessing the risk for respiratory aspiration.

Predicting progression in ALS is more difficult. Decline is generally non-linear, with early and late phases showing the most rapid rates of change.[35] Older age and bulbar signs are associated with a more rapid decline across a population sample, but variation is wide, and correlations with individual patients are poor.

Whilst baseline phenotypic characteristics poorly predict disease course in ALS, attempts to create mixed-parameter models to predict decline, using clinical and laboratory measures, have proved slightly more successful, albeit into just two categories of high- and low-risk.[36]

The ALS functional rating scale (ALSFRS-R) is a validated rating instrument for monitoring progression of ALS - revised in 1999 to incorporate respiratory dysfunction as an important component of ALS quality of life.[37] It scores across multiple clinical domains, such as speech, swallowing, handwriting, dressing and hygiene, climbing stairs and respiratory insufficiency, to provide a total score out of 48. A decreasing score marks disease decline. It is therefore a useful marker of disease status, but

prognostic potential is uncertain. One recent study has reported that a decline in ALSFRS-R motor subscores in patients with spinal-onset disease, and a decline in ALSFRS-R bulbar subscores in patients with bulbar-onset disease, may predate reported disease onset dates. They also emphasise that the domain-specific subscores are perhaps more valuable than the single combined score.[38]

Brain imaging

The search for more objective measures of disease type and burden has paralleled the advances in neuroimaging, where technology and research have rapidly translated to patient care.

MS

Magnetic resonance imaging (MRI) brain scans are currently our primary source of objective information in assessing MS disease status, in terms of neurodegeneration and possibly prognosis. Measurements of brain atrophy have shown worsening rates are higher in untreated MS patients compared with healthy controls[39] and also correlate with subsequent disability status eight years later.[40]

However, brain atrophy measures sometimes reveal paradoxical outcomes, particularly of white matter atrophy, where normal or increased volume as a result of pathological processes, such as tissue damage and repair, can impact upon the measures.[41] This concept of the 'clinico-radiological paradox' in MS is frequently seen, with the association between clinical findings (including cognitive function[42]) and radiological extent of disease generally poor.[43]

Several studies have considered the potential for MRI to provide some estimate of individual risk stratification, for newly diagnosed patients or first presentation with CIS, by examining the brain lesions. Despite measurement challenges in either manual or semi-automated assessment of 'lesion burden', it is thought that greater number - and volume - of initial T2 weighted brain MRI lesions predicts long-term disability.[28] MRI T1 'black holes' or cerebral atrophy of course suggest irreversible axonal injury.[44]

Within treatment trials, advanced MRI measures of tissue integrity such as diffusion tensor imaging (DTI) and magnetisation transfer ratio (MTR), rather than simple brain or lesion volume, are showing greater sensitivity in characterising disease status.[45]

Dementia

Positron emission tomography (PET) imaging has shown some promise in identifying Alzheimer's disease at an early stage.[46] Using radiotracers with an affinity for amyloid or tau deposition in the brain, PET can discriminate between normal ageing and disease with high specificity and sensitivity.[47] It is expensive, and invasive, but work continues on developing even more specific markers.

Single-photon emission computer tomography (SPECT) also uses gamma radiation and radiotracers, but is a lot cheaper than PET. The images have less resolution than PET, but it may have a role in distinguishing between different dementia types.[48]

MRI is more accessible, though less specific in dementia. It can aid diagnosis by the pattern of atrophy, but is less useful in very early disease. Regarding conversion from MCI to AD, one study found that the combination of left hippocampal volume, occipital cortex theta power, and clock drawing copy subtest scores predicted conversion from MCI to AD with 100% of sensitivity and 94.7% of specificity.[49] Other MRI measures for predicting decline include higher grade white matter lesions.[33] Also, vascular factors (assessed with both general vascular risk scoring (e.g. Framingham Coronary Heart Disease Risk score) and also carotid plaque measured with ultrasound) both predict conversion from MCI to AD.[50, 51]

ALS

Attempts to use advanced MRI methods to provide biomarkers of disease progression and survival in ALS have proved challenging, with no overall consensus as a result of studies being too small, and with varied methodologies.

Consortia such as the Canadian ALS Neuroimaging Consortium (CALSNIC) have been established to attempt to overcome the weaknesses of small single centre reports, by coordinating a prospective multicentre biomarker validation study, with harmonised imaging clinical and imaging protocols. Their imaging protocol includes MR spectroscopy, diffusion tensor imaging and resting state fMRI. They are attempting to look at several aspects of proposed ALS pathology, such as neuronal and white matter integrity, gliosis, and structural and functional connectivity.

Some studies have shown that when MRI data is added to clinical scoring systems such as ALSFRS-R, it improves the predication accuracy of 18-month survival.[52]

Cerebrospinal fluid

Cerebrospinal fluid (CSF) analysis is a developing focus in the area of biomarkers of neurodegeneration, particularly in diseases with known misfolded protein accumulation as part of the pathological process, such as prion protein in Creutzfeldt-Jakob disease (CJD), or α-synuclein in Lewy-body dementia (LBD).

The detection and reliable quantification of these proteins is complex, and innovative technologies such as Real-time quaking induced conversion (RT-QuIC) are gaining traction as highly sensitive diagnostic tests.[53]

MS

The down-grading of the role of CSF detection of oligoclonal bands in the diagnostic criteria for MS has reduced the need for CSF examination in these patients. Nevertheless, work continues on investigating the utility of novel CSF biomarkers, such as microRNA profiles[54], that may more precisely quantify inflammation.[55]

Dementia

It is in dementia diagnosis where we have seen greater utility for CSF biomarkers, with the discovery of extracellular protein aggregation as a key disease marker.

The major component of amyloid plaques in the brain of patients with AD is amyloid-β (Aβ). Multiple forms are seen, with oligomers of amino acid fragments length 42 thought to the main contributor of disease.

Whilst the presence of this amyloid can be measured at post-mortem in brain using immune-staining or ELISA methods, *in vivo* measurement is more difficult. PET imaging is attempting this, as discussed above, but direct physical measurement in CSF should in theory be more accurate.

Decreased CSF amyloid-beta 1-42 ($A\beta_{1-42}$) concentrations in combination with raised CSF total-tau (t-tau) and CSF phosphorylated-tau (*P*-tau) concentrations have been repeatedly demonstrated as features characteristic of AD when evaluated against patients with MCI and healthy controls.[56] This CSF pattern likely reflects the neuronal injury caused by abnormal accumulation of amyloid beta peptide and tau protein with subsequent formation of plaques and neurofibrillary tangles in AD.[57]

In addition, these markers may also distinguish AD from FTD with the *P*-tau/$A\beta_{1-42}$ ratio being the most discriminant value.[58]

Lewy body dementia (LBD) is not easily distinguished from other dementias in its early stages, however a recent systematic review concluded that measuring CSF α-synuclein may be of sufficient sensitivity to differentiate between LBD and AD.[59]

ALS

Neurofilaments are a cytoskeletal protein with the neurone, providing structural support. Following neuronal loss, there is accumulation of these neurofilament proteins in the local area, and some will migrate into the CSF (and serum). Therefore, there is a hypothesis that elevated levels of neurofilament light chain (NfL) levels in the CSF may be a marker of neuronal loss. With ALS characterised by loss of large neurones with abundant NfL, ALS is a candidate disease for this biomarker evaluation.

The measurement of NfL requires electrochemiluminescence immunoassay, and early studies suggested it identifies ALS with high sensitivity and specificity.[60]

CSF NfL levels appear to be elevated at an early stage of the disease (with no difference between sporadic or genetic ALS), correlate with progression, and may have prognostic value.[61, 62]

However, CSF analysis requires invasive lumbar puncture procedure, and is expensive. Incorporating this as a regular investigation in routine clinical care would be challenging. And there is insufficient data thus far demonstrating superiority of CSF NfL measurement over plasma NfL in phenotyping disease, although it may be better for monitoring progression.

Genetic/Biochemical/Molecular markers

MS

Despite the frequent observation of MS occurring more than once within families, a genetic cause remains elusive. Susceptibility genes have been identified - such as retinoic acid receptor-related orphan receptor alpha (RORA)[63] - which support the hypothesis of MS being a more complex group of clinically similar diseases.

Diagnostic exclusion has been facilitated by the finding of aquaporin-4 (AQP4) IgG autoantibody in serum, distinguishing neuromyelitis optica (NMO) from MS, with 97-99% specificity.[64] Patients with NMO are frequently also seropositive for other autoantibodies such as ANA and anti-TPO, though these are less specific to NMO, and so of less diagnostic utility.[65]

Dementia

Three genetic mutations identified as causative in Alzheimer's disease - mutations of the presinilin genes 1 and 2, and amyloid precursor protein (APP) - actually only account for around 5% of cases.[24] In sporadic AD, an important genetic risk marker is the apolipoprotein E (APOE) gene. The exact gene function and expression is unclear, but it is thought to play a role in systemic lipid distribution and metabolism.[66] There are at least 3 alleles of the gene: ε2, ε3, and ε4. The commonest is ε3, which is likely healthy, whereas APOE ε4 genotype is associated with a higher risk of AD[67] as well as an earlier age of onset.[68]

Plasma biochemical measures of tau and amyloid are attractive tests, being low-cost and easy to perform. Whilst some studies suggest they are insufficiently specific to separate disease from normal ageing[69], they form part of the screen of tests being used in large prospective cohort studies looking for early mid-life predictive biomarkers of later-life dementia.[70]

ALS

The genetics of ALS is a hot-topic field of research at present, integrating research across multiple fields from clinical registers to laboratory stem cell models of the disease. Rapid advances in the isolation of genes relating to different cellular processes in ALS pathophysiology highlights the complexity of this disease, as well as generating new hypotheses regarding the interplay between neurometabolic and environmental factors in the pathophysiology of the disease.[71, 72]

From the early identification of the genes SOD1, TARDBP, C9ORF72 and others, through to modern genome-wide association studies, the prospect of a molecular taxonomy for sporadic disease, as well as familial, is intriguing and will translate to patient stratification.[73, 74]

Biochemical plasma markers of ALS progression are also under investigation, particularly humoral pro-inflammatory factors/cytokines.[75]

Summary

Clinical measures, neuroimaging, genetics, CSF and biochemical markers, all have a role to play in phenotyping neurodegenerative disease. The pace of new discoveries is rapid, and the complex interplay between biology and environment is pervasive. However, despite these advances in molecular and radiological diagnostics, post-mortem neuropathology currently remains the (only) gold standard, particularly in syndromic dementias.[24]

Each category of marker has strengths and weaknesses; none provide the whole picture, and none inform with 100% sensitivity. It is likely that the future lies in multi-modal combination markers, with each system targeted at a specific facet of disease. Current momentum in research is aimed at elucidating new biochemical markers, particularly in relation to genetics. But this is expensive. Pragmatic solutions are required.

In summary, there is therefore a clear persistent need for novel, affordable, and patient-acceptable (non-invasive) biomarkers of neurodegenerative disease, to assist with diagnosis, prognosis and impact of interventions. And these biomarkers need to be sensitive, specific and precise.

Retinal Imaging

Note: Excerpts of this section have been published – in "Retinal imaging as a source of biomarkers for diagnosis, characterisation and prognosis of chronic illness or long-term conditions", TJ MacGillivray, E Trucco, JR Cameron, B Dhillon, JG Houston, EJR van Beek. Br J Radiology 2014; 87: 20130832. doi: 10.1259/bjr.20130832

History of fundus photography

With the invention of the ophthalmoscope by Von Helmholtz over 150 years ago, the black void beyond the pupil became visible and a new field of medical examination was born. (Figs. 1.4, 1.5) The development of colour photography in the years following led to many researchers' attempts to photograph the fundus, with the complex optics and magnification required proving challenging. After many experimental prototypes, the first commercially available fundus camera was released in 1925 in partnership with the Zeiss Camera Company.[76] Four years later, in 1929, the first retinal photo atlas was published.[77]

Figure 1.4: Illuminating the dark void beyond the pupil - unlocking the hidden landscape of the retinal neurovascular architecture

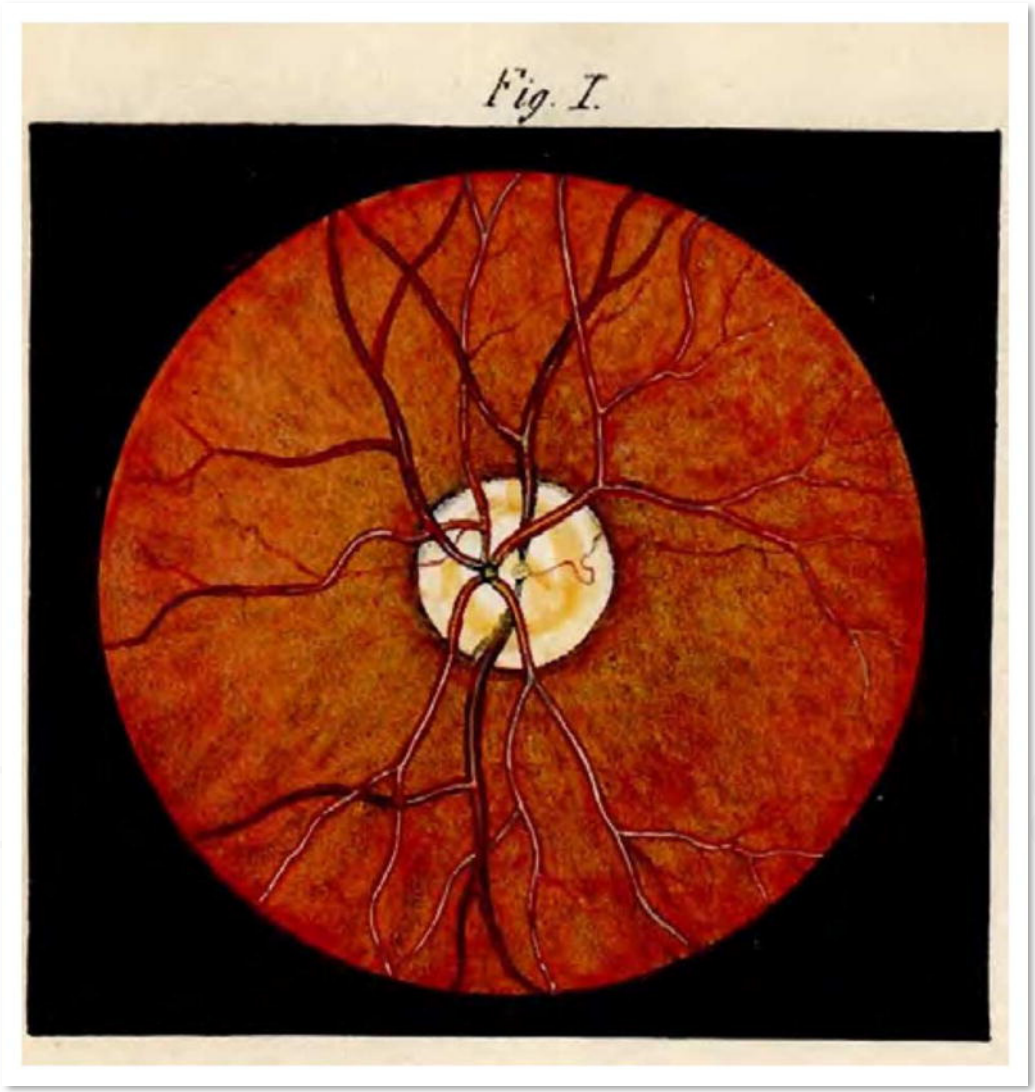

Figure 1.5: First known image of the human retina, as drawn by Van Trigt in 1853 [78]

Colour fundus photography today remains a core mainstay of clinical practice, with the enormous advantage of digital photography. Other developments, such as fluorescein angiography (FA) which became popular in the 1960s, and indocyanine green (ICG) angiography coming later, have added great value to fundus photography, in providing both structural and functional information about the retinal and choroidal vasculature, particularly in retinal pathology. Wide-angle imaging with new devices such as the Optos wide-field scanning laser ophthalmoscope (SLO) have also dramatically widened our field of view. (Fig. 1.6)

Figure 1.6: Retinal imaging modalities. a) digital colour fundus photography b) fluorescein angiogram c) wide-field Optos SLO

Optical coherence tomography

First described by Huang *et al.* in 1991, optical coherence tomography (OCT) is a non-invasive and non-contact method for *in vivo* cross-sectional imaging of the internal retinal structures.[79]

OCT is an optical scanning method, which can be thought of as 'optical ultrasound' in use, and in image interpretation; albeit with a limited tissue depth of just ~ 2mm.

Huang himself created the term 'OCT', reflecting the physical principles of low-coherence interferometry and tomography used in the technology. The conversion of signal reflectance intensities at adjacent A-scan positions into 2-dimensional B-scan greyscale (or false colour) cross-sectional images creates a highly visual representation of the retina in section, whist somewhat concealing the advanced and complex technology required to produce these images.

Multiple advances in the technology of the light source and detector over the past two decades have brought new generations of the technology, with greater axial resolution and considerably faster scanning speeds. (Fig. 1.7) This has provided us with even higher-resolution images of the internal retinal configuration, allowing identification of specific cellular layers (and accurate measurement of these layers) in a way only previously seen in histological samples.

Ocular OCT is not confined to the retina. Anterior segment OCT is now available, providing similarly detailed reflectance images of the cornea and iris. This is proving very useful in the assessment of patients for corneal surgery, particularly lamellar corneal transplant surgery.[80] It is also being used to evaluate the angle structures in angle closure glaucoma, with mixed results.[81, 82] There are even developments of the technology to enable imaging of the pre-corneal tear film, to allow quantification of abnormalities or the effect of eye drop treatments.[83]

Within ophthalmic clinical practice, the role for retinal OCT has expanded greatly in recent years, with its quality and resolution refining in coincident timing with the emergence of treatments for retinal conditions previously deemed untreatable, such as neovascular age-related macular degeneration (ARMD). OCT is now an essential tool in the eye clinic - both in its powerful diagnostic support role in retinal disease, and also its monitoring of disease and treatment response in ARMD, diabetic macular oedema, and others. Indeed, current guidelines on treating these retinal conditions that result in retinal leakage and thickening require the use of OCT measurements as criteria for re-treatment and management plans.

The newest generation of machines are now of sufficient resolution to clearly demarcate the individual retinal layers. This has transformed not only how we treat retinal diseases, but changed our understanding of the pathology, pathogenesis, evolution and natural history of many disease processes affecting the retina. No other imaging modality has had this kind of profound impact upon clinical ophthalmology.

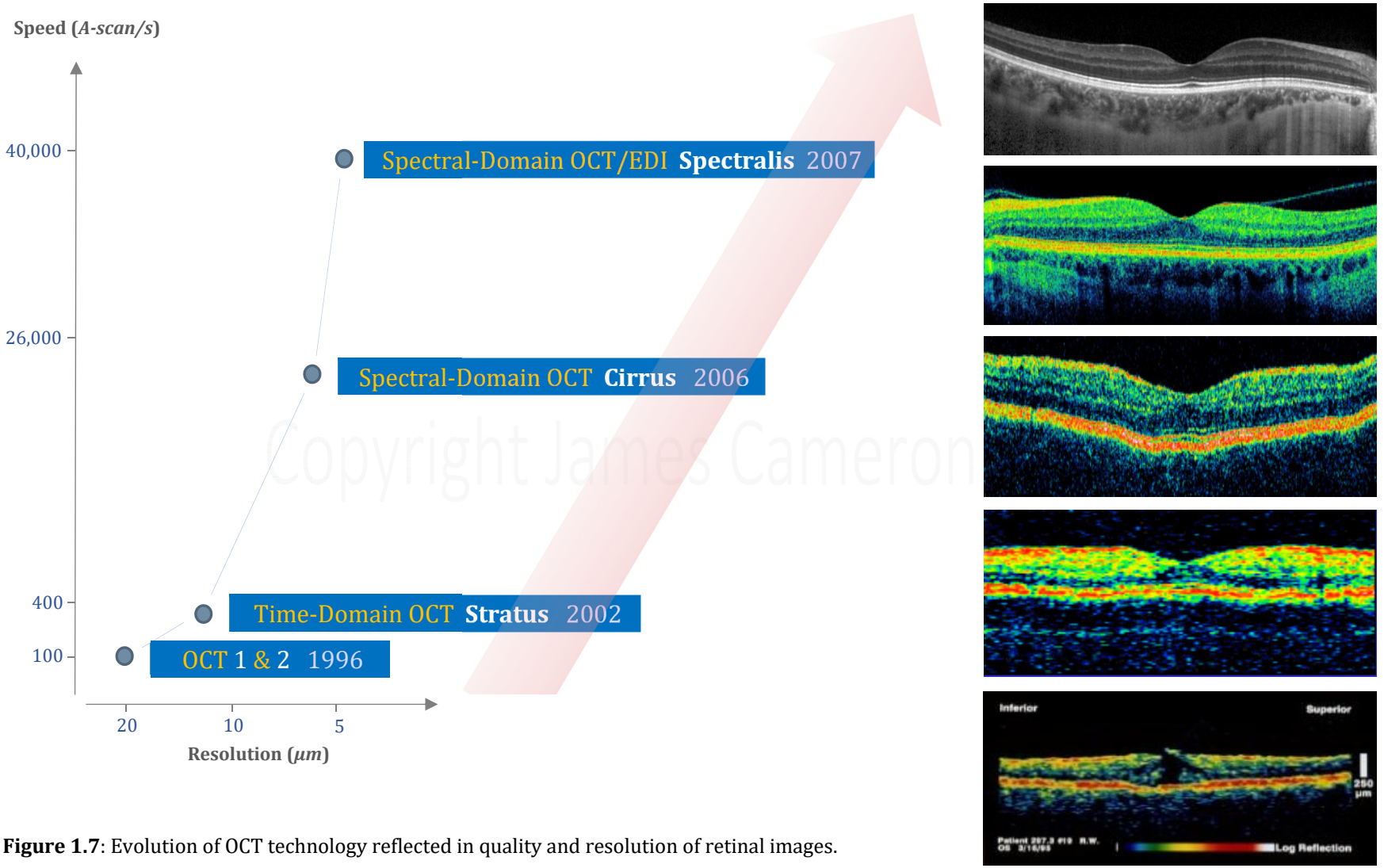

Figure 1.7: Evolution of OCT technology reflected in quality and resolution of retinal images.

Imaging the Retinal Layers

The evolution of OCT technology has enabled greater visualisation of the retinal structure, with varying amounts of reflectivity producing an image that resembles the known histological structure of the retina. Caution however must still be advised in the interpretation of such a high-resolution image of the retina, as the matching of OCT reflectivity to retinal layer is not simple, and incorrect assumptions continue to be prevalent amongst ophthalmologists. This is particularly true of the outer retinal layers where we see high reflectivity bands on the OCT image which do not correspond with the thickness of an anatomical retinal layer. The layer previously known as the "inner/outer photoreceptor junction" is essentially an indicative intracellular boundary, and not the thick hyper-reflective region seen on OCT. A recent consensus review of retinal layer designations has addressed this discrepancy in traditional nomenclature, and recommended a new term for this hyper-reflective band - "ellipsoid zone" - as well as reviewing the terms for the other retinal layers.[84] (Fig. 1.8)

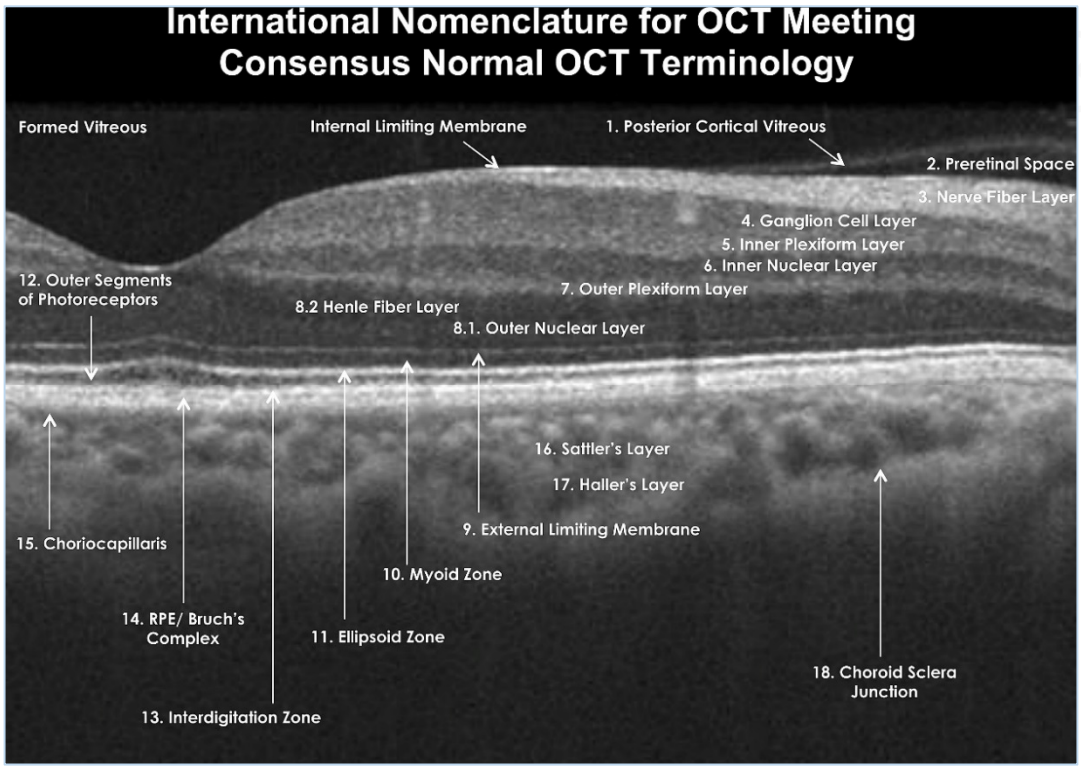

Figure 1.8: Nomenclature for normal anatomic landmarks seen on spectral domain optical coherence tomography (OCT) images proposed and adopted by the International Nomenclature for Optical Coherence Tomography Panel.

[Image from Staurenghi et al. Ophthalmology 2014 [84]]

Retinal Ganglion Cells

The retinal ganglion cells (RGC) are the neurones that connect the retina with the brain. With their cell body residing in the retina, and receiving neurological inputs from adjacent intra-retinal neurones, their axons coalesce to form the optic nerve, then optic tracts, and finally synapsing in the thalamus or midbrain. Second-order relay neurons then transmit visual information from the thalamus to the visual cortex. (Fig. 1.9)

There are approximately 1.6 million RGCs per eye, with around 90% connecting to the lateral geniculate nucleus (LGN), and being responsible for image-forming information. There is a small population of photosensitive RGCs, which synapse with the suprachiasmatic nucleus, and control circadian rhythm. The remaining ~10% of RGCs carry non-image-forming information, such as detecting movement in the far peripheral visual field, and connect with the superior colliculus (SC).[85]

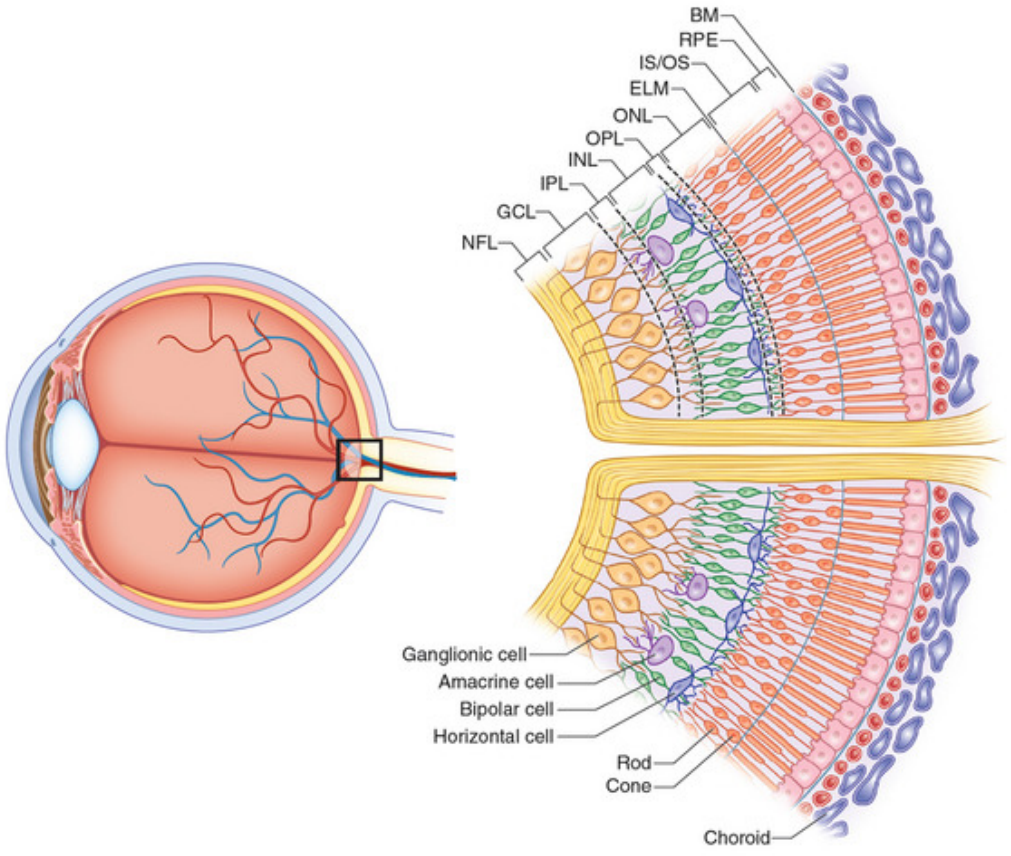

Figure 1.9: Schematic representation of the retinal layers.

[Image from 'The Retina Reference'; accessed at www.retinareference.com]

Retinal Nerve Fibre Layer (RNFL)

The RNFL consists predominantly of the long axons of the retinal ganglion cells (RGCs) sweeping forward and across the innermost surface of the retina, before converging to form the optic nerve. The pattern of distribution of these axons in the RNFL is precise, and important in the understanding of ocular disease diagnosis and assessment, for example the strict horizontal[a] midline division.[86, 87] (Fig. 1.10)

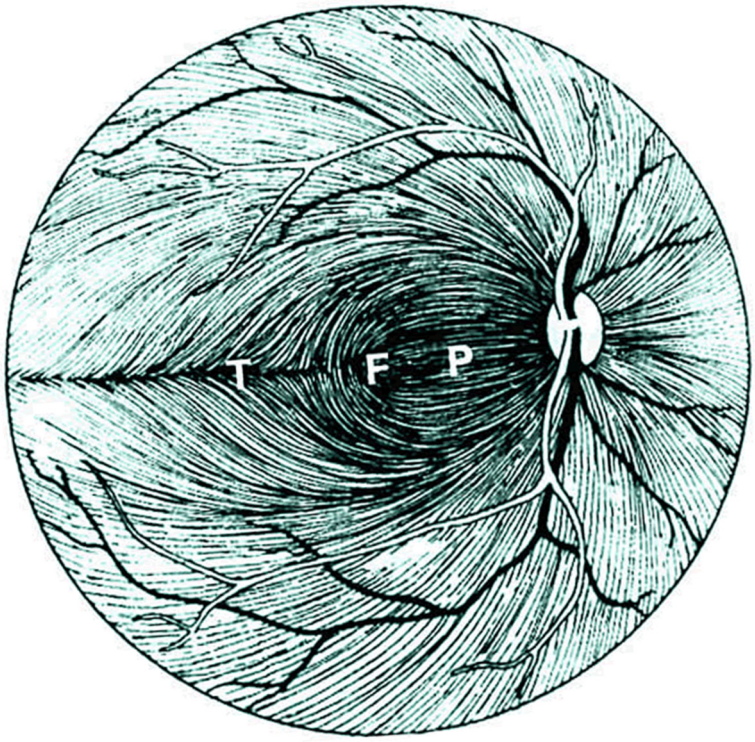

Figure 1.10: RNFL axon orientation-distribution map.

The RNFL is unsurprisingly thickest around the optic nerve head, but quickly thins out within a few millimetres, and is barely measurable on OCT beyond about 4mm from the optic disc margin.[88] (Fig. 1.11) Although it remains artificially thickened around the vessel arcades, which lie within this layer.

[a] The horizontal raphe is not actually horizontal, but in fact at a small angle of around 1-3° from the true horizontal, known as the 'temporal raphe to horizontal meridian angle'. Though it is closer to the horizontal than the axis of the papillomacular bundle, which is at around 5-10°, known as the 'disc fovea angle' (DFA).[87]

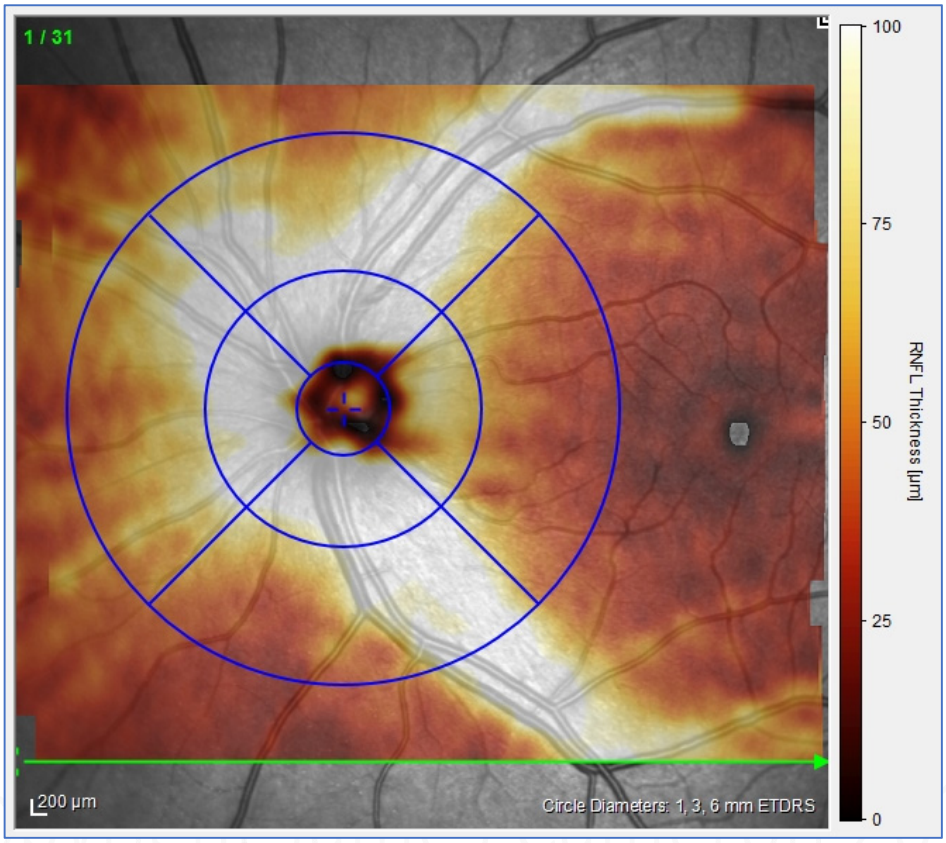

Figure 1.11: OCT volume scan at optic nerve head, segmented to show en face RNFL thickness map, demonstrating rapid reduction of RNFL thickness with distance from the optic disc.

It is therefore logical to study the RNFL in this region, near the optic disc, and in addition, the circumpapillary RNFL measurement is not affected by optic disc size (provided there is adjustment for axial length).[89]

A circular peripapillary OCT scan with automated segmentation of the RNFL has therefore become a standard measure for assessing the RNFL, both in optic nerve disease such as glaucoma, but also in neurological brain disease research. (Fig. 1.12)

This scan protocol is now a pre-set imaging protocol in the current generation of OCT devices available.

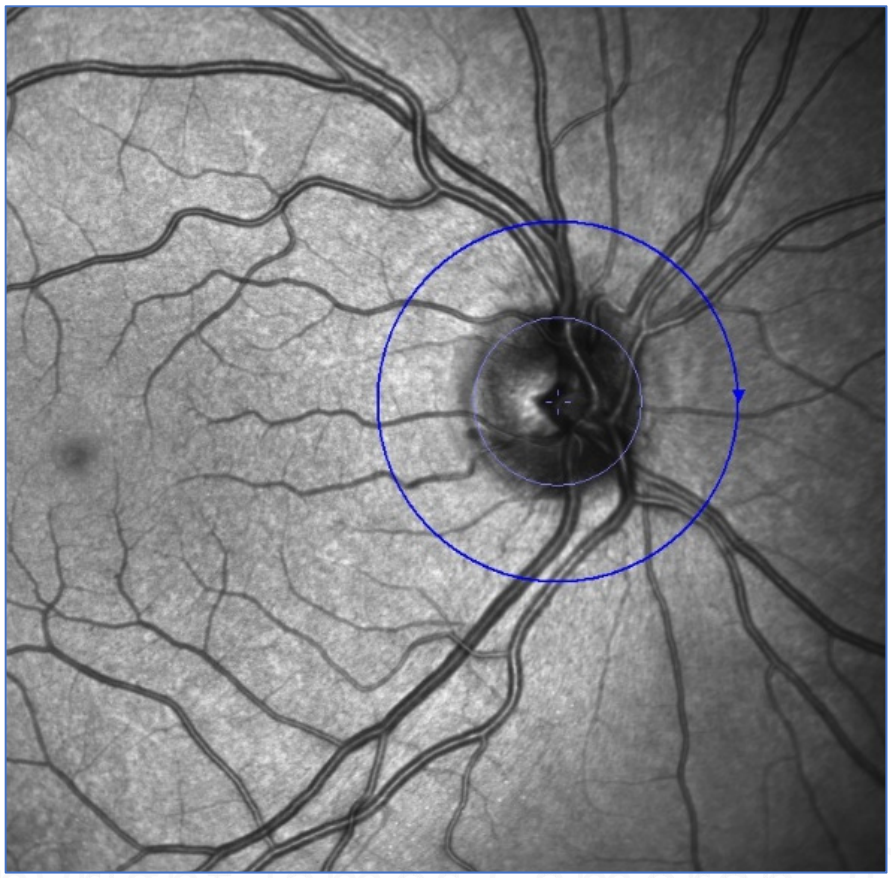

Figure 1.12: Standard peripapillary circular OCT line scan pattern, centred over the optic disc, for subsequent RNFL analysis.

Ganglion Cell Body Layer (GCL)

Whilst the density of RGC axons (and therefore RNFL thickness) increases towards the optic disc, the highest density of the cell bodies of these RGCs lies within the macula, likely reflecting the importance of macular visual function. (Fig. 1.13)

Anatomically we know that the macular RGC cell bodies correspond to the temporal peripapillary RNFL (and temporal optic nerve), however once again, partly for reasons of measuring a retinal layer at its maximal thickness to reduce error and improve ability to detect change, it is the macula area of the RGC layer that has become a standard OCT protocol for measuring RGC in relation to ocular disease, such as glaucoma.[90]

The required OCT scan protocol for this is a macular volume scan, centred over the fovea. (Fig. 1.14)

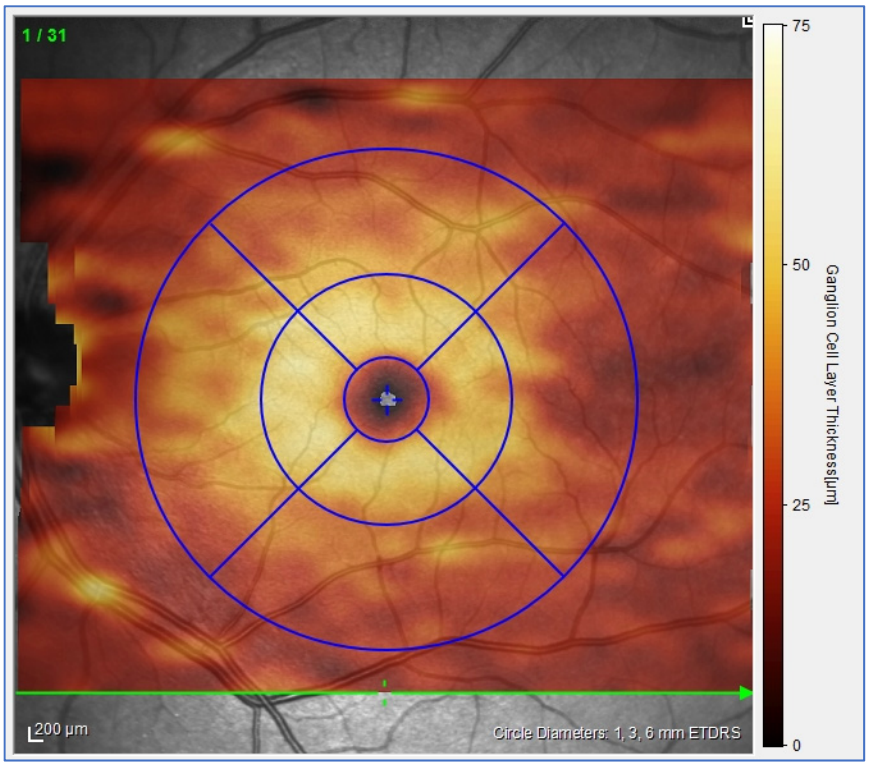

Figure 1.13: OCT volume scan of the macula, segmented to show en face GCL thickness map, demonstrating highest density of RGC cell-bodies in the macula.

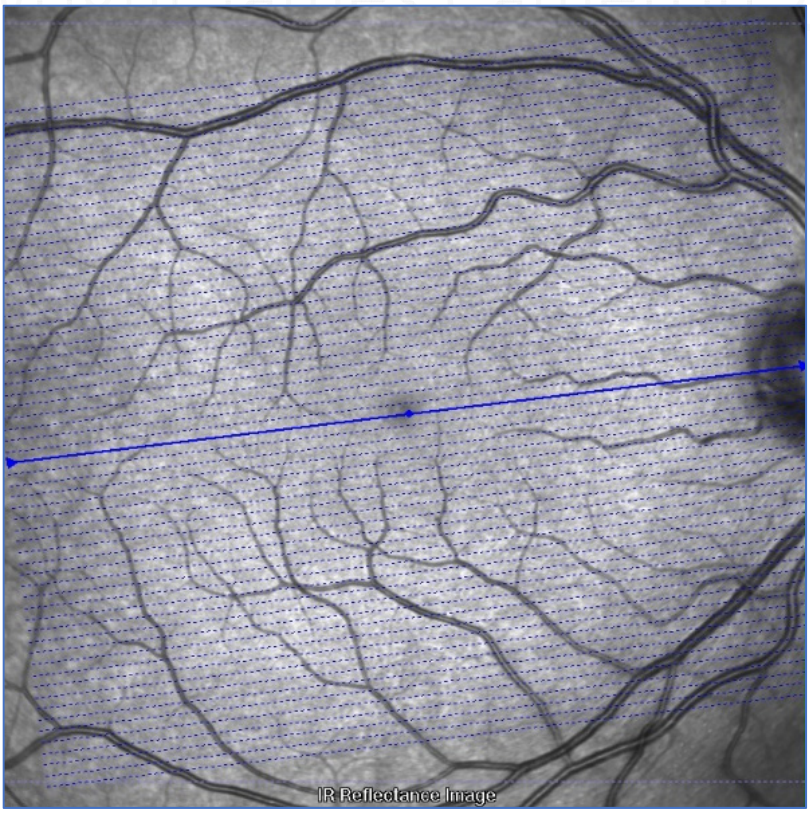

Figure 1.14: Standard macular volume OCT scan pattern, centred over the fovea, for subsequent thickness and volume analysis of the macula including individual layers.

Choroidal vasculature

Choroidal visualisation

The choroid is a vascular layer, supplying oxygen and nutrients to the outer retina, as well as supportive homeostatic mechanisms.[91] Lying deep to the retina, it is less easily visualised with OCT, with the limited tissue penetration of current SD-OCT technology. However, the SPECTRALIS OCT features an additional function within the OCT scan known as enhanced depth imaging (EDI). This scan mode re-focuses the OCT beam for further tissue penetration, and gains greater resolution of the deeper layers - the outer retina and choroid - at the expense of the vitreous and inner retinal surface. (Fig. 1.15)

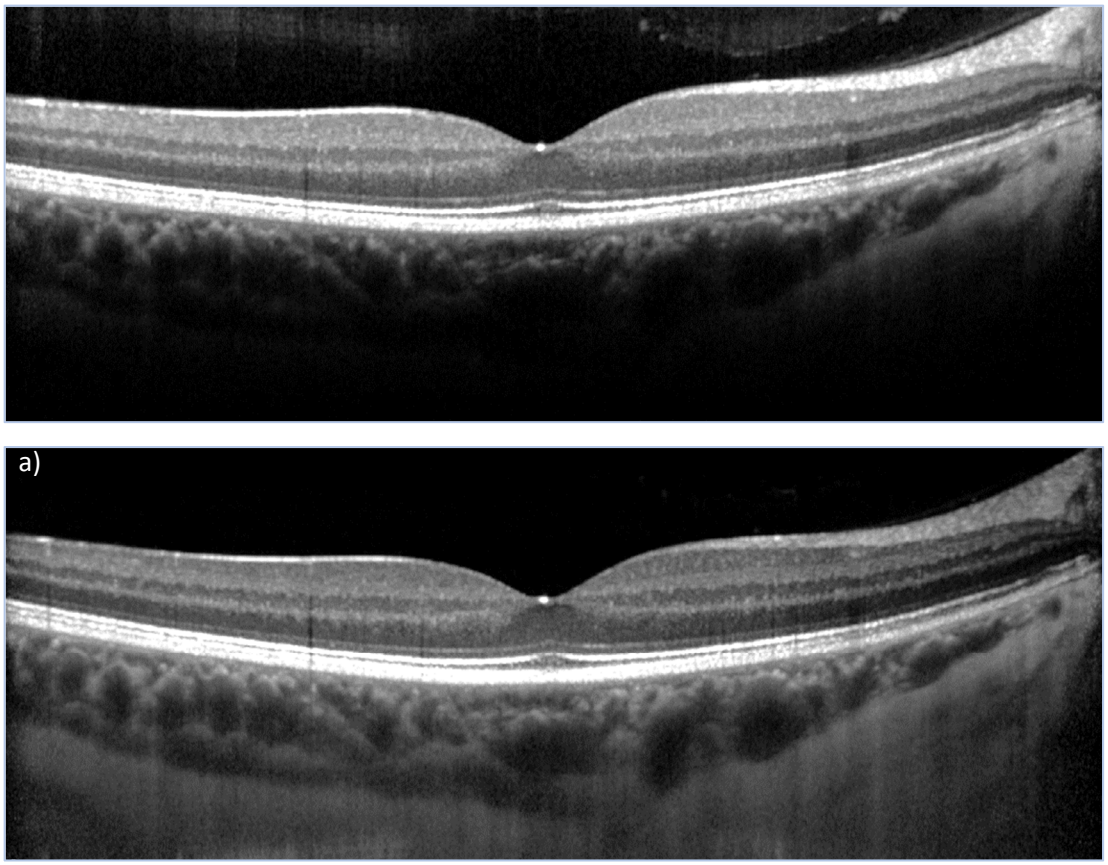

Figure 1.15: Horizontal line OCT scan through the fovea a) without and b) with EDI activated; demonstrating the greatly improved visualisation of the choroid, particularly the choroidal-scleral junction, enabling choroidal thickness measurements.

This greater visualisation of the vascular choroid enables closer examination of this important layer of the eye, and the potential to measure it. There continues to be poor

agreement on the most reliable and precise method for measuring the choroid, whether thickness or volume, or even where to measure it. This is partly due to the variable quality of choroidal imaging, both between machines but also inter-visit repeatability issues. Nevertheless, some authors have called for at least a greater objective understanding of what they are measuring and reporting in studies that are looking at the choroid.[92, 93] Confusion often arises from the appearance of the outer choroid on these images, with a hyper-reflective stromal line and a very thin hypo-reflective space underneath. This hypo-reflective space is the suprachoroidal potential space, and is not always or completely visible in OCT scans. Consequently, an error can be made by measuring to the inner border of the hyper-reflective outer choroidal stroma, incorrectly interpreting it as the sclera. This may still give rise to consistent measures of the choroidal vessel layers, but results may be over-interpreted.

Certainly, it seems sensible and scientific to at least accurately define the outer border of the choroid that you are measuring to, whether intra-luminal, stromal, or actual scleral border. (Fig. 1.16)

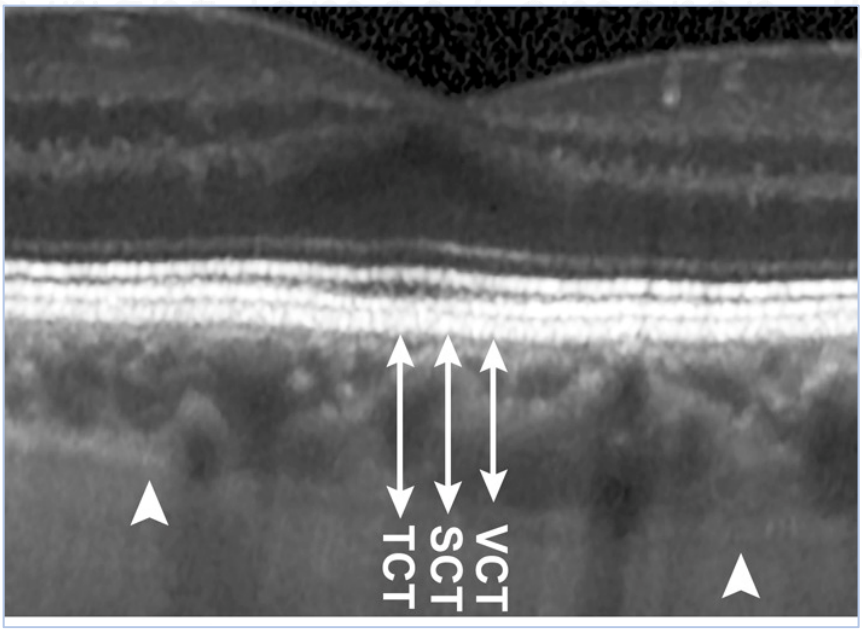

Figure 1.16: Measuring choroidal thickness with three different posterior boundaries: total choroidal thickness (TCT), stromal choroidal thickness (SCT) and vascular choroidal thickness (VCT).
Arrowheads mark the hypo-reflective line of the visible suprachoroidal layer, enabling precise location of the inner scleral border, and used for the TCT measure.

[Image from Vuong et al. Am J Ophthalmology 2016 [92]]

Retinal vessel morphology

The retinal vascular network develops in a way that is optimised for efficient flow and deliver of oxygen and nutrients to the inner neuroretina.[94] Deviations away from this optimal state occur in abnormal micro-environmental conditions, as in disease. The impact of microvascular damage directly, or damage to the adjacent retina releasing vessel-impacting factors that indirectly alter the vasculature, can be seen and measured on fundus images, with quantitative assessment of the vessel morphology.

Over recent years, standardised terminology has arisen for describing the retinal vessels and their morphology, in a way that provides key measures relevant to describing the optimality of the vascular tree, as well ensuring inter-operability between research groups. Vessel diameters, bifurcation geometry, tortuosity and fractal dimension are all methods of measuring distinct characteristics of the retinal vasculature. (Fig. 1.17)

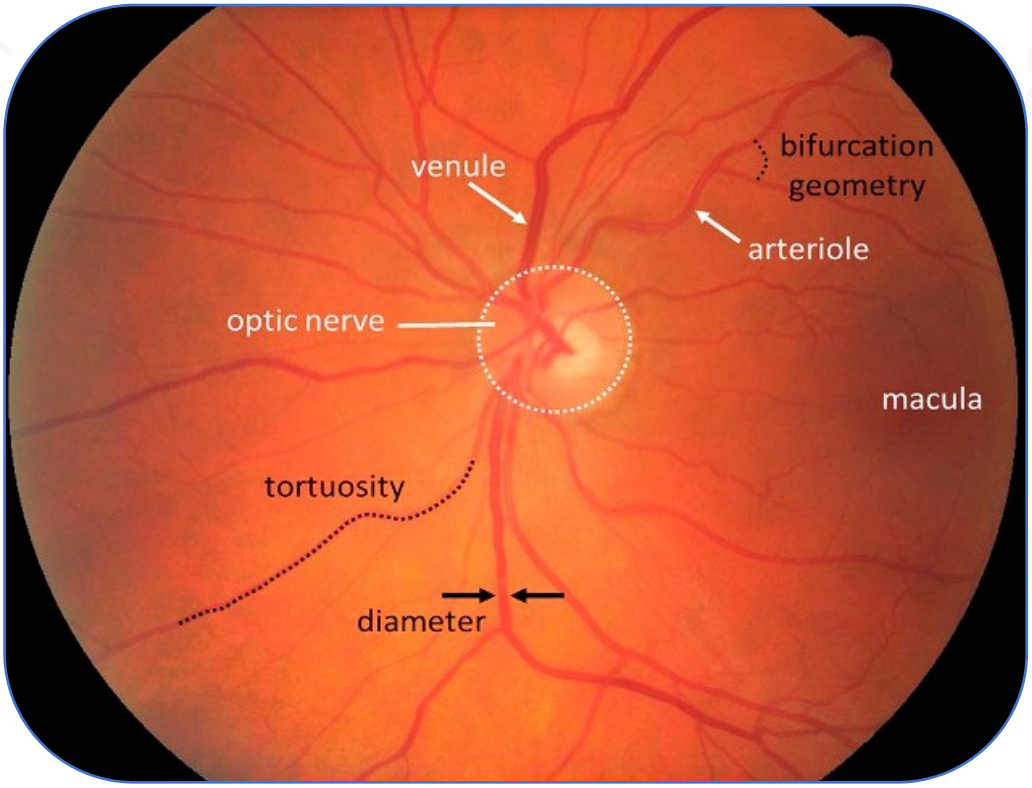

Figure 1.17: Features of interest in a fundus image. The optic nerve head boundary provides a reference point for locating and quantifying other features of interest.

Zones

Defining the regions of the posterior pole in a way that facilitates repeatable measurement of the blood vessels is essential. However, there is no ideal solution to this, with the population variance in ocular size, optical refraction and magnification, and retinal features. Given that the fundal image with maximal vessels visible is one centred on the optic disc, it is reasonable to use the optic disc itself as the reference for location, with the optic disc diameter as the measurement interval for defining concentric zones of the retina around the disc.

There is some population variance in optic disc size, but this is partly a property of the magnification effects of the ocular optics, and the instrument of examination. The true optic nerve head diameter is really only measurable during vitreoretinal surgery, or histologically. Studies have shown this to be a more consistent size between people than fundus photographs would suggest.[95]

Therefore, the utilisation of the optic disc as the reference location and measure has become standard within the retinal image analysis community.[94, 96]

Immediately adjacent to the optic disc, the retinal vessels frequently overlap, bifurcate into temporal and nasal main branches, and are less distinct. Instead the proximal measurement point of vessels is taken as one half a disc diameter from the optic disc margin. The segment of vessel between this point, and a further half disc diameter represents a reasonable segment of proximal vessel for the prime measures of vessel calibre.

Known as 'Zone B', This measurement location on the retina can be more easily visualised as the ring (or annulus) 0.5 - 1 optic disc diameters from the optic disc margin - or alternatively 1 - 1.5 optic disc diameters from the centre of the optic disc. 'Zone C' describes the larger area extending from the optic disc boundary to the ring that is 2 optic disc diameters further away (i.e. a radius of 2.5 optic disc diameters). This region is used for the vessel metrics that rely on longer segments of vessels, e.g. tortuosity and fractal dimension measurement. (Figs. 1.18, 1.19)

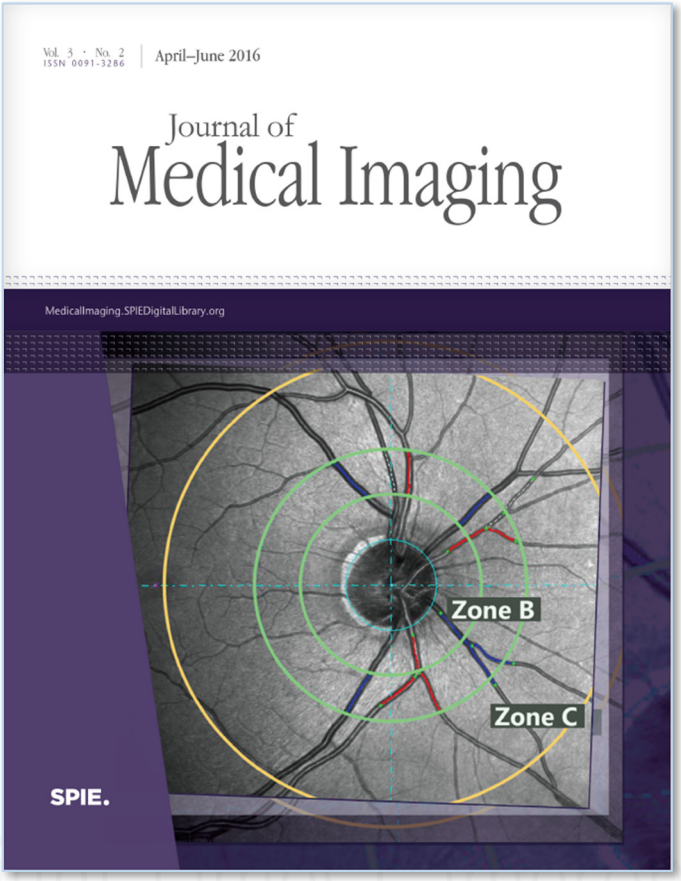

Figure 1.18: Front cover of Journal of Medical Imaging - 3(2) June 2016, featuring Zone map illustration from our published paper on VAMPIRE software modulation.[97]

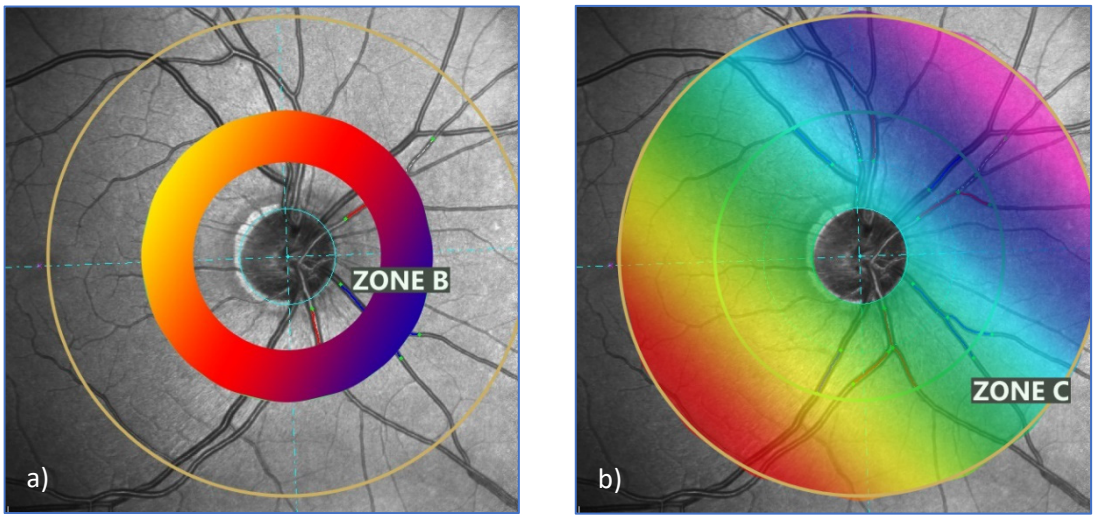

Figure 1.19: Highlighted standard zones of retinal vessels for analysis - a) zone B b) zone C

Vessel calibre (luminal width)

The central retinal arteriolar equivalent (CRAE) and central retinal venular equivalent (CRVE) are summary metrics to essentially describe the average overall calibre of the arteriolar or venular trees, around their thickest areas.

The visible vessel on colour fundus images (or SLO images) actually represents the luminal contents of the vessel. The vessel wall is poorly visible on these images, being very thin, and of low optical density, and therefore relatively transparent when compared to the higher contrast of the vessel contents and the background pigmented contrast of the retina. (Fig. 1.20) Therefore, the measured vessel width from these images structurally represents the internal luminal width of the vessel. The preferred term for this is 'calibre', thus avoiding confusion with the term 'width' which could be misinterpreted as referring to the overall width of a vessel, including the vessel wall.

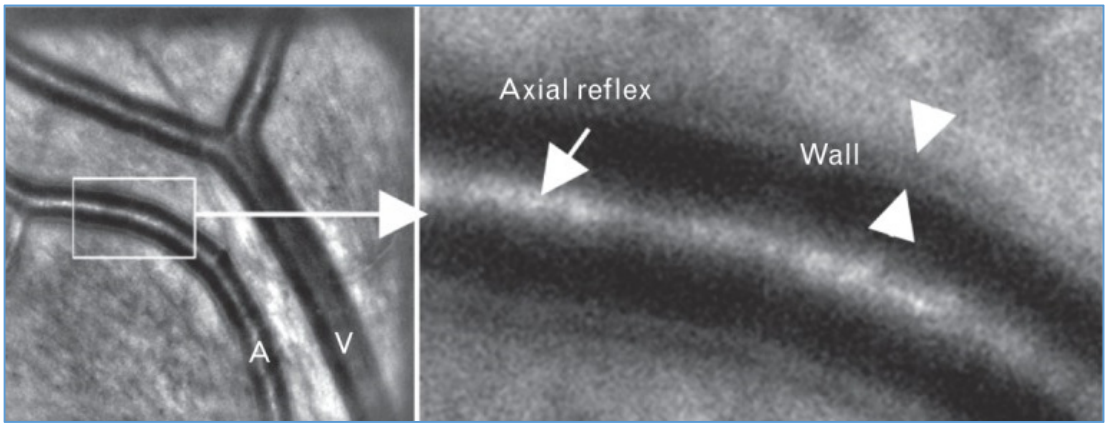

Figure 1.20: High-magnification adaptive optics image of a retinal arteriole, showing the vessel wall; and illustrating the familiar central (axial) reflex in the appearance within the vessel lumen, signifying the higher reflectivity of the central column of blood flow

To calculate the CRAE and CRVE, the six thickest arterioles (and venules) in zone B are identified, and their thickness throughout the segment length measured, and then averaged for that segment. These six calibre measures are then averaged, but with weighting given depending upon the vessel segments' bifurcation geometry - so-called branching coefficients.[98]

The ratio between the two measures, CRAE and CRVE, is known as the arteriovenous ratio (AVR). As a quotient, it is a dimensionless figure, and thus bypasses some of the

potential confounders from optical magnification in measuring vessel calibres. The weakness of AVR is of course that it will fail to detect where pathology results in changes in both CRAE and CRVE. Nevertheless, it is a widely-used measure in ophthalmic studies that seek to correlate vessel calibres with a systemic phenotype.

Tortuosity

Tortuosity measurement is an attempt to quantify the curvature of a wiggly line. In the retina, increasing tortuosity of vessels is a well-established sign of specific pathologies (e.g. the venular tortuosity and dilation associated with a central retinal vein occlusion, a sight-threatening event usually associated with hypertension). It would therefore be advantageous to include some measure of this in the range of vessel metrics available.

Whilst visually identifying a vessel as tortuous is simple, defining mathematically what it is that makes a vessel tortuous, and how to quantify that is more challenging. One method of mathematically calculating tortuosity is to see it as the ratio between the distances a vessel travels between two points, and the shortest distance between those points, as if drawn by a straight line. Alternatively, we can attempt to define the degree of curvature in the vessel path, as a function of its length. Of course, it is not just the curvature of a vessel that represents its tortuosity, but the rate of change of that curvature over the length of that vessel, in a sinusoidal oscillation. In addition, the calibre of the vessel can alter how the same degree of curvature is measured.

Fractal Dimension

Retinal vascular fractal dimension (D_f) is a quantitative measure of the complexity and density of the retinal vessel network, as if projected onto a 2-dimensional plane. It is an attempt to define how optimal the branching pattern of the retinal vascular tree is, but in a mathematical way that includes the density and calibre of the vessels in the calculation.

The concept of fractal dimension is one from pure mathematics, but has been applied to many disciplines, from quantum physics[99] to coastline geography.[100] Fractal geometry is a complex branch of mathematics, dealing with self-similarity of a pattern at all scales of magnification, also known as expanding symmetry. Fractal dimension is an attempt to quantify the *degree* of complexity of a pattern or image, that ultimately becomes a dimensionless value, thus avoiding the confounding of infinite complexity at increasing scale.

A simplification of fractal dimension would be to think of it first as the density, or space-filling of the pattern to be quantified. This gives us our reference values: a straight line has a D_f of 1. A filled-in (2-dimensional) square has a D_f of 2, and finally a complete (3-dimensional) cube has a D_f of 3. Within these reference values, incomplete filling of the shape will result in a D_f in-between the values. For example, a partially-filed in square will have a D_f somewhere between 1 and 2 (e.g. the retinal vasculature falls into this boundary). A solid object that does not completely fill-in the limits of its surrounding cube will have a D_f in between 2 and 3 (e.g. a visual illustration of this is the vegetable broccoli - the typical D_f of broccoli is 2.66). (Fig. 1.21)

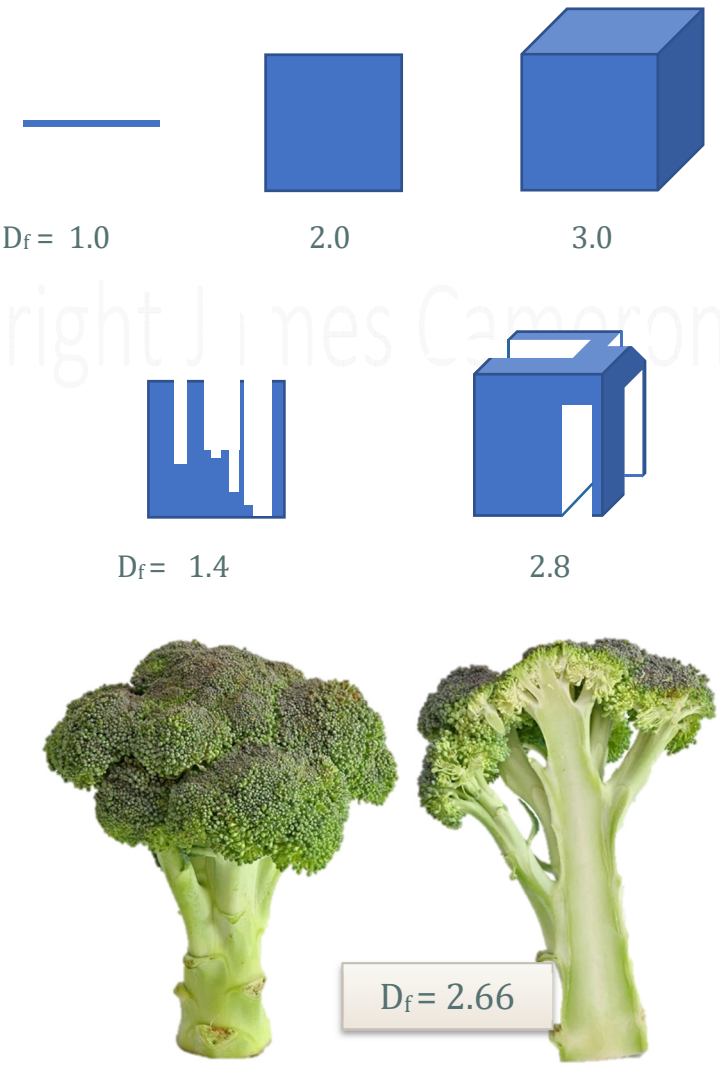

Figure 1.21: Fractal dimension in terms of mathematical dimension density

The retinal vasculature D_f can be calculated automatically from retinal images, via the use of algorithms that incorporate the vessel morphology as well as the vessel metrics of calibre and branching angle. Mono-fractal analysis is the basic method for calculating retinal vascular D_f, providing a single measure that represents the whole network. It assumes homogeny across the vessel tree, and is calculated with box-counting.[101] More sophisticated analysis has more recently been proposed, called multi-fractal analysis.[102] It attempts to overcome the limitation of assuming a single fractal dimension is true across the whole vascular tree by measuring D_f at 1000 random points across the vascular network, and integrating those measures in different ways, with different algorithms proposed: D_0, D_1 and D_2 are commonly referred to as the capacity dimension, the entropy dimension and the correlation dimension, respectively.[103]

The assumption in measuring the retinal vasculature fractal dimension is similar to that given above, for measuring other parameters of vessel morphology. That there is an optimal retinal vascular network density and complexity, which can be quantified by some dimensionless measure of D_f, and that changes in this measure reflect a sub-optimal vascular network, which may be correlated with, a marker of, or a consequence of, systemic vascular disease. The figure often cited for the optimal D_f of the retinal vasculature is 1.7. It is not clear if that has been measured across a high number of healthy eyes, or a mathematical extrapolation of Murray's law for the optimal branching angle of arterioles of 75°. Murray's law states *"The most efficient circulation across a vascular network can be achieved if blood flow is proportional to the cubed power of the vessel's radius"*.[104] Thus the inclusion of vessel calibre as an important component of understanding an optimal vessel network, not merely the number and angle of branches.

Of course, this assumes the absence of ocular disease, for as we know, several ocular diseases (for example, retinal vein occlusion, diabetic retinopathy, posterior uveitis) result in changes to the retinal vasculature, particularly the emergence of new vessels and intra-retinal microvascular abnormalities (IRMA). Even high myopia is known to be associated with reduced D_f.[105]

Mono-fractal calculation of the retinal vasculature has been used and correlated with cognitive dysfunction[106], stroke[107] and cardiovascular disease[108]. All studies finding a lower value of D_f (considered 'sub-optimal' D_f) in association with the disease or dysfunction being studied.

Newer - and more sensitive - multi-fractal techniques have been used and compared with cognitive ageing.[103] It is likely that future studies of physiological associations with retinal vascular D_f will use the superior multi-fractal techniques.

Finally, the software offers reporting of D_f for either all the vessels, just the arteriolar tree or just the venular tree. It is unclear which is the more appropriate - or sensitive - measure to assess the optimality of the retinal vasculature.

Vessel measures in relation to ocular anatomy

The measurement of retinal vessel morphology has become more precise and reliable, with the development of semi-automated software packages (see section below). However, meaningful interpretation, and correlation with systemic disease, requires appreciation of the potential effects of axial length and refractive optics of the eye.

Dimensional parameters such as CRAE and CRVE are inevitably subject to magnification effects, as the retinal image is created via external camera and its size will be affected by axial length, and refractive power of the eye. The Blue Mountains Eye Study and Beaver Dam Eye Study found an association between myopic refraction and reduced retinal fractal dimension and smaller retinal vessel diameters respectively.[105, 109] Longer axial length has been associated with the narrowing of arterioles and venules, increased arteriolar and venular branching coefficients and less tortuous arterioles.[110, 111]

Dimensionless parameters such as arteriole-to-venule ratio (AVR) and bifurcation angles are not affected by axial length or refraction. This makes them more attractive for studies where ocular biometry is not readily available.

Automated software platforms

Several groups worldwide have recognised the importance of retinal vasculature morphology in the context of chronic systemic disease. A few multi-disciplinary teams have developed software packages for the measurement of the vessel metrics described above, such as vessel calibre, branching angles and tortuosity, with interesting findings already published across cardiovascular and neurological domains.

Two of the most well-known and evaluated systems, are VAMPIRE ('Vascular Assessment and Measurement Platform for Images of the Retina' - *Universities of Edinburgh/Dundee*)[112] and SIVA ('Singapore I Vessel Assessment' - *Singapore*).[113]

Both analyse conventional colour digital fundus camera images, and use standardised protocols for reporting vessel measurement, despite implementing different algorithms for the vessel detection and measurement. Comparison studies between the software have not yet been done. (Fig. 1.22)

a)

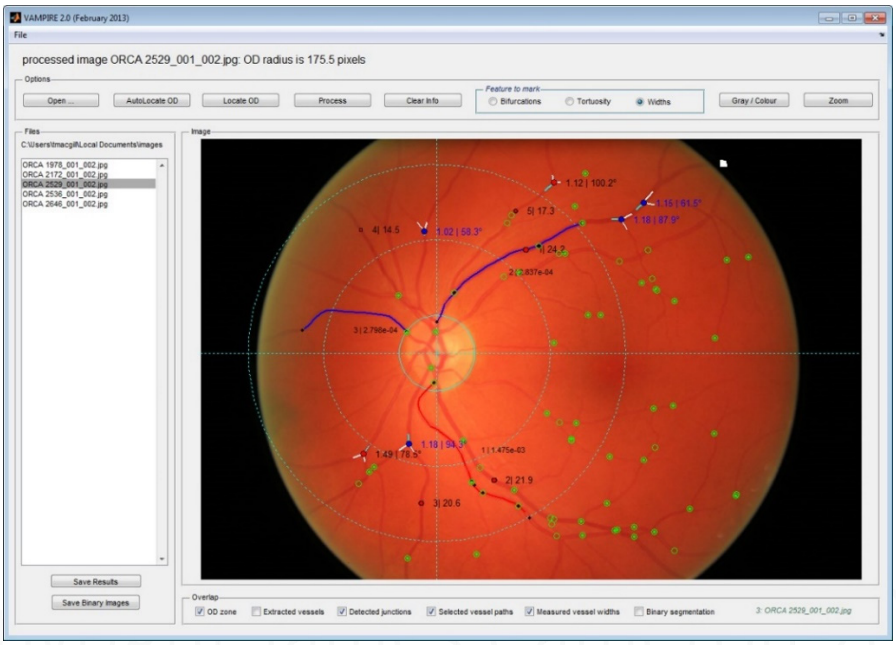

b)

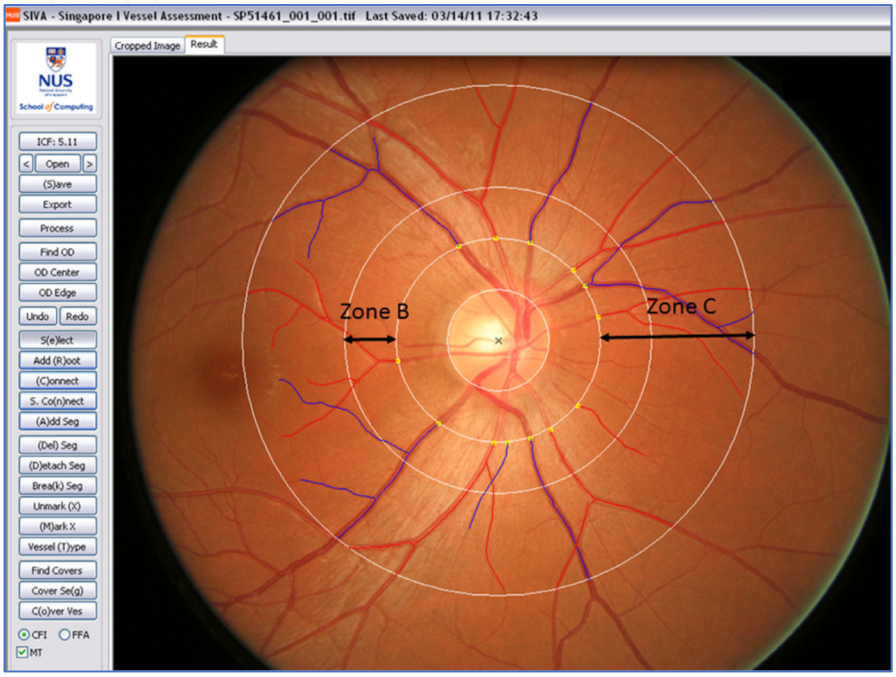

Figure 1.22: Software platforms for retinal vascular analysis - a) VAMPIRE b) SIVA

[Image of SIVA from Cheung et al. Stroke 2013 [114]]

Other software systems in use include: ARIA ('Automated Retinal Image Analyser' - *Queen's University Belfast*)[115], IVAN ('Vasculomatic ala Nicola' - *University of Wisconsin, Madison*)[116], and some project-specific bespoke systems such as 'Retinal Vessel Measurement System', which was used for the quantitative measurement in the Rotterdam Study of retinal vessels in dementia.[117]

I have worked with the VAMPIRE group locally for several years, advising on its development, and using the software for several imaging projects. It was therefore a sensible choice to use it in this research work. *Further information on the history and development of VAMPIRE is provided in Chapter 3.*

Role in systemic disease

Retinal imaging has transformed ophthalmological practice, and is essential in the management of retinal disease. Quantitative retinal image analysis has proliferated in research environments, but has quickly also had a profound clinical impact for many retinal diseases, where there is a need for precise and reproducible measures within the retina to stratify diagnosis and guide new treatments.

There are also systemic diseases with retinal signs that can be imaged and measured, to provide quantitative metrics that may influence management. This includes systemic disease with known ocular manifestations/retinopathy, but also those systemic conditions without a clinical ocular involvement but potentially have subclinical retinal changes.[118]

Diabetes

Diabetic retinopathy screening has been a pathfinder in the large scale use of retinal screening with image analysis, to detect disease at an early stage.[119] Proposals to increase the level of automation in image processing and grading[120] continue to be highlighted, with potential for multi-modal screening programmes - with OCT, and wide-angle retinal imaging - to enhance specificity, and reduce costs.[121] (Fig. 1.23)

Figure 1.23: Proliferative diabetic retinopathy with maculopathy - SLO colour wide-angle image

[Image from MacGillivray et al. Br J Radiology 2014 [118]]

Hypertension

Like diabetes, hypertension is a systemic disease that affects the whole body, including ocular manifestations that can impact upon vision. Modern community screening programmes for hypertension, along with effective treatments, have reduced the incidence of severe hypertensive retinopathy seen in ophthalmic clinics. However, mild retinopathy is often observed, and may influence medical management. (Fig 1.24)

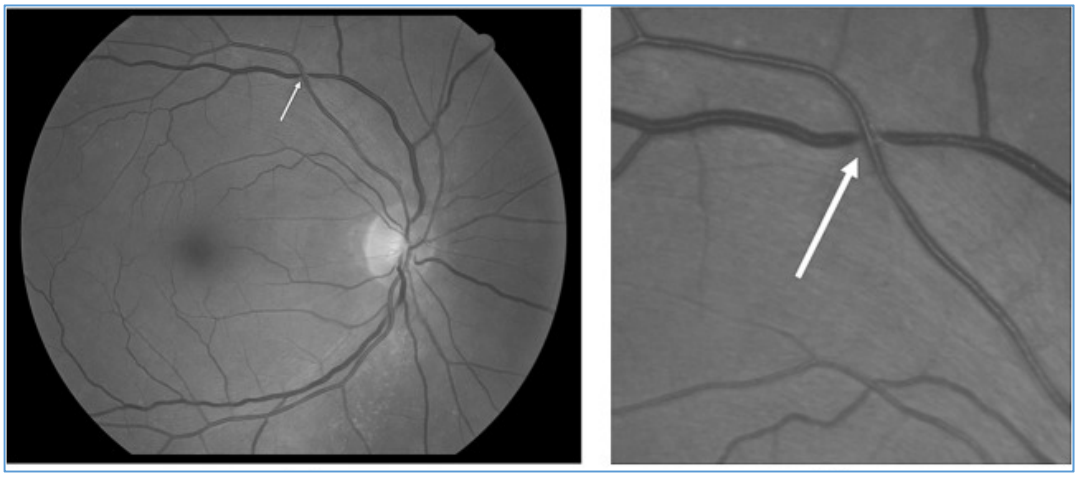

Figure 1.24: Early hypertensive retinopathy with arterio-venous nipping

[Image from MacGillivray et al. Br J Radiology 2014 [118]]

Stroke and cardiovascular disease

Stroke is not classically associated with retinopathy, (though its systemic risk associations, such as hypertension, are). However, with the similarity between retinal and cerebral small blood vessels, several studies have investigated the potential for using retinal imaging in small vessel cerebrovascular disease.[122, 123] Lacunar stroke in particular is known to be a small vessel disease, and is associated with wider retinal venules and a loss of retinal vessel branching complexity.[107, 124]

I have recently worked on a study investigating the potential for retinal imaging to inform on kidney disease.[125] In this pilot study, we found that both retina and choroid were thinner in chronic kidney disease, and that the degree of choroidal thinning was highly correlated with several markers of kidney damage, inflammation and endothelial dysfunction. (Fig. 1.25)

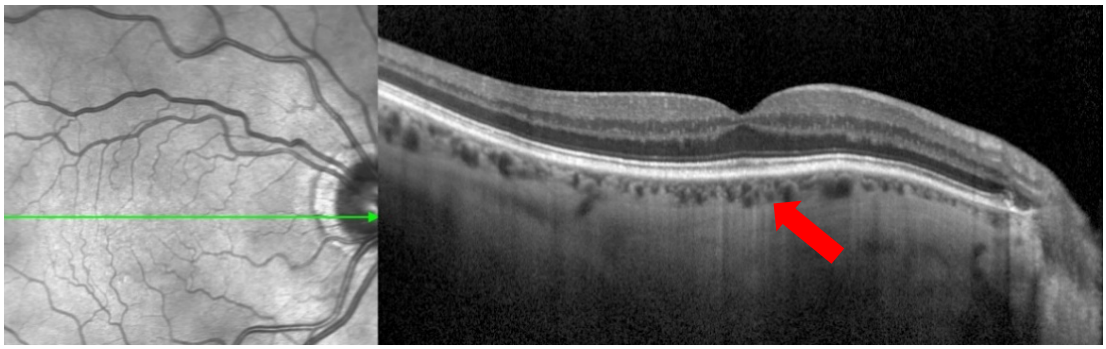

Figure 1.25: Choroidal thinning seen in chronic kidney disease

Biomarker identification

Several large scale longitudinal studies, incorporating retinal imaging along with thorough medical history and follow-up, have been undertaken internationally with the shared aim of improving the prevention, diagnosis and treatment of these and other chronic conditions. (Table 1.2)

The aim has been the identification of biomarkers that will enable systematic patient surveillance and the identification of high-risk patients, as well as surrogate end-points that will accelerate the discovery of new interventions.

Table 1.2: A summary of large-scale longitudinal studies featuring quantitative analysis of retinal imaging (predominantly fundus camera imaging)

Study name	Aims	Participants	Findings
Wisconsin Epidemiologic Study of Diabetic Retinopathy	Establish frequency and incidence of complications associated with diabetes, and to identify contributing risk factors	2366	Good control of blood sugar associated with reduced risk of incidence and progression of DR[126]
Atherosclerosis Risk in Communities	Investigate the causes of atherosclerosis and its clinical outcomes and variation in cardiovascular risk factors	>10,000	Lower AVR predicted 3-year risk of CHD events[127] Retinal microvascular abnormalities were related to current and past blood pressure, and to various markers of inflammation and endothelial dysfunction[128]
Beaver Dam Eye Study	Inform on the prevalence and incidence of common eye diseases causing loss of vision in an ageing population, and examine other ageing problems such as kidney and heart disease	4926	Narrower arterioles and wider retinal venules predicted higher CHD mortality in persons aged 43–69 years[129]
Blue Mountains Eye Study	Assess visual impairment and common eye diseases of a representative older sample, as well as other ageing problems	3654	Thinner arterioles and lower AVR associated with hypertension, after adjustment for age, gender, body mass, smoking[130]
Rotterdam Study	Investigate the prevalence and incidence of and risk factors for chronic diseases in the elderly	7983	Arteriolar narrowing associated with an increased risk of hypertension[131] Wider venules associated with an increased risk of vascular dementia[117] and stroke[132]
Multi-Ethnic Study of Atherosclerosis	Investigate the prevalence, correlates and progression of subclinical CVD and risk factors that predict progression to clinically overt CVD	6814	Retinal arteriolar and venular calibre associated with CVD risk factors - hypertension, diabetes, measures of obesity and dyslipidemia[133] Narrower retinal arterioles in non-diabetic participants associated with increased risk of stroke independent of traditional risk factors[134]
UK Biobank	Creation of a databank, accessible to international researchers, for improving the prevention, diagnosis and treatment of a wide range of long-term conditions and chronic illness	67,716	Central macular thickness positively correlated with older age, female gender, myopia, smoking, body mass and white ethnicity[135] RPE thickness decreases with age, raised IOP and smoking[136]

Abbreviations: DR, diabetic retinopathy; CHD, coronary heart disease; CVD, cardiovascular disease; IOP, intraocular pressure

[Table adapted from MacGillivray et al. Br J Radiology 2014 [118]]

These studies all featured retinal fundus imaging, with retinal vessel analysis, as a potential non-invasive proxy of microvascular health. Latterly, some have included OCT derived measures of macular volume in these tests of association with systemic disease.

The consistency of results, for example the strong association between thinner retinal arterioles - and lower AVR - with hypertension and heart disease, is encouraging and certainly gives power to the potential of using the retinal vessels as a view into the systemic circulation.

OCT measures of the neuroretina and choroid have been far less investigated across such large populations to uncover systemic associations. However, smaller and more targeted studies with neurological disease are revealing some important links and directions for research.[137]

Benefits and challenges

Retinal imaging in relation to systemic disease is clearly an exciting area of research. There are tremendous advantages to using retinal imaging, but also some challenges.

Benefits

- patient-friendly, non-invasive imaging
- rapid image acquisition, seldom requires repeating
- cheap and easy to use devices, with operator-friendly software systems

Challenges

- Variation in equipment and protocols can limit data interoperability
- Presence of co-existent ocular pathology affects interpretation
- Requires experienced eyes to review images to avoid misinterpretation or incorrect data extraction
- Limited population studies so far with OCT imaging means several unanswered questions about range of normality, and influence of individual variation in ocular size/shape/refraction on retinal measures

Embryology of the eye

Development of the eye begins at around 3 weeks of gestation, from a small region of neuroepithelium in the developing forebrain. Two symmetrical optic grooves are formed, which expand, becoming the optic vesicles. As these optic vesicles enlarge further, they contact the overlying non-neural surface ectoderm, which induces vesicle invagination, forming the double-walled optic cup.[138]

The contacted area of surface ectoderm thickens, forming the lens placode. This invaginates and separates from the ectodermal surface, forming the primitive lens vesicle, and becoming enclosed within the optic cup. The surface ectoderm also forms the cornea.

The stalk of the invaginating optic vesicle maintains a fissure for the passage of the developing vasculature (hyaloid vessels) and neurones (optic nerve). It closes at around 8 weeks. Failure of this closure can result in the clinical finding of coloboma - of anterior or posterior eye segment structures.

The neuroretina is formed from the inner layer of the optic cup. (The outer layer of the optic cup forms the retinal pigment epithelium). The neuronal differentiation begins around the 7th week, with full retinal layer formation taking several months.[139] The retinal ganglion cells are apparent early, sending out their axonal processes by the 8th week. Molecular signalling guides these axons in a precise pattern to the lateral geniculate nucleus of the thalamus.[140, 141]

Blood vessels are separately derived from extracellular mesenchyme, which also forms the sclera and vitreous. The retinal blood vessels emerge from the optic disc during the 4th month of development, as continuations of the hyaloid artery - later to become the central retinal artery. Again, molecular signalling guides the vascular patterning through the retina, and this angiogenesis continues until a few months post-partum.[142]

Nerve and vessel tissue, comparing eye and brain

Nerve

The optic nerve is developmentally and genetically an extension of the brain, and histologically same as brain, in contrast to the other cranial nerves which are peripheral nerves.[143] Thus the optic nerve IS brain, and the retinal ganglion cells are properly determined as brain neurones. White matter atrophy within the optic nerve is therefore CNS white matter change.

Therefore, when we observe changes in the RNFL and GCL of the neuroretina, we are observing changes in the brain. Pathological processes affecting brain neuronal tissue will of course have characteristic patterns of location within the brain, and therefore not necessarily be observable in the retina. However, no part of the brain is as accessible and visible in such high detail as the retina, and therefore it is an extremely attractive point of observation and research when considering complex brain disease.

Vessel

Comparing vascular features between the retinal vessels and the brain, reveals an extensive similarity in geometry, topology, and physiology.[144] Metabolic demand of retina and brain tissue is also comparable, and higher than any other tissue or organ.[145]

Multiple studies have demonstrated a strong association between both acute and chronic cerebral vascular diseases, and observable retinal vascular changes. In addition, some measures of retinal vascular morphology have shown to be predictive of cerebral vascular pathology. (Table 1.2)

This homology between the retinal and cerebral vasculature characterises the hypotheses for imaging the retina as a window to the cerebral circulation.

Blood-retinal and blood-brain barrier

Both retinal and cerebral micro-circulations are 'barrier' circulations, with a priority function of maintaining the environment of the adjacent neural tissue. This barrier is both mechanical and metabolic, and importantly dynamic.[122]

Blood-retinal barrier

The blood-retinal barrier (BRB) is essential to the regulation of the retinal micro-environment. Breakdown of the BRB is directly implicated in many retinal diseases such as diabetic retinopathy (DR) and age-related macular degeneration (ARMD).[146]

There are two components of the BRB, corresponding to the dual blood supply to the retina. The inner two-thirds of the retina is supplies by the retinal arterioles, and the outer one-third by the choroidal circulation.

The inner BRB consists of the tight junctions between the endothelial cells of the (non-fenestrated) retinal capillaries.

A secondary (outer) component of the BRB is the retinal pigment epithelium. In addition to acting as a barrier between the retina and the fluid choriocapillaris below, one of the many roles of the RPE is the active transport of any percolating water within the retina, across and into the sub-RPE space which is osmotically linked with the choroid. Maintenance of the tight junctions between the RPE cells protects from fluid ingress from the sub-RPE space, and maintenance of the RPE function keeps the retina dry.[147]

Breakdown of the BRB with fluid accumulation into the retinal extracellular space is clinically observed as macular oedema, and symptomatically produces blurred or distorted vision. More extensive BRB breakdown permits immune cell migration into the retina, which may manifest as retinal inflammation, infiltration or even necrosis.

Blood-brain barrier

The blood-brain barrier is very similar to the (inner) BRB. It is also responsible for maintenance of the adjacent neural tissue environment, with responsibilities for water impermeability and ion gradients, delivery of nutrients, and as a barrier to inflammatory cells and excitotoxic compounds.

Of course, the cerebral circulation is more complex than in the retina, however there are sufficient homologies between the topology and function of the BRB and the BBB for biologically plausible hypotheses to be generated with regards to observing the retinal in BRB breakdown as a surrogate of the BBB in similar states.[144]

Inflammation in MS

Retinal periphlebitis (inflammation of the small retinal venules) is a known clinical finding in some MS patients, with the fundal appearance of white sheathing around the retinal venules.[148] This has been confirmed on fluorescein angiography as venous leakage, secondary to BRB breakdown, and like BBB disruption, the timing is usually unrelated to clinical neurological relapses in MS patients.[149] Not always symptomatic, an early screening study estimated the prevalence of retinal vessel sheathing in MS at around 11.5%, though more recent reports suggest that it may be present at some stage in up to a third of patients.[150] (Fig 1.26)

The white retinal appearance represents granulomatous infiltration of lymphocytes and plasma cells.[151] This is thought to be histologically very similar to the inflammatory white matter foci seen perivenular in the brain[152], and so there is a plausible link between the inflammation seen in the retina and the brain in MS. Given the high prevalence on screening studies compared with the low incidence that present with ophthalmic symptoms, it is likely to be a fluctuating sign, that may be transient in some patients, representing a period of local inflammation, that spontaneously settles.

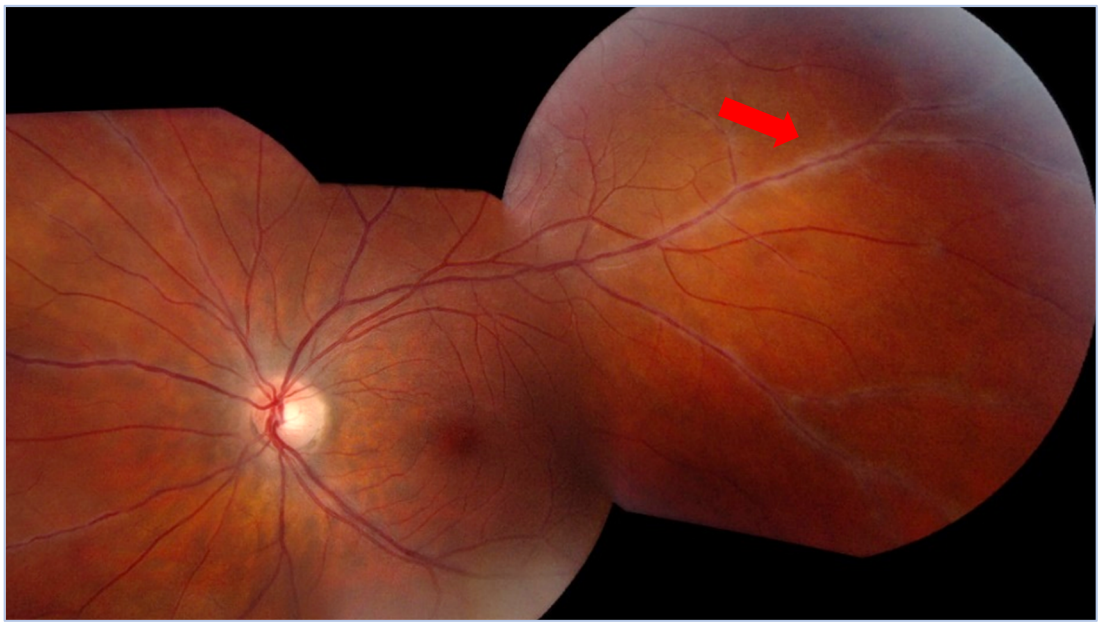

Figure 1.26: White sheathing around the peripheral retinal venules (red arrow), representing retinal periphlebitis

[Image from 'EyeRounds'; accessed at webeye.ophth.uiowa.edu/eyeforum/atlas/pages/Retinal-Periphlebitis/index.htm]

In some patients, however, there is persistent retinal vasculitis, which becomes occlusive vasculitis, with permanent damage to the vessel structure, and can result in ischaemia of the adjacent retina. This can progress to retinal neovascularisation and even tractional or rhegmatogenous retinal detachment.[153, 154] Therefore, the presence of such proliferative retinopathy is an indication for local ocular treatment with peripheral scatter photocoagulation laser treatment, and if uncontrolled, vitrectomy may be required. (Fig 1.27)

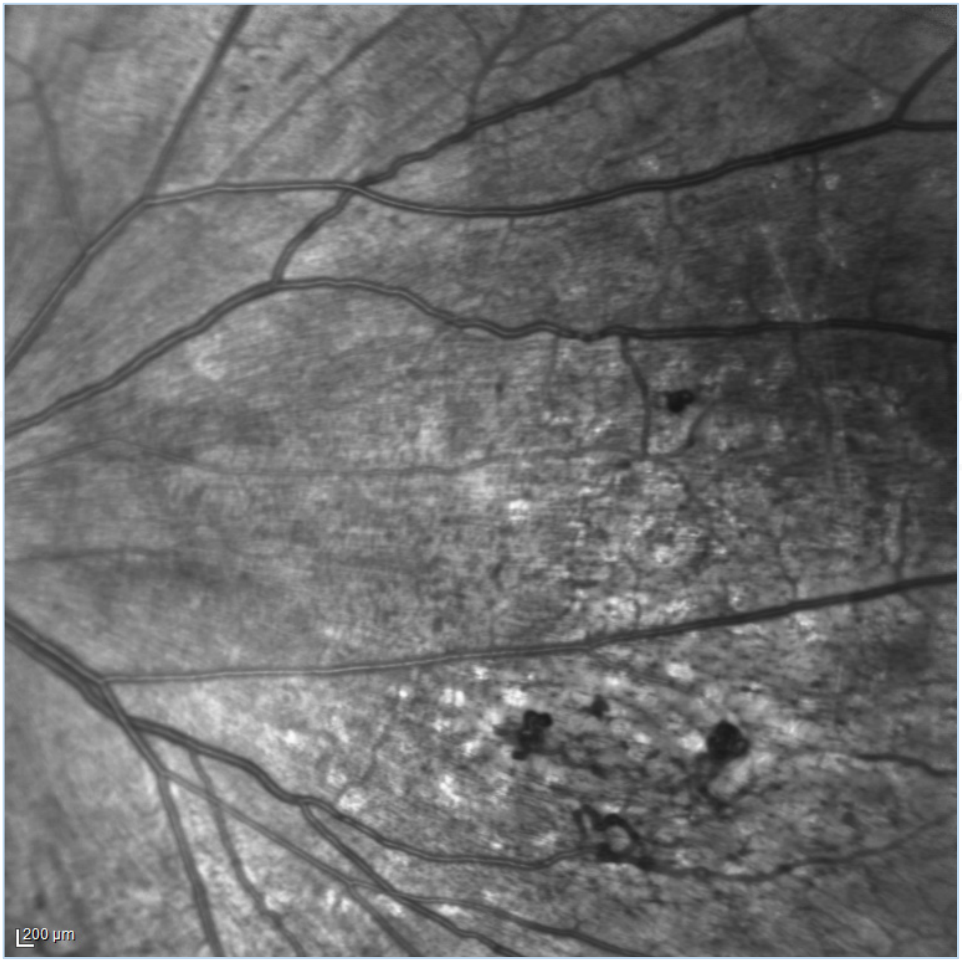

Figure 1.27: Ischaemic proliferative retinopathy in the nasal retina of a 44-year-old female with MS, secondary to vasculitis of unknown duration. The patient was asymptomatic, with the vascular changes identified at a routine optometrist examination. Some photocoagulation laser has already been applied, but the neovascularisation persists, and so more laser treatment is required. The patient remained neurologically clinically stable throughout.

Integration of nerve and vessel data

Retinal nerve and blood vessel tissues cannot be viewed in isolation. Whilst they can be anatomically imaged and measured individually, the two are closely connected in physiology and interdependency, in health and in disease.

Common pathways

With common signalling during precursor differentiation, and similarity between neurogenesis and angiogenesis, there is much to support the integration of nerve and vessel data in the study of the nervous system.[155] In addition, evidence for the neuronal influence on vascular patterning suggests an intriguing hypothesis for the interaction between nerve and vessel in disease states.[156]

With similar nutritional requirements, and susceptibility to inflammatory insult in the presence of systemic disease, there appears merit in observing both structures and considering them in any investigation of systemic biomarkers.

Data integration

How then might we integrate metric data concerning the structure of the neural and vascular tissue in close proximity within the retina? Atrophy, or thinning, of both tissues is a measurable response to damage. However, inflammation can cause leakage, swelling and scarring, all of which can add to tissue volume, hence the paradox sometimes seen with neuroradiological brain imaging.

Therefore, measurements must be taken in context, with a clinical history important before data extraction. For example, neural tissue measurements should be avoided in the immediate period following an inflammatory episode (e.g. optic neuritis) as localised tissue swelling artificially inflates measures of nerve fibre layer thickness.

Ease of interpretation and combination of data could be achieved by dichotomisation of structural measures, allowing a normal/abnormal status for each tissue. However, this loses the value of the tools available to calculate precise measures within the retina.

It is therefore necessary to investigate and determine sensitivity and specificity levels for each proposed biomarker of neural or vessel measure, and then integration into scoring systems becomes possible, in a similar way to cardiovascular risk scoring systems that have been developed to provide a measurable system for correlating risks and determining treatment thresholds.

Aims and hypotheses

Retinal imaging has the potential to provide powerful and precise measures of neuronal and vascular integrity within the neuroretina, that has a biologically plausible link to neurodegenerative disease in the brain.

With a need for new biomarkers of these devastating diseases, the retina offers an opportunity to act as a window into the brain, to observe and measure pathology, at a resolution that has never previously been possible, with any imaging investigation.

Broad questions

- Is retinal imaging clinically useful in the diagnosis and monitoring of multiple sclerosis, dementia and amyotrophic lateral sclerosis?
- Does retinal imaging provide sensitive biomarkers of brain pathology, with sufficient specificity and sensitivity to identify different phenotypes, as well as to characterise disease severity and progression?
- Therefore, does retinal imaging not only aid us in treating patients, but also provide us with more clues about disease pathophysiology?

Biological hypotheses

The core hypothesis is that the retina, as an extension of the brain, contains clues to what is occurring a few centimetres posteriorly, in the core brain.

Both nerve and vessel tissue within the retina are of the same embryological derivation as in the central brain, and increasing evidence supports their similar functional behaviour and response to insult.

Therefore, observation of the retina should provide some clues about pathology within the brain, if we have sufficiently sensitive tools.

Aims of the study

The aims are:

- To explore the current state of the field with regards to retinal imaging derived biomarkers of neurodegenerative disease, both with OCT measures of neuronal integrity, and also vascular morphology assessment.
- To explore retinal imaging methodology in depth, to provide biological foundation for measurement accuracy, and therefore clinical relevance
- To develop new methods of image analysis, by extracting maximum neuroretinal measurements from a single patient imaging episode, to extend value
- To image a large cross-section of patients with different neurological diseases, to enable robust cross-sectional data analysis, and determine best candidate biomarkers
- To advance our knowledge focussing on how we might extend the potential of retina imaging-derived biomarkers to provide more clinical utility, towards a personalised and stratified approach to patient care.

2 LITERATURE REVIEW

OCT in neurological disease - systematic review

Note: Excerpts of this section have been published – in "A Window to Beyond the Orbit: the value of optical coherence tomography in non-ocular disease", JR Cameron & AJ Tatham. Acta Ophthalmologica 2016; 94(6): 533-539. doi: 10.1111/aos.12978

And in "Retinal imaging as a source of biomarkers for diagnosis, characterisation and prognosis of chronic illness or long-term conditions", TJ MacGillivray, E Trucco, JR Cameron, B Dhillon, JG Houston, EJR van Beek.
Br J Radiology 2014; 87: 20130832. doi: 10.1259/bjr.20130832

The evolution of SD-OCT technology, with automated segmentation and measurement of the neuroretina, has transformed ophthalmic research, and extended the potential utility of retinal imaging in ophthalmic disease research and understanding.[157]

In addition, OCT imaging of the eye is now being increasingly explored as a possible tool for identifying ocular biomarkers of predominantly non-ophthalmic diseases, ranging from multiple sclerosis to cardiovascular disease. This potential value for OCT imaging informing on neurological or vascular disease beyond the orbit is an area of research in its early stages, but one of great interest, not least because of the low impact of retinal imaging in terms of cost and patient acceptability.

The recognition of the neuroretina as an extension of the brain white matter creates a highly plausible biological hypothesis that changes in the brain may be reflected in the neuroretina, where they can be measured at far greater resolution and precision than any existing brain imaging modality.

Literature review timing

In this literature review, I set out the scope and evidence thus far for the use of OCT in informing on neurological disease. This search and review was carried out at the beginning of my PhD research, to provide an overview of the field, and highlight unanswered questions that would be appropriate for my work. However, I continued to update this search throughout my PhD, as this is a rapidly developing field, and in 2016

published a summary review of the field.[137] This time-point is where I place the published work for critical review.

Methods

A PubMed and Medline database search was performed on 20 September 2015 using the following search terms: ((((((((((“optical coherence tomography”[Title/Abstract]) NOT ("Eye Diseases"[Mesh])) AND English[Language]) NOT Review[Publication Type]) NOT Comment[Publication Type]) NOT animals[MeSH Terms]) NOT mice[MeSH Terms])))) AND ((eye OR retina OR macula OR "retinal nerve fibre layer")).

This search yielded 2,059 results. Although searching with Medical Subject headings (MeSH terms) may exclude newer citations and articles that do not yet include MeSH subject terms, I avoided this problem by excluding rather than including articles based on MeSH terms. Therefore, a manuscript describing an animal study without a MeSH term for animal would not have been excluded at this stage.

Article titles were then manually reviewed and those relating primarily to ocular diseases (such as glaucoma or age-related macular degeneration) or studies in healthy subjects were excluded. Studies relating to the use of OCT for non-ocular imaging or anterior segment imaging were also excluded. I also purposefully excluded animal studies, letters, comments, review articles and articles not published in English. I also excluded articles describing OCT in systemic diseases with well know ocular manifestations such as hypertension, diabetes and albinism.

References of the articles retrieved from the above search were also manually scanned to identify additional studies.

Results

A flow diagram of the manuscript selection is shown below (Fig. 2.1) along with a table of the diseases with studies remaining after the initial search, and prior to full-text eligibility review, demonstrating the range of diseases of research interest. (Table 2.1)

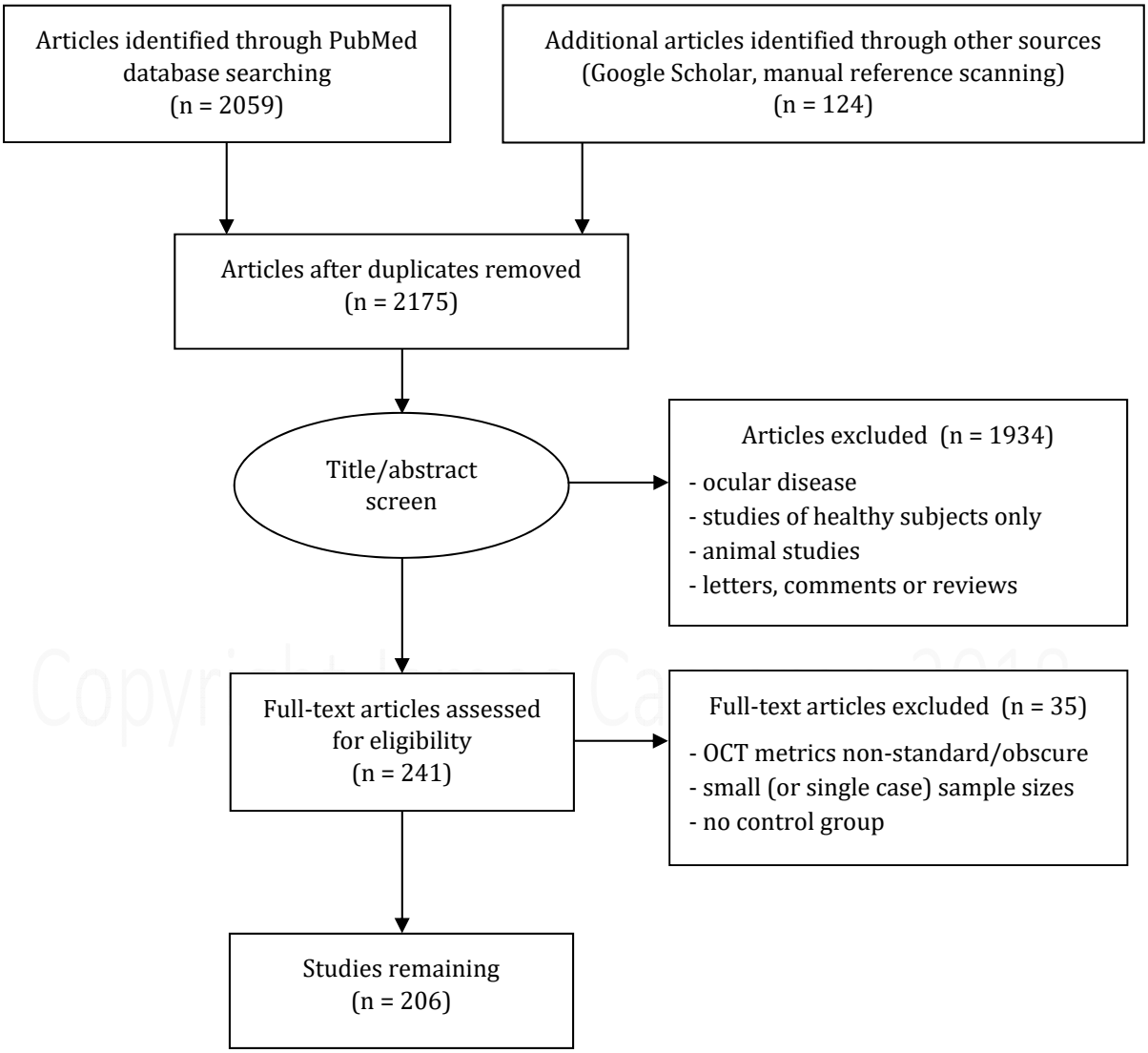

Figure 2.1: OCT in neurological disease: Flow diagram of manuscript selection

Table 2.1: Summary of papers reporting OCT studies in non-ocular diseases from initial PubMed search, prior to full-text eligibility screening.

	Case Report	Case-control / Cohort-study	Random allocation	Meta-analysis
Multiple sclerosis	6	132	0	0
Neuromyelitis Optica	3	18	0	0
Dementia	0	12	0	3
Parkinson's Disease	2	27	0	1
Multiple System Atrophy	0	5	0	0
Motor Neurone Disease	0	2	0	0
Autism	0	1	0	0
Traumatic brain injury	1	3	0	0
Chiasmal compression	2	6	0	0
Optic pathway glioma	0	2	0	0
Schizophrenia	0	2	0	0
Neurosarcoid	0	1	0	0
Stroke	0	3	0	0
Migraine	0	6	0	1
Cluster headache	0	1	0	0
Systemic lupus erythematosus	0	1	0	0

It is clear from this search that the most work on OCT in neurological disease has been done with multiple sclerosis. Indeed, it is this work that was the stimulus for my research project.

A moderate presence of papers on dementia and Parkinson's disease shows how the field is widening, and the spread of small numbers of papers on diseases as diverse as schizophrenia and migraine demonstrate the creative interest this topic of retinal imaging in relation to neurological disease is having.

Discussion

Perhaps more notable are the absences from this list. Within the dementia category, the focus is almost exclusively Alzheimer's Disease (and mild cognitive impairment). There were no papers on other dementia subtypes/syndromes, for example frontotemporal dementia, or primary progressive aphasia. And even within the AD group, the populations studied were elderly, with no studies looking at the early-onset of dementia.

It was therefore straightforward to identify those groups of potential interest and match them with the local expertise and patient groups potentially available to me for research. Clearly as the leading focus of published work, multiple sclerosis must be included - it clearly warrants further and deeper review, to identify the progress in the field, potential unanswered questions, as well as identifying best practice in the field for application to other diseases.

Early-onset dementia, including non-AD diagnoses, is certainly an unmet need. And finally, motor neurone disease, or ALS, is an interesting choice for research, as a disease not thought to have any ocular manifestations, and with only 2 published papers at the time of this review.

OCT for diagnosis

It is now over a decade since the first proposal for OCT to have a role in the assessment of multiple sclerosis, by examining the nerve fibre layer - the anterior portion of the retinal ganglion cell. Conceptually, this was a reasonable hypothesis, given the frequency with which MS affects the anterior visual pathway, often early in the disease.

The hope was that it could document the severity of optic neuritis episodes, as a surrogate marker of disease. However, it quickly proved to be more useful, and could reflect the disease status more globally.

The first paper to investigate OCT as a potentially useful biomarker in MS was published in 2006, by a group in Philadelphia.[158] They used OCT to measure RNFL thickness in MS eyes with and without a history of optic neuritis (ON), as well as in disease-free control eyes. They found not only reduced RNFL thickness in MS eyes with a history of ON, but also in those without any history of ON, although not to the same degree of reduction. They also measured low-contrast visual acuity in the participants, and found correlation between RNFL thinning and reduced vision (one line decrease in visual acuity for every 4μm of RNFL thinning). However, this was calculated as a cross-sectional average across all patients, and therefore does not imply an individual's gradient of visual decline; which we also know is non-linear.

The same group (now in conjunction with Baltimore) followed this up quickly with another paper subdividing the analysis between MS clinical subtypes.[159] They reported RNFL thinning in all MS subtypes (RRMS, PPMS, SPMS), and all with or without a history of ON. The greatest loss of RNFL was seen in SPMS, and in history of ON.

In contrast, a UK study from 2007 reported RNFL thinning (and reduced macular volume) in SPMS, but not in PPMS in the absence of ON history.[160]

Reproducibility

However, it must be emphasised that at this stage, these studies were using the lower resolution time-domain OCT systems (TD-OCT), resulting in wide confidence intervals, despite statistical significance. In addition, there were sources of bias in the studies, which the authors acknowledged - recall bias and ambiguity regarding episodes of ON

as opposed to Uhthoff's phenomenon - and also the lack of protocol in their recruitment and imaging methodologies. They subsequently improved upon the latter, with a study in 2008 to determine the reproducibility of OCT measurement of RNFL thickness by trained technicians in their MS centre.[161] Their refined methods showed excellent interrater, intrarater and intervisit agreement, boosting the validity of their reported results.

A systematic review and meta-analysis published by A Petzold *et al.* in 2010 demonstrated a consistent finding of RNFL thinning in MS eyes with or without a history of ON.[162]

At the same time, development was progressing with high resolution spectral-domain OCT (SD-OCT). Within a few years of its release, a new surge of publications appeared, as teams saw the potential with the higher resolution and speed/accuracy/quality of image capture. The Philadelphia/Baltimore team carried out their reproducibility study once again, but this time with the Cirrus SD-OCT.[163] The popular Heidelberg SPECTRALIS 'HRA+OCT' SD-OCT machine was also released at this time, and studies using it confirmed RNFL thinning compared with controls[164] and characteristic variations within the MS sub-types.[165]

It should be remembered that retinal measurements from different machines, and between TD-OCT and SD-OCT, are not comparable or interchangeable.[166] This is important for large multi-centre studies, or longitudinal studies.

Diagnostic discrimination

Surprisingly little has emerged on the ability of OCT to discriminate between neurological diseases. The emerging phenotypic pattern in MS of predominantly temporal RNFL loss invites such investigation.

One study attempted to generate a linear discriminant function for RNFL in MS, yielding an area under the ROC curve (AUC)=0.834.[167] What is interesting about their final function is that despite weighting thickness measurements from four regions of the pRNFL, the resulting AUC did not improve over just using the temporal quadrant alone, though they were able to achieve higher sensitivity.

The natural first comparator with MS is the near relation Devic's disease - or neuromyelitis optica (NMO). There have been several studies demonstrating the RNFL thinning in patients with NMO, the earliest from 2008[168] and more recent work with

SD-OCT examining the macular GCL as well as the RNFL.[169] A couple of studies have directly compared the findings in MS with NMO, after an ON event, finding that the RNFL loss after an ON event is greater in NMO than in MS.[170] In addition, there appears to be more global loss of the peripapillary RNFL, compared with the selective temporal loss in MS, and an increased incidence of microcystic macular oedema.[171]

Structure/function correlations may be higher in NMO, with one study showing a better correlation between RNFL thinning and impact on the patient's visual field, in NMO, compared with MS.[172]

Refining OCT methods and measures

Larger cross-sectional studies in 2012-2014 also identified reduction in total macular volume (MV) as a significant finding in MS.[165, 173, 174] This provides more evidence for the importance of temporal RGCs in this disease.

The importance of rigor and expertise in OCT imaging and processing is often ignored by study groups, but fortunately some authors in the field of neurodegeneration research acknowledge the value of clear and robust methodology.[175]

OCT correlations with brain imaging

From an early stage, researchers recognised the need to compare the OCT findings of RNFL thinning with the best existing measures of neuronal loss, which means MRI-brain measures of atrophy.

Again, the group from Philadelphia/Baltimore (led by L Balcer and P Calabresi) who continue to be amongst the world leaders in the field, were the first to measure this. Their paper in 2007 imaged 40 MS patients, and showed correlation of RNFL thickness with MRI-measured brain parenchymal fraction (BPF), using linear regression modelling.[176]

Further studies from other groups confirmed this finding, with additional associations found between RNFL thickness and normalised whole brain volume, and T2-lesion volume.[177-179]

With SD-OCT available, their findings became more robust, with increasing evidence of retinal measures reflecting global CNS pathology.[180]

Some studies have examined the relationship between RNFL measures and other neuroimaging modalities such as diffusion tensor imaging (DTI).[181, 182]

Perhaps the most significant of studies published are the pair of papers from the Philadelphia/Baltimore group, published in 2015.[183, 184] They report findings from a 4-year prospective study of over 100 patients of all MS subtypes, who have had regular OCT and MRI imaging (with multiple sequences and analyses), as well as full clinical assessments. Cross-sectional multivariate analysis demonstrated strengths of OCT imaging when compared with spinal cord imaging[184], and the 4-year prospective analysis has fairly established OCT as a valid and reliable tool for monitoring MS disease progression, and as an outcome measure in clinical trials.[183]

OCT for prognosis

Correlation with MRI indices and disease phenotype are important first steps in understanding neuroretinal biomarker candidates in MS. The next stage is to investigate their role in the visible manifestations of the disease, with physical disability status, and prognosis.

The first paper to suggest that OCT measures of RNFL thickness could have prognostic value was in 2007, by a group in Pamplona, Spain.[185] Their 2-year prospective study involved neurological and ophthalmological assessments every 3 months. They found that baseline temporal quadrant RNFL atrophy was associated with new relapses and changes in the Expanded Disability Status Scale (EDSS) by the end of the study.

Other studies have since also shown temporal quadrant atrophy associated with physical disability.[186] Though direct correlations with EDSS are modest at best, even in treatment-naïve MS patient populations.[187]

One interesting study from Calgary, Canada, followed up 50 consecutive patients with a single ON event, to determine whether RNFL measurements were predictive of conversion to clinically definite MS.[188] They found 21 patients (42%) developed MS, with a mean conversion time of 27 months. These patients had more RNFL loss by the second year, but had also had more recurrent ON events, compared with those who had not converted to definite MS. There was no difference between the baseline measurements that would have been predictive.

To determine the natural history of the RNFL changes, a collaborative study between many of the published authors on this topic appeared in 2010, following 299 patients with MS, with OCT and low contrast visual acuity.[189] They found that eyes with visual loss showed more RNFL thinning compared to eyes with stable vision, and that in general, RNFL thinning increased over time, with or without prior history of ON.

The first study of progression using SD-OCT was published in 2011, from Vienna.[190] They followed 37 patients with MS, without a recent history of optic neuritis. Whilst their initial scans showed a broad range of RNFL thickness patterns, there was no significant difference between baseline and 2-year follow-up.

A Spanish group followed 34 MS patients after an episode of optic neuritis, and compared their affected and un-affected eyes.[191] Whilst they unsurprisingly found RNFL thinning in the eye affected by ON, the background progressive loss was similar between the two eyes, suggesting that whilst ON gives a single dramatic kick, the chronic degeneration continues in the background, secondary to the disease. The same group published further results on a larger study population, this time showing that patients with MS relapses showed a greater reduction of RNFL thickness, compared with non-relapsing cases.[192] This Spanish group (led by E Garcia-Martin) have joined the world leaders in the field, and have continued to lead on important studies of OCT for monitoring MS, as well as other neurological conditions such as dementia.

A longitudinal study from K Galetta *et al.* agreed with this model of a constant background rate of RNFL thinning, even in patients judged to have 'benign MS'.[193]

Clinically isolated syndrome (CIS) progresses to MS in around 45% of individuals. Whilst MRI has been used to predict the risk of progression, clinical trials of treatments to delay a second clinical event/definite MS would benefit from additional markers of risk of progression.

A Spanish cross-sectional study prospectively followed a small group of such individuals.[194] 13 out of 24 patients had decreased RNFL thickness in at least one quadrant at presentation; and this finding had a sensitivity of 75% and specificity of 56% for predicting progression to MS. They report these findings positively, however given the small numbers and low predicative probability, more evidence is needed.

OCT in clinical trials

The accumulating evidence for RNFL measurement as a marker of disease status and progression have given it weight for use as an outcome measure in clinical trials of new treatments. The ease of patient participation, with it being a rapid and non-invasive test, make it ideal for trials where test burden is an important consideration for patients and their on-going compliance with a study.

There are challenges to using OCT in MS treatment trials. Some neurology sites may be unfamiliar with the technology, and the possibility of operator error or variability must be considered. In addition, several different OCT machines are available, and results are not interoperable or equivalent.[195] Many large, well-funded studies make use of 'reading centres' to handle the quality assurance, processing, interpretation, reporting and storage of images.

A 3-year study from Spain published at the end of 2012 followed-up 94 MS patients, and 50 healthy controls, for 3 years, measuring multiple ophthalmic items, including OCT.[196] Around half of the MS patients were receiving treatment - with beta interferon 1b, beta interferon 1a or glatiramer. Not only did the MS group show RNFL thinning, but untreated MS patients showed more degeneration in the mean and superior RNFL thicknesses, than the treated. There was no difference between the treatments.

In the UK, I have been involved with an important trial of repurposing treatments for secondary progressive MS (MS-SMART), where we are using OCT measures of axonal loss as a secondary outcome measure.[197] OCT is carried out at baseline and after 2 years of treatment (double-blinded) with the aim of observing a change in the gradient of decline in axonal integrity being associated with any useful treatment.

Below the nerve fibre layer

High resolution spectral-domain OCT has transformed ophthalmological practice, giving us access to imaging of the retinal architecture in greater detail than ever before, allowing us to distinguish, and measure, individual retinal layers.

Much of the work described thus far has involved measuring the RNFL - the axons of the ganglion cells, that run across the inner retina, to the optic nerve, and onwards. But with new and improved OCT images, we now have an opportunity to look at the

immediate adjacent layer, the ganglion cell layer (GCL), which consists of the main body of the ganglion cell or neurone.

The Philadelphia/Baltimore group used the SPECTRALIS SD-OCT to measure the GCL in MS eyes, versus controls.[198] They found similar results to RNFL measuring, with GCL thinning in MS eyes, particularly those with a history of ON. This was consistent with their work on post-mortem histological evidence of GCL thinning, in all MS sub-types.[199] They speculate as to what the role and timing of neuronal vs axonal loss in MS eyes may be. Caution should be noted with this study, however, as the GCL layer was marked and measured manually, rather than automated segmentation and analysis as per the RNFL analysis.

In 2012, they improved their technique by using software algorithms originally designed for glaucoma assessment to measure the retinal layers - GCL+IPL, ONL+PRL, OPL+INL - finding that GCL+IPL thinning was most significantly correlated with visual function.[200]

Later, the Baltimore group used a prototype software algorithm for the Cirrus SD-OCT machine that was designed for these studies in MS, to investigate GCL pathology after optic neuritis, in MS patients. It featured automated layer segmentation for the first time, and indeed found GCL thinning after ON.[201] Using this system, they also found accelerated GCL+IPL thinning in patients with clinical and/or radiological signs of (non-ocular) disease activity.[202]

A German study using the SPECTRALIS SD-OCT and new incorporated software to measure different retinal layers, found thinning in all MS subgroups - both peripapillary RNFL and GCL+IPL layer. They found INL thinning only in PPMS.[203]

Interestingly, as OCT machine software has improved, with more reproducibility in the automated retinal layer segmentation programs, we have seen more agreement between different OCT machines.[204] However, the current guidance on the lack of equivalency and interoperability between machines stands.

Recent work to link retinal measures and current pathology understanding

The onset of RGC involvement in MS-related axonopathy is unclear. The working hypothesis of RGC axonal loss as a retrograde degeneration in conjunction with brain white matter disease insufficiently explains the OCT changes we observe in patients with different disease trajectories.

No study has attempted to determine the point of onset of RGC involvement. A recent study of CIS patients without ON history found significant GCL volume reduction, even at this early stage, and before significant RNFL thinning could be detected.[205] This may suggest either the greater sensitivity in measuring the GCL, or a new theory in the timeline of GCL involvement in MS. Both possibilities are intriguing.

Retinal vessels in MS

There is a distinct lack of publications on retinal vessel characteristics in neurodegenerative disease. Some early work in dementia is emerging, from retrospective analysis of large fundus camera image datasets. However, little prospective hypothesis-driven work exists.

The potential for retinal vessel morphology to inform on diseases such as MS is speculative, but plausible, given our developing understanding of the inflammatory influence - and perhaps initiator - on the disease.

My initial literature search focussed on neuroretinal markers. I therefore performed additional searches to identify any studies of retinal vessels in MS, and found just two.

Retinal vasculature

The two papers found are both from a group in Basel, Switzerland, and were published in the German language journal 'Klinische Monatsblätter für Augenheilkunde', in 2009.[206, 207] English abstracts are available, and describe two studies of the retinal vasculature in patients with MS.

The first study measured choroid-to-retina pulse delay with a 'Retinal Vessel Analyzer' as a surrogate marker of retinal vessel rigidity, and found it reduced in MS patients, with or without a history of optic neuritis. They concluded that patients with MS have increased rigidity of the retinal vessels.[206]

The second study used the same tool to measure retinal vessel widths, finding thinner arterioles and thicker venules in MS eyes, than in controls.[207] This finding certainly warrants further investigation.

Choroidal vasculature

No studies investigating choroidal thickness in MS were found.

Dementia

OCT in Alzheimer's disease

Following the publication of several positive studies in MS, it became clear that OCT-derived measures of RGC axonal loss had the potential to be a useful marker of disease burden in neurodegeneration. The high prevalence of dementia, and Alzheimer's disease particularly, made this an attractive next disease to study.

Earlier work from a Californian group on post-mortem tissue from patients with AD had demonstrated optic nerve involvement in AD, and specifically RGC axonal loss.[208] The same group further investigated this and later characterised this RGC atrophy as "vacuolated" cytoplasmic appearance, and no abnormal protein acculumulation.[209]

The significance of this finding became relevant with the emergence of OCT technology, enabling quantification of RGC axonal loss in patients. The first study of OCT in AD was published in 2001.[210] Whilst a small study (17 patients) and using early generation of OCT hardware and software, they were able to demonstrate RNFL thinning.

There are weaknesses in their study, such as the low level of cognitive characterisation of the patients, with their inclusion criteria also allowing mild cognitive impairment, and their OCT imaging protocol which used 3 non-consecutive scans, and averaged the results. They do not report on any quality assurance, processing or failed/excluded images.

A recurring weakness in several of the studies published since on OCT in AD is this challenge of establishing a well characterised patient group for study, and also a standardised and quality-assured OCT imaging protocol.

As a result, the 20 or so published studies on OCT in AD to date vary greatly in their methodology, and also in their findings.

I therefore wished to carry out a more detailed systematic review of OCT in dementia, with a meta-analysis of RNFL thickness from these studies.

Meta-analysis of OCT in Alzheimer's disease and MCI

Note: Excerpts of this section have been published – in "A systematic review and meta-analysis of retinal nerve fiber layer change in dementia, using optical coherence tomography", KL Thomson, JM Yeo, B Waddell, JR Cameron & S Pal. Alzheimers Dement (Amst) 2015; 1(2): 136-143.

Thanks are due to:
Kelsey Thomson – student, performed the initial library systematic search
Jing Yeo – statistician, performed the meta-analysis and produced the Forest plots

The identification of retinal thinning in association with Alzheimer's disease (AD) was first reported in 2001, using an early OCT device.[210] Since then, several studies have reported thinning of the neuroretina, and specifically the RNFL, in patients with AD[211-219], and in mild cognitive impairment (MCI).[216-218] The principal hypothesis is that following white matter atrophy in the brain of patients with AD, retrograde degeneration of the retinal ganglion cell (RGC) occurs.[216]

With a small number of published papers on the subject, and each with a small number of patients, it was therefore appropriate to perform a systematic review and meta-analysis to investigate the utility of RNFL measurement in AD and MCI, to provide a foundation for my research.

Methods

Search Strategy

We systematically searched PubMed and the Excerpta Medica Database (EMBASE) via OVID for all human studies published until September 2014, in all languages. The Medical Subject Heading (MeSH) search terms used were: "dementia", "Alzheimer disease", "dementia, vascular", "dementia, multi-infarct", "Lewy body disease", "mild cognitive impairment" AND "tomography", "tomography, optical coherence", "OCT".

We also searched Web of Knowledge, Scopus and Google Scholar for all studies published prior to and including September 2014 using the MeSH terms: "optical

coherence tomography", "OCT" AND "dementia", "Alzheimer", "mild cognitive impairment", "MCI". Further studies were identified through manual reference scanning of retrieved articles.

Inclusions / exclusions

Inclusion criteria were an original study of the diagnostic utility of OCT, a confirmed diagnosis of dementia based on appropriate criteria, a comparison of RNFL thickness between patients and an appropriate control group, and with at least 10 participants.

Studies that were excluded were reviews, abstract-only reports, case reports and studies relating to CADASIL (Cerebral Autosomal-Dominant Arteriopathy with Subcortical Infarcts and Leukoencephalopathy) dementia.

Data extraction

All studies identified in the systematic search of the online databases were initially screened by abstract and title. Irrelevant or duplicate studies were removed, and the remaining articles were assessed for eligibility by full-text review. Data extracted from these studies included: title, authors, centre, publication year, aim of study, study type, disease focus, number of patients and controls, characteristics of patients including male:female ratio, mean age, and participant selection criteria, diagnostic criteria, method of OCT used, results and authors' suggestions.

Quality Assessment

All full-text studies to be included in the data analysis were assessed using the Quality Assessment for Diagnostic Accuracy Studies (QUADAS) tool to determine the risk of bias and variability in each study.[220]

Statistical Analysis

Original data was extracted from the studies (means, standard deviations, sample sizes) and where required, calculated data which were not available.

The meta-analysis was performed using RevMan 5.3 (Cochrane Collaboration, Oxford, United Kingdom), calculating the summary estimates including 95% confidence intervals (CI). Using the means, standard deviations and sample sizes extracted from the studies, the weighted mean difference (WMD) was calculated using the inverse-variance random-effects model. A p value of less than 0.05 was considered to be

statistically significant. Heterogeneity was assessed with the chi-squared test, tau-squared, and the Higgins I^2 test, with an I^2 value of more than 50% being significantly heterogeneous. A funnel plot was produced to assess for possible publication bias.

Results

555 articles were identified in the database search, with an additional 3 articles from scanning references. After screening titles and abstracts, with removal of duplicates and irrelevant articles, 26 articles were left for full-text review.

7 further articles were removed at this stage: 3 did not measure RNFL, 1 was a duplicate study, 1 did not compare patient with controls, and 2 reported insufficient data for analysis. This left 19 articles for inclusion in the meta-analysis. (Fig. 2.2)

Of these 19 studies, 17 compared AD to controls (totalling 702 AD eyes and 790 control eyes) with 5 studies comparing MCI to controls (totalling 214 MCI eyes and 421 control eyes). [3 of the 19 studies compared both AD and MCI.]

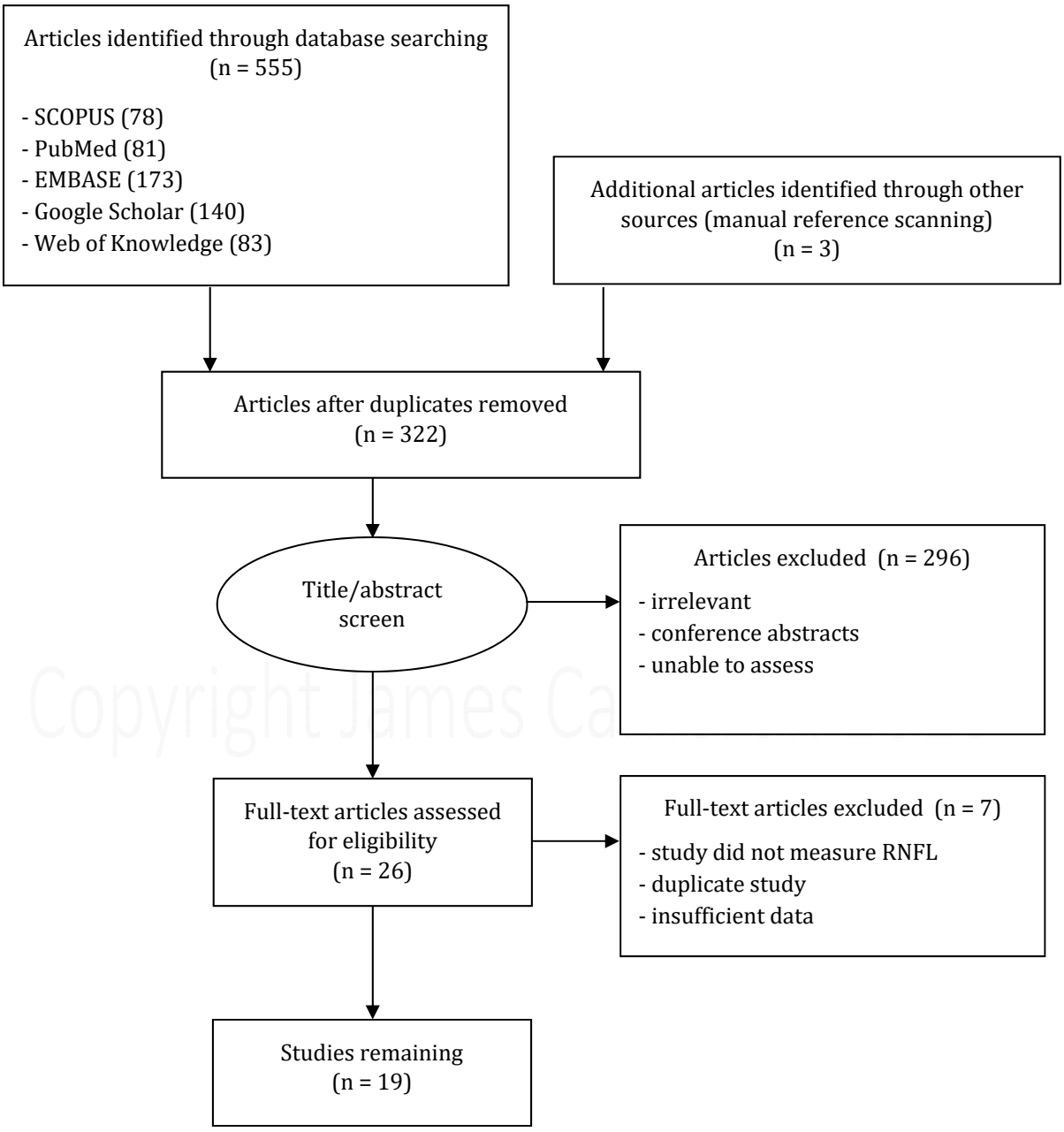

Figure 2.2: OCT in Alzheimer's disease: Flow diagram of manuscript selection

RNFL thickness in AD compared with controls

This analysis comprised 17 studies including 702 AD eyes and 790 control eyes.

There was a significant reduction in the overall mean RNFL thickness in AD patients compared with controls (WMD= -12.44, 95% CI [-16.64, -8.25], p<0.0001). (Table 2.2) (Fig. 2.3)

Sub-division of the RNFL measures by peripapillary quadrant was available in 14 of the 17 studies, including 588 AD eyes and 698 control eyes. All quadrants of the peripapillary RNFL demonstrated significant reduction in patients with AD compared with controls; superior quadrant (WMD= -17.07, 95% CI [-25.26, -8.89], p<0.0001); inferior (WMD= -16.62, 95% CI [-24.48, -8.76], p<0.0001); temporal (WMD= -8.71, 95% CI [-13.66, -3.76], p=0.0006); and nasal (WMD= -9.35, 95% CI [-14.33, -4.38], p=0.0002). (Table 2.3) (Figs. 2.5, 2.7, 2.9, 2.11)

Significant heterogeneity was identified between the studies, with values of heterogeneity for overall mean RNFL thickness of tau^2=67.27, chi^2=377.84, df=16 (p<0.00001), and I^2=96%.

A subgroup analysis according to the type of OCT used (TD-OCT or SD-OCT) demonstrated statistically significant reductions in the overall, inferior and temporal RNFL thickness regardless of whether TD-OCT or SD-OCT was used. The TD-OCT studies showed a larger weighted mean difference for the overall mean RNFL thickness compared with the SD-OCT studies (TD-OCT WMD= -20.89, 95% CI [-29.32, -12.45], p<0.00001; SD-OCT WMD= -6.92, 95% CI [-11.66, -2.18], p=0.004).

A sensitivity analysis was also performed, with exclusion of studies where the required data had to be calculated from the data provided (Ascaso *et al.*[216], Berisha *et al.*[221], Garcia-Martin *et al.*[222], Paquet *et al.*[218], Polo *et al.*[213]). Statistically significant reductions in the overall, superior, inferior, temporal, and nasal RNFL thickness remained.

Funnel plots did not show any correlation between the study size and effect size. (Figs. 2.4, 2.6, 2.8, 2.10, 2.12)

Table 2.2: AD vs. normal controls: overall RNFL thickness

Study	OCT Type	One or Both Eyes	Number of Subjects (Eyes)		Mean Age ± SD (Years)		Overall Mean RNFL Thickness ± SD (μm)	
			AD	Controls	AD	Controls	AD	Controls
Ascaso *et al.*[216]	TD	Both	18 (36)	41 (82)	72.1 ± 8.7	72.9 ± 7.9	64.96 ± 16.71***	103.1 ± 8.04
Berisha *et al.*[221]	TD	One	9 (9)	8 (8)	74.3 ± 3.3	74.3 ± 5.8	85.5 ± 7.4	93.8 ± 10.4
Chi *et al.*[223]	TD	One	12 (12)	17 (17)	75.39 ± 7.30	75.29 ± 5.84	93.18 ± 11.36	99.44 ± 8.88
Garcia-Martin *et al.*[222]	SD	One	20 (20)	28 (28)	79.3 ± 4.1	72.1 ± 5.1	88.6 ± 20.5	89.2 ± 20.9
Gharbiya *et al.*[224]	SD	Both	21 (42)	21 (42)	73.1 ± 6.9	70.3 ± 7.3	96.8 ± 6.9	95.9 ± 8.5
Günes *et al.*[212]	SD	One	40 (40)	40 (40)	75.02 ± 6.34	74.15 ± 5.76	84.0 ± 7.0 ***	107.1 ± 6.3
Iseri *et al.*[219]	TD	Both	14 (28)	15 (30)	70.16 ± 9.7	65.1 ± 9.8	87.46 ± 23.78***	113.16 ± 6.72
Kang *et al.*[215]	SD	Both	8 (16)	8 (16)	71.5	67.4	80.44 ± 16.73*	92.50 ± 9.8
Kesler *et al.*[217]	TD	Mix	30 (52)	24 (38)	73.7 ± 9.9	70.9 ± 9.2	84.7 ± 10.6*	94.3 ± 11.3
Kirbas *et al.*[214]	SD	Both	40 (80)	40 (80)	69.3 ± 4.9	68.9 ± 5.1	65.0 ± 6.2***	75.0 ± 3.8
Kromer *et al.*[225]	SD	Mix	22 (42)	22 (42)	75.9 ± 6.1	64.0 ± 8.2	105 ± 17.0	101.8 ± 10.7
Larrosa *et al.*[226]	SD	One	151 (151)	61 (61)	75.29	74.87	97.55 ± 14.12	100.55 ± 12.99
Moreno-Ramos *et al.*[227]	SD	Both	10 (20)	10 (20)	73.0 ± 6.5	70.2 ± 5.5	94.5 ± 2.2***	108.0 ± 2.2
Paquet *et al.*[218]	TD	Both	26 (52)	15 (30)	78.5 ± 4.91	75.5 ± 5.1	83.4 ± 7.19**	102.2 ± 1.8
Parisi *et al.*[210]	TD	One	17 (17)	14 (14)	70.37 ± 6.1	Age-matched	59.5 ± 16.7**	99.9 ± 8.95
Polo *et al.*[213]	SD	One	75 (75)	75 (75)	74.15 ± 9.15	73.98 ± 9.05	97.40 ± 11.2	99.21 ± 9.9
Zhu *et al.*[228]	SD	*NR*	10 (*NR*)	167 (*NR*)	79.6 ± 8.6	75.5 ± 7.7	90.7 ± 15.8***	96.7 ± 9.6

Abbreviations: AD, Alzheimer's disease; RNFL, retinal nerve fiber layer; OCT, optical coherence tomography; SD, standard deviation; TD, time-domain; SD, spectral domain; NR, not reported.

NOTE. One or both eyes or a mix of one and both eyes used per subject in the evaluation of mean RNFL thickness.

*P < 0.05, **P < 0.01, ***P < 0.001.

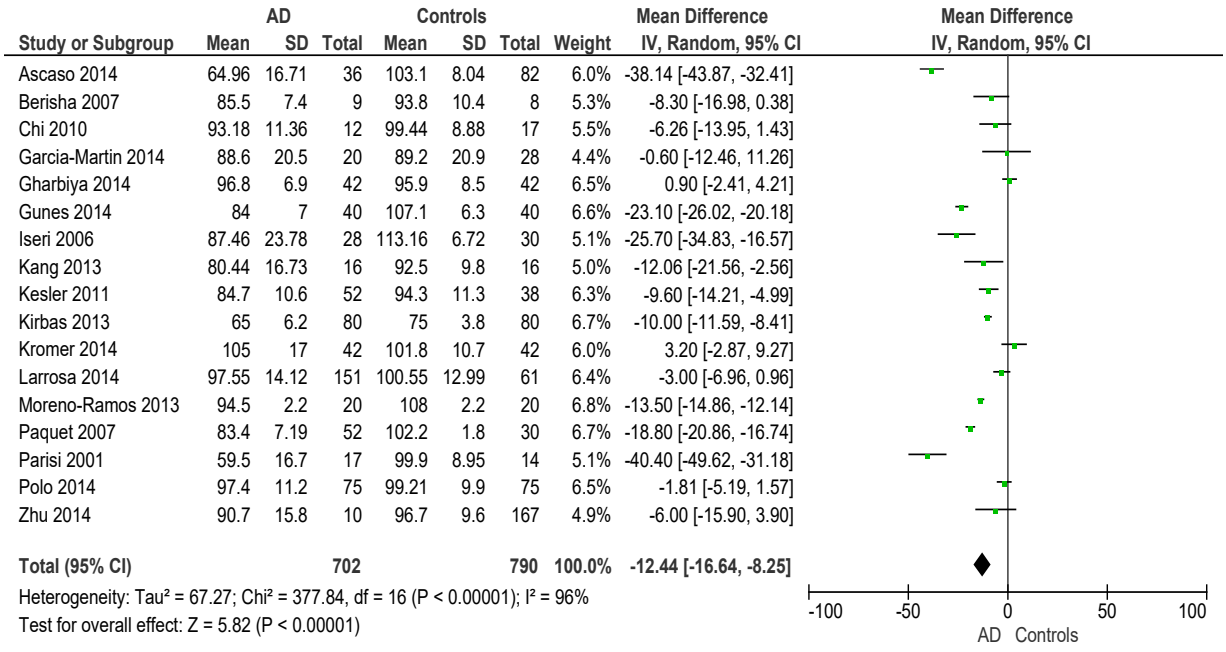

Figure 2.3: Meta-analysis of Alzheimer's disease vs. normal controls: overall RNFL thickness.

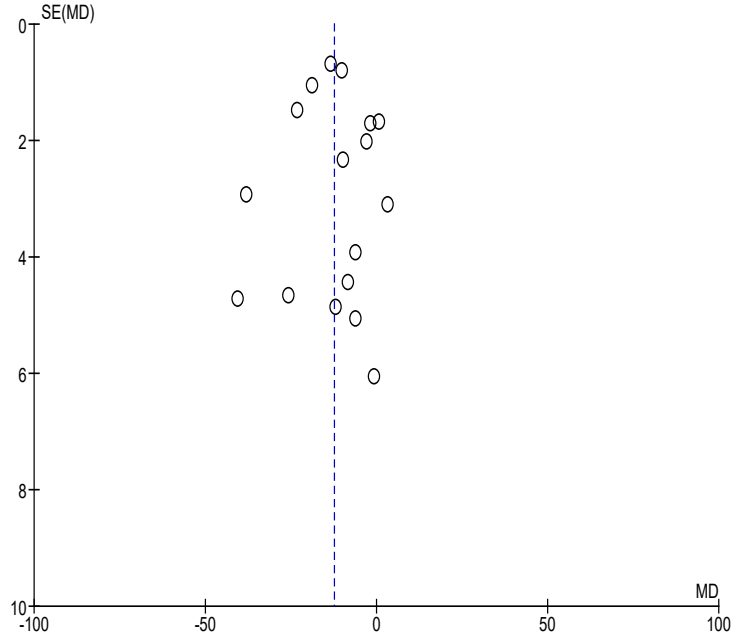

Figure 2.4: Funnel Plot of Alzheimer's disease vs. normal controls: overall RNFL thickness.

Table 2.3: AD vs normal controls: RNFL thickness by quadrant

Study	Superior		Inferior		Temporal		Nasal	
	AD	Controls	AD	Controls	AD	Controls	AD	Controls
Ascaso *et al.*[216]	76.58±21.90***	127.4±14.0	85.47±25.70***	134.2±15.57	56.47±15.86***	75.34±15.05	44.59±21.67***	76.84±15.0
Berisha *et al.*[221]	92.2±21.6*	113.6±10.8	117.0±15.3	128.1±11.4	67.0±15.0	69.5±11.1	65.7±15.1	64.1±7.3
Chi *et al.*[223]	115.09±14.05*	127.94±12.29	120.64±17.99	129.56±15.17	72.36±17.85	74.69±11.72	65.81±13.02	65.31±8.99
Garcia-Martin *et al.*[222]	101.4±16.5	102.2±10.8	110.8±11.1	111.8±10.8	71.8±12.5	70.6±11.6	70.5±12.8	72.3±10.6
Gharbiya *et al.*[224]	114.9±13.8	116.3±14.5	126.9±12.7	124.0±13.6	72.6±14.9	69.8±13.9	74.9±11.5	73.7±12.2
Günes *et al.*[212]	104±14.2 ***	126.5±14.0	101.3±16.2 ***	135.9±16.3	66.6±15.0 ***	80.2±16.7	67.7 ± 17.0 ***	85.4 ± 13.5
Iseri *et al.*[219]	112.64±35.32**	137.16±16.48	103.10±33.64***	141.56±19.09	64.92±17.70	72.30±16.42	63.57±19.09***	96.00±34.39
Kang *et al.*[215]	103.8±26.71	113.5±20.75	104.8±24.97*	126.1±19.34	58.38±13.24	61.50±10.71	55.31±12.61**	68.81±11.35
Kesler *et al.*[217]	99.0±18.0*	110.0±16.7	110.1±19.1*	127.0±15.5	61.7±10.9	67.8±15.1	66.8±14.5	76.4±21.8
Kirbas *et al.*[214]	76±6.7***	105±4.8	106±11.5	108±8.7	74±6.7	77±7.3	75±2.8	76±2.7
Larrosa *et al.*[226]	113.22±18.67**	117.81±19.00	120.44±20.98***	127.38±20.99	64.47±21.76*	67.83±20.01	72.67±17.31	74.55±17.26
Parisi *et al.*[210]	72.1±21.4**	104.6±12.1	77.9±26.4**	116.2±9.87	37.9±17.60**	85.6±8.21	50.4±23.2**	93.4±13.7
Polo *et al.*[213]	113.59±14.5**	118.58±10.8	121.96±16.9*	127.97±15.9	65.00±10.2	66.96±9.2	71.61±15.0	72.12±14.5
Zhu *et al.*[228]	110.9±27.4**	125.2±20.6	122.1±19.9	131.4±20.1	62.1±19.5***	84.3±13.8	67.9±9.2	67.1±14.0

*P < 0.05, **P < 0.01, ***P < 0.001.

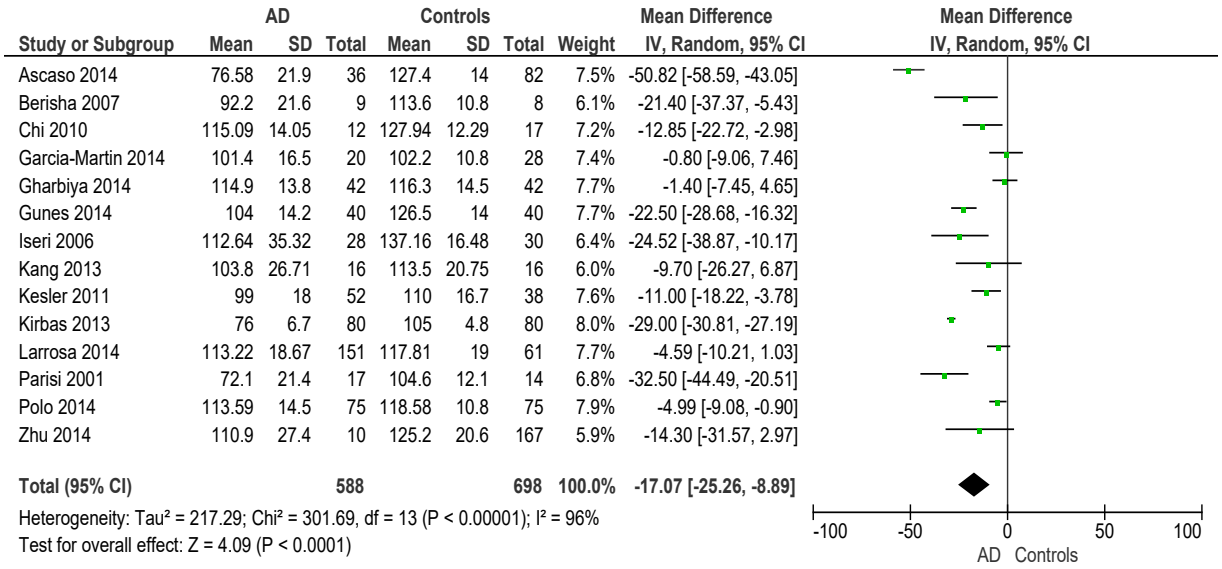

Figure 2.5: Meta-analysis of Alzheimer's disease vs. normal controls: RNFL thickness SUPERIOR quadrant.

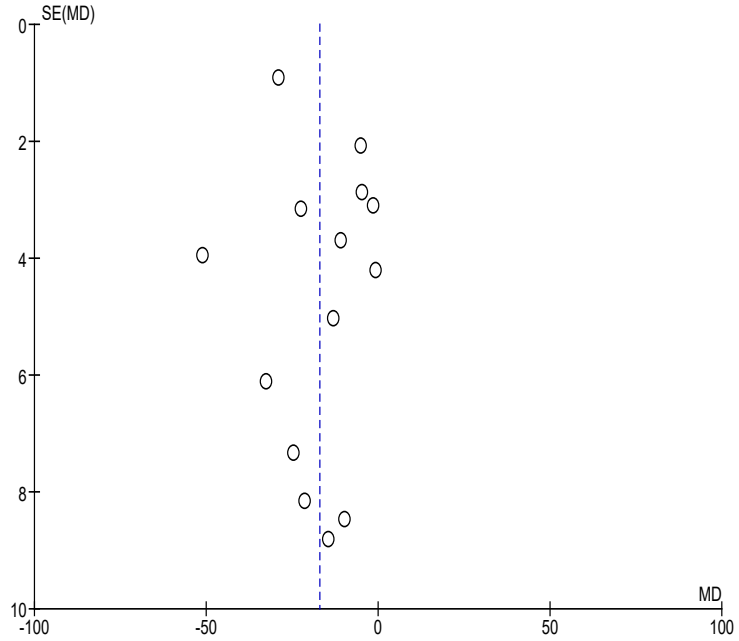

Figure 2.6: Funnel Plot of Alzheimer's disease vs. normal controls: RNFL thickness SUPERIOR quadrant.

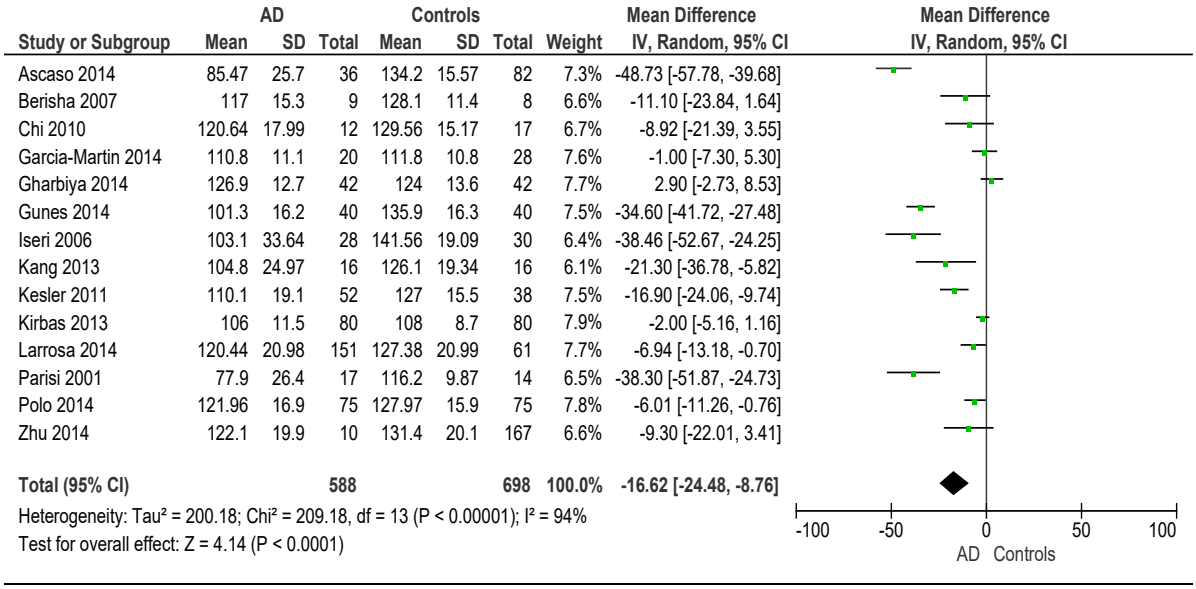

Figure 2.7: Meta-analysis of Alzheimer's disease vs. normal controls: RNFL thickness INFERIOR quadrant.

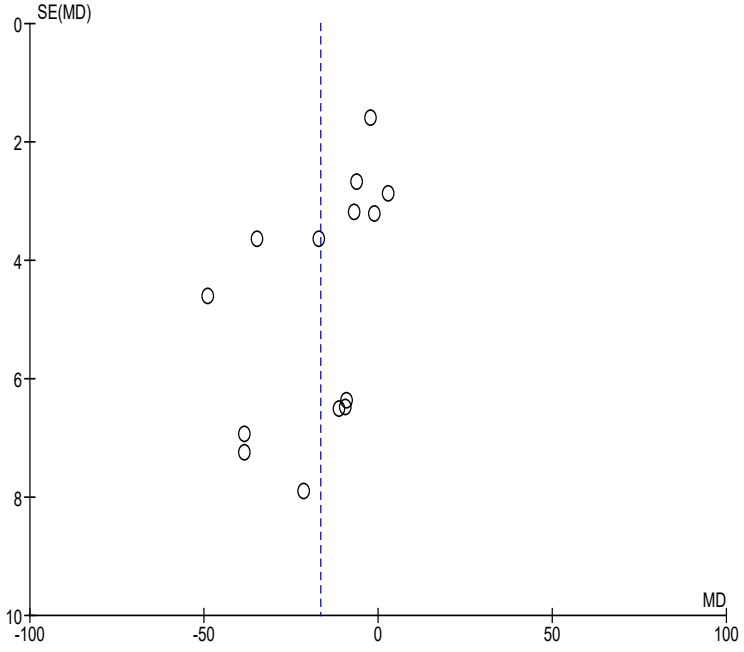

Figure 2.8: Funnel Plot of Alzheimer's disease vs. normal controls: RNFL thickness INFERIOR quadrant.

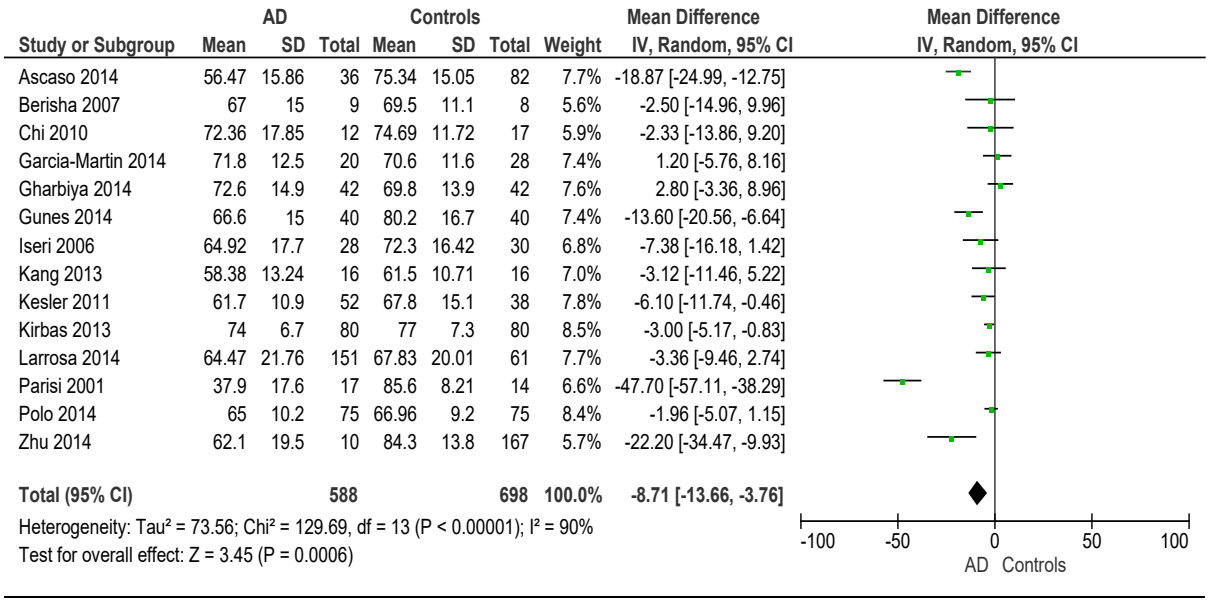

Figure 2.9: Meta-analysis of Alzheimer's disease vs. normal controls: RNFL thickness TEMPORAL quadrant.

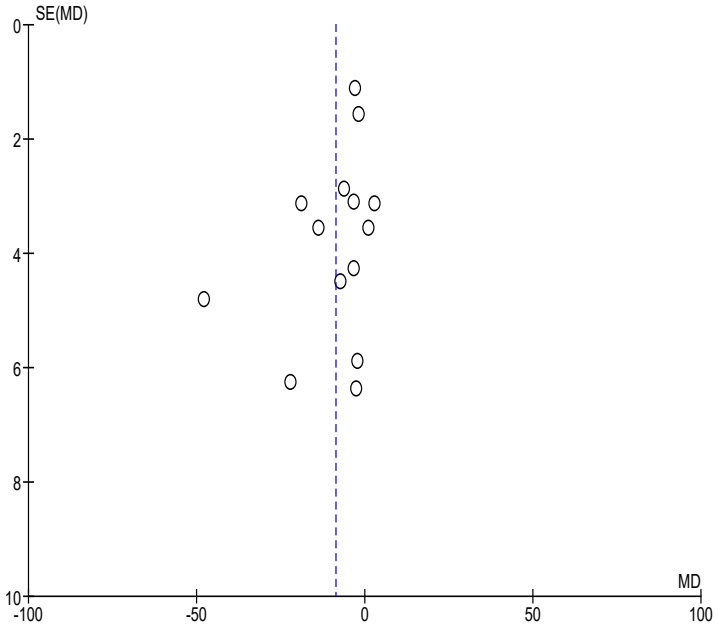

Figure 2.10: Funnel Plot of Alzheimer's disease vs. normal controls: RNFL thickness TEMPORAL quadrant.

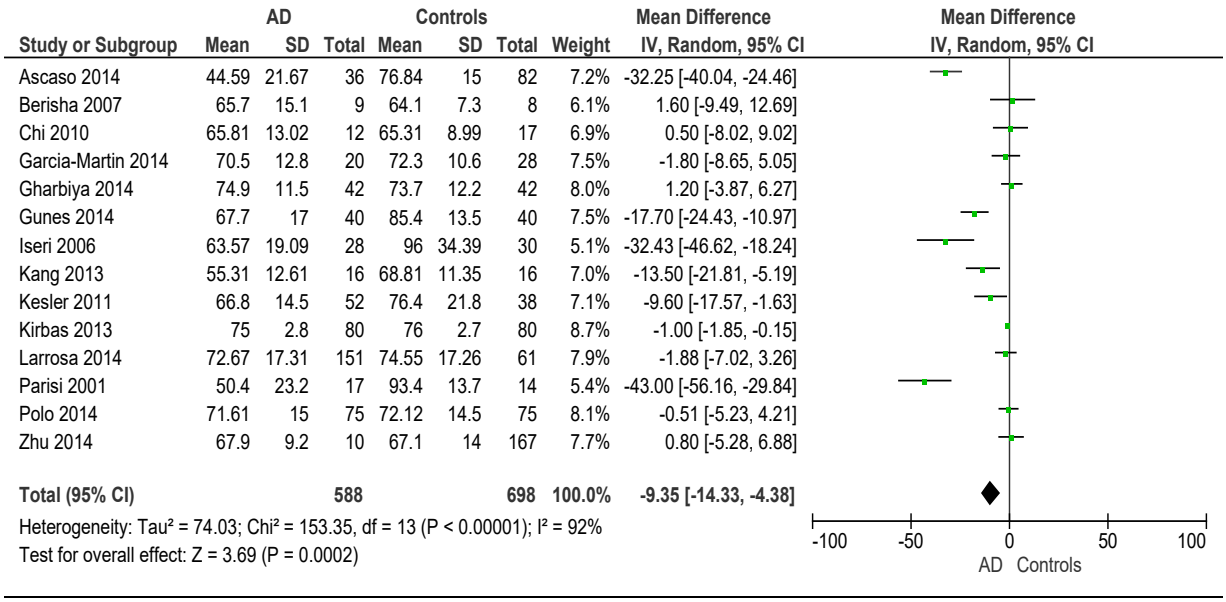

Figure 2.11: Meta-analysis of Alzheimer's disease vs. normal controls: RNFL thickness NASAL quadrant.

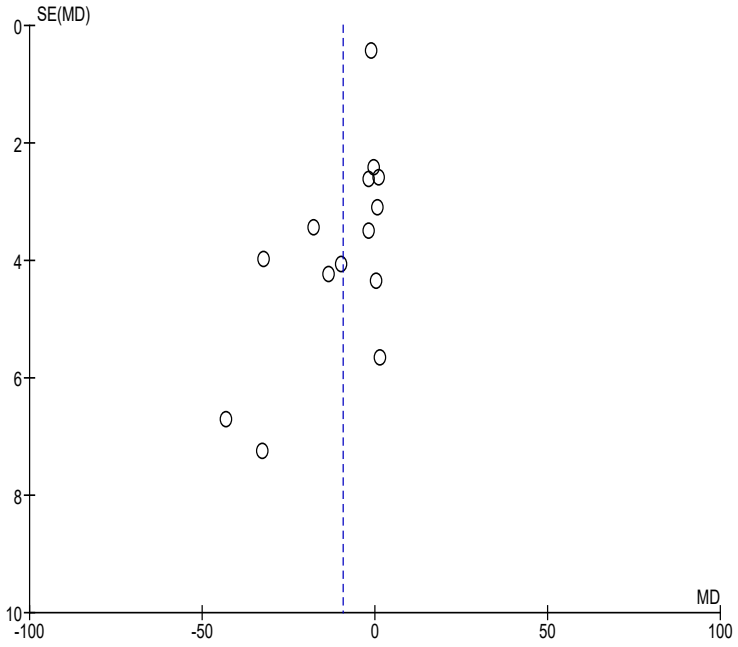

Figure 2.12: Funnel Plot of Alzheimer's disease vs. normal controls: RNFL thickness SUPERIOR quadrant.

RNFL thickness in MCI patients compared with controls

This analysis comprised 5 studies including 214 MCI eyes and 421 control eyes.

There was a significant reduction in the overall mean RNFL thickness in patients with MCI compared with controls (WMD= -8.23, 95% CI [-14.00, -2.45], p=0.005) (Table 2.4) (Fig. 2.13).

There were 4 studies including 168 MCI eyes and 391 control eyes for the mean RNFL thickness by quadrant, showing significant reduction in all four quadrants; superior (WMD= -11.72, 95% CI [-22.59, -0.85], p=0.03); inferior (WMD= -11.45, 95% CI [-21.00, -1.90], p=0.02); temporal (WMD= -6.47, 95% CI [-10.74, -2.20], p=0.003); and nasal (WMD= -4.34, 95% CI [-8.50, -0.19], p=0.04). (Table 2.5) (Figs. 2.14, 2.15, 2.16, 2.17)

There was again significant heterogeneity between the studies, with values of heterogeneity for overall mean RNFL thickness of tau^2=40.61, chi^2=91.67, df=4 (p<0.00001), and I^2=96%.

A subgroup analysis according to the type of OCT used (TD-OCT or SD-OCT) showed that the TD-OCT studies showed a significant reduction in the overall, inferior, temporal, and nasal RNFL thickness, whereas the SD-OCT studies only showed a significant reduction in the superior RNFL thickness. Heterogeneity became nonsignificant within the TD-OCT studies for the inferior, temporal, and nasal quadrants, and within the SD-OCT studies for the overall, superior, inferior, and nasal quadrants.

A sensitivity analysis (excluding Ascaso *et al.*[216], where the required data had to be calculated) only showed a significant reduction in the superior and temporal RNFL thickness, with no significant reduction in the overall, inferior, and nasal RNFL thickness.

Table 2.4: MCI vs. normal controls: overall RNFL thickness

Study	OCT Type	One or Both Eyes	Number of Subjects (Eyes)		Mean Age ± SD (Years)		Overall Mean RNFL Thickness ± SD (µm)	
			MCI	Controls	MCI	Controls	MCI	Controls
Ascaso *et al.*[216]	TD	Both	18 (36)	41 (82)	72.1 ± 8.7	72.9 ± 7.9	86.7 ± 7.18***	103.1 ± 8.04
Kesler *et al.*[217]	TD	Mix	24 (40)	24 (38)	71.0 ± 10.0	70.9 ± 9.2	85.8 ± 10.0*	94.3 ± 11.3
Paquet *et al.*[218]	TD	Both	23 (46)	15 (30)	78.7 ± 6.2	75.5 ± 5.1	89.3 ± 2.7***	102.2 ± 1.8
Shen *et al.*[229]	SD	Mix	23 (45)	52 (104)	74.4 ± 3.2	74.1 ± 2.6	82.6 ± 10.5	85.6 ± 10.2
Zhu *et al.*[228]	SD	*NR*	47(NR)	167 (NR)	76.1 ± 8.2	75.5 ± 7.7	96.8 ± 9.9***	96.7 ± 9.6

NOTE. One or both eyes or a mix of one and both eyes used per subject in the evaluation of mean RNFL thickness.
*P < 0.05, **P < 0.01, ***P < 0.001.

Table 2.5: MCI vs normal controls: RNFL thickness by quadrant

Study	Superior		Inferior		Temporal		Nasal	
	MCI	Controls	MCI	Controls	MCI	Controls	MCI	Controls
Ascaso *et al.*[216]	100.3±15.5***	127.4±14.0	110.6±18.1***	134.2±15.57	67.38±14.32***	75.34±15.05	68.43±17.16***	76.84±15.0
Kesler *et al.*[217]	101.3±15.2	110.0±16.7	111.9±16.1*	127.0±15.5	64.2±13.9	67.8±15.1	65.9±15.1	76.4±21.8
Shen *et al.*[229]	101.8±16.8	104.7±15.4	104.5±17.6	109.3±21.3	62.7±12.2	65.5±10.1	61.5±8.1	64.8±8.4
Zhu *et al.*[228]	117.1±18.3**	125.2±20.6	128.7±17.2	131.4±20.1	73.1±13.5***	84.3±13.8	67.6±12.2	67.1±14.0

*P < 0.05, **P < 0.01, ***P < 0.001.

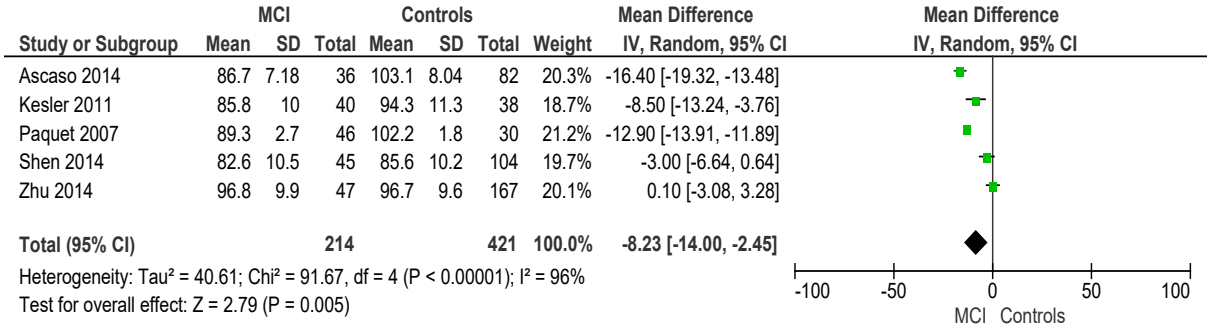

Figure 2.13: Meta-analysis of MCI vs. normal controls: overall RNFL thickness.

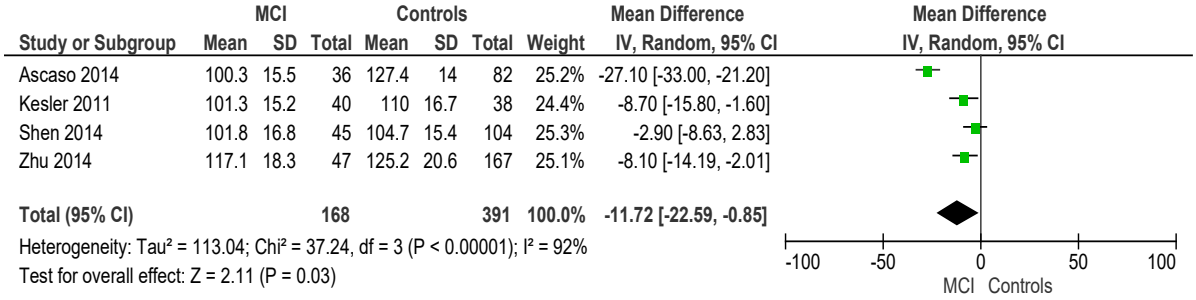

Figure 2.14: Meta-analysis of MCI vs. normal controls: RNFL thickness SUPERIOR quadrant.

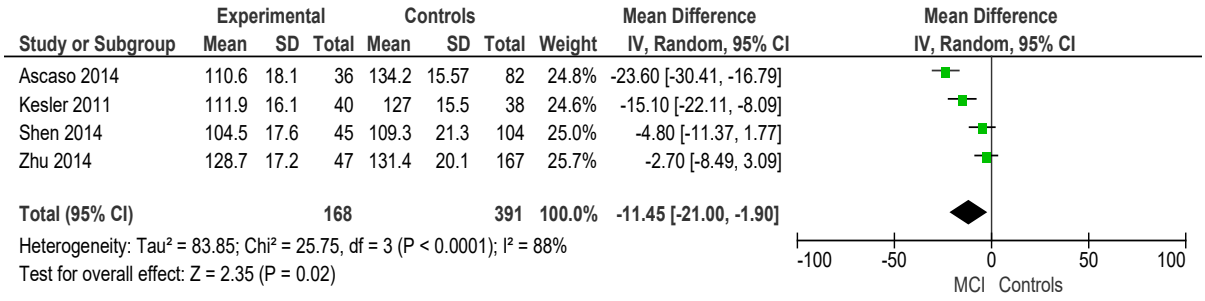

Figure 2.15: Meta-analysis of MCI vs. normal controls: RNFL thickness INFERIOR quadrant.

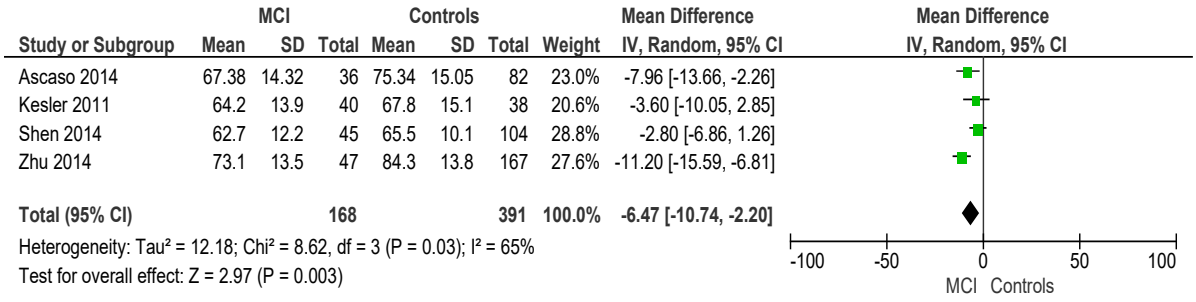

Figure 2.16: Meta-analysis of MCI vs. normal controls: RNFL thickness TEMPORAL quadrant.

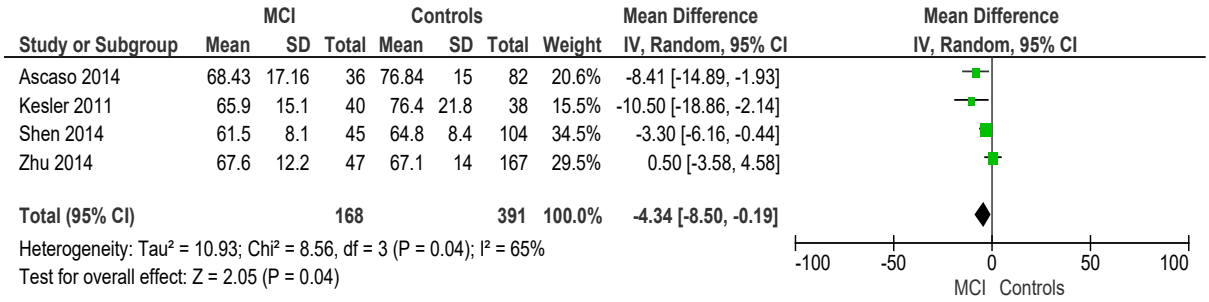

Figure 2.17: Meta-analysis of MCI vs. normal controls: RNFL thickness NASAL quadrant.

Discussion

RNFL thickness appears to be significantly different between AD eyes and healthy controls. In addition, MCI eyes also show a smaller, but still significant difference.

The mean overall RNFL thickness is the primary measurement of all the reported studies, but several studies have also investigated the four quadrants of peripapillary RNFL thickness, and found reductions in each quadrant, although the superior and inferior quadrants show the most thinning in AD eyes.

Whilst this meta-analysis confirms the significant difference, the effect size is relatively modest: mean overall RNFL thinning= -12.44μm, 95% CI [-16.64, -8.25], p<0.0001. This difference falls well within the normal variation of mean overall RNFL thickness in the population, despite the meta-analysis containing 790 control eyes. It is less than 0.5 of the highest reported standard deviation (23.78) in the AD studies.[219] The sub-division by RNFL quadrant showed a small preponderance for the superior and inferior quadrants, but insufficiently specific for any quadrant(s) to be regarded as phenotypic of AD.

Therefore, the diagnostic discrimination between AD and controls of RNFL thickness is not established by these studies. More work will be required to refine this figure, and identify both the sensitivity and specificity of RNFL measurement as a diagnostic marker. It is noticeable that none of the studies acknowledged this shortcoming, although perhaps this reflects the infancy of this research area.

A limitation of this analysis is the inclusion of studies with both older TD-OCT technology as well as the newer SD-OCT. Multiple studies in the ophthalmic literature have shown that the two technologies are very different, and often measure things differently, with SD-OCT vastly superior and more precise. Sub-group analysis revealed similar findings between TD-OCT and SD-OCT, but with a much-reduced effect size with the newer and more reliable SD-OCT.

The correlation between severity of AD and degree of RNFL thinning has not been established. Although some studies have reported cognitive scores - e.g. Mini-Mental State Examination (MMSE) - of participants, no clear correlation has yet been shown. There were also no studies correlating RNFL thinning with other biomarkers of dementia, for example imaging or cerebrospinal fluid.

No prognostic information was reported or can be inferred from these cross-sectional studies. One conference proceeding reports prospectively recruiting patients and found that RNFL thickness may predict the risk of cognitive decline in healthy patients.[230] This is an interesting hypothesis, but one that has not been tested further or confirmed.

MCI

Despite only 5 articles being eligible for inclusion in the meta-analysis of MCI eyes compared with controls, a significant difference was found, although with a very low effect size: mean overall RNFL thinning= -8.23, 95% CI [-14.00, -2.45], p=0.005. This is a smaller difference that in AD, and therefore is consistent with the hypothesis, but nonetheless represents a small difference in means, and low specificity.

In addition, the significant heterogeneity between the studies - particularly in the chosen control groups - limits the conclusions that can be drawn from this meta-analysis.

Non-AD dementia

There were no articles found or included in this meta-analysis that studied non-AD dementia, and none that addressed early-onset (age < 65 years) AD. Therefore, these remain untested patient populations.

Nevertheless, this meta-analysis has shown that there does appear to be a detectable, and reproducible, degree of RNFL thinning in patients with AD, and to a lesser degree, MCI. It certainly warrants further investigation to further elucidate the potential of using this as a disease biomarker, in AD and also in other dementia syndromes.

Since publication of this meta-analysis, three further meta-analyses of retinal thinning in AD have been published[231-233], and one in MCI.[234] Their findings of significant differences between RNFL in AD, MCI and healthy controls matched ours, and they also agreed with high heterogeneity between studies.

The most recent of the meta-analyses of AD included 25 articles (reflecting the proliferation of studies over the last year), and also examined the evidence for macular thickness differences between AD and controls.[232] They found that this too showed evidence of thinning in patients with AD, particularly in the outer ring of the standard ETDRS circular grid pattern.

Early-onset dementia

OCT in early-onset and other dementia types

Despite the proliferation of OCT studies in AD, they have exclusively focussed on AD (and MCI) in the elderly.

The mean age of the patient groups are all > 69 years, with the majority of studies with a mean age at the upper end of the eighth decade. (Table 2.2)

In addition, no studies investigating OCT in any other dementia subtypes - behavioural variant frontotemporal dementia (bvFTD), primary progressive aphasia (PPA), corticobasal dementia (CBD), posterior cortical atrophy (PCA) - were found.

OCT correlations with other biomarkers

Cognition

Whilst several of the studies reported above included some cognitive assessment in their study protocol, few explored this in any detail.

The commonest test used was the Mini-Mental State Examination (MMSE). Despite its limited sensitivity, studies such as that by Iseri et al[219] found a significant correlation between MMSE and OCT measure of total macular volume (r=0.696, p=0.006). This hypothesis that retinal atrophy might occur in line with cognitive decline is perhaps less intuitive than might be expected, when we know the pattern of white matter atrophy in the brain is often localised in early dementia, rather than diffuse.

Electrophysiology

Comparison of OCT measures with electrophysiological testing such as visual evoked potentials (VEP) has been included in some studies, such as Kromer *et al.*[235] The findings have generally been either inconclusive or insignificant. This may reflect challenges of reproducibility and confounders in the reporting of VEP outcomes.

Cerebrospinal Fluid / Biochemical / Molecular

No studies investigating OCT correlations with CSF or plasma markers of disease were found.

Retinal vessels in dementia - systematic review

Note: Excerpts of this section have been published – in "The application of retinal fundus imaging in dementia: a systematic review", S McGrory, JR Cameron, E Pellegrini, C Warren, F Doubal, IJ Deary, B Dhillon, J Wardlaw, E Trucco & TJ MacGillivray.
Alzheimers Dement (Amst) 2017; 6(1): 91-107.

Thanks are due to:
Sarah McGrory - lead author, and systematic analysis

Retinal microvascular abnormalities in relation to cognitive dysfunction have been previously described in both age-related cognitive decline and in dementia[236, 237], and in association with diabetes.[238]

However, wide variability in the results and conclusions from the studies of retinal vessel morphology in dementia limits our ability to make robust conclusions.

I therefore carried out a more detailed systematic review of the utility of retinal vessel analysis from fundus camera imaging, in relation to dementia. I worked with colleagues who are researching this topic specifically, under a large EPSRC funded project.

Methods

Search Strategy

We systematically searched PubMed, MEDLINE and EMBASE for all human studies published until March 2016, in all languages. The Medical Subject Heading (MeSH) search terms used were: "retina," or "fundus," or "retinal vasculature," or "retinal microvasculature," or "retinal vascular," or "retinal vessel," or "retinopathy" and in combination with "dementia," or "Alzheimer," or "Lewy bodies," or "cognition," or "cognitive".

We also searched Google Scholar for all studies published prior to and including March 2016 using similar keywords. Further studies were identified through manual reference scanning of retrieved articles.

Inclusions / exclusions

Inclusion criteria were an original study applying fundus camera imaging to examine the association between retinal vasculature and any form of dementia, an English manuscript available, and a diagnosis of any dementia based on appropriate criteria.

Studies that were excluded were reviews, single-case reports, non-human research, conference proceedings, studies without details of dementia diagnosis and studies examining retinal features via imaging modalities other than fundus camera imaging.

Data extraction

All studies identified from the search of online databases were initially screened by abstract and title. Irrelevant and duplicate studies were removed, and the remaining articles were assessed for eligibility by full-text review. Data extracted from the studies included: title, authors, year of publication, study aim and type, numbers of patients and controls, mean age, diagnostic criteria, participant selection criteria, method of fundus imaging and image analysis used, results and conclusions.

Results

1567 studies were identified in the literature search. After screening titles and abstracts, with removal of duplicates and irrelevant articles, 59 articles were considered to be potentially relevant and were assessed by full-text review. (Fig. 2.18)

10 studies met the inclusion criteria. The populations samples came from the US (2), UK (2), Iceland (1), the Netherlands (3), Australia (1) and Singapore (1). They comprised three prospective cohort studies[117, 239, 240], three population-based cross-sectional studies[241-243], and four case-control studies.[244-247]. Although several articles had overlapping samples, each article assessed different retinal features. (Table 2.6)

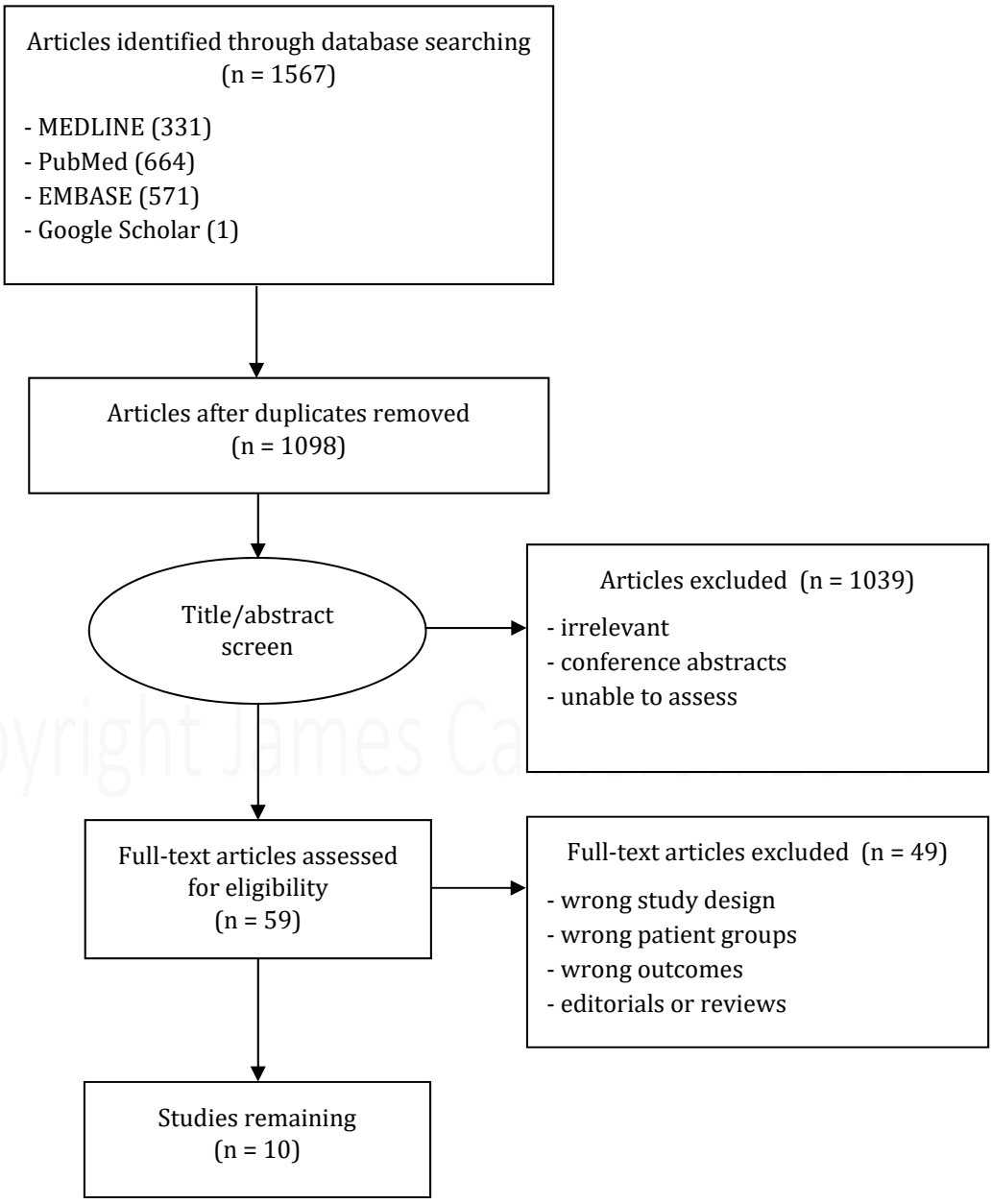

Figure 2.18: Retinal fundus imaging in dementia: Flow diagram of manuscript selection

Table 2.6: Included studies using fundus imaging methods to examine retinal associations with dementia

Study	Study design and total sample size	Dementia	Retinal measures	Software/grading	Region measured
Klaver *et al.*[239] 1999 Rotterdam Study	Prospective population-based study. (n=1438)	AD (n=62 incident cases)	ARMD	Grading of fundus according to international classification system	Macula
Baker *et al.*[241] 2007 Cardiovascular Health Study	Population-based cross-sectional study (n=2,211)	AD (n=99); VaD (n=11); mixed AD VaD (n=49) other types (n=5)	Retinopathy; AVN; FAN; Retinal vascular calibre	Observer graded. Calibre was measured and summarised	Centred between the OD and macula. Calibre measured one disc diameter from the OD margin
Baker *et al.*[242] 2009 Cardiovascular Health Study	Population-based cross-sectional study (n=2,088)	Dementia (n=135); AD (n=86)	ARMD	Observer graded	Macula
Qiu *et al.*[243] 2010 AGES-Reykjavik Study	Population-based cross-sectional study (n=3,906)	AD (n=66); VaD (n=31); possible AD and VaD (n=20)	Retinopathy; AVN; FAN,	Observer graded	Two images, centred on the OD and the macula
De Jong *et al.*[117] 2011 Rotterdam Study	Population based prospective study (n=5,553)	Incident dementia: AD (n=519); VaD (n=73); other subtypes (n=63)	CRVE; CRAE	Retinal Vessel Measurement System	Centred on the OD
Schrijvers *et al.*[240] 2012 Rotterdam Study	Population-based cross-sectional and prospective study (n=6078)	AD (n=149); VaD (n=29); other subtypes (n=17)	Retinopathy	Observer graded	Macula
Frost *et al.*[245] 2013 Australian Imaging, Biomarkers and Lifestyle (AIBL) Study of Ageing	Case-control study (n=25: 123)	AD (n=25)	CRAE; CRVE; AVR; D_f; BSTD; BC; AF; JE; LDR; Tortuosity; Num1stB	SIVA	Centred on OD; 0.5–1.0 disc diameters or 0.5–2.0 disc diameters away from the disc margin

Cheung *et al.*[244] 2014 Singapore Epidemiology of Eye Disease (SEED) program	Case-control study (n=136:290)	AD (n=136)	CRAE; CRVE; D_f; Tortuosity; BA	SIVA	Two images of each eye: one centred at the OD and the other centred at the fovea. Measurements taken between 0.5 and 2.0 disc diameters away from the disc margin
Williams *et al.*[246] 2014	Case-control study (n=258:322)	AD (n=258)	ARMD	Observer graded	6mm AREDS macula grid centred on fovea
Williams *et al.*[247] 2015	Case-control study (n=213: 294)	AD (n=213)	CRAE; CRVE; D_f; Tortuosity BA	SIVA	0.5 and 2.0 disc diameters away from the disc margin

* For longitudinal studies age at baseline;

Abbreviations: AD, Alzheimer's disease; VaD, vascular dementia; OD, optic disc; FAN, Focal arteriolar narrowing; AN, Arteriovenous nipping; CRAE/CRVE, central retinal arterial/venular equivalent; AVR, arteriole-to-venule ratio; D_f, fractal dimension; BA, branching angle; BC, branching coefficient; AF, asymmetry factor; BSTD, Zone B standard deviation; JE, Junctional exponent deviation; Num1stB, number of first branching vessels in Zone C; LDR, Length diameter ratio; RNFL, retinal nerve fibre layer; ARMD, age related macular degeneration; SIVA, Singapore I Vessel Assessment; AREDS, Age-Related Eye Disease Study; APOE, Apolipoprotein E.

Measurements

The assortment of retinal features being measured across these studies not only demonstrates the infancy of the field, but is frustrating in the lack of a cohesive and interoperable approach to retinal biomarker research.

A combination of visual grading and computerised analysis has been used across the studies, and with different grading systems between studies.

Retinal features under investigation fell into three general categories:

1. retinopathy (haemorrhage, microaneurysms, ischaemia - cotton wool spots, exudation, neovascularisation, evidence of laser treatment)

2. macular degeneration (drusen, haemorrhage, pigment migration)

3. retinal vessel morphology (calibre, focal narrowing or nipping, tortuosity, bifurcation angles and coefficient, fractal dimension)

My focus is on (computerised analysis of) retinal vessel morphology, and so will consider the 5 studies that investigated this.[117, 241, 244, 245, 247]

Retinal vessel calibre

From the 3 case-control studies, associations between arteriolar calibre and dementia were inconsistent. Using CRAE as a summary measure of arteriolar vessel calibre, Frost *et al.*[245] and Cheung *et al.*[244] found arteriolar narrowing in AD (area under the curve (AUC)=0.612, SD=0.082; age, sex, and ethnicity–adjusted OR=2.02, 95%CI [1.59, 2.58]), whereas Williams *et al.*[247] found evidence of arteriolar widening in AD (age and sex–adjusted OR=1.37, 95% CI [1.08, 1.75]. However, associations were lost once cardiovascular risk factors were controlled for: OR=1.22, 95% CI [0.78–1.91][244] and OR=1.1, 95% CI [0.83, 1.47].[247]

In our subsequently published meta-analysis from this review[248], we determined a reduction in arteriolar width in AD, with a mean difference of -7.52, 95% CI [-18.88, 3.84], with significant heterogeneity between these 3 studies. (Fig. 2.19)

Associations between venular calibre and dementia were also mixed. Using CRVE as a measure of venular calibre, Frost *et al.*[245] found evidence of narrower venular widths in AD (AUC=0.703, SD=0.067, p=0.0049). Cheung *et al.*[244] also found that patients with AD (n=136) had narrower venules (p<0.001; age, sex, and ethnicity-adjusted OR=2.17,

95% CI [1.69, 2.79]; multivariate-adjusted OR=2.01, 95% CI [1.27, 3.19]). Williams *et al.*[247] did not find a significant difference between CRVE in patients with AD (n=213) and control subjects (n=294) (d=0.006, p=0.951) (multivariable-adjusted OR=0.99; 95% CI [0.75, 1.32], p=0.960).

From the meta-analysis of these studies, we observe a trend for reduction in venular calibre in AD, (MD= -10.74, 95% CI [-24.09, 2.61] and again with significant heterogeneity between studies. (Fig. 2.19)

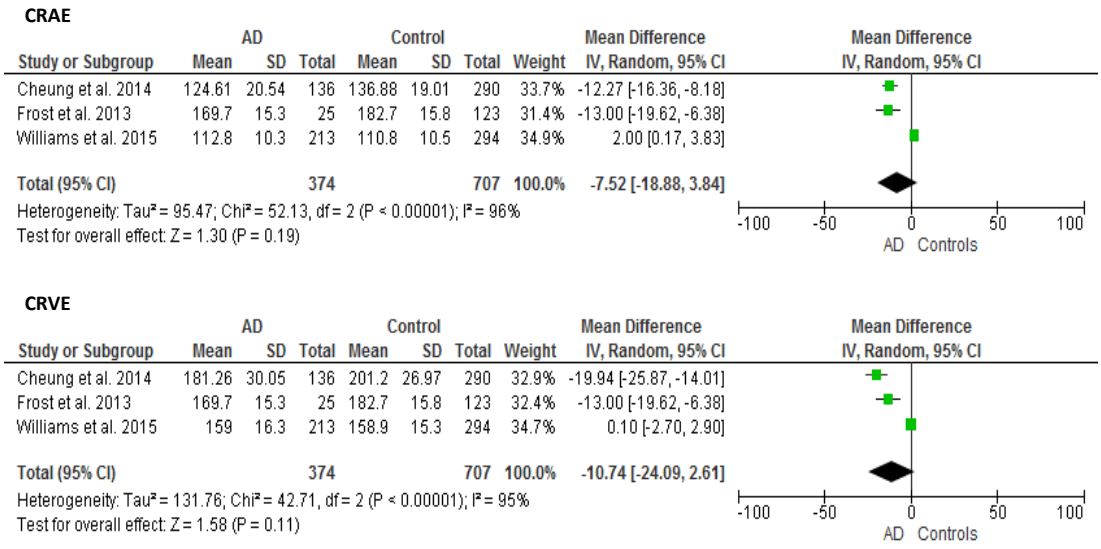

Figure 2.19: Meta-analysis of Alzheimer's disease vs. normal controls: CRAE and CRVE. Unadjusted results reported.

[Figure from McGrory et al. Alzheimer's & Dementia (Amst) 2017 [248]]

The Cardiovascular Health Study population-based study failed to find a significant association between arteriolar calibre and dementia (multivariate-adjusted OR=1.42, 95% CI [0.74, 2.96]).[241]

The prospective Rotterdam Study investigated the association between retinal vessel calibre and prospective risk of incident dementia - both AD and VaD.[117] They found increasing venular calibre was associated with increased risk of dementia (age and sex–adjusted HR=1.09, 95% CI [1.01, 1.18]; multivariate-adjusted HR=1.11, 95% CI [1.00, 1.22]). However, further analysis revealed that this increase was driven by the association with VaD, and that there was no significant increased risk of AD with

increasing venular calibre, following exclusion of those with cardiovascular disease. No association between arteriolar calibre and risk of dementia was found.

The only study using arteriovenous ratio (AVR) found no significant difference between patients with AD and the control group.[245]

Fractal dimension

The three studies that looked at fractal dimension (D_f) in AD all reported a reduced D_f, both arteriolar and venular, in AD compared with healthy controls.[244, 245, 247]

Frost *et al.*[245] found that patients with AD demonstrated reduced complexity of the branching pattern in comparison with control subjects with lower arteriolar (AUC=0.644, SD=0.075, p=0.021) and venular D_f (AUC=0.716, SD=0.074, p=0.0033). Cheung *et al.*[244] and Williams *et al.*[247] both reported reduced arteriolar, venular and total D_f in AD patients. Those with lower venular D_f (multivariate-adjusted OR per SD increase=0.77, 95% CI [0.62, 0.97], p=0.025) were more likely to have AD, however the association between total and arteriolar D_f and AD did not persist in the final models.

Meta-analysis reveals no significant heterogeneity between the studies, and a small but significant MD= -0.02, 95% CI [-0.03, -0.01]. (Fig. 2.20)

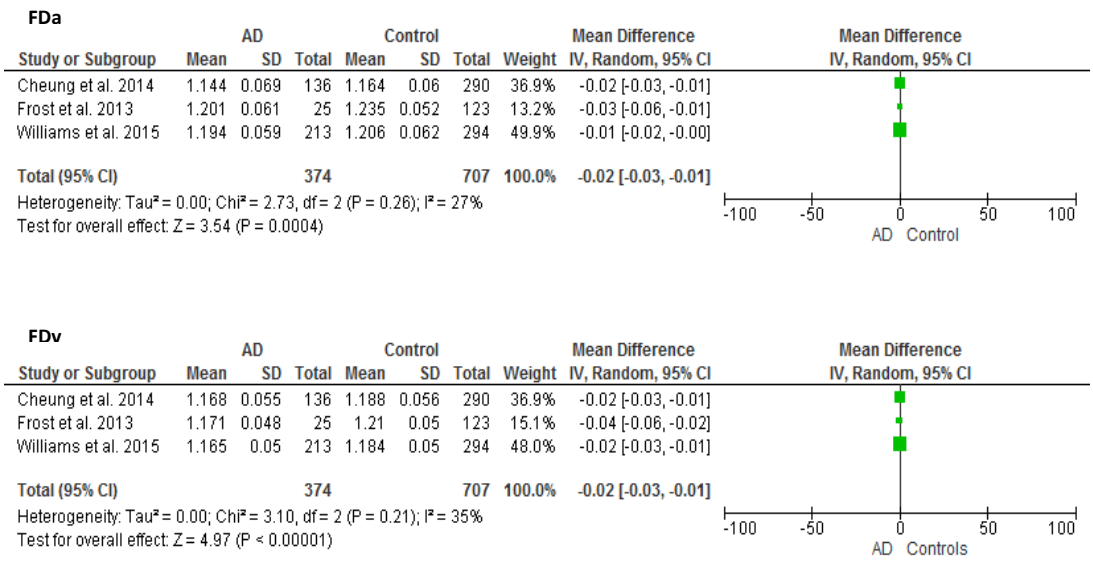

Figure 2.20: Meta-analysis of Alzheimer's disease vs. normal controls: arteriolar and venular fractal dimension. Unadjusted results reported.

[Figure from McGrory et al. Alzheimer's & Dementia (Amst) 2017 [248]]

Vessel tortuosity

More inconsistency was seen in the results of vessel tortuosity analysis.

More tortuous arterioles and venules were observed in AD than in control subjects (d=0.2, p=0.001) in the Singapore Epidemiology of Eye Disease study.[244] Those with higher arteriolar and venular tortuosity were more likely to have AD (multivariable-adjusted OR per SD increase=1.8, 95% CI [1.48, 2.53]; OR=1.94, 95%CI [1.48, 2.53] respectively).

Frost *et al.*[245] found less tortuous venules (AUC=0.706, SD=0.073, p=0.042) in AD, with no significant difference in arteriolar tortuosity. Conversely, Williams *et al.*[247] observed lower arteriolar tortuosity in AD (d=0.2, p=0.030, multivariable-adjusted OR=0.78, 95% CI [0.63, 0.97], p=0.27), and not venules (d=0.07, p=0.458).

Discussion

Despite the appeal of investigating the retina for consistent markers of dementia, the number of published studies that passed through manuscript selection was small. And within these ten studies, the research methods and outcome measures were very variable. Half looked at features of ARMD as a comparator with dementia, and I have not reported on their findings. The other five did examine retinal vessel morphology, but with different approaches and in the case of vessel tortuosity, different results.

The most consistent finding was a reduced D_f in AD. This is similar to that seen in hypertension[113] and stroke.[107, 249] The presumed mechanism for a reduced D_f is the loss of small blood vessels due to vessel wall damage and capillary occlusion, as seen in the micro-angiopathy of diabetic retinopathy.[250] If this loss of optimal vascular pattern is paralleled in cerebral small vessels, resulting in relative downstream hypoxia, then this becomes a biologically plausible biomarker for the vascular component of cerebral disease.

Retinal vessel calibre was a less consistent finding in AD, with both narrower and wider arterioles reported. Narrower arterioles are a known association of hypertension, both existant[251] and future risk.[252] Wider retinal arterioles are a less studied phenomenon, but known to be associated with early ARMD.[253] In this review, we identified larger venular calibre associated with increased risk of VaD, but not with AD.[117]

The relevance of vessel tortuosity in dementia was also unclear from this analysis, with mixed reports. Multiple ocular diseases are known to affect retinal vessel tortuosity, and short-term changes in tortuosity in response to environmental effects have also been reported.[254] Therefore we may be measuring a morphological parameter with too many contributing factors, and so will not see a consistent finding in any dementia. Alternatively, it could be a marker of vascular health and so better correlate with indices of severity and decline, rather than diagnosis.

This review has confirmed the variability in both the methodology and results, from studies of retinal vessel morphology in dementia. Whilst fractal dimension has emerged as the most (relatively) consistent finding, the evidence is limited, and lacks more detailed phenotypic correlation.

The only dementia subtype encountered was AD. No studies investigating retinal vessels in bvFTD, PPA, CBD or PCA were found. In addition, within the AD studies, all patient populations were elderly, with no exploration of early-onset AD.

Choroidal vasculature

In a follow-up literature search, two studies were found that reported on choroidal thickness (CT) changes in AD.[224, 255]

In 2014, Gharbiya *et al.*[224] demonstrated significant choroidal thinning in their group of 21 patients with mild to moderate AD. Using the EDI mode of the SPECTRALIS OCT, they manually measured the subfoveal choroid thickness, and again at 500μm and 1500μm from the fovea, both horizontally and vertically. The found the choroid to be significantly thinner at all locations in AD, compared with control eyes, with around a 60μm difference.

The second study, from 2016, by Bulut *et al.*[255] examined both eyes of 41 patients with AD, 38 with MCI and 44 control subjects. Again, they measured CT at several locations of the posterior pole, and found all regions of the choroid significantly thinner, with a mean difference of -57μm at the subfoveal location in AD, and -44μm in MCI.

Failing to account for the cluster bias of using both eyes as independent subjects in their analysis is an important weakness of the study.

Whilst they also reported a positive correlation between CT and MMSE score in AD, there was no further discussion on how CT might be developed to become a potential biomarker in AD or other dementias. They speculate that the observed choroidal thinning is atrophy secondary to toxicity caused by Aβ accumulation. This amyloid angiopathy is known in the cerebral vessels, but not yet demonstrated in the retinal or choroidal vasculature.

No studies investigating choroidal thickness in early-onset AD, or other dementia types were found.

Amyotrophic lateral sclerosis (motor neurone disease)

OCT in ALS

Just three studies have been published on the use of OCT neuroretinal measures in patients with amyotrophic lateral sclerosis (ALS).

The first study of OCT in ALS was published in 2013, from a collaboration group between Germany and Philadelphia.[256] They included 76 patients - of which 15 were clinically definite ALS, 41 clinically probable, and 20 possible ALS. They found no difference in any measurement between patients and controls; and in ALS patients no correlations with disease severity measures, concluding that "*involvement of the anterior visual pathway is not one of the non-motor manifestations of ALS*."

This was followed a year later with another study from Germany, this time with less overall patients - 24, but a better sample with 20 clinically definite and 4 clinically probable ALS patients.[257] They used a different OCT device (the SPECTRALIS rather than the Cirrus used by the previous study). They used similar scan protocols of the peripapillary RNFL and macular volume scans, but added in manual segmentation of the other retinal layers. They found the RNFL was significantly thinner in ALS (by 6.7%) and a slight reduction of the macular volume (by 2.6%). Of the manually segmented retinal layers, they also revealed a significant thinning of the inner nuclear layer.

They comment that the presence of microglial activation - a known pathophysiological element within ALS - could be occurring in the retina and affecting the thickness measures, however given the better phenotyped cohort of ALS patients in this study, they conclude that ALS is associated with measurable neurodegeneration.

A third study, also from Germany, was published in 2015, and examined 71 patients with ALS (all clinically definite, or clinically probable).[258] Again they used the SPECTRALIS OCT, and reassuringly comment that "*Scans that did not pass the OSCAR-IB criteria for retinal OCT quality assessment were excluded from the analysis*". This provides more confidence that the study utilised ophthalmic image analysis expertise. A subgroup of just under half of the participants also underwent MRI with DTI analysis of fractional anisotropy of the corticospinal tract.

They found that RNFL thinning was observed in the ALS group, though when sub-divided into spinal and bulbar-onset groups, in only the spinal-onset group was the RNFL thinning statistically significant. Like the two previous studies, no other correlations were found between the OCT measures and any other clinical characteristics.

Regarding the DTI analysis, they observed a significant positive correlation between RNFL and fractional anisotropy of the corticospinal tract, which was not present in the control group. With DTI a more established marker of disease severity and progression in ALS[259], this does suggest that RNFL measurement may have potential as an additional marker of disease progression, but without any impression of its sensitivity.

The weakness of this third study was that no ophthalmological examination was performed, and so they could not exclude patients with ophthalmic co-morbidity. This is an important weakness, as with small sample sizes, it is imperative to rigorously exclude potential confounders where even one participant could influence the study findings. It is also surprising, given the evidence from the paper suggesting a high level of ophthalmic imaging expertise oversaw the imaging.

In summary, these three studies are somewhat heterogenous in study design, in patient population and in their conclusions. No analyses were adjusted for duration of disease/time since onset of symptoms, and clinical characterisation of the study population was limited. Each study has certain weaknesses tempering their conclusions, and it therefore remains unclear if neuroretinal thinning is indeed a feature of ALS.

Retinal vessels in ALS

No studies investigating retinal vessel morphology in ALS were found.

Choroidal vasculature

No studies investigating choroidal thickness in ALS were found.

Summary

This literature review with systematic searches has described the current state of retinal imaging markers in neurodegenerative disease research. Whilst there have been many published studies, particularly in MS, there remain many unanswered questions, and scope for further research.

MS

In MS, large longitudinal studies in the key MS research centres have provided evidence for the use of RNFL measures as a strong surrogate of brain atrophy measures in MS. Correlation with other disease markers is less strong, and some recent work has started to explore other retinal markers such as thicknesses of other retinal layers. It is not clear which markers are best, and for what purpose.

Whilst both RNFL and RGC layer thicknesses have been shown to fall in MS, and in a particular distribution (temporal), no study has looked at the chronological sequence of this, i.e. whether axonal loss precedes cell body degeneration, vice versa, or simultaneously. The answer to this may have implications for understanding the pathological process that results in RGC loss in MS. The clear preferential targeting of the visual pathways in MS in contrast to other neurological conditions suggests that perhaps there is an immunological target within the retinal ganglion cell, rendering it susceptible in this disease. In which case RGC loss may be primary, and not secondary to retrograde degeneration travelling forward from the brain white matter into the retina.

Evidence for this hypothesis exists in the animal model, where a study examining this process in the rat model of MS - experimental autoimmune encephalomyelitis (EAE) - observed that "before manifestation of optic neuritis, characterized by inflammatory infiltration and demyelination of the optic nerve, degeneration of retinal ganglion cell bodies had already begun." They also observed early activation of resident microglia in the retina, supporting the hypothesis that primary neurodegenerative changes can occur in the retina independent of optic nerve inflammation.[260] Of course, EAE is a somewhat capricious model of MS, with a low conversion rate of treatments that show

promise in EAE converting to successful human trials.[261] Nevertheless, it provides a useful source of hypotheses for investigation.

There are also gaps in MS research regarding the discriminatory potential of these neuroretinal markers, including retinal vascular morphology, and their relationship with function assessments, such as visual acuity.

Dementia

The focus in dementia has been exclusively AD and MCI. The meta-analyses have shown good potential for RNFL in AD, but mixed opinion on retinal vascular markers.

However, there were no studies found relating to AD in younger patients, or in any non-AD dementia, such as bvFTD, PPA, CBD or PCA. And no studies of correlation with other AD markers, such as CSF biomarkers.

Amyotrophic lateral sclerosis

With just a couple of studies published - with conflicting results - it is not yet known whether neuroretinal markers have clinical utility in ALS. In addition, there are no studies of retinal vascular markers or the choroid in ALS.

Whilst ALS is not thought to have visual pathway involvement in any clinically relevant way, that does not exclude the potential for sub-clinical changes to be measurable, and important.

Retinal Ganglion Cell - choice of layer

Measuring for atrophy of the retinal ganglion cell can be done with OCT looking either the RFNL (the ganglion cell axon, that forms the RNFL, optic nerve and anterior visual pathway) or the GCL (the cell bodies of the ganglion cells).

Advantage of the GCL is that it is more 'stable' - i.e. doesn't swell like the RNFL. If there is optic disc oedema, then by definition there will be some swelling of the RNFL near the optic disc. RNFL thickness will therefore be mixed measure of this axonal swelling plus any established adjacent axonal atrophy, therefore normalised, and not reflecting either pathology. Optic disc oedema can last several weeks in some pathologies, therefore it can be some time before RNFL measurement can reasonably reflect the resultant axonal damage.[262]

In contrast, evaluation of the retina more distal from the optic disc, for example the macula (including individual layers of the macula such as the GCL) will be less prone to this swelling, and represent only any progressive atrophy from normality.[262]

Retinal vessel morphology

Automated software platforms for measuring retinal vessel geometry are enabling prospective studies to be undertaken with reasonable reliability and precision, encouraging this added value within retinal imaging research.

Whether changes in retinal vascular geometry are related to CNS degeneration is yet to be elucidated. Although, there is evidence that retinal vessel geometry and axonal layer integrity are indeed linked, with correlations found in the elderly population of the Lothian Birth Cohort 1936 study.[263]

Biologically plausible hypotheses of vessel changes within neurodegenerative disease, accepting the assumption of retinal and brain vasculature homogeny, are intriguing and certainly feasible to study.

Amyloid angiopathy is a known component of brain amyloid accumulation disorders, causing fragility of small-to-medium sized arteries, with potential for intracranial haemorrhage.[264] It has not been described outside the brain, but has been speculated as a putative hypothesis for the small vessel changes potentially encountered in the eye, and elsewhere.

Choroidal thickness

Measurement of this vascular layer under the retina has only become possible with recent advancements in OCT technology - namely swept-source OCT or EDI functioning within SD-OCT. The choroid is thickest at the fovea, and therefore this is frequently the site of measurement.[265]

The choroid provides nutrition to the outer retina, and is implicated in several ocular diseases, such as age-related macular degeneration (ARMD) where thinning of the choroid is observed[266] - thought to be atrophy - and central serous chorioretinopathy (CSCR) where thickening is seen[267] - due to choroidal vessel dilation.

Choroidal changes in response to systemic vasculopathy has been less investigated. Recent work by our group has looked at the choroid in patients with chronic kidney disease and/or hypertension, with findings of choroidal thinning that correlates

significantly with circulating inflammatory biomarkers and also clinical measures of kidney dysfunction.[125]

Increasing reporting of the relevance of systemic microvascular health to diseases like MS and dementia provide sufficient interest to include a hypothesis for measuring sub-foveal choroidal thickness (sfCT) in this study. Whilst the choroid may be simply a window to generalised microvascular integrity, there are perhaps additional pathophysiological reasons for observing changes in the choroid, in neurological disease. As with the retinal vasculature, the impact on the choroid of amyloid angiopathy could also contribute to the thinning and atrophy observed.

Measuring only single point-thickness of the choroid is a somewhat crude method of assessing this vascular structure. Ideally, we would extract volume measures, and sub-divide this by choroidal tissue - medium or small vessels, choriocapillaris, etc. Whilst newer processing methods of OCT-angiography systems are looking in more detail at the choroidal vasculature, quantitative measures are not yet available, and so full thickness point measures will have to suffice at present.

Studies that have measured CT at multiple locations on the horizontal and vertical lines cans through the fovea have shown similar findings at all locations, and therefore no advantage to this method of multiple location measures. Therefore, for explorative pilot studies, and in the absence of more advanced choroidal assessment, a simple subfoveal CT measure is sufficient. Indeed, with the choroid being thickest at this location, it is potentially superior to other locations, as more sensitive to small changes, as well as being the most straightforward to obtain a high-quality OCT image from which to make the measurement.

Research Questions

This literature review has supported the aims of my study, as stated in Chapter 1. Having explored the current state of the field in retinal imaging derived biomarkers of neurodegenerative disease, it is clear that there are many unanswered questions.

By exploring retinal imaging methodology in more detail, and modulating the image analysis tools to gain retinal vessel data from the imaging episodes, I can analyse a large volume of cross-sectional data, in these patient populations.

The literature review has identified particular areas of weakness and absence in the literature for example, non-AD dementias, and the general absence of retinal vessel analysis in these conditions.

I can therefore highlight research questions that I am well placed to engage with.

MS

- What are the OCT and vessel findings in MS of all subtypes, in a Scottish population?
- What is the specificity and sensitivity of RNFL and other retinal measures for discriminating MS from controls, and MS from NMO
- Is temporal or global RNFL better at discriminating diseases, measuring disease severity and monitoring change?
- Does GCL loss occur with, before or after RNFL loss?
- Which MS subtype is associated with choroidal changes, and do choroidal measurements correlate with other retinal measures?
- Are retinal venules thicker in MS? And if so, does the degree of thickening correlate with any other markers of clinical inflammation/severity, such as being predictive of relapse rate in RRMS?
- Does treatment status in RRMS affect the retina or retinal vasculature?
- Do any retinal measures correlate with EDSS?
- Which retinal measure best correlates with visual acuity?
- Which low-contrast visual acuity chart is best to use in monitoring MS?

Dementia

- What are the OCT and vessel findings in early-onset dementias of all types (specifically AD, bvFTD, PPA, CBD and PCA), in a Scottish population?
- What is the specificity and sensitivity of RNFL and other retinal measures for discriminating dementia from controls, and between dementia types
- Is temporal or global RNFL better at discriminating disease, and measuring disease severity?
- Does retinal vessel data improve the discrimination of neuroretinal metrics?
- What is the relationship between neuroretinal markers and cognitive status? Do any of the markers predict cognitive decline?

ALS

- What are the OCT and vessel findings in ALS, in a Scottish population?
- What is the specificity and sensitivity of OCT markers in discriminating ALS from controls, and ALS from progressive MS?
- Is there a difference in neuroretinal markers between spina-onset and bulbar-onset ALS? And do they correlate with any other disease phenotypic features?
- Does RNFL correlate with ALS subtype, or phenotypic features?
- Does treatment status in ALS affect the retina or retinal vasculature?

3 METHODS

Research design

Setting

The Anne Rowling Regenerative Neurology Clinic (ARRNC) is a charitable University of Edinburgh, purpose-built, dedicated research clinic, for patients with neurological conditions, particularly neurodegenerative diseases. From inception, the aims of the facility are to progress high-impact research, integrating all domains of laboratory science and clinical trials, in a way that integrates with immediate patient care, supported by a wide-experienced and multi-specialty research team.

This concept of a synergistic partnership with patients carries many advantages, not least clear engagement and involvement with this group of patients who have a clear and immediate need for scientific advances in the understanding of their conditions.

Since its official opening in October 2013, the spectrum of patients being seen has increased. The main conditions being seen are multiple sclerosis, motor neurone disease and early-onset cognitive disorders/dementia. It is with these three groups upon which this research is focused.

Patient Groups

MS

The majority of MS clinics and management in Lothian now comes through the ARRNC.

Data from the locally managed clinical MS database reveals the known population within Lothian of 2078 patients with MS (and 95 with CIS who have attended the specialist MS clinic at some point for assessment). Around 250 new referrals are seen per annum,

The clinic participates in several MS treatment trials, and other clinical assessment trials. Therefore, the infrastructure and environment for recruiting patients is excellent, as well as the patients themselves being familiar with the research-partnership vision for the clinic.

The clinical MS database can record many aspects of a patient's disease status, treatment journey, and other important clinical information. Like any clinical data system, it relies upon frequent and accurate data entry, and the staff were able to advise me on the patient groups with most useful data.

Dementia

The cognitive disorders clinic in ARRNC is a tertiary referral, multi-disciplinary specialist clinic for patients aged 65 years or younger, with dementia symptoms.

Held weekly, referred patients receive a comprehensive workup, combining a clinical assessment with a neurologist and/or psychiatrist, with access to comprehensive investigations such as cognitive and psychological testing, DNA analysis, CSF analysis, MRI and SPECT neuroimaging, and now retinal imaging.

In the 18 months before I started, there have been 280 new patients assessed in the clinic. The forward projection was for 150-160 new patients per year, along with a similar number of established patients being reviewed.

Given the broad referral criteria, the range of pathology seen is broad. Whilst a number of patients are found to have only subjective memory impairment without evidence of a neurodegenerative disease, there are a significant number of diagnoses across the disease spectrum. The diagnosis mix is approximately: ⅓ have early onset AD, ⅓ have early onset FTD (including behavioural and language variants), and the rest have mixed pathologies (including vascular dementia, multiple co-morbidities, epilepsy, HIV etc).

ALS

The specialist ALS/MND clinic in ARRNC is a bi-weekly, multi-disciplinary service, providing specialist neurologist, respiratory, speech therapy and nursing support. Whilst much input for patients with ALS is carried out in their home, attendance at the clinic facilitates not only this additional team input, but the opportunity for engagement with vital patient-focussed research, including skin cell donation for stem cell work.

Despite challenges in mobility and physical positioning, the patient-friendly nature of retinal imaging is such that image capture is still possible despite wheelchairs and reduced physical motor ability. Requiring only a supported lean forward towards the chin-rest of the device, many patients are able to position for satisfactory retinal imaging, where other investigations may be more problematic, uncomfortable or even

impossible. This is a strength of retinal imaging; and future hand-held devices will make this even more accessible.

Healthy controls

For comparisons with normal healthy data, I recruited healthy control subjects from staff, university colleagues, and friends/partners of patients attending the clinic. The same exclusion criteria and consent process applied to these healthy controls.

As a trained ophthalmologist, I was able to assess any incidental findings as they occurred, and reassure, treat or refer as necessary.

Methodology

The research study is a prospective, cross-sectional, case-control retinal imaging study, with opportunistic recruitment from a secondary care facility.

The sampling technique was a non-probability opportunity sampling, from the patient population attending the clinic for their clinical care. This method of sampling carries a limitation of population representation unless the numbers are significantly high and there is a reason for the population to be well and randomly represented. I can achieve both, by seeing high numbers, and recruiting from new, routine return and intervention (treatment) follow-up clinics.

This sampling approach carries the additional advantage of allowing me to be blinded to diagnosis and other clinical phenotype information at the time of imaging.

Essential to the work is close collaboration with clinical colleagues in the clinic, for recruitment, as well as providing ophthalmological input and support. The clinical relevance of retinal imaging in these patients is approaching importance clinical value, and therefore a beneficial and synergistic relationship between clinical and research value in my work enhances patient care and adds value to the clinical service.

For recruitment sample sizes, power calculations were performed - detailed in the 'Data Analysis and Statistical Plan' section of this chapter. These provide minimum numbers for recruitment, based on estimated mean differences in the principal outcome metrics. However, I plan to recruit considerably more, to enable subtype analysis and minimise type 2 errors.

Blinding

The advantage of an opportunistic recruitment methodology is that I can be initially blinded to patient diagnosis, subtype, and all clinical measures. Inviting successive patients to participate in a study would normally be an inefficient recruitment method, however with my capacity to recruit a large number of patients across several disease types, this was not a concern.

I was therefore blinded to patient details during scanning, image processing, and correction of any automated segmentation errors.

I could not be blinded to healthy controls, as I recruited these participants separately. However, I carried out the image processing in blocks at the end of imaging sessions, so mixed patients and controls were processed together to minimise bias, by ignoring the patients details during processing.

Approvals

Ethical approval was obtained for the study from the Scotland A Research Ethics Committee, on 11 March 2014, REC reference: 14/SS/0033.

This included approval for patients lacking capacity to consent, under the Adults with Incapacity (Scotland) Act 2000.

NHS Lothian R&D site approval was gained 18 March 2014, reference: 2014/0057.

Patient recruitment and clinical assessment

Inclusion and exclusion criteria

The inclusion criteria for this study are:

Patients attending ARRNC, with a confirmed diagnosis, willing and consent to be in the study (or in cases of incapacity, agreement to retina imaging and consent from family member with them for research use of images), able to physically position their head on the chin-rest of the OCT machine, and follow brief simple instructions on fixation.

Exclusion criteria are:

Ocular disease including significant media opacity, prior ocular surgery, history of uveitis, refractive error > ±5 dioptres or astigmatism > 2 dioptres, or any new finding found on eye examination.

- A refractive error of > ±5 dioptres is usually related to the eye being shorter or longer than normal. This impacts on the retinal structure, for example in a long eye, the retina is effectively stretched a bit thinner, to cover the posterior pole. In doing so, the retina - and hence the retinal layers - are thinner than normal, despite this not being strictly pathological.
- In addition, measurement of vessel morphology may be affected by long or short eyes, due to magnification effects. Although this is offset by using dimensionless parameters for vessel analysis, excluding these eyes reduces this potential.

Medical conditions of hypertension, diabetes, or kidney disease.

- We know that in diabetes, significant neuroretinal thinning can be observed early in the disease, even in the absence of visible diabetic retinopathy.[268]

Additional exclusion criteria in MS population

To minimise confounding of OCT measurements, patients within 3 months of optic neuritis, or 1 month of steroid therapy are usually also excluded.

Assessment

As well as retinal imaging with OCT, patients received additional examination or investigations, dependant on their diagnosis, as part of their routine clinical care. Consent for the study included access to this data for imaging comparisons.

Baseline demographic information could usually be accessed during, or at the end of the clinic, from the clinical team. (Table 3.1) Additional investigation results were retrospectively obtained from online patient records, or in discussion with the clinical team. (Table 3.2)

Ophthalmic assessment included an eye examination for all patients, as well as checking for exclusion criteria, such as high refractive error. In MS patients, visual acuity was obtained, including low-contrast Sloan acuity for a selected subgroup. In the dementia population, intraocular pressure was checked whenever there was any suspicion of glaucoma, for example optic disc cupping, optic disc haemorrhage, or RNFL loss in a pattern consistent with early glaucomatous change. (Table 3.3)

Table 3.1: Baseline demographic and phenotype data capture

Sex (male/female)
Age (years)
Diagnosis and classification or sub-type
Symptoms at onset
Years/months since onset of symptoms
Years/months since diagnosis
Past medical history
Past ophthalmic history, including history of optic neuritis
Current medications, and history of medications related to current neurological disease

Table 3.2: Disease-related measures

Relapses (in MS) – annualised relapse rate
Addenbrooke's Cognitive Score (in dementia) – ACE-III
CSF biomarkers (dementia sub-study) - $A\beta_{1\text{-}42}$, t-tau, *P*-tau
Expanded Disability Status Scale (EDSS) (in MS)

Table 3.3: Ophthalmic examination and imaging measures

Visual acuity (ETDRS full contrast, plus Sloan low contrast 5%, 2.5% & 1.25% for sub-study)
Refractive error (spherical equivalent in dioptres)
Intraocular pressure (if suspicion of glaucoma, or for sub-study)
Ocular examination for previous or subclinical ocular disease
OCT: pRNFL (global, 7 sectors, nasal/temp ratio), macular thickness and volume (9 sectors and full ETDRS 6mm circle) – full retinal thickness and GCL, sub-foveal choroidal thickness (sfCT)
Retinal vasculature: CRAE, CRVE, AVR, aTort, vTort, D_f ($D_{0,1,2,BOX}$ for a, v, both)

OCT imaging protocol

Note: Excerpts of this section have been published – in "Retinal imaging in early Alzheimer's disease", TJ MacGillivray, S McGrory, T Pearson, JR Cameron.
Book chapter in 'Biomarkers for Preclinical Alzheimer's Disease': NeuroMethods Vol. 137, Robert Perneczky (Ed.), Humana Press. (2017) doi: 10.1007/978-1-4939-7674-4

OCT technique

All participants underwent a single examination of both eyes using the Heidelberg SPECTRALIS® Spectral-Domain OCT machine (software version 6.0, Heidelberg Engineering, Heidelberg, Germany).

Each examination comprised three scan pattern protocols, repeated for each eye:

1. A horizontal line scan through the fovea, centred over the fovea, and with enhanced depth imaging (EDI) enabled for greater choroidal visualisation. (Fig. 3.1)

2. A peripapillary circular line scan centred over the optic disc, with segmentation of the retinal nerve fibre layer (RNFL). (Fig. 3.2)

3. A macular volume scan consisting of 61 horizontal B-scans, with a separation of 120µm, covering the whole macula area. (Fig. 3.3)

Together these three scans per eye provide a wealth of neuroretinal metrics, in an efficient scanning protocol - taking approximately 30-40 seconds per eye to perform. Extensive measurements of retinal thicknesses and volumes, of specific layers and within designated sectors, can be easily extracted. RNFL thickness, GCL volume and subfoveal choroidal thickness (sfCT) are the core parameters of interest in this study.

A key benefit of the SPECTRALIS system is the latest generation software featuring automated retinal layer segmentation, and active eye-tracking. These leading advances facilitate highly precise and repeatable measures, and have made the SPECTRALIS system the leading device for this area of research.

The Heidelberg Nsite Axonal Analytics™ software automates segmentation of the peripapillary RNFL, and provides a control database for the peripapillary RNFL thickness of each sector.

Whilst not used for the analysis in this study, the control database presents a visual colour coding to the RNFL thickness measurement graph - green for normal, yellow for borderline (1st to 5th percentile), and red for abnormal (< 1st percentile). This is useful in the clinical setting, enabling rapid initial assessment for the operator, as well as visual representation context for explaining the image to the patients.

Automated segmentation of the macula volume scan is a feature of the version 6.0 software, and uses the latest algorithms for accurately segmenting the retinal layers, and enabling 3D re-construction and volume measurements from any retinal layer in the scan area.

Each scan also takes advantage of the proprietary TruTrack™ active eye tracking and ART™ (Automatic Real-Time) software, which averages the image over 100 scans, to generate a single high-resolution scan image. By 'freezing' the eye position, the SPECTRALIS can acquire artefact-free images even in the presence of ocular movement, or blink. I have even been able to acquire images in patients with nystagmus. It also improves the quality of an image in patients with ocular media opacity (e.g. cataract, unstable tear film, corneal scar) by averaging scans whilst the operator can subtly re-align the axis of the OCT scan.

Choroidal thickness measures

The subfoveal choroidal thickness (sfCT) was measured manually using software calipers, on the horizontal EDI line scan. The measurement was taken in a vertical line perpendicular to the horizontal retinal pigment epithelium RPE, from the outer hyper-reflective line corresponding to the base of the RPE (RPE/Bruch's complex), to the choroidal-scleral junction. (Fig. 3.1)

Peripapillary RNFL measures

The ppRNFL thickness has become an important measure, and the scan protocol is now standardised. A circle of fixed diameter 12^0 (with millimetre diameter dependent upon eye axial length) and consisting of 1536 A-scans, is centred over the optic disc manually. Whilst the manual location of the scan invites a possibility for error, studies have shown that the SPECTRALIS has not only excellent reproducibility of this scan protocol, but exceeds rival machines.[269]

The scan is then segmented for measurement of the RNFL thickness, which is shown as a continuous line graph. Peri-papillary sectoral averages are also calculated, and

provided in a circular chart that corresponds anatomically to the optic disc; with the sectors: papillo-macular bundle (PMB), temporal (T), temporal-superior (TS), nasal-superior (NS), nasal (N), nasal-temporal ratio (N/T), nasal-inferior (NI) and temporal-inferior (TI), along with the global (G) mean. (The PMB sector is located within the temporal quadrant, between -22° and +8°). (Figs. 3.2, 3.6)

The software processing of the segmentation of the ppRNFL scan takes approximately 2 seconds.

Macular volume measures

From the macular volume scan, measurements of average retinal thickness and sector volumes are based around the ETDRS macula grid protocol.[b] The SPECTRALIS software offers the ETDRS macula grid as an option for analysing these measures, dividing the macula into 9 subfields.[270] The circular grid is centred over the fovea and consists of three concentric rings of diameters 1, 3 and 6mm. The middle and outer rings are further divided into quadrants: temporal, nasal, superior and inferior. (Fig. 3.3) Again, these measures are calculated automatically after selection by the operator. The software processing of the segmentation of the macular volume scan takes approximately 25 seconds.

[b] ETDRS was a multicentre, randomised trial of over 300 patients with diabetic retinopathy (DR), over a 4-year period.[270] It was designed to evaluate the use and effectiveness of laser treatment in DR, but had the additional benefit of defining a number of standards relating to vision and ocular measurements that remain in place today, and help ensure interoperability across clinical trials.

a)

b)

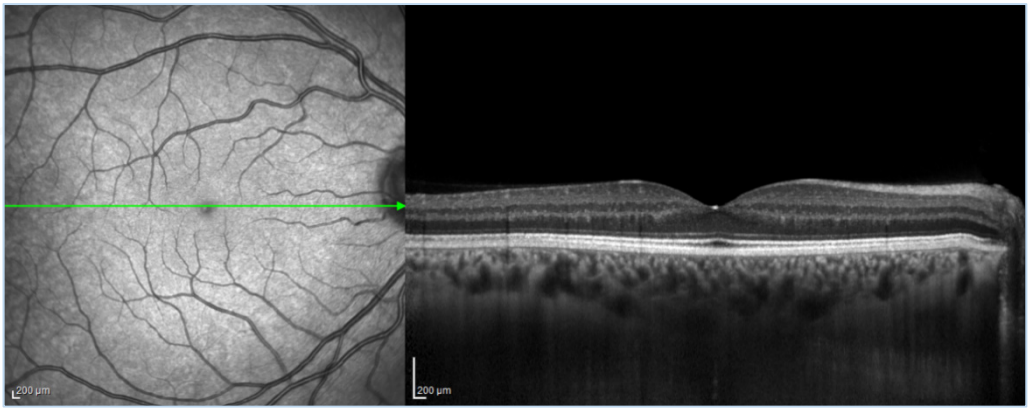

c)

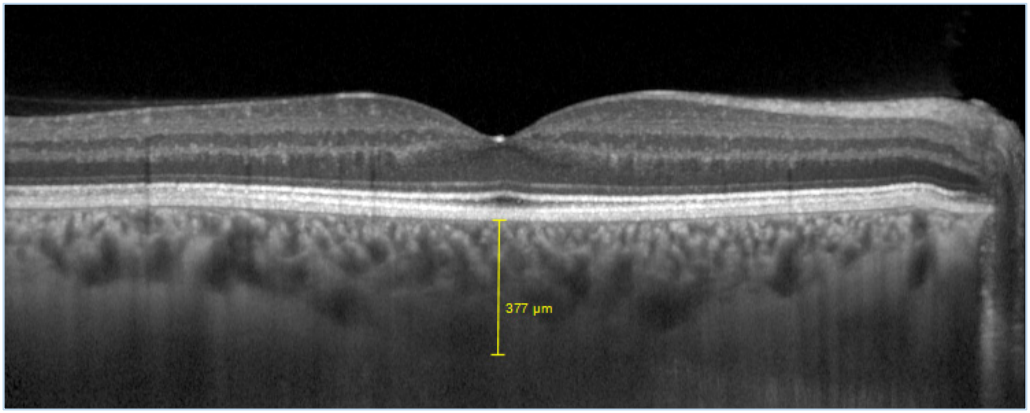

Figure 3.1: OCT scan protocol: horizontal line scan through the fovea, with EDI activated. a) scan reference b) scan image c) choroidal measurement

a)

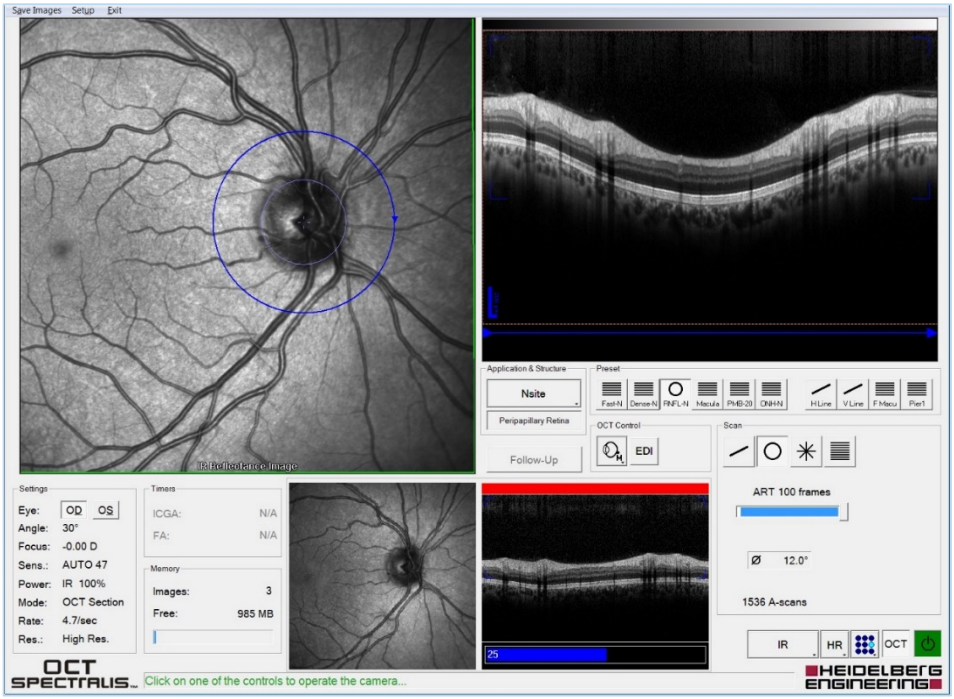

b)

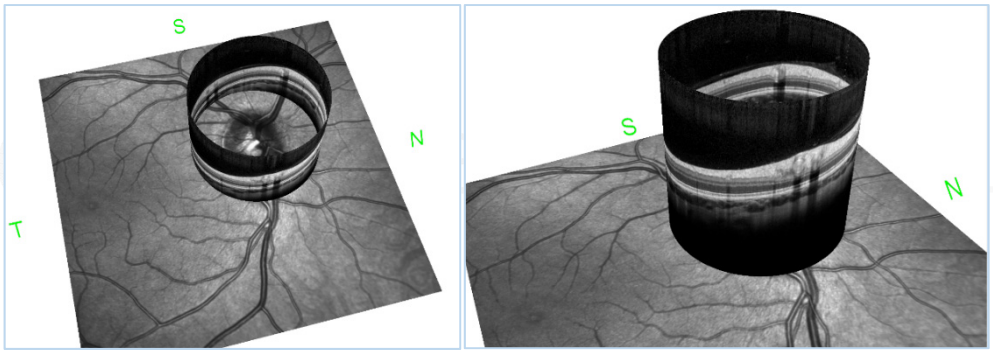

c)

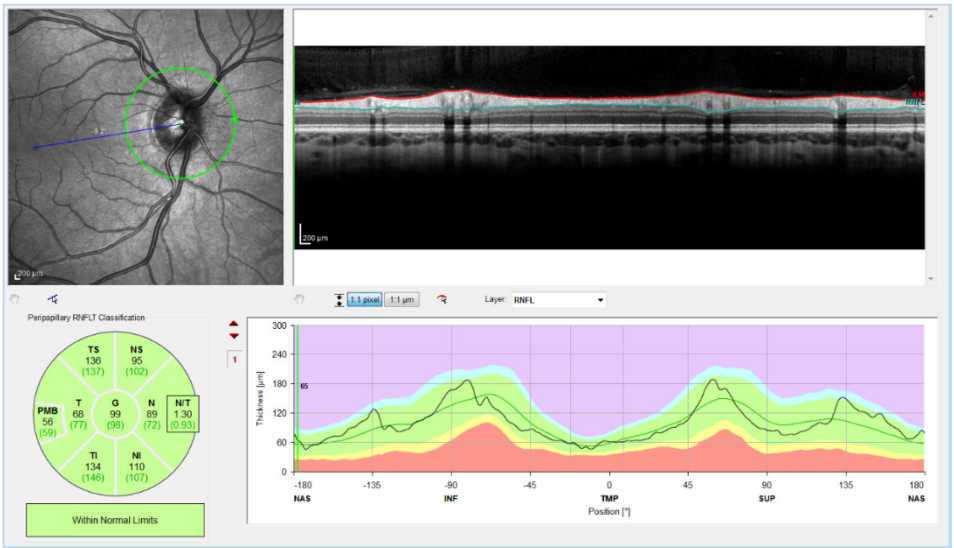

Figure 3.2: OCT scan protocol: peripapillary circular line scan centred over the optic disc, with RNFL segmentation. a) scan reference b) scan image c) RNFL measurement

a)

b)

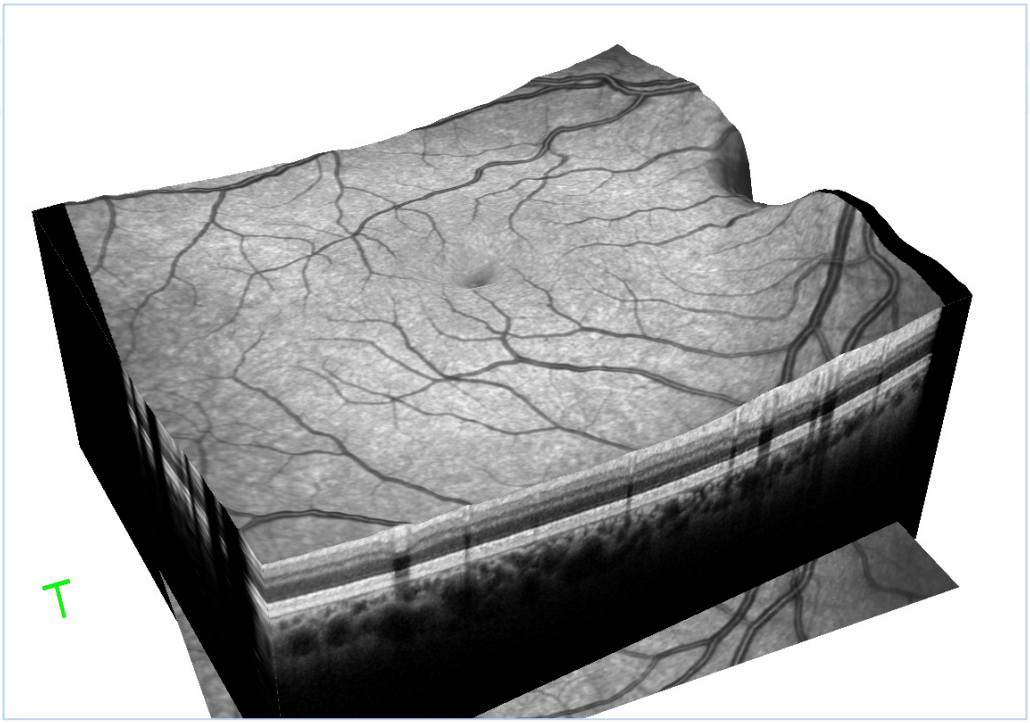

Figure 3.3: OCT scan protocol: macular volume scan centred over the fovea, with GCL segmentation. a) scan reference b) 3D macula reconstruction c) retinal layer segmentation d) scan profile showing full macular thickness e) macular volume measurements f) scan profile showing GCL thickness g) (macular) GCL volume measurements

c)

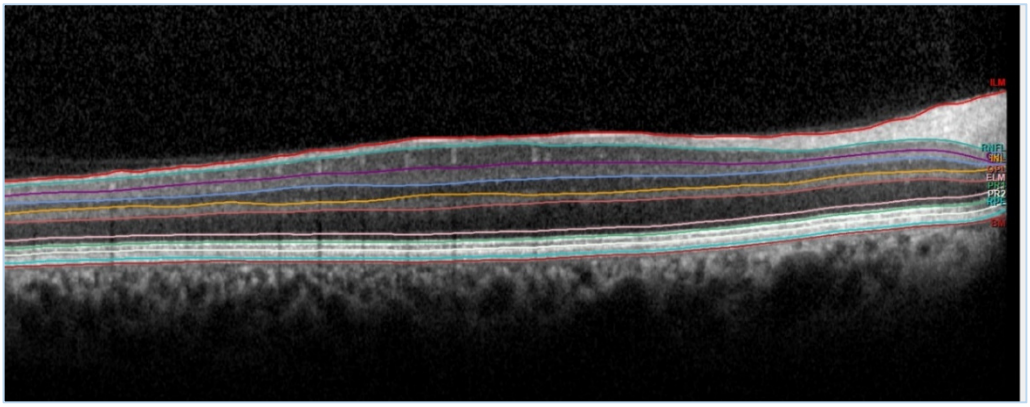

d)

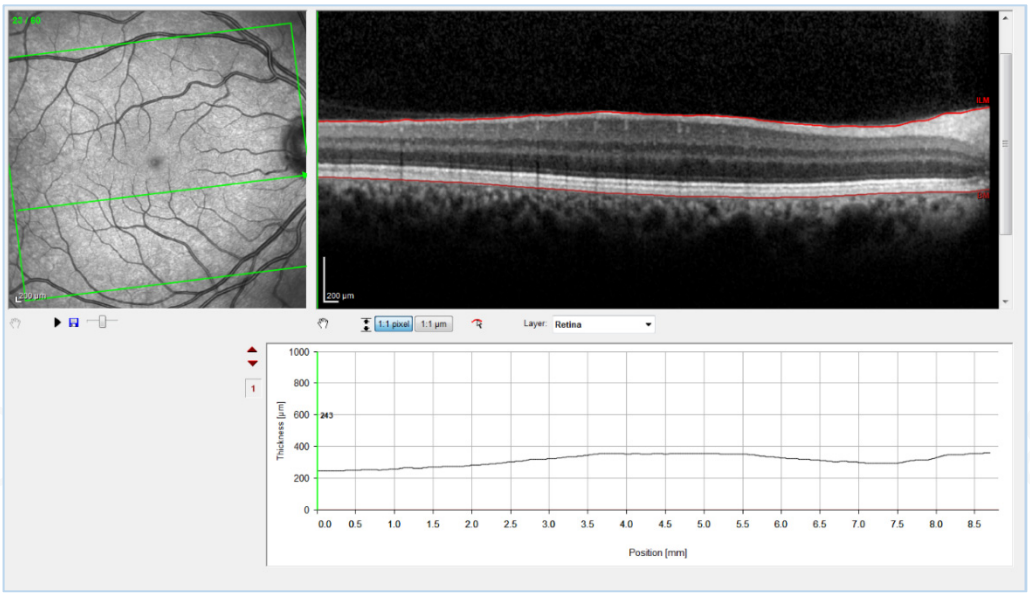

e)

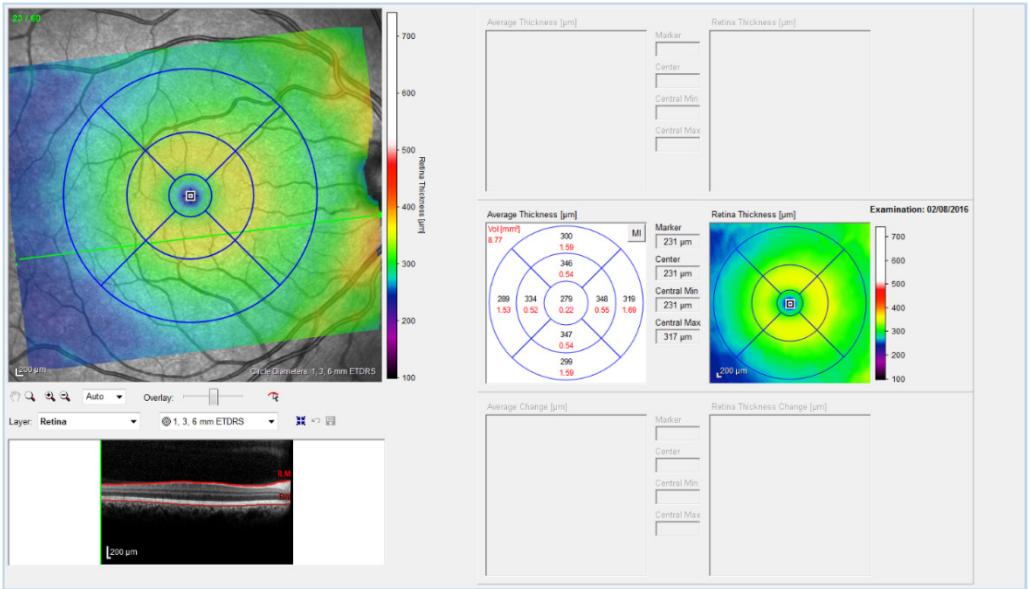

Figure 3.3: continued

f)

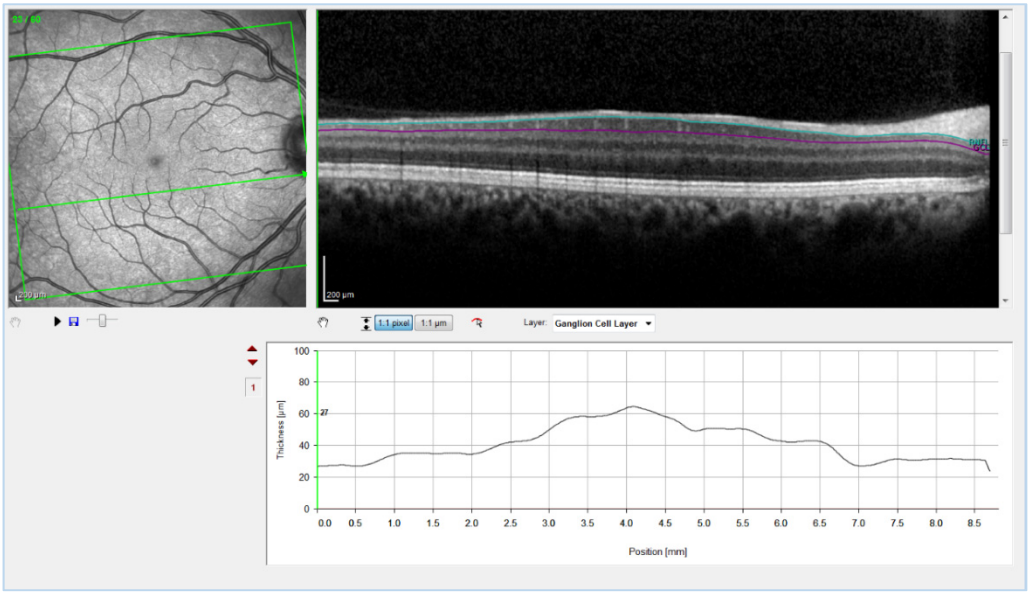

g)

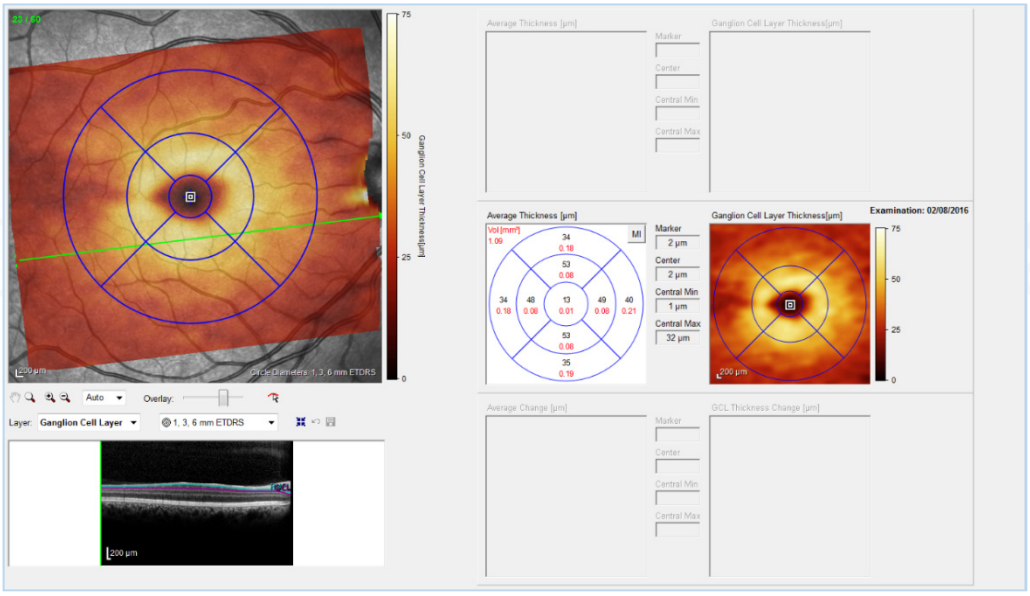

Figure 3.3: continued

OCT image processing

Quality assurance of image

The first stage of image processing is ensuring adequate quality of images. Whilst visual inspection can quickly decide whether an image is satisfactory, more objective assessment is desirable. This has been provided by the international OSCAR-IB criteria for OCT scan quality[271], a prospective multicentre study to develop a consensus on criteria to judge quality in OCT imaging in relation to MS. (Table 3.4) They showed much higher inter-rater agreement on deciding acceptability of an OCT image, when following these criteria, compared to previous general inspection.

Table 3.4: Synopsis of the OSCAR-IB criteria. *[Table from Tewarie et al. PLoS One 2012* [271] *]*

O	Obvious problems not covered by any of the other items. (poor focus, wrong scan protocol, etc.)
S	Is the OCT signal sufficient? Signal strength > 15 (ring and volume scans) with appropriate averaging of multiple scans (ART activated).
C	Is the ring scan correctly centred over the optic disc?
A	Is there an algorithm failure? (correct location of red segmentation lines)
R	Is there visible retinal pathology which may potentially impair the RNFL reading?
I	Is the fundus well illuminated?
B	Is the measurement beam placed centrally? Homogenous outer plexiform layer reflectivity (ring and volume scans)

The process begins during the actual scanning, when a real-time image is seen, and quality concerns visible immediately, permitting some attempt at adjusting the scan or patient. Identification of a poor tear film, or incorrect head position can be corrected. Accurate focus is essential, and should be constantly checked and adjusted, as patient focus/accommodation will alter their lens power and move the image quality out of focus. Media opacity can sometimes be overcome by redirecting the scan off-axis.

Following this, image quality is more objectively assessed. Each scan is automatically allocated a Scan Quality score (out of 40, on the SPECTRALIS OCT) based upon focus, illumination and low noise. The OSCAR-IB criteria recommend a scan quality > 15 for inclusion in subsequent analysis. I set myself a higher threshold of > 25 to ensure as best image quality as possible, based upon my experience with using OCT technology.

Accurate focus is achieved during scanning by manual adjusting the focus control, whilst observing retinal structures with sharp edges, such as the optic disc margin or the retinal vessels. Significant astigmatism will markedly impact the ability to focus, as there is only the facility to adjust spherical focus.

Uniform illumination of the image is achieved by the vertical and lateral movement of the OCT scan head. This becomes an intuitive skill with scanning experience, but is often the main challenge for new users, and a common pitfall for the inexperienced.

During this movement of the OCT scan to achieve uniform illumination, it is preferable to also align the cross-sectional OCT image as close to the horizontal as possible. This assists with avoiding tangential measurement errors, although the automated segmentation algorithms in the SPECTRALIS OCT cleverly seem to cope with any orientation of the OCT image.

There are also scan protocol-specific checks, such as the peripapillary circular scan which requires the operator to accurate locate the scan centrally over the optic disc. This cannot be corrected after the scan has been done, so if the scan has not been placed accurately, it is necessary to re-scan the patient.

Image registration

A key benefit of the Heidelberg SPECTRALIS system is the proprietary TruTrack™ active eye tracking. As well as enabling high-resolution scan images via averaging of repeated imaging of the same region, it ensures inter-visit repeatability by ensuring imaging in the same identical region of the retina. Using the SLO image as a localisation map for image registration, this eliminates any inter-scan variability related to position change of the OCT image.

Scan alignment

The next step of image processing is to ensure correct alignment of the scan measurements, in relation to the eye anatomy.

In the peripapillary circular scan, it is the foveal alignment that corrects for any head or ocular rotation, as well as anatomical variation, to enable the temporal and other zones of the circle to be correctly orientated. The axis between the centre of the optic disc and the fovea is now agreed as the reference axis for defining the sectors (superior, inferior, etc) of the disc / peripapillary region for RNFL analysis.[86, 272, 273]

The automated FoDi (Foveal Disc alignment) software is generally highly accurate, however if it has mislocated the fovea (Fig. 3.4) simple manual correction allows correct placement. (Fig. 3.5) Automatic calculation of sectoral average thicknesses can then proceed, according to the anatomical sectors shown. (Fig. 3.6)

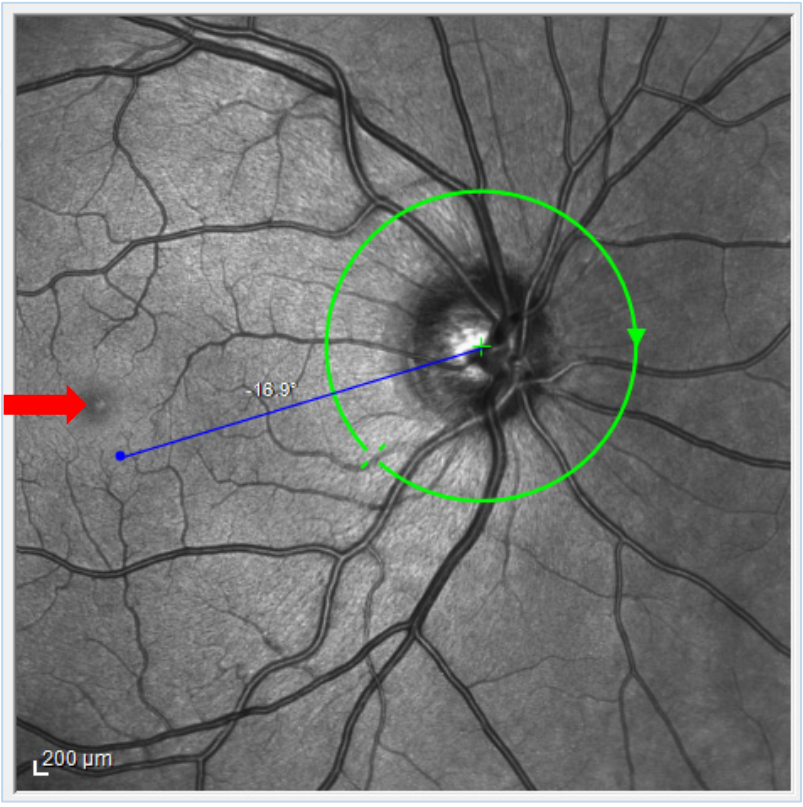

Figure 3.4: Fovea not identified correctly (red arrow marks true foveal location)

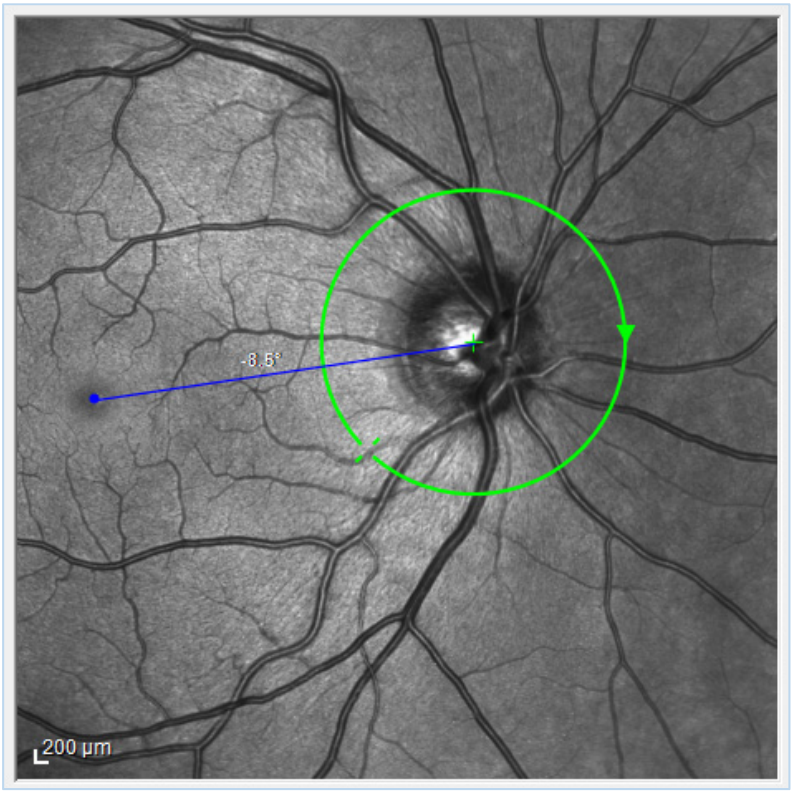

Figure 3.5: Relocation of foveal marker to correct location

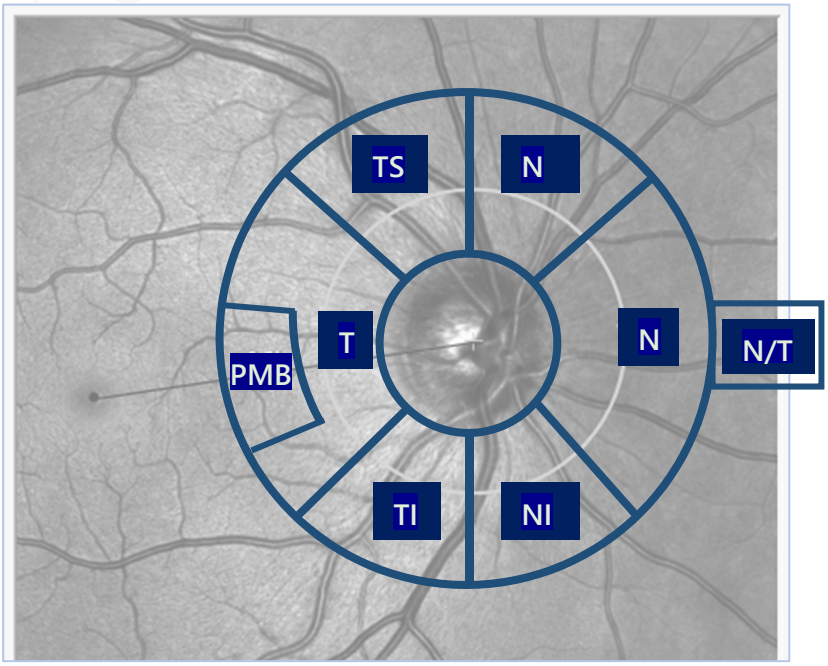

Figure 3.6: Overlay of peripapillary sector classification: TS=temporal-superior, NS=nasal-superior, N=nasal, N/T=nasal/temporal ratio, NI=nasal-inferior, TI=temporal-inferior, T=temporal, PMB=papillomacular bundle

In the posterior pole macular volume scan, the thickness map superimposes a standard ETDRS circular grid pattern, for sector thicknesses and volumes. This grid requires centration over the fovea. Again, the software correctly locates this grid the majority of the time, but small adjustments are occasionally required to precisely locate it centrally over the macula and fovea.

The ETDRS grid may be obviously seen to be misaligned (Fig. 3.7) or a smaller deviation can be identified with the measures of centre and central minimum, which should be identical if the grid is perfectly centrally aligned. The grid can then be moved into correct position (Fig. 3.8) with the thickness and volume measures re-calculated automatically. (Fig. 3.9)

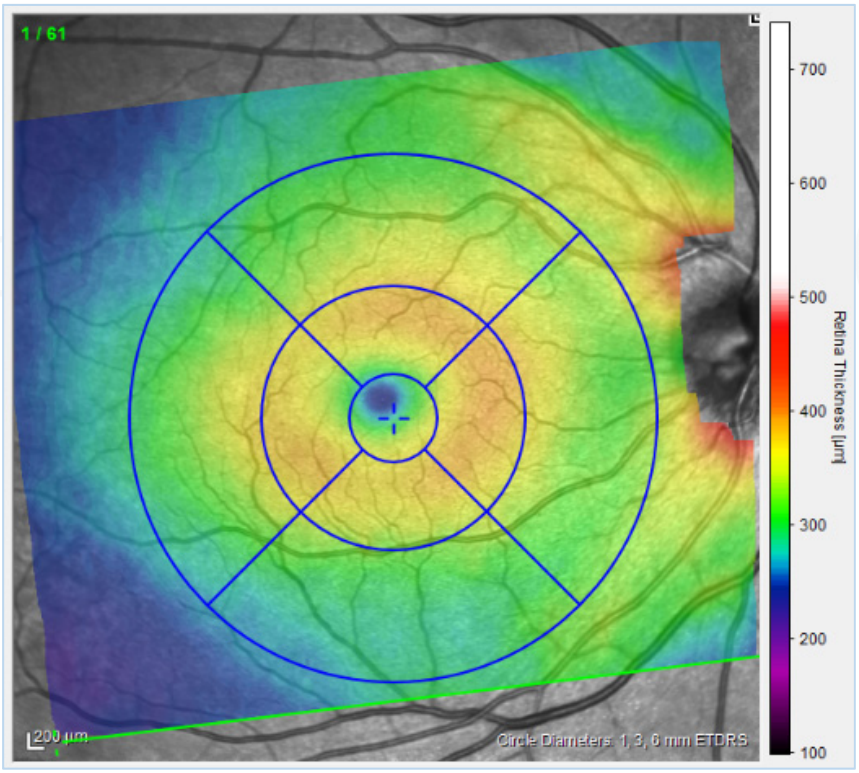

Figure 3.7: Misaligned ETDRS grid

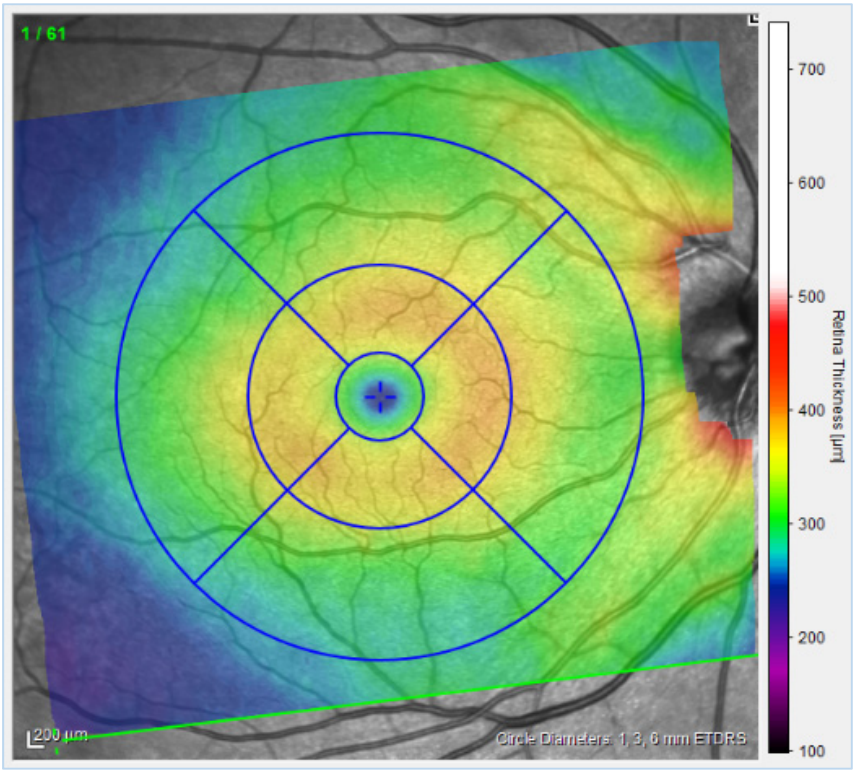

Figure 3.8: Corrected position for ETDRS grid

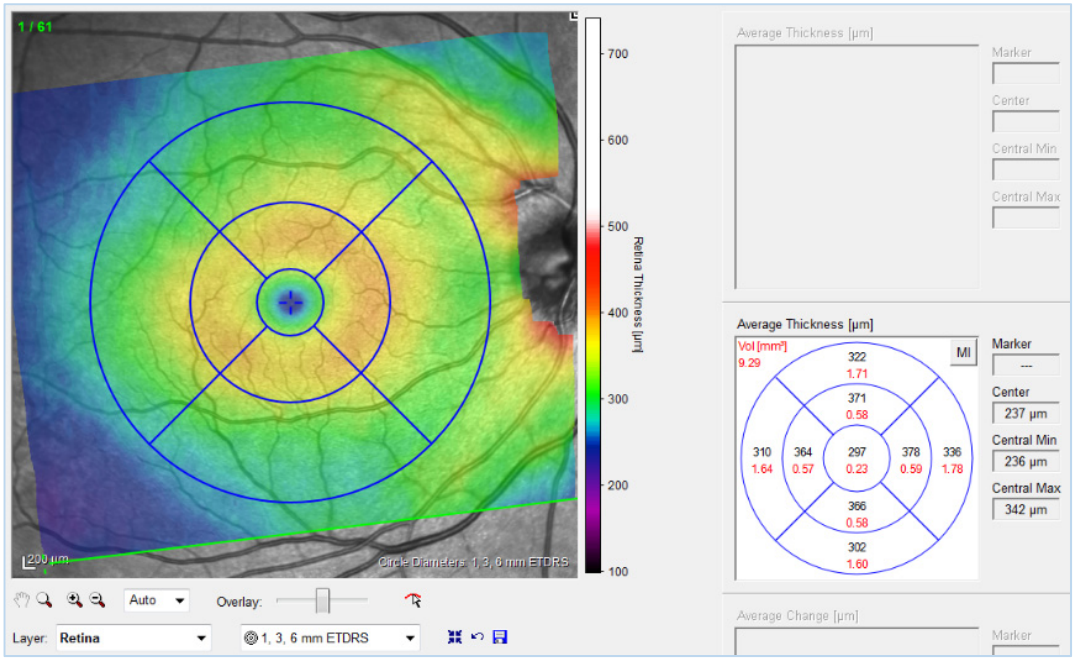

Figure 3.9: Corrected ETDRS grid with sample thickness and volume data

Segmentation errors

The next stage of image processing is to closely examine the automated segmentation of the retinal surface, basement membrane, and intra-retinal layers. Whilst the automated software works extremely well, subtle variations in pathology, or lower quality images, can result in erroneous segmentation lines. These require manual correction, which can be performed at high-zoom to minimise user error.

Around 5% of images required some intervention with the automated segmentation lines, usually a single-point correction, and therefore of low impact on the overall thickness or volume measurement, regardless of error correction. However, a few images required a greater amount of correction, following erroneous identification of the posterior vitreous face as the inner limiting membrane. (Figs. 3.10, 3.11)

The segmentation editor (Fig. 3.12) facilitates correction by a zoomed-in image, and outline of the segmentation line with point reference spots that can be manually moved, pulling the segmentation line into correct alignment and resultant thickness measures recalculated. (Figs. 3.13, 3.14)

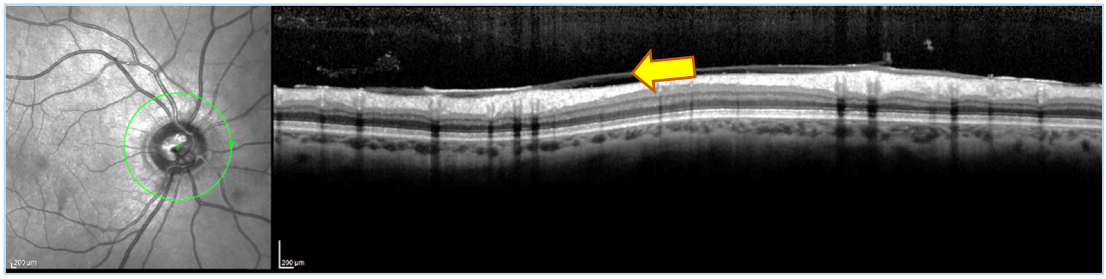

Figure 3.10: Patient with thickened posterior vitreous face (marked with yellow arrow)

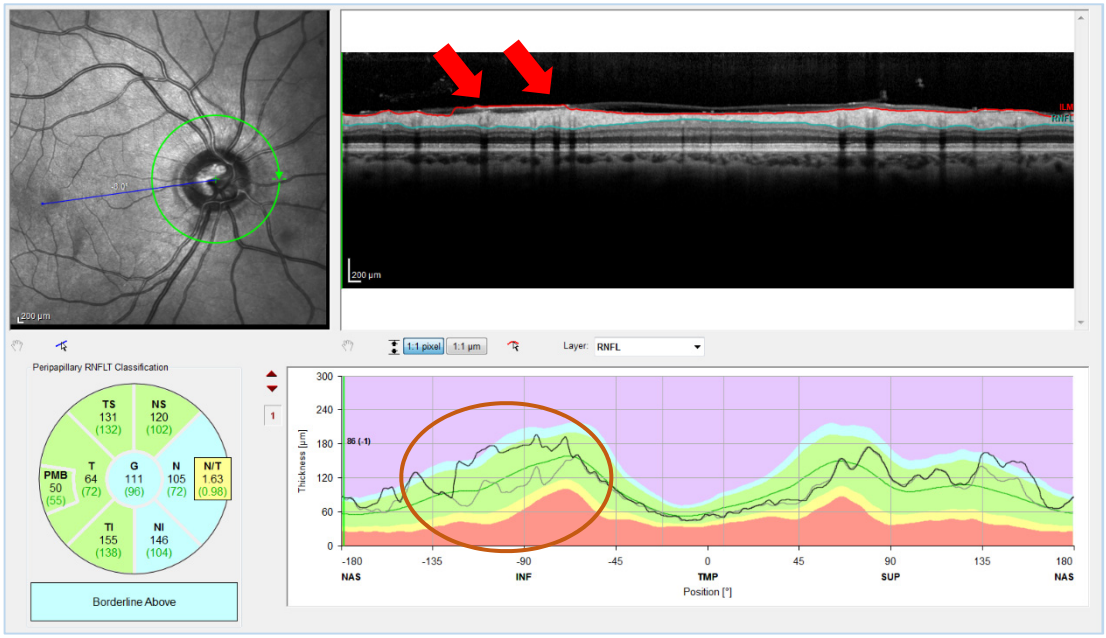

Figure 3.11: Automated segmentation, showing erroneous identification of inner retinal limit, in an area of thickened posterior vitreous face (marked with red arrows), and as a result, over-measuring nasal/nasal-inferior RNFL thickness (circled)

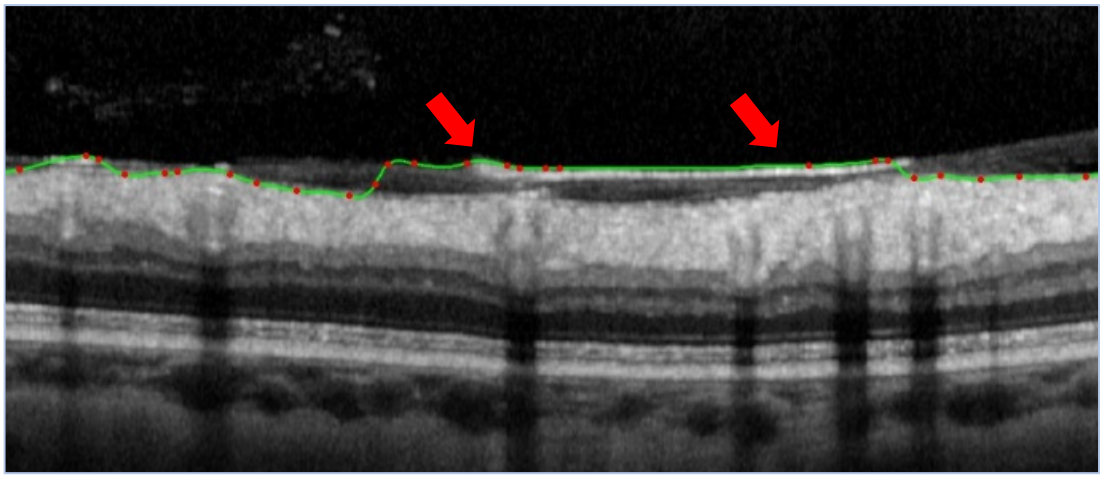

Figure 3.12: Segmentation editor: zoomed view of segmentation error - wrongly interpreting thickened area of posterior vitreous face as the inner retinal surface. Segmentation line highlighted in green, ready for manual correction by moving red dot points to correct location

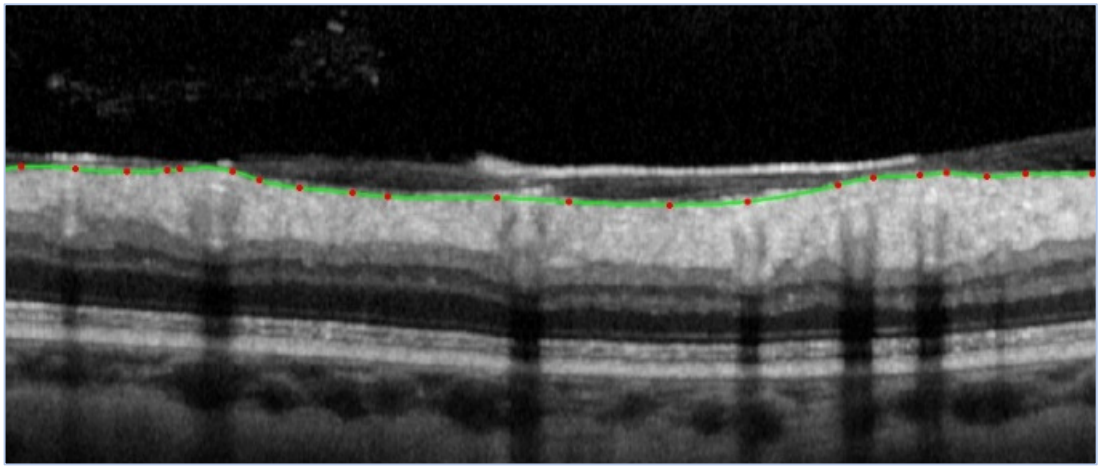

Figure 3.13: Segmentation editor: zoomed view of segmentation error - now corrected

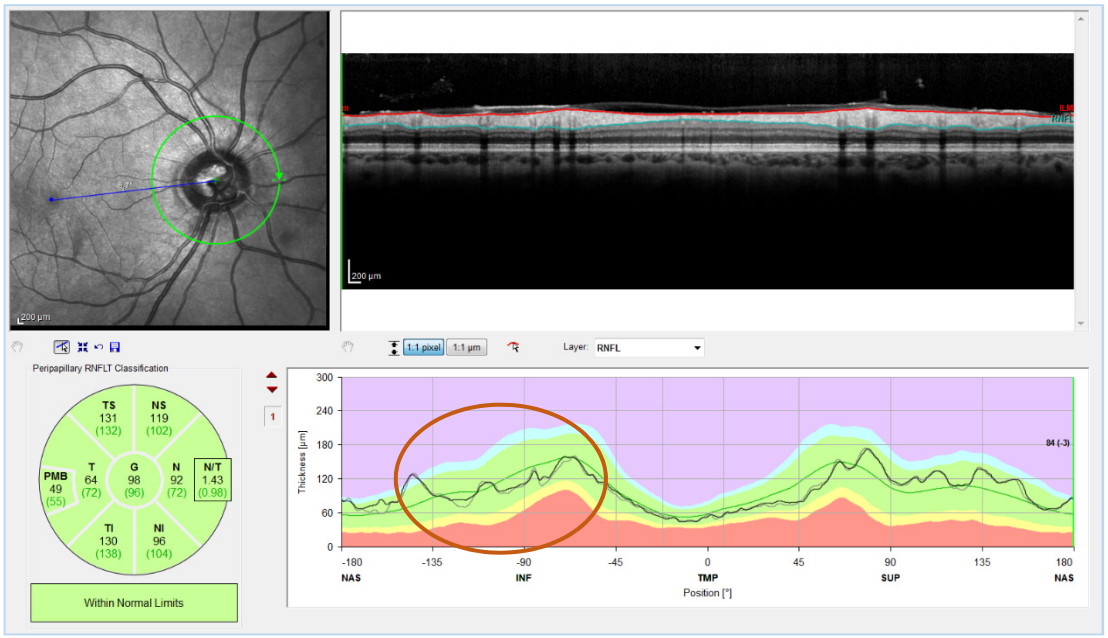

Figure 3.14: Automated segmentation, now showing correct segmentation of inner retinal limit, with adjusted RNFL thickness graph

Data extraction

The SPECTRALIS OCT software currently supports only a limited data export option, into an XML file. As not all the required OCT data is exported in this process, and the comma delimited extraction requires reformatting to align with a patient-orientated database, the data handling in onwards transfer could increase the potential for transcription errors, and so I proceeded with manual data transcription from the OCT into a separate database.

Manual transcription is extremely laborious, but has some additional benefits. With the necessity to open and display each imaging episode, with original image and data, there is a final opportunity to review image quality and processing.

The potential for transcription error when re-typing a very large number of data values is low but present. Familiarity with the expected range of data values for each measurement reduces this potential for error, and is an advantage of me performing the data entry myself, rather than someone unfamiliar with the data values.

Audit

To check for typographical or transposition errors during transcription of data values, I also performed an audit of the data transcription, re-checking the data of a random sub-set of 100 images.

Within this sub-set there were zero errors in the data, and no transposition errors.

Nevertheless, a clear need for future software versions of this device is an automated and configurable data export function.

Modulation of vascular analysis software

Note: Excerpts of this section have been published – in "Modulation of retinal image vasculature analysis to extend utility and provide secondary value from optical coherence tomography imaging", JR Cameron, L Ballerini, C Langan, C Warren, N Denholm, K Smart, TJ MacGillivray.
Journal of Medical Imaging. 3(2):020501. (2016) doi:10.1117/1.JMI.3.2.020501

Thanks are due to:
Clare Langan, Claire Warren, Nicholas Denholm and Katie Smart – students who carried out the training image segmentation, and the processing for the evaluation
Tom MacGillivray and Lucia Ballerini – VAMPIRE programmers

Vampire evolution

VAMPIRE (Vascular Assessment and Measurement Platform for Images of the REtina) is a semi-automatic bespoke software platform, developed under an academic collaboration between the University of Edinburgh, University of Dundee, Universita degli Studi Di Palermo and Universita degli Studi di Verona.[112, 274] This group comprising software engineers, and specialists in ocular imaging and image analysis, has worked together over the past decade developing and refining the software algorithms and user interface to create an established tool that is now integral in many clinical studies involving retinal imaging. Analysing conventional digital colour fundus photographs, it provides efficient quantification of standard retinal vascular parameters as well as the complexity of the visible vascular network (through fractal analysis).

With established utility in cerebrovascular disease[124], cognitive ageing[103], and other chronic diseases[118], VAMPIRE was also the first tool to be used in assessing fundus camera images held in the UK Biobank – the largest retinal image repository in a prospective population-based medical data resource – to deliver computational quantification of retinal vascular parameters in relation to cardiovascular disease.[275]

Evaluation and validation

Validation of image analysis algorithms is essential if the results are to be clinically meaningful.[276]

VAMPIRE has undergone continuous evaluation with each extension and study such as with automatic optic disc and fovea detection[277, 278], retinal arteriole and venule classification[279], and measurement of vessel calibre.[280, 281]

Modulation for other modalities of fundus imaging

Modulation of the software for the purposes of analysing other types of fundus image, such as those produced by a scanning laser ophthalmoscope (SLO), to provide automated vascular measures as required, is also a goal of the VAMPIRE project. A recent report described the process of adaptation to images captured by the ultra-widefield Optos P200C SLO device.[280] This method involved the development and validation of a new vessel detection algorithm incorporating multi-scale matched filters, a neural network classifier and hysteresis thresholding.

The Heidelberg SPECTRALIS OCT being used in this study is a dual-modality imaging device. As well as the 4μm resolution cross-sectional OCT image, the instrument also simultaneously acquires a SLO image. This is a sharp, high-contrast confocal SLO, with a viewing angle of 35°, utilizing a laser light of 785nm, and generating an image of 1536×1536 pixels. It is primarily used for guiding location of the OCT imaging and enabling image registration for follow-up scans, ensuring the same precise location is re-imaged. However, there is potential to evaluate the retinal vessels appearing in these SLO images in much the same way as previous work featuring standard fundus camera photographs.

This would add value to the already acquired patient imaging, and provide a unique opportunity for the development of dual-mode image analysis derived from a single instrument and a single patient imaging event. As well as efficiency and patient convenience, this development brings additional advantages: it allows direct point-to-point correlation between the OCT and SLO image, and also the SLO-generated fundus image is of high contrast potentially facilitating more accurate measures of the retinal vessels. This will provide a rich dataset for my study, featuring reliable vessel morphology data alongside neuroaxonal measures, in an efficient, patient-friendly way.

In partnership with the Vampire software development team, I therefore sought to adapt the software for use with the SLO images generated by the SPECTRALIS OCT device, to provide the vascular measures for this study, from the same patient episode of retinal imaging.

Software modulation

The SLO images from the SPECTRALIS are very different from those produced by the Optos SLO device – a different field-of view, image resolution and illumination source (the SPECTRALIS utilizes near-infra-red light, and requires no visible light flash.) Therefore, the previous modulation of VAMPIRE for Optos ultra-widefield imaging described above could not be used.

Binary map

The process for vessel segmentation therefore started with the current VAMPIRE (version 3.0) for colour fundus images. The processing algorithms were then retrained for SPECTRALIS SLO images.

All algorithms were implemented in Matlab (The Mathworks Inc., USA).

The uneven contrast of these SLO images prevented the use of raw pixel classification (for vessel/not-vessel classification of each pixel), therefore an algorithm based around background correction followed by filtering was used to even out the contrast variation across the image. For automatic detection of vessels, a 2-D Gabor wavelet approach for fundus camera images was adapted to emphasize the appearance of vessels captured with SLO, followed by supervised pixel classification with a Bayesian classifier.[282]

This vascular detection algorithm was retrained to work on the SLO images by manually delineating vessels in 16 images (randomly selected from a study using the SPECTRALIS OCT), taking 1,000,000 samples of pixels with 6 features (i.e. original grayscale intensity and response to Gabor filters of size 2-6 pixels) to create a supervised classifier which is applied to new images to automatically create pixel-by-pixel maps of the vessels.

Further post-processing based on mathematical morphology was also adapted to vessels in SLO images where the central reflex is more evident than in images acquired by a fundus camera. This caused misclassified gaps in vessels with the supervised classification technique, and this effect was lessened by removing such regions or holes with size less than 200 pixels to create an improved map of the vessel. This size was chosen following experimental investigation. Vessel contours were deemed satisfactory at pixel level, therefore no spline-fitting[283] process was required.

Using this vessel map, VAMPIRE creates a tree-like representation of the vasculature as a pre-processing step for performing vascular measurements. (Fig. 3.15)

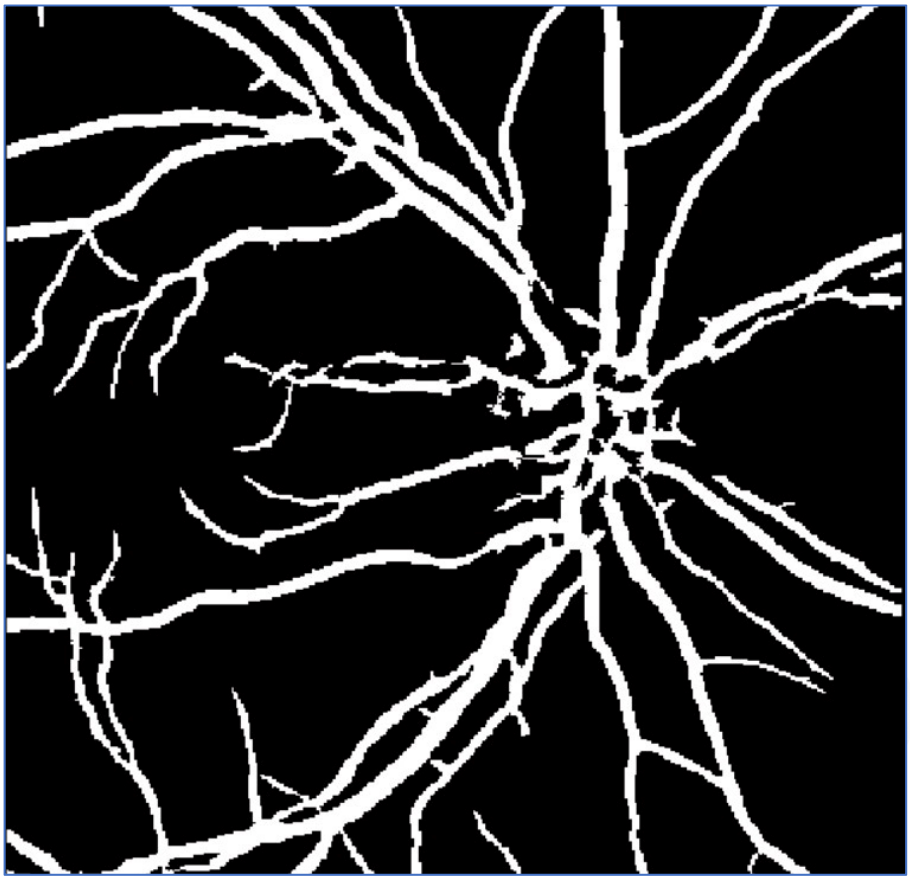

Figure 3.15: VAMPIRE version 3.1.1: binary map of retinal vessels

Vessel measurement

From the vessel tree the software automatically selects the 6 widest arterioles and venules crossing zone B (Fig. 3.16) and measures vessel calibres using a supervised algorithm[281] that was retrained on these SLO images by manually annotating widths at 200 locations in 5 images.

These measurements were used to calculate the well-recognized summary parameters – central retinal arteriole equivalent (CRAE) and central retinal venule equivalent (CRVE) – yielding the arteriole to venule width ratio (AVR).[98] Similarly, for tortuosity, VAMPIRE selects the 6 widest arterioles and venules crossing zone C, evaluates the

tortuosity for each using an established technique[284] and calculates the median values (plus standard deviation and range).

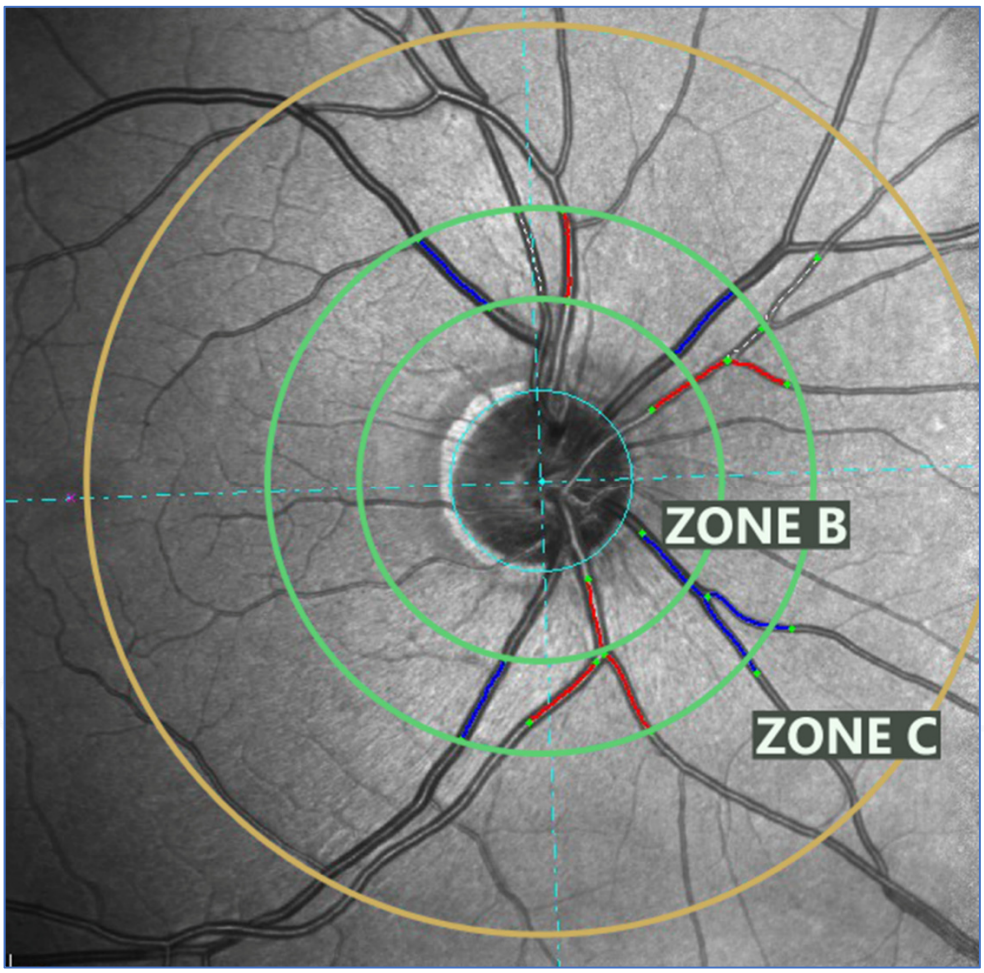

Figure 3.16: VAMPIRE version 3.1.1: Overlay of the standard set of circular measurement zones commonly used in the analysis of fundus camera images – zone B which is the ring 0.5-1 optic disc diameters away from the disc margin, and Zone C which is the ring extending from optic disc boundary to 2 optic disc diameters away.

VAMPIRE automatically detects and selects the 6 widest arterioles (red) and venules (blue) crossing zone B to calculate AVR, CRAE and CRVE. The vessels in zone C (not marked in this example) were used to calculate arteriolar and venular tortuosity.

Automated identification of vessels (as either arteriole or venule) has not yet been implemented in this modulated version of VAMPIRE, therefore the operator is still required to click and identify the vessels. Whereas VAMPIRE for analysis of fundus camera pictures features automatic classification, this is facilitated by the colour

information inherently contained in a fundus photograph, where the vessels have distinct and measurable differences in colour features.

If the operator is unsure of a vessel classification or believed the vessel to have been detected incorrectly, or erroneous segmentation, it can be deselected. In such cases the software provides a replacement vessel that was the next widest in calibre. This manual review process takes approximately 1-2 minutes per image.

The final modulated software user interface is shown below. (Fig. 3.17)

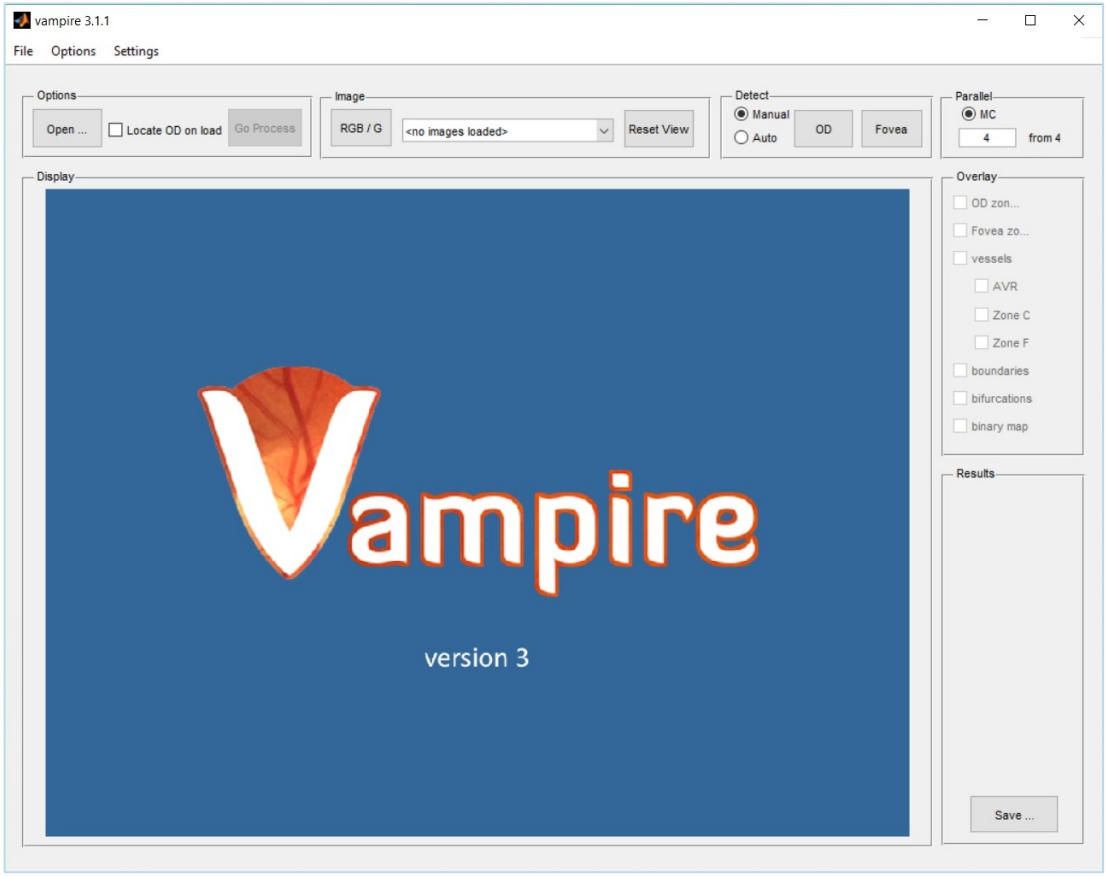

Figure 3.17: VAMPIRE version 3.1.1: user interface

Inter-operator evaluation

The modulated software was evaluated by assessing inter-operator reliability.

Methods

We obtained optic disc centred SLO images from 78 participants - 48 males, 30 females, all white Caucasian, and an age range of 39-69 years (mean 52) - using the SPECTRALIS OCT device. We also employed the use of two students as operators of the software, who received training on the use of the software, but had not previously had experience of retinal vessel analysis.

Each image was uploaded into the modulated VAMPIRE software. The optic disc and fovea were manually selected by the operator. The software then creates a circular approximation to the optic disc outline and also places the standard set of measurement zones used in conventional analysis of fundus camera pictures[98], as previously described.

The two operators were blinded to each other's use of the software and a comparison between their results was assessed as an outcome measure of the successful modulation of VAMPIRE to these SLO retinal images. Inter-operator reliability was assessed using intraclass correlation coefficients (ICC) and a Bland-Altman approach to display the extent of agreements.

Results

Of the 78 images available, 2 were not analysed due to insufficient image quality. A further 2 participants' images were not included due to insufficient vessel selection (a selection of less than 3 of either arterioles or venules was deemed insufficient for accurate analysis).

Each operator analysed the images independently, recording values for AVR, CRAE, CRVE, arteriolar tortuosity and venular tortuosity. The total manual operator time for these 78 images was around 3 hours.

The ICCs were > 0.9 for all metrics demonstrating very high reliability and repeatability of these measurements with the modulated software. (Table 3.5)

Table 3.5: VAMPIRE evaluation: intraclass correlation coefficients (and 95% confidence intervals) for absolute agreement between two operators, of the retinal parameters.

	AVR	CRAE	CRVE	A tortuosity	V tortuosity
Intraclass Correlation Coefficient	0.961	0.936	0.961	0.955	0.958
95% CI	0.939-0.975	0.900-0.959	0.938-0.975	0.930-0.971	0.934-0.973

The Bland-Altman analysis demonstrated a high level of consistency between the operators, for all five measures. (Fig. 3.18) The narrow limits of agreement seen in all five plots provides reassurance regarding the inter-operator reliability of the modulated software.

In addition, the low level of image rejection is reassuring, given the challenge of adapting the software to a new fundal image representation that whilst recognizably similar to the human viewer, represents greater challenge to the software interpretation of vessel and background.

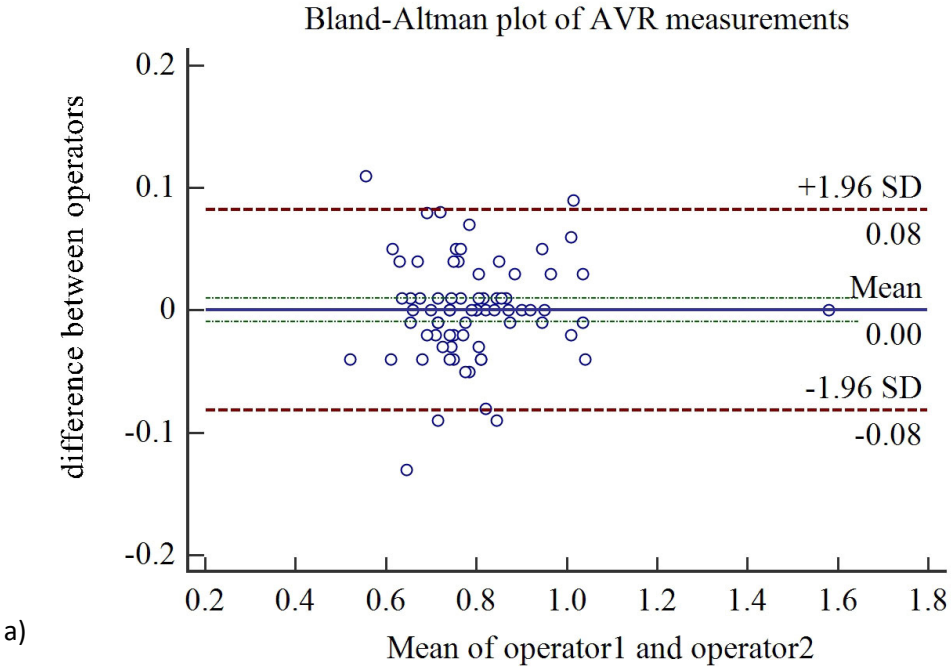

a)

Figure 3.18: Bland-Altman plots of agreement between two operators (with 95% CIs for limits of agreement) for a) AVR, b) CRAE, c) CRVE, d) arteriolar tortuosity and e) venular tortuosity

b)

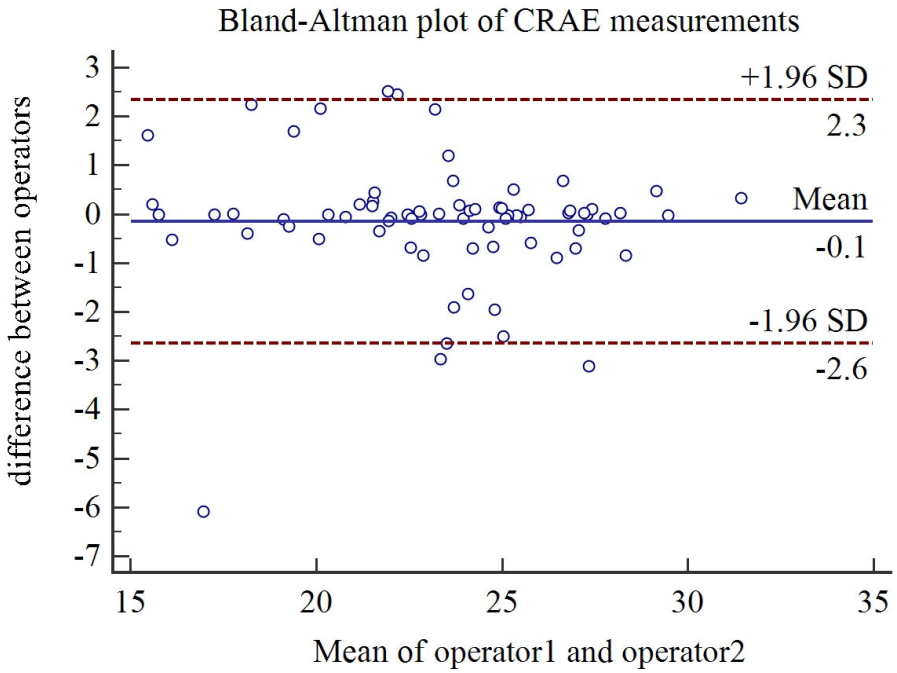

c)

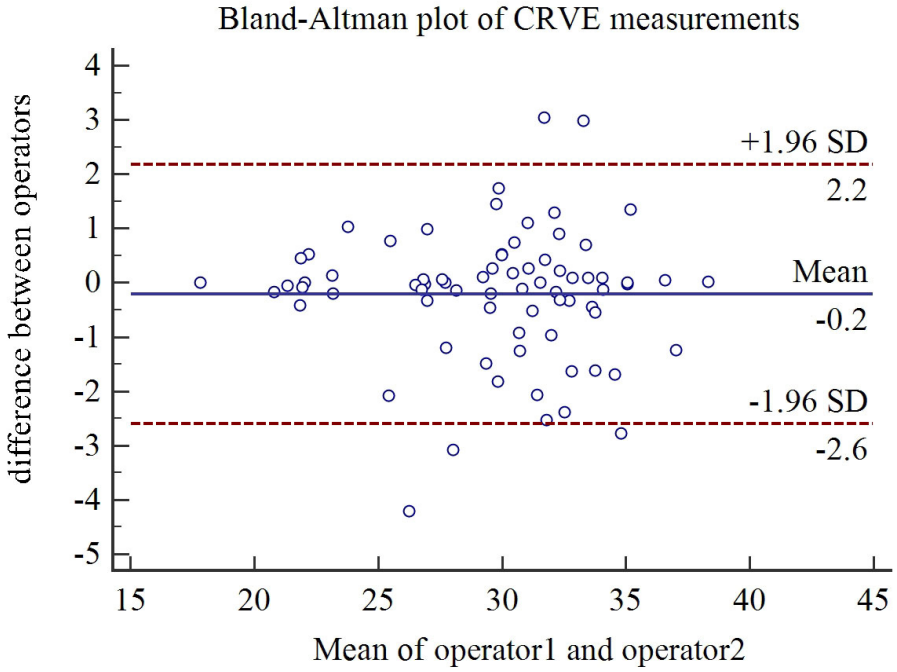

Figure 3.18: continued

d)

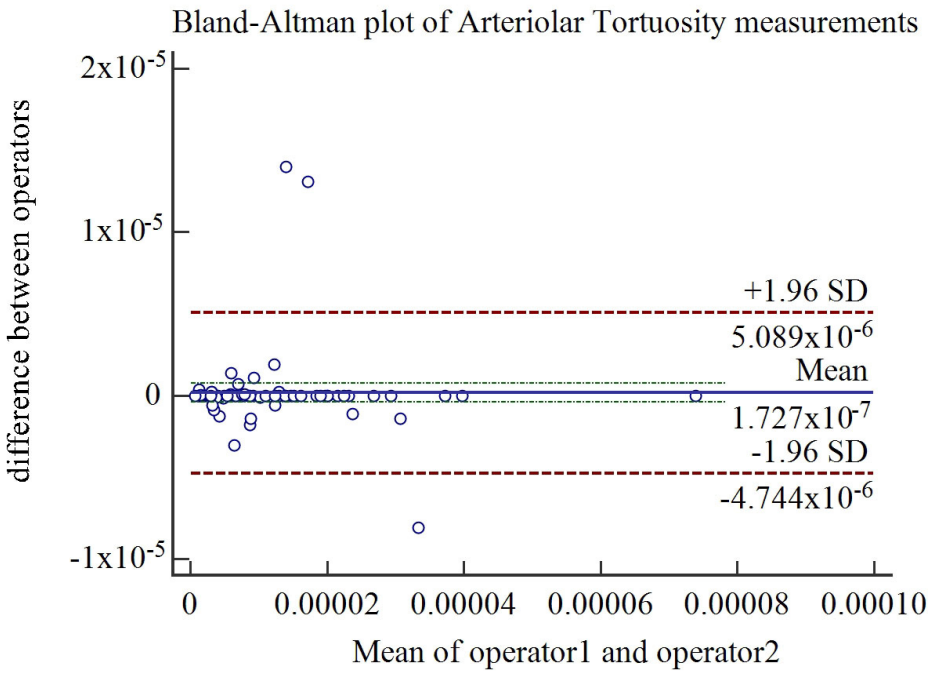

e)

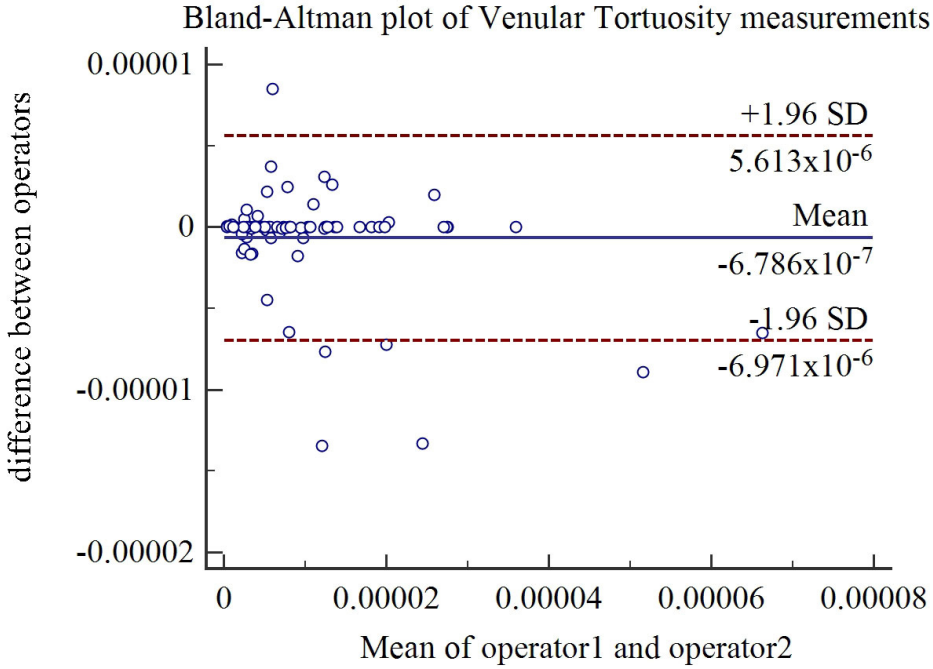

Figure 3.18: continued

SLO image analysis

Image extraction

The SPECTRALIS OCT machine features a high-resolution scanning laser ophthalmoscope (SLO) which generates a high contrast grayscale fundus image, for the purposes of scan localisation and tracking. The peripapillary circular OCT scan is centred over the optic disc, and provides the most retinal vessel content - as well as being the commonest used fundus location for vessel analysis.

This SLO image can be extracted from the OCT scan file, and exported as a single image: a high-resolution (1536x1536 pixels) uncompressed TIFF image file, of ~ 7MB file size. No brightness or contrast enhancement is applied to the image. (Fig. 3.19)

Figure 3.19: Scanning laser ophthalmoscope (SLO) image, extracted from OCT peripapillary scan, and exported as a high-resolution, non-compressed image.

Image processing

The processing of the SLO images takes place within the newly modulated VAMPIRE software platform, version 3.1.1.

Whilst the software is capable of batch processing many images, this quickly becomes processor intensive and RAM hungry, and therefore small batches of 8-12 images are more manageable, and avoid potential slowdown crashes, or operator frustration.

However, it does feature parallel processing for systems with multi-core processors.

Localisation of landmarks

After loading the images, the operator is required to first identify the optic disc and fovea. (Fig. 3.20) These steps are automated in the general version of VAMPIRE, but have not been fully adapted for SLO images as yet. Nevertheless, it is a quick step, and has the additional benefit of quality checking the SLO images as the operator proceeds.

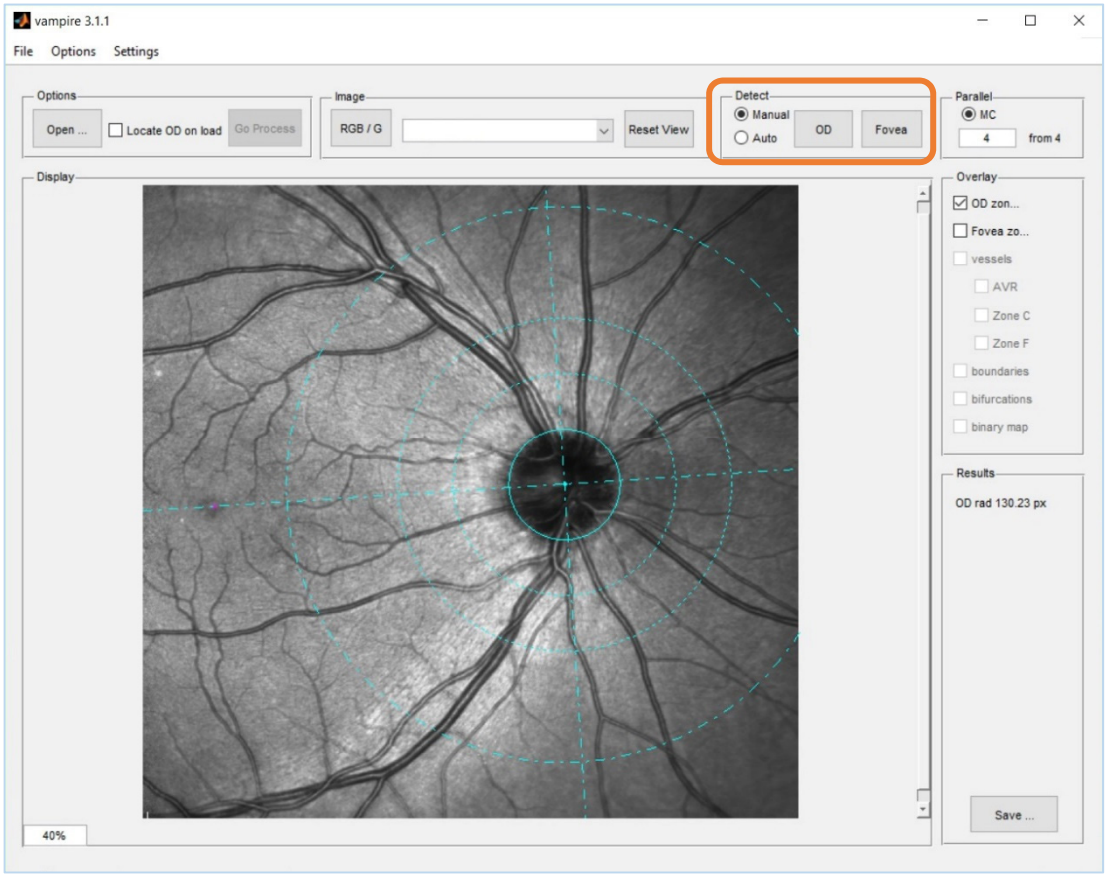

Figure 3.20: VAMPIRE: manual annotation of the optic disc and fovea.

After the annotations are completed for all images in the batch, the automated processing can be started by clicking 'Go Process'. (Fig. 3.21)

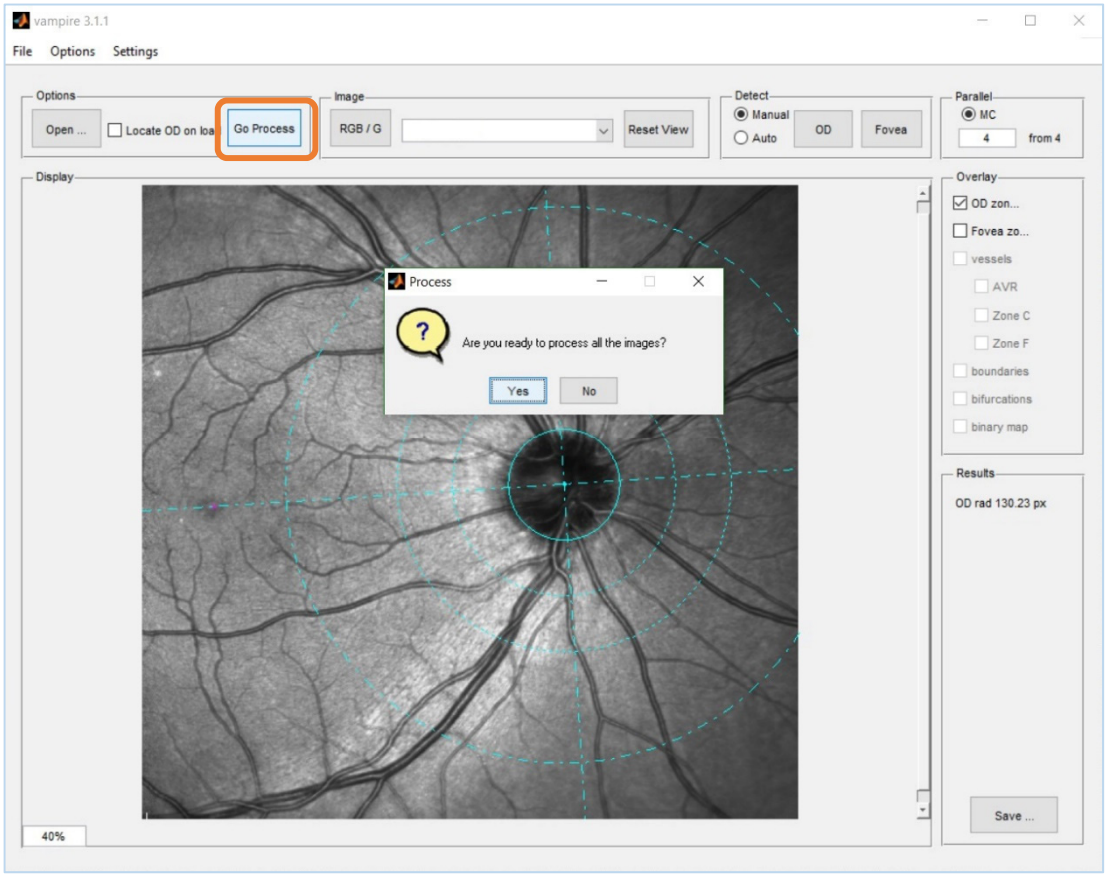

Figure 3.21: VAMPIRE: automated processing of retinal image.

Automated generation of binary map

The automated processing takes approximately 10-17 minutes per image. There is no operator intervention during this process. The processing comprises 4 stages: preprocessing, segmentation, creating (a binary) tree and measuring. (Fig. 3.22)

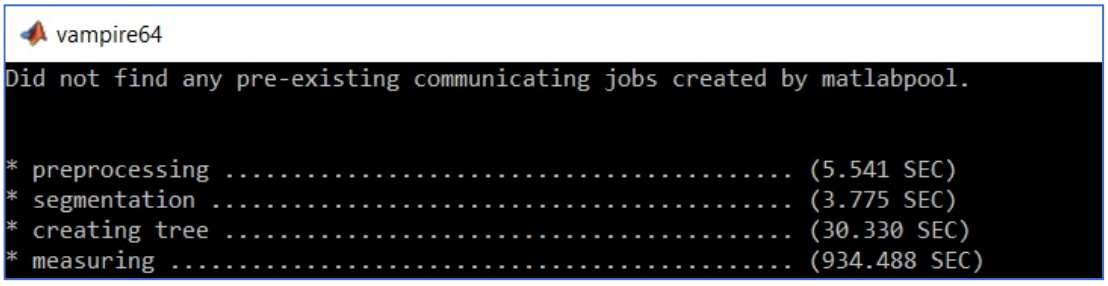

Figure 3.22: VAMPIRE: image processing progress indicator window.

The result is a generation of a binary map of the retinal vascular tree, marking all the vessels that the processing has identified and measured. (Fig. 3.23) At this stage the 'Results' window is inaccurate, as vessels have not yet been identified or selected for inclusion.

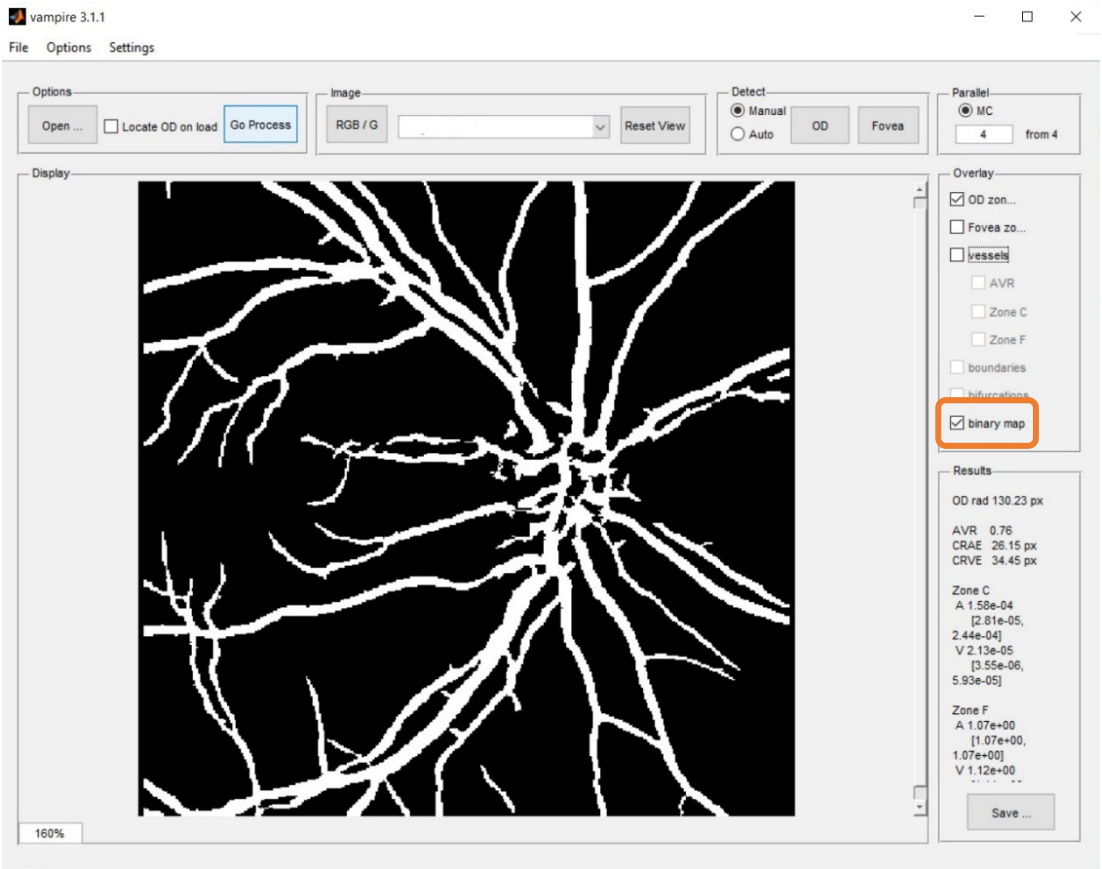

Figure 3.23: VAMPIRE: retinal vascular binary map.

Arteriole / venule classification

The operator is then required to manually identify each vessel as arteriole or venule. The software has randomly assigned this classification, with red segmentation lines denoting arteriole, and blue segmentation lines denoting venule. A single click on each vessel line changes the designation. When complete, the colour coding neatly matches the vessel designations across the vascular tree. (Fig. 3.24)

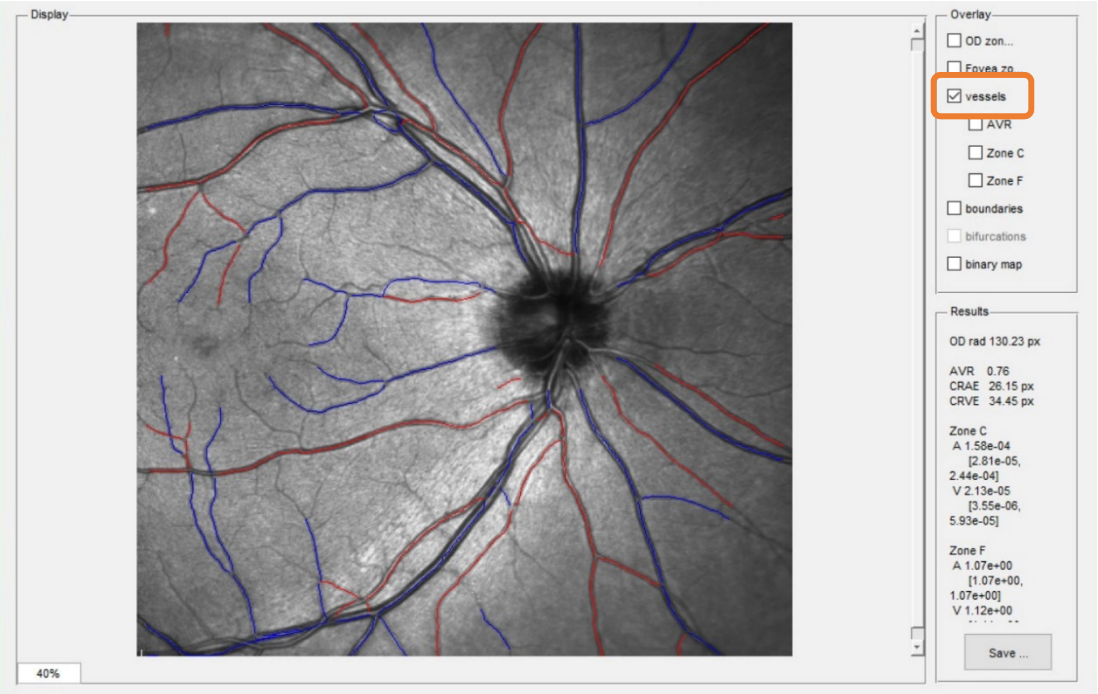

Figure 3.24: VAMPIRE: red and blue vessel designations for arterioles and venules.

Segmentation errors

After extensive beta-testing and feedback with the modulated VAMPIRE software, errors have been reduced to occurring very infrequently.

If a segmentation error is identified, such as linking two crossing vessels as a single vessel with a 90° turn (Fig. 3.25) the vessel segment(s) can be excluded from further analysis by clicking on the segment and selecting 'Delete'.

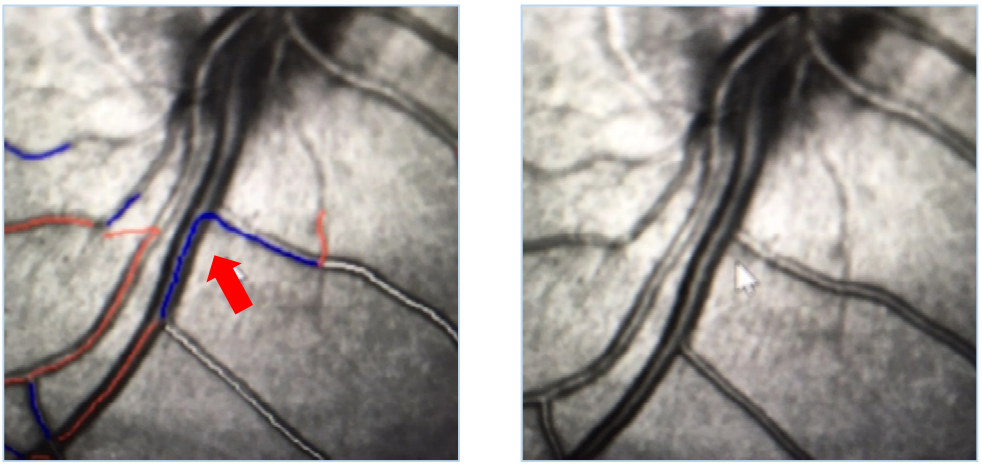

Figure 3.25: VAMPIRE: segmentation error - identifying and labelling two crossing vessels as a single (angled) vessel segment.

Calculation of vessel metrics

The vessel measurements produced by this version of VAMPIRE are the same measures and core calculations as for the colour fundus images version, which have been well tested and evaluated.[112] One improvement in the user interface with the recent software development is the real-time vessel metrics on display next to the image. As the operator adjusts the vessel designations as arteriole or venule, the software automatically calculates and updates the Results window, for the required vessel measurements in accordance with the standard zone locations.

CRAE, CRVE

The central retinal arteriolar equivalent (CRAE) and central retinal venular equivalent (CRVE) are automatically calculated. During image processing, the continuous vessel widths of all the vessels in the binary map are stored. To calculate the CRAE and CRVE, the six thickest arterioles (and venules) in zone B are used, and their continuous thickness averaged for that segment. (Fig 3.26)

Figure 3.26: VAMPIRE: six arteriole and six venule segments within Zone B selected for CRAE, CRVE and AVR calculation. (Thick coloured lines are the six thickest, and used for calculation.)

These six segment calibre measures are then averaged, but with weighting given depending upon the vessel segments' bifurcation geometry. These so-called branching coefficients allow us to adjust for vessels with a larger calibre because they have more

bifurcations distally. Modified algorithms to account for these different coefficients and allow weighting for averaging the segments were initially reported by Knudtson[98] and based upon the Parr-Hubbard formaula[285] but VAMPIRE incorporates its own modification of these.[286] The units for the CRAE and CRVE measures are in pixels.

AVR

The arteriovenous ratio (AVR) is simply the quotient of the ratio between CRAE and CRVE. It is automatically calculated by VAMPRIE, and reported to two decimal places.

There is no published normal range for AVR, however experience suggests a range of 0.75-0.90, reflecting that retinal venules are normally slightly thicker than the corresponding arterioles.

Tortuosity

The tortuosity calculations again use the six thickest arterioles - and venules - but uses the longer segment length of zone C. (Fig. 3.27) The software then evaluates the tortuosity for each vessel using an established technique[284] and calculates the median values (plus standard deviation and range).

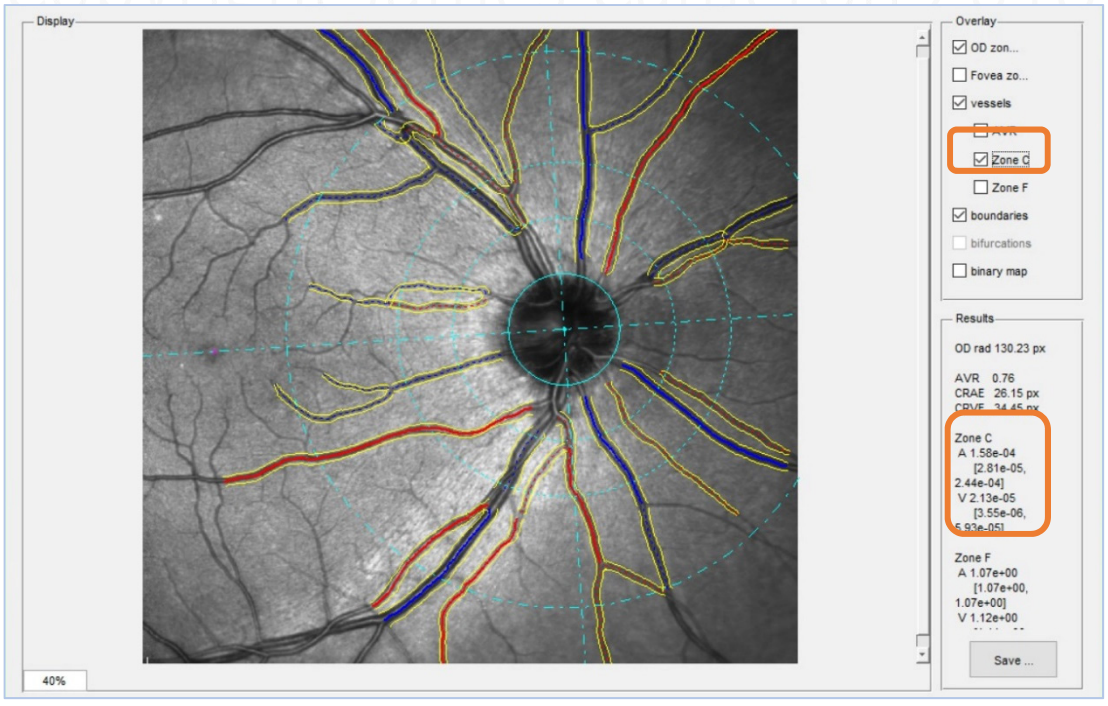

Figure 3.27: VAMPIRE: six arteriole and six venule segments within Zone C selected for arteriolar and venular tortuosity. (Thick coloured lines are the six thickest, and used for calculation. Dotted lines are the remaining segments that have been measured, but will not be included in calculation.)

The raw tortuosity measures are a little difficult to handle in calculations, as firstly they are very small numbers of five or six decimal places from zero (where zero would represent a perfectly straight line, and increasing positive values correspond to increasing tortuosity). And secondly, the nature of the tortuosity calculation generates positively skewed data. Therefore, it is appropriate to apply natural log transformation to the data, in order to normalise the data, better visualise the variation and enable more robust calculations of correlation. As all values of tortuosity are <1, then $\log_n$ numbers will be negative, with values higher/approaching zero corresponding to increased tortuosity.

Fractal Dimension

The software algorithms for calculating fractal dimension (D_f) are not yet fully incorporated within the Vampire platform 3.1.1. Therefore, this required separate processing within a command line system, with the assistance of a programmer.

For each SLO image, multiple fractal calculations were retrieved:

Multi-fractal analysis:

D_0, D_1, D_2 (for each of artery, vein, and combined) = 9 values
(capacity dimension, entropy dimension and correlation dimension)

Mono-fractal analysis:

D_{BOX} (for each of artery, vein, and combined) = 3 values
(box counting method)

Total of 12 values per image.

The calculation of fractal dimension required a higher quality of image, and therefore some images were rejected, with no measures possible. Reasons for rejection include:
- high noise in the vessel segmentation map, for example circles of noise, which the software is unable to resolve, and crashes.
- too few vessels in the segmented map, for a reliable calculation

The calculation of fractal dimension from these extracted SLO images is novel, and so it is not yet clear which fractal calculation is most appropriate.

Data storage and management

Data type and quantity

The raw image data is stored in an encrypted proprietary format on the hard disk drive (HDD) of the OCT machine PC. This means the images and associated measurement data can only be viewed on the OCT machine itself, and not directly transferred to - or viewed on - another PC.

Therefore, for secondary analysis of the SLO image as described above, the SLO image must be exported from the OCT machine (as an uncompressed TIFF file) via a removable USB hard disk.

The storage space required for each patient image file depends upon the number and type of scans performed, but typically takes 300-500 MB disk space.

The clinical information for each participant scanned was stored in categorised text, in an encrypted spreadsheet.

Hardware requirements, security and backup

The primary data storage is the HDD within the OCT machine, with a storage of 1 TB. An attached portable 1 TB HDD connected with USB-3.0 provides a first level backup as a software-driven real-time archive process maintains a direct copy of all the image data.

The OCT machine is located within a lockable clinic room, within the ARRNC facility, that is only open during working hours when staff are present on the reception desk. Outside those hours, the clinic is locked and alarmed.

A second tier of backup involves password-protected encrypted DVD backup of the proprietary data. This DVD backup is held in off-site secured locked filing cabinet storage.

Data analysis and statistical plan

Note: Excerpts of this section have been published – in "Lateral thinking - interocular symmetry and asymmetry in neurovascular patterning, in health and disease",
JR Cameron, RD Megaw, AJ Tatham, S McGrory, TJ MacGillivray, FN Doubal, JM Wardlaw, E Trucco, S Chandran, B Dhillon.
Progress Ret Eye Res 2017; 59: 131-157. doi: 10.1016/j.preteyeres.2017.04.003

Sample size calculation

Limited data exists for the expected effect size for many of the groups I plan to study, therefore I based my sample size calculation on the known mean RNFL thickness difference in MS, and the calculated weighted MD in global RNFL thickness from my meta-analysis of AD.

For MS, the necessary minimum sample size was projected to be 10 in each group, on the basis of the following assumptions: the expected effect size was 14µm, alpha error of 0.05, and the power of the study 95%.

{Mean RNFL thicknesses: normal 106µm (SD 12), MS 92µm (SD 12).
Therefore Cohen's d = (106-92)/12 = 1.2.
For power .95, minimum sample size is therefore 10 (1-sample Z-test) }

For dementia, the necessary minimum sample size was projected to be 11 in each group, on the basis of the following assumptions: the predicted effect size from the meta-analysis was 12.44µm, alpha error of 0.05, and the power of the study 95%.

{WMD in RNFL thickness: -12.44, 95% CI [-16.64, -8.25].
Therefore Cohen's d = 12.44/12 = 1.04.
For power .95, minimum sample size is therefore 11 (1-sample Z-test) }

With the effect sizes unknown for non-AD dementia subtypes, (and for ALS), recruitment will be in line with the above calculations.

Recruitment of patients was targeted at a minimum of 20% above these calculations to allow for subsequent exclusions based on incidental findings, study withdrawal, etc. In addition, to ensure adequate sample sizes when subtyping MS according to history of

optic neuritis, treatment history, and other phentotypic details, a considerably higher overall MS recruitment number is necessary. This can be monitored during the study to ensure the minimum sample size is achieved for each intended subgroup.

For recruitment of controls, it was necessary to ensure not only a comparable number to the patient sample size, but also sufficient breadth of age range to allow reasonable age-matching in each study. A target of 80 controls was set, with an age range of 18-65.

Unit of analysis

The independence of discrete data values within an analysis is essential, if statistical tests are to reasonably represent the sample, and avoid misleading the reader. Non-independence, such as multiple observations from the same individual, create bias within the data, as well as artificially inflating the sample size, which can result in spurious statistical significance.[287] This important concept of 'units of analysis' is particularly relevant to studies involving our eyes, and necessitates caution and consideration before planning ophthalmic studies, as well as in the critical interpretation of published work.

Studies that wish to utilise the data from both eyes of participants need to address the statistical challenges that this produces. Two eyes from one participant cannot be independent subjects, due to the paired cluster bias associated with our eyes being highly similar, and therefore statistical strategies are required to account for this. The choice of how we use both eye data will depend upon the nature of the study, and whether the observations are subject to confounding from the paired eye.

Using one eye data per patient avoids this potential for bias, however has the disadvantage of wasting half of the measured data. One suggestion is that we use one random eye from each participant for initial analysis, and the paired eye data as a repeat analysis for validity.[288] However, this process assumes a high level of symmetry between the eyes, and I would suggest some modification is needed to this advice, given my recent work on the pervasive interocular asymmetry.[289]

In this study, where there is no reason to exclude one eye from a participant, or use an eye for its own ophthalmic history (optic neuritis in MS) I have selected the right eye for analysis. Where necessary to deviate from this, I have outlined the reasons for this, the limitations, and the strategies to reduce bias.

Data analysis methods

Descriptive and comparisons

In general, categorical data are presented using frequencies and percentages, whilst continuous variables are presented using the mean and standard deviation (SD).

All statistical tests and confidence intervals will be two-sided. 95% confidence intervals will be presented with the significance of raw p-values assessed based on a 5% significance level. Outliers will be identified by viewing boxplots and/or histograms of the outcome variables of interest and will be queried at the data checking stage if an error is suspected.

For each study, a sample of controls were selected to be age and sex matched to the population of comparison. Matching of controls was tested with one-way ANOVA for age, and χ^2 for gender ratio.

Normality will be tested with the Shapiro-Wilk test. Independent (unpaired) 2 samples t-test is used for comparison of normally distributed variables, and the Matt-Witney U test for non-normal distributions. The Pearson correlation test will be used to determine the relationship between continuous variables, and Spearman's rho for ordinal variables. For all tests, a p value below 0.05 was deemed statistically significant.

Discrimination between diseases with ROC curve and discrimination function analysis

The area under the ROC curve (AUC) is a measure of discrimination between two outcomes (diseases). A high area under the curve suggests that the model or factors accurately predict the outcome. (Table 3.6) ROC curves can be generated for multiple classes, with AUC values for each comparator. This 'one versus all' approach can be used to test for discrimination between multiple possible diagnostic subtypes/syndromes. Youden's J statistic can be used for determining cutoff scores.

Table 3.6: General guidelines for interpreting AUC values from a ROC curve.

AUC = 0.5	No discrimination (no better than flipping a coin)
0.7 ≤ AUC < 0.8	Acceptable discrimination
0.8 ≤ AUC < 0.9	Very good discrimination
AUC ≥ 0.9	Excellent discrimination

For more rigorous discrimination between disease categories, discrimination function analysis will be used, by assessing Wilks' statistic with exact F-test. This provides a joint test of the means, and is possibly a better assessment of the predictive variables.

Age adjustment

We know that RNFL thickness slowly declines with age, therefore age adjustment of RNFL thickness values in study populations is required, despite age-matching the control groups as far as possible.

For background guidance on this, normal values and ranges for RNFL thickness across age-ranges were retrieved from the normal database within the SPECTRALIS OCT software. (Table 3.7)

Whilst I will recruit healthy controls within this study for data comparison, it is nonetheless helpful to review the content of this normal database in the OCT machine.

Of particular note was that the values for male and female were identical, as were the values for left and right eyes.

Table 3.7: Normal RNFL thickness values across age-ranges, as per SPECTRALIS OCT software normative data.

Age Range	G	PMB	T	TS	NS	N	N/T	NI	TI
10-19	99	59	78	138	102	72	0.92	108	147
20-29	99	59	78	138	102	72	0.92	108	147
30-39	98	58	76	136	102	72	0.94	107	145
40-49	97	57	75	135	102	72	0.95	106	143
50-59	96	56	73	133	102	72	0.96	105	141
60-69	96	55	72	132	102	72	0.98	104	138
70-79	95	54	70	130	102	72	0.99	103	136
80-89	94	53	69	128	102	72	1.00	103	134

For every RNFL scan performed on a patient, not only are reference 'normal' values provided, but also a colour-coded scale of normal percentiles, facilitating a visual reference for rapid clinical interpretation. The data for this is not just calculated from the raw normal data, but has already undergone an age-adjustment transformation.

From the FDA 510(k) premarket notification report for the device[290], we can obtain more detail on the creation of the normative database in the device:

"The normative database includes 201 subjects of Caucasian origin enrolled in a patient registry. Demographically, the subjects included: 111 male, 90 female, mean (SD) age 48.2 ± 14.5 years, age range 18 to 78 years. Included subjects had no history of glaucoma. normal intraocular pressure, normal visual field, normal appearance of optic disc, etc. Screening for entry into the study included patient history and physical examination to determine if eyes were 'normal' by two ophthalmologists.

… RNFL thickness measurements made with the Spectralis HRA+OCT are compared to the normative database. For that purpose, an age-adjustment of the normal database is performed and percentile limits of the normal distribution are computed as follows.

For each subject in the normative database, RNFL thickness at each point along the circle scan, mean RNFL thickness along the whole circle scan (global), and mean RNFL thickness within certain sectors of the circle scan (temporal, temporal-superior, temporal- inferior, nasal, nasal-superior, nasal-inferior) were measured. From these measurements, the age-adjusted percentiles of the database sample of 201 healthy Caucasians were determined. These age-adjusted percentiles form the basis for highlighting a result as being within or outside the normal limits (greater than the 5th or less than the 1st percentile of the database sample). The meaning of the nth percentile is that n percent of normal Caucasian subjects from the database sample have a RNFL thickness of less than or equal to this value.

Age-adjustment of the normal data is based on the linear regression of RNFL thickness vs. age of the normal subjects. Global RNFL thickness and RNFL thickness in the sectors temporal, temporal-superior, temporal-inferior, and nasal-inferior showed negative slopes (decrease of RNFL thickness) with age in the normal data and are adjusted. RNFL thicknesses in the sectors nasal and nasal-superior showed insignificant positive slopes with age in the normal data and are not adjusted.

As an example for the effect of age, the following tables show the values of the 1st and 5th percentile of RNFL thickness global and in the six sectors for ages 45 and 65 years. All values are in microns; the numbers in brackets represent the 95% confidence intervals of the respective percentiles." (Tables 3.8, 3.9)

Table 3.8: SPECTRALIS normal database: 1st and 5th percentiles for age 45 years

	1st percentile (95% CI)	5th percentile (95% CI)
Global	76.0 (73.2-78.2)	82.1 (79.9-83.9)
sector T	46.9 (42.8-49.5)	54.9 (51.7-57.0)
sector TS	96.3 (90.8-100.0)	107.4 (103.1-110.4)
sector TI	99.1 (92.7-103.1)	111.6 (106.6-115.0)
sector N	38.3 (34.0-42.0)	48.1 (44.6-51.0)
sector NS	57.8 (52.0-62.6)	70.7 (66.1-74.6)
sector NI	53.6 (46.7-59.2)	68.8 (63.4-73.3)

[Table from FDA 510(k): K121993 2012 [290]]

Table 3.9: SPECTRALIS normal database: 1st and 5th percentiles for age 65 years

	1st percentile (95% CI)	5th percentile (95% CI)
Global	74.5 (71.7-76.7)	80.6 (78.4-82.4)
sector T	43.9 (39.8-46.5)	52.0 (48.8-54.1)
sector TS	93.0 (87.6-96.8)	104.1 (99.8-107.2)
sector TI	94.6 (88.2-98.6)	107.1 (102.1-110.4)
sector N	38.3 (34.0-42.0)	48.1 (44.6-51.0)
sector NS	57.8 (52.0-62.6)	70.7 (66.1-74.6)
sector NI	51.9 (45.0-57.5)	67.2 (61.7-71.7)

[Table from FDA 510(k): K121993 2012 [290]]

This explains the static values for N (nasal) and NS (nasal-superior) for all ages, as revealed from the normal database. (Table 3.7) It is a timely reminder that the natural history of retinal ganglion cell loss over our lifetime remains incompletely understood, and approximate percentages of micron loss per annum are a convenient method for extrapolating and comparing health and disease, but may lead to erroneous conclusions, consequent to our insufficient knowledge of this cellular behaviour over

time. I suspect we will need devices with greater resolution and higher precision to gain a more accurate understanding of retinal ganglion cell natural history.

Choroidal thickness is also known to decrease with age, at an approximate rate of around 16μm every 10 years.[291] Therefore age adjustment here is also possible, though given the many other factors that also influence choroidal thickness, it is perhaps of less importance.

Missing data

Where data was incomplete for any participant, they were removed before statistical analysis.

Software

All statistical analyses and graphs were produced with Minitab® v17.0 (Minitab Inc., State College, Pennsylvania, USA); except for the meta-analyses in chapter 2 which used RevMan® 5.3 (Copenhagen: The Nordic Cochrane Centre, The Cochrane Collaboration), and ROC curve analysis using GraphPad Prism® v6.0 (GraphPad Software Inc., La Jolla, California, USA).

4 MULTIPLE SCLEROSIS

Introduction

Multiple sclerosis (MS) has been a pathfinder disease in the use of neuroretinal measures as surrogate marker of white matter degeneration. It was the first disease to be studied with OCT, and now has the highest number of published papers.

The key findings are that RNFL is thinner in MS patients, of all sub-types, and the degree of thinning correlates to varying degrees with other markers of disease. In particular, MRI measures of white matter damage, which have been studied in large MS facilities, where routine imaging data has been collected for many years, and across many patients.

However, there remain unanswered questions regarding the clinical utility of RNFL measures (and GCL) as relevant to individual patients. Few have commented on the sensitivity and specificity of neuroretinal measures in patients, and how they may discriminate between patients, both phenotypically within MS, but also between MS and other neurodegenerative conditions.

The relationship between structure and function in the neuroretina is a source of current interest, and worthy of further exploration.

The potential use of vascular morphology measurements has also not been explored. There would be great interest in a non-invasive marker of inflammatory burden in MS patients, and vascular imaging studies are of current interest.

The aim of this chapter then is to explore in more depth how these neuroretinal derived markers can be of clinical utility in MS, by recruiting a large number of MS patients across the disease spectrum. Not only will this help to answer these questions of clinical utility, but should also generate new hypotheses relating to the pathophysiology of visual pathway involvement in MS, a consequence well known, but poorly understood.

The setting for the study was the ARRNC, with patients recruited from the specialist MS clinics. The patient case mix within each clinic list is mixed across subtype, duration and severity. I could therefore be assured of recruiting sufficient numbers across all subtypes of disease, to enable subgroup analysis later.

Healthy control patients were recruited from family members and friends attending the clinic, and staff colleagues. (See Chapter 3 for more detail on recruitment methods)

Patient population

Data from the locally managed clinical MS database reveals the known population within Lothian of 2078 patients with MS (and 95 with CIS who have attended the specialist MS clinic at some point for assessment), including data on duration of disease and EDSS at last visit (if recorded). (Figs. 4.1, 4.2, 4.3)

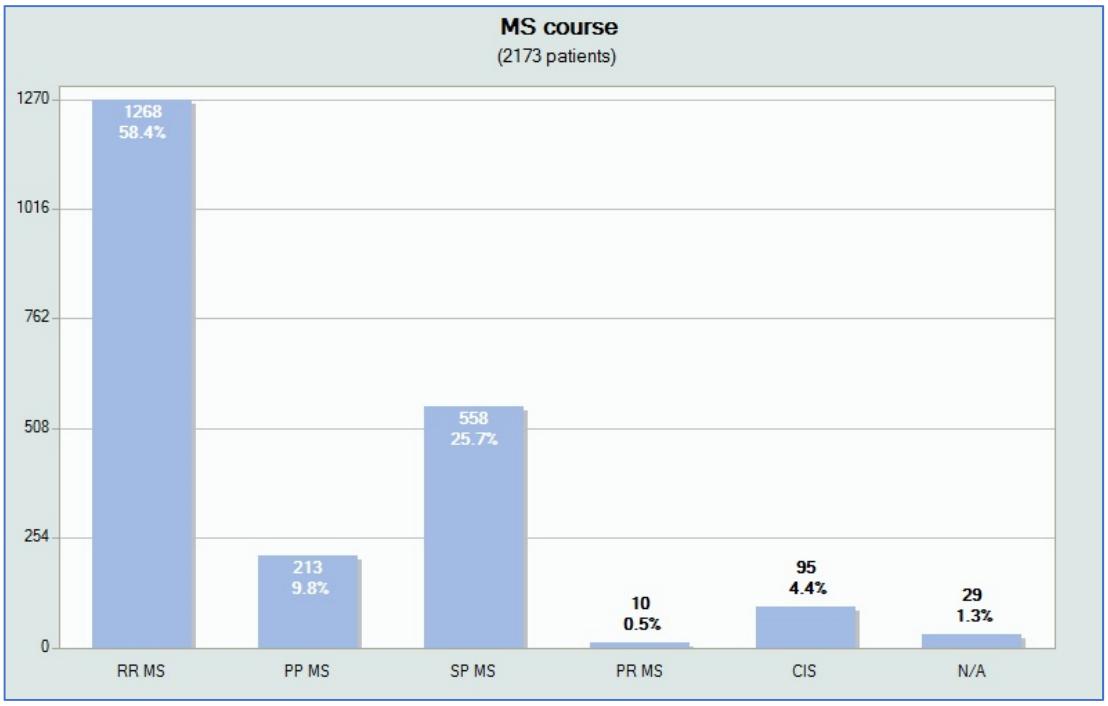

Figure 4.1: MS in Lothian region: distribution of subtypes

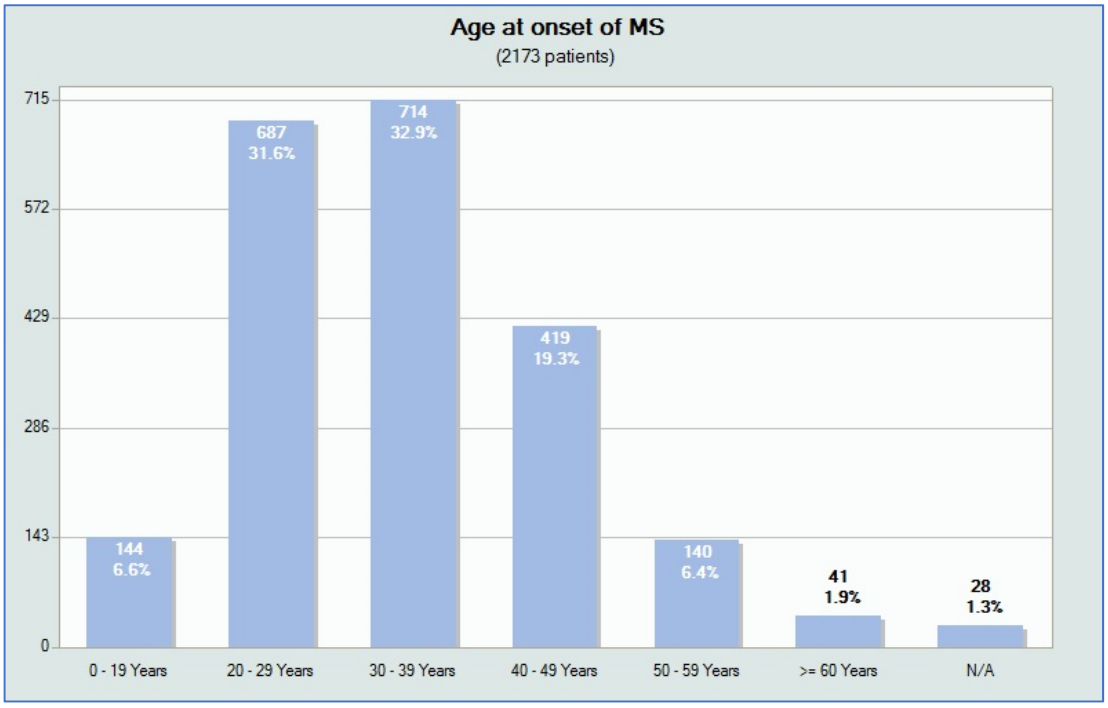

Figure 4.2: MS in Lothian region: age at onset

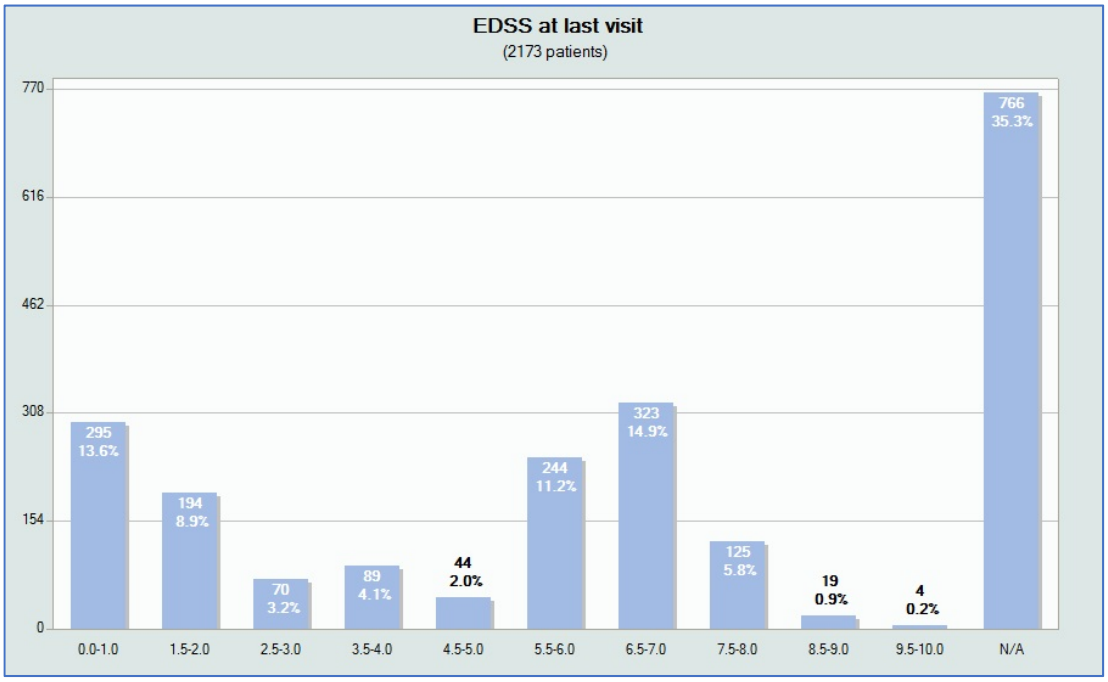

Figure 4.3: MS in Lothian region: current level of EDSS

607 patients are currently on treatment, at the time of this data retrieval. (Fig 4.4)

This represents 29% of all MS patients, or more relevantly 48% of RRMS patients.

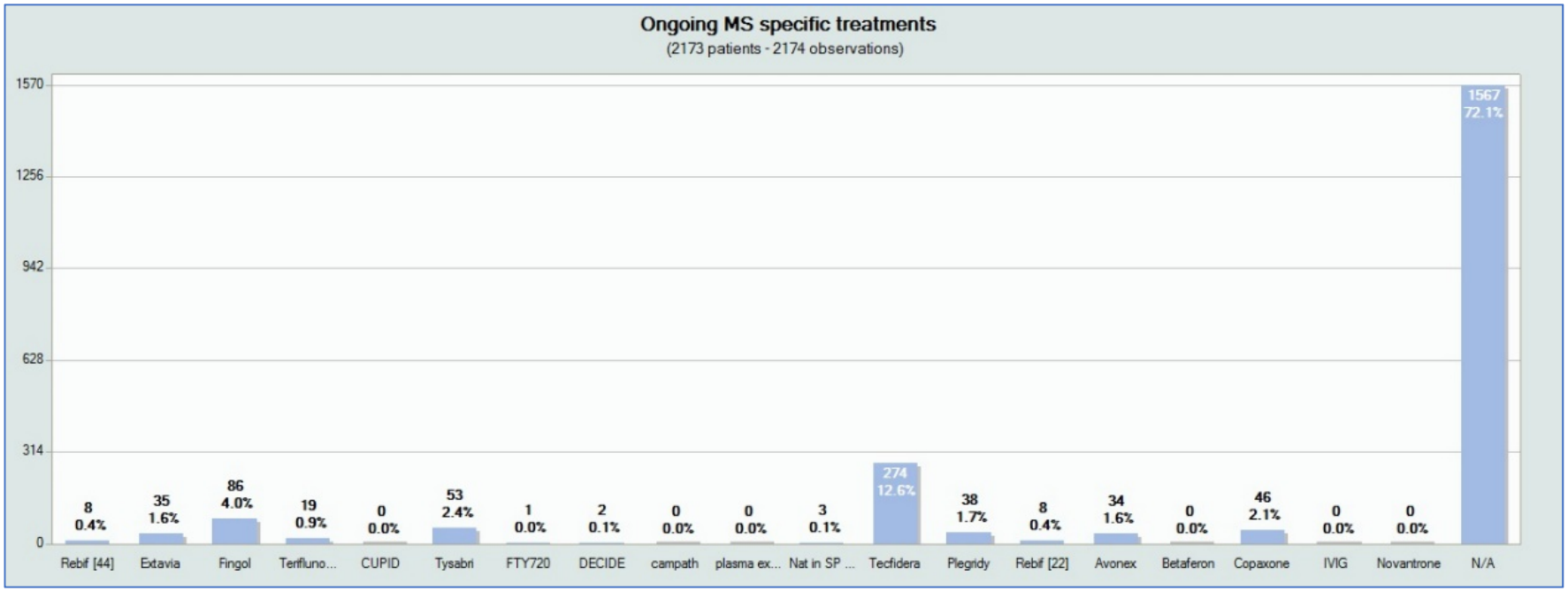

Figure 4.4: MS in Lothian region: patients on disease-modifying treatment (Note the separations within this system of alternate names or doses of the same treatment, for example fingolimod and FTY720, or the distinction made between 22µg and 44µg doses of Rebif)

Clinical Assessment

Treatments

Over the past few years, several disease-modifying treatments (DMT) for relapsing MS have been made available, initially for patients with highly active relapsing disease, but increasingly used earlier in the disease course for some patients. At present, there are 11 drugs approved within the NHS. (Table 4.1) Effectiveness of the drugs has been classified by the Association of British Neurologists according to the results from large clinical trials. (Table 4.2) They have not yet been shown to provide benefit to patients with PPMS.[44]

Table 4.1: Disease-modifying treatments for relapsing MS

Drug name	generic name	method of admin	effectiveness
Avonex	interferon beta 1a	injection; weekly	moderately effective
Betaferon	interferon beta 1b	injection; every other day	moderately effective
Extavia	interferon beta 1b	injection; every other day	moderately effective
Plegridy	interferon beta 1a	injection; 2 weekly	moderately effective
Rebif	interferon beta 1a	injection; 3 times a week	moderately effective
Copaxone	glatiramer acetate	injection; daily	moderately effective
Aubagio	teriflunomide	oral; daily	moderately effective
Tecfidera	dimethyl fumarate	oral; twice daily	more effective
Gilenya	fingolimod	oral; daily	more effective
Tysabri	natalizumab	infusion; monthly	highly effective
Lemtrada	alemtuzumab	infusion; two, 12 months apart	highly effective

Table 4.2: Effectiveness classification of disease-modifying treatments for relapsing MS

category		relapse reduction
1.1	"moderately effective"	30%
1.2	"more effective"	50%
2.0	"highly effective"	70%

Disease Activity

Defining the level of activity of a patient's disease is challenging. Like defining the level of severity or progression, there is no objective 'gold standard' measure of activity. In relapsing disease, the frequency of relapses, or severity of symptoms experienced, can be used as a broad assessment of activity. This is not ideal, as it can occasionally be difficult to distinguish between a relapse and day to day fluctuations in symptoms.

A good clinical definition is that a relapse is the appearance of a new symptom (or reappearance of an old symptom) that lasts more than 24 hours, but more commonly for several days or weeks. Annualised relapse rate (ARR) (i.e. relapses/year) has been used as a clinical indicator of disease activity, with the benefit of being easy to measure. It is also used in clinical trials as an outcome measure, which is reasonable particularly as prevention of relapses directly and immediately benefits patients.[292]

Disease Severity - EDSS

The (Kurtzke's) Expanded Disability Status Scale (EDSS) is an ordinal scale for indicating neurological impairment in MS, widely used in the clinical setting as a means of evaluating disability status and over time demonstrating disease progression. It is assessed by a neurological examination across seven functional systems (FS) – visual, brain stem, pyramidal, cerebellar, sensory, bowel & bladder, and cerebral functions.[293] Scores from each domain are combined to form an overall score, from 0 to 10. (Table 4.3)

In this study, EDSS was assessed by a trained rater - either neurologist or MS specialist nurse.

Critics of the scale note its weight towards motor disability and noncontinuous scoring, questioning its reliability. As such, it is not expected to be a 'gold standard' reference of disability status to which retinal metrics should be judged.

Table 4.3: Expanded Disability Status Scale (EDSS) - score and clinical correlation

0	Normal Neurological Exam
1	No disability, minimal signs in 1 functional system (FS)
1.5	No disability, minimal signs in more than 1 FS
2	Minimal disability in 1 FS
2.5	Mild disability in 1 or Minimal disability in 2 FS
3	Moderate disability in 1 FS or mild disability in 3 - 4 FS, though fully ambulatory
3.5	Fully ambulatory but with moderate disability in 1 FS and mild disability in 1 or 2 FS; or moderate disability in 2 FS; or mild disability in 5 FS
4	Fully ambulatory without aid, up and about 12hrs a day despite relatively severe disability. Able to walk without aid 500 meters
4.5	Fully ambulatory without aid, up and about much of day, able to work a full day, may otherwise have some limitations of full activity or require minimal assistance. Relatively severe disability. Able to walk without aid 300 meters
5	Ambulatory without aid for about 200 meters. Disability impairs full daily activities
5.5	Ambulatory for 100 meters, disability precludes full daily activities
6	Intermittent or unilateral constant assistance (cane, crutch or brace) required to walk 100 meters with or without resting
6.5	Constant bilateral support (cane, crutch or braces) required to walk 20 meters without resting
7	Unable to walk beyond 5 meters even with aid, essentially restricted to wheelchair, wheels self, transfers alone; active in wheelchair about 12 hours a day
7.5	Unable to take more than a few steps, restricted to wheelchair, may need aid to transfer; wheels self, but may require motorized chair for full day's activities
8	Essentially restricted to bed, chair, or wheelchair, but may be out of bed much of day; retains self-care functions, generally effective use of arms
8.5	Essentially restricted to bed much of day, some effective use of arms, retains some self-care functions
9	Helpless bed patient, can communicate and eat
9.5	Unable to communicate effectively or eat/swallow
10	Death due to MS

Visual Acuity

The easiest and more frequently used tool of assessment of function of the visual system is visual acuity. Snellen (full contrast) visual acuity (VA) is ubiquitous within the ophthalmology clinic and forms the initial phase of every ophthalmological examination. Despite its many weaknesses and limitations, it remains a useful screening tool of visual function, and most people are very familiar with the test.

In retinal and optic nerve disease, a more refined version of VA assessment is necessary, to distinguish smaller degrees of functional change, to compare with the slight structural changes we can now measure with OCT and other tools.

Firstly, an improved acuity chart has become increasingly prevalent - an 'ETDRS' chart of 70 letters (with 5 letters on every line), compared with the 37-46 total letters (and only 1 letter on the top line) of most Snellen charts. (Fig. 4.6)

This chart design also facilitates a better system of documenting acuity - the LogMAR. LogMAR stands for Logarithm of the Minimum Angle of Resolution, referring to the stroke width of the letters, which is one fifth of their vertical angular subtense. Thus a 6/6 (Snellen) letter which subtends 5 minutes of arc, equates to a MAR of one minute and a LogMAR of 0 (Log_{10} 1=0). Tables of Snellen to LogMAR conversion are readily available, and newer LogMAR charts print on the equivalent Snellen, decimal and LogMAR values next to each line of letters. LogMAR is far superior for inter-visit comparison, and meaningful statistical analysis.[294]

Secondly, low contrast visual acuity (LCVA) letter charts have been developed, where the black contrast of the letters has been lowered to specific percentages, making them more difficult to read against the same fixed white background. These LCVA charts have been shown to better pick up and discriminate small degrees of impaired visual function, for example in patients who are otherwise asymptomatic and can easily complete the full contrast VA chart. This makes them particularly appropriate for neurological/optic nerve disease, where subtle visual change is an early and important finding.[295] The charts are available in a range of contrast percentages - the most commonly used are 5%, 2.5% and 1.25%. (Fig. 4.5) These charts also require standardised retro-illumination for accurate assessment.

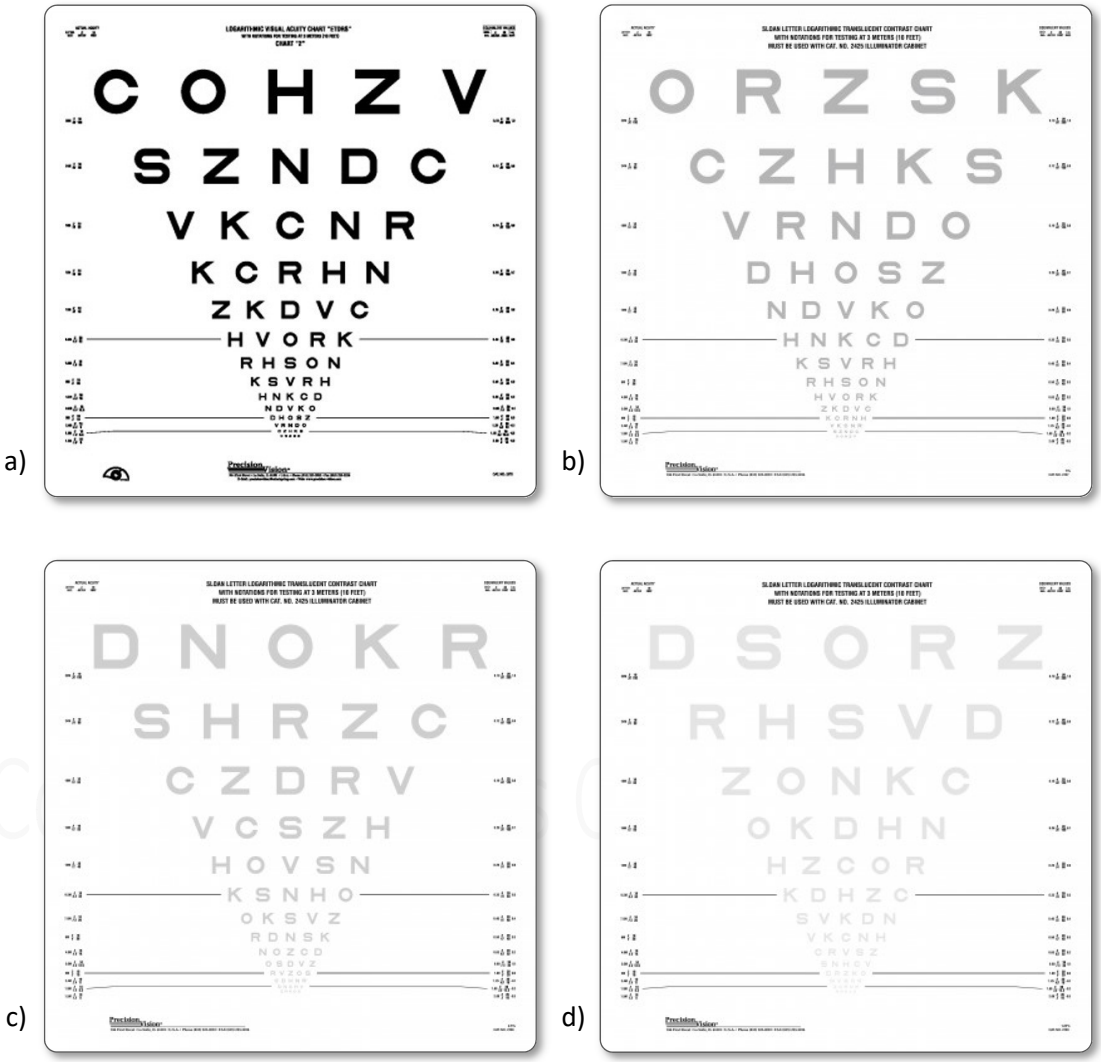

Figure 4.5: Visual acuity charts. a) ETDRS full contrast b) ETDRS 'Sloan' low contrast 5% c) ETDRS 'Sloan' low contrast 2.5% d) ETDRS 'Sloan' low contrast 1.25%

Retinal imaging and analysis

All participants had the full OCT imaging protocol as outlined in Chapter 3.

All images were of satisfactory quality for processing and analysis, as per the OSCAR-IB criteria.

Results

Participant characteristics

I recruited and imaged 655 MS patients, and 106 healthy controls.

The mean ages of the MS patients and controls were 43.7 ± 11.8 years, and 42.1 ± 12.2 years respectively; with around two-thirds females in each group. The mean refractive errors for each group were also comparable, both being -0.4 with small SDs.

Within the MS patients, representative samples of each MS subtype were recruited: 502 RRMS, 21 PPMS and 132 SPMS. Full details of their disease duration, treatment, optic neuritis history and EDSS are given below. (Table 4.4)

Table 4.4: Baseline participant characteristics

	Controls	**All MS**	**RRMS**	**PPMS**	**SPMS**
Number	106	655	502	21	132
Mean age (years)	42.1 ± 12.2	43.7 ± 11.8	40.8 ± 10.9	49.1 ± 12.9	53.9 ± 8.4
Sex (male:female)	28:78 (=35.9% male)	179:476 (=37.6% male)	135:367	8:13	36:96
Refractive error * (dioptres)	-0.4 ± 1.5	-0.4 ± 1.4	-0.4 ± 1.2	-0.37 ± 1.52	-0.29 ± 2.06
Disease duration (months)	-	139 ± 109	114 ± 91	135 ± 109	235 ± 118
Age of onset (years)	-	32.1 ± 9.1	31.3 ± 8.6	37.0 ± 11.5	34.2 ± 9.9
On treatment (%)	-	32.7 (n=214)	41.8 (n=210)	4.7 (n=1)	2.2 (n=3)
Previous optic neuritis * (%)	-	24.4 (n=160)	22.7 (n=114)	23.8 (n=5)	31.1 (n=41)
EDSS	-	2.9 ± 2.1	2.5 ± 1.9	3.2 ± 1.9	4.6 ± 1.9

NOTE. Data are shown mean ± SD
* in right eye, as image analysis data will be from right eye images only

Treatment

Of the 502 RRMS patients, just under half (210) are on disease-modifying treatment. This is close to the Lothian population figure of 48%, as retrieved from the iMed database. (Fig. 4.4) This is a lower rate of treatment than many reported figures, particularly North America, where DMT use is almost 75%.[296]

However, this facilitates some useful analysis in this study, with there being a large treatment-naïve group for comparisons where treatment could be considered a confounding factor.

Optic neuritis

Across all MS patients, the rate of previous ON (in the right eye) was 24.4%.

388 RRMS patients had no ON history, either reported, or documented in notes.

It would be interesting to improve the granularity of optic neuritis events: number, timing, severity or pattern, etc, however this data is seldom recorded in sufficient detail, and patient memory of events varies considerably, therefore this was not taken further.

OCT analysis

RNFL thickness

Peripapillary RNFL (pRNFL) was significantly thinner in all MS subtypes, and in all peripapillary sectors, with the exception of PPMS where the nasal sector thinning did not reach significance. (Table 4.5)

Global pRNFL was significantly thinner in PPMS (MD= -11.07, 95% CI [-17.63, -4.50], p=0.002), SPMS (MD= -19.93, 95% CI [-23.22, -16.63], p<0.001), and RRMS with no ON history (MD= -10.72, 95% CI [-13.20, -8.24], p<0.001). The greatest amount of thinning was seen in RRMS with ON history (MD= -24.65, 95% CI [-28.21, -21.09], p<0.001).

For temporal pRNFL the findings were similar. Temporal pRNFL was significantly thinner in PPMS (MD= -11.11, 95% CI [-18.03, -4.18], p=0.003), SPMS (MD= -22.55, 95% CI [-25.96, -19.14], p<0.001, and RRMS no-ON history (MD= -13.92, 95% CI [-16.47, -11.38], p<0.001). Again, the greatest amount of thinning was seen in RRMS +ON (MD= -26.38, 95% CI [-29.67, -23.10], p<0.001).

Table 4.5: OCT analysis: peripapillary scan, RNFL thickness by sector

	healthy controls	RRMS - no ON	RRMS + ON	PPMS	SPMS
pRNFL thickness: global	101.0 ± 10.9	90.2 ± 13.2***	76.3 ± 15.5***	89.9 ± 13.8**	81.1 ± 14.8***
PMB	57.5 ± 7.7	46.2 ± 10.9***	37.8 ± 10.1***	48.9 ± 12.1**	40.3 ± 12.1***
T	74.9 ± 10.8	61.0 ± 14.7***	48.5 ± 13.8***	63.8 ± 14.5**	52.4 ± 15.8***
TS	140.2 ± 17.7	127.9 ± 18.8***	110.2 ± 21.7***	127.1 ± 25.8 **	115.6 ± 20.5 ***
NS	101.2 ± 20.7	93.7 ± 19.3***	86.0 ± 25.5***	89.8 ± 15.8**	89.6 ± 20.1***
N	76.5 ± 13.1	70.6 ± 14.8***	58.1 ± 14.2***	70.8 ± 15.4	63.5 ± 15.6***
N/T	1.045 ± 0.23	1.219 ± 0.363 ***	1.254 ± 0.345***	1.166 ± 0.359	1.294 ± 0.397 ***
NI	115.1 ± 26.5	105.3 ± 25.6***	90.8 ± 26.6***	101.6 ± 22.5*	95.3 ± 23.3***
TI	148.7 ± 18.4	132.0 ± 23.3***	110.8 ± 25.5***	132.2 ± 25.2**	116.0 ± 25.3 ***

Abbreviations: PMB, papillo-macular bundle; T, temporal; TS, temporal-superior; NS, nasal-superior, N, nasal; N/T, nasal-temporal ratio; NI, nasal-inferior; TI, temporal-inferior
NOTE. Right eye analysis only. Data are shown mean ± SD (μm)
*P < 0.05, **P < 0.01, ***P < 0.001.

The finding of a greater RNFL loss in patients with a history of ON concurs with the literature on this. Comparing global and temporal RNFL thinning as percentage loss, global MD equates to a 24.4% thinning, temporal MD equates to a 35.2% loss of RNFL. In other words, the effects size is considerably larger for temporal RNFL in thinning relating to ON history.

For the remaining RNFL sectors, the RNFL thinning MD is around 10-20% from healthy mean value.

Macular thickness

Macular thickness averages were significantly reduced in all MS subtypes, and in all macular sectors, with the exception of PPMS where central macular thickness was no different from the controls. (Table 4.6)

The greatest mean reductions were seen in SPMS.

Table 4.6: OCT analysis: macular volume scan, macular average thickness by sector

	healthy controls	RRMS - no ON	RRMS + ON	PPMS	SPMS
Macular average thickness: central	275.2 ± 18.4	270.7 ± 19.3*	265.3 ± 19.3***	277.7 ± 18.7	265.6 ± 20.3***
IN	348.8 ± 12.4	333.8 ± 20.6***	324.5 ± 20.1***	336.1 ± 22.1*	321.5 ± 20.1***
IS	347.2 ± 12.2	333.7 ± 19.5***	324.4 ± 17.4***	334.8 ± 20.1*	321.3 ± 19.2***
IT	333.7 ± 12.7	322.7 ± 18.0***	314.9 ± 17.2***	325.4 ± 17.3*	311.8 ± 18.1***
II	344.9 ± 12.6	330.4 ± 19.6***	320.0 ± 19.1***	332.2 ± 19.2**	318.1 ± 19.1***
ON	320.6 ± 14.1	303.9 ± 19.6***	293.0 ± 17.1***	302.3 ± 22.6**	289.8 ± 19.8***
OS	301.4 ± 12.2	292.7 ± 16.8***	286.4 ± 14.1***	287.7 ± 17.4**	282.5 ± 15.4***
OT	286.1 ± 13.6	279.7 ± 13.6***	275.1 ± 12.8***	277.8 ± 14.7*	270.8 ± 14.4***
OI	292.9 ± 13.7	282.5 ± 15.3***	273.8 ± 14.2***	280.0 ± 13.8**	271.7 ± 15.4***

Abbreviations: IN, inner nasal; IS, inner superior; IT, inner temporal; II, inner inferior; ON, outer nasal; OS, outer superior; OT, outer temporal; OI, outer inferior

NOTE. Right eye analysis only. Data are shown mean ± SD (μm)

*P < 0.05, **P < 0.01, ***P < 0.001.

Central macular thickness was significantly reduced in SPMS (MD= -9.60, 95% CI [-14.56, -4.64], p<0.001), RRMS no-ON (MD= -4.50, 95% CI [-8.53, -0.48], p=0.029) and RRMS +ON (MD= -9.93, 95% CI [-14.95, -4.91], p<0.001).

Inner ring macular sectors were significantly thinner in all subtypes, for example inner nasal sector: PPMS (MD= -12.68, 95% CI [-23.02, -2.33], p=0.019), SPMS (MD= -27.29, 95% CI [-31.50, -23.09], p<0.001), RRMS no-ON (MD= -15.00, 95% CI [-18.15, -11.84], p<0.001), and RRMS +ON (MD= -24.34, 95% CI [-28.77, -19.92], p<0.001).

And the inner superior sector: PPMS (MD= -12.44, 95% CI [-21.83, -3.04], p=0.012), SPMS (MD= -25.96, 95% CI [-30.00, -21.92], p<0.001), RRMS no-ON (MD= -13.53, 95% CI [-16.58, -10.48], p<0.001), and RRMS +ON (MD= -22.85, 95% CI [-26.83, -18.88], p<0.001).

Outer ring macular sectors were similarly affected, with significant thinning seen in all MS subtypes, for example the outer superior sector: PPMS (MD= -13.72, 95% CI [-21.97, -5.47], p=0.002), SPMS (MD= -18.94, 95% CI [-22.49, -15.40], p<0.001), RRMS no-ON (MD = -8.72, 95% CI [-11.61, -5.83], p<0.001), and RRMS +ON (MD= -15.08, 95% CI [-18.58, -11.57], p<0.001).

The remaining macular sectors showed similar thinning.

Macular volume including GCL

Macular volume was significantly reduced in all MS subtypes. The greatest reductions were seen in SPMS and RRMS +ON. (Table 4.7)

Macular volume was significantly reduced in PPMS (MD= -0.34, 95% CI [-0.556, -0.115], p0.004), SPMS (MD= -0.62, 95% CI [-0.719, -0.526], p<0.001), RRMS no-ON (MD= -0.30, 95% CI [-0.382, -0.228], p<0.001), and RRMS +ON (MD= -0.54, 95% CI [-0.634, -0.437], p<0.001).

Macular GCL volume was also significantly reduced in all MS subtypes. Again, the greatest reductions were seen in SPMS and RRMS +ON.

Macular GCL volume was significantly reduced in PPMS (MD= -0.17, 95% CI [-0.242, -0.093], p<0.001), SPMS (MD= -0.25, 95% CI [-0.283, -0.220], p<0.001), RRMS no-ON (MD= -0.15, 95% CI [-0.171, -0.128], p<0.001), and RRMS +ON (MD= -0.24, 95% CI [-0.270, -0.211], p<0.001).

Table 4.7: OCT analysis: macular volume scan, macular volume of full 6mm circle

	healthy controls	**RRMS - no ON**	**RRMS + ON**	**PPMS**	**SPMS**
Macular full thickness volume MV	8.74 ± 0.33	8.43 ± 0.43***	8.21 ± 0.41***	8.41 ± 0.46**	8.12 ± 0.42***
Macular GCLV	1.12 ± 0.08	0.97 ± 0.14***	0.88 ± 0.13***	0.95 ± 0.16***	0.86 ± 0.15***

Abbreviations: MV, macular volume; GCLV, ganglion cell layer volume
NOTE. Right eye analysis only. Data are shown mean ± SD (mm^3)
*P < 0.05, **P < 0.01, ***P < 0.001.

Choroidal thickness

The subfoveal choroid was significantly thinner in RRMS and SPMS. The greatest reduction was seen in SPMS. (Table 4.8)

The sfCT was reduced in SPMS (MD= -47.3, 95% CI [-70.2, -24.4], p<0.001), RRMS no-ON (MD= -23.0, 95% CI [-43.7, -2.3], p=0.030), and RRMS +ON (MD= -27.6, 95% CI [-53.2, -2.1], p=0.034).

Table 4.8: OCT analysis: horizontal EDI scan, choroidal thickness

	healthy controls	RRMS - no ON	RRMS + ON	PPMS	SPMS
sfCT	322.3 ± 92.5	299.3 ± 106.4*	294.7 ± 99.7*	281.1 ± 111.4	275.0 ± 84.4***

Abbreviations: sfCT, sub-foveal choroidal thickness
NOTE. Right eye analysis only. Data are shown mean ± SD (μm)
*P < 0.05, **P < 0.01, ***P < 0.001.

Data Analysis

In summary, all MS subtypes were associated with neuroretinal thinning. However, no clear pattern of thinning emerged to distinguish the MS subtypes.

RRMS with an ON history was associated with the greatest thinning of the RNFL, and SPMS was associated with the greatest reduction in all the other measured neuroretinal layers.

For RNFL measures, the temporal peripapillary sector is affected the greatest, in all MS subtypes.

Macular thickness and macular volume were significantly reduced in all MS subtypes, but with SPMS most affected, closely followed by RRMS +ON. This includes macular GCL volume, which again was most significantly affected in SPMS and RRMS+ON.

These measures therefore distinguish optic neuritis history more than MS subtypes.

ROC curve analysis for distinguishing ON history for each measure reveals: Global RNFL AUC=0.753, 95% CI [0.699, 0.806), p<0.0001. Temporal RNFL AUC=0.798, 95% CI [0.726, 0.849], p<0.0001. Macular volume AUC=0.695, 95% CI [0.603, 0.716], p<0.0001. Macular GCL volume AUC=0.685, 95% CI [0.632, 0.738], p<0.0001.

Correlation between these measures and EDSS was generally poor. (Table 4.9) There were moderate correlations between RNFL thinning and EDSS in the RRMS +ON group, but otherwise the correlations were weak.

Table 4.9: Correlation between neuroretinal parameters and EDSS in MS

	Spearman's rank correlation coefficient (p-value)			
	RRMS - no ON	**RRMS + ON**	**PPMS**	**SPMS**
global RNFL	-0.452 (<0.001)***	-0.744 (<0.001)***	0.068 (0.770)	-0.273 (0.002)**
temporal RNFL	-0.368 (<0.001)***	-0.603 (<0.001)***	-0.227 (0.322)	-0.214 (0.014)*
MV	-0.178 (<0.001)***	-0.436 (<0.001)***	0.397(0.074)	-0.128 (0.143)
macular GCLV	-0.264 (<0.001)***	-0.511 (<0.001)***	-0.676 (0.001)**	-0.205 (0.019)*
sfCT	-0.144 (0.004)**	-0.198 (0.035)*	0.103 (0.656)	0.124 (0.157)

Abbreviations: MV, macular volume; GCLV, ganglion cell layer volume; sfCT, sub-foveal choroidal thickness

NOTE. Right eye analysis only. Data are shown Spearman's rho (p-value)

*P < 0.05, **P < 0.01, ***P < 0.001.

Regarding choroidal thickness, the subfoveal choroid is thinner in MS, with or without ON history. The degree of thinning does not correlate with duration of disease, visual acuity, EDSS or central macular thickness.

However, further analysis revealed that in RRMS, the choroid is thinner in patients on treatment, versus treatment-naïve patients (MD= -40.47, 95% CI [-58.65, -22.29], p<0.001).

Retinal vessel analysis

Vessel calibre

CRVE was significantly higher in RRMS, but not in PPMS or SPMS. AVR was correspondingly lower in RRMS. There was no difference in CRAE in any of the MS subtypes. (Table 4.10)

Table 4.10: Retinal vessel analysis: vessel calibre

	healthy controls	RRMS - no ON	RRMS + ON	PPMS	SPMS
CRAE	28.08 ± 2.17	28.47 ± 2.29	28.29 ± 2.30	28.56 ± 2.93	28.20 ± 2.36
CRVE	35.37 ± 2.41	36.57 ± 2.89**	37.30 ± 3.15***	35.42 ± 2.80	34.93 ± 2.97
AVR	0.80 ± 0.06	0.76 ± 0.06***	0.75 ± 0.07***	0.80 ± 0.07	0.81 ± 0.09

Abbreviations: CRAE, central retinal arteriolar equivalent; CRVE, central retinal venular equivalent; AVR, arterio-venous ratio

NOTE. Right eye analysis only. Data are shown mean ± SD (pixels)

*P < 0.05, **P < 0.01, ***P < 0.001.

The clear finding here is that AVR is significantly lower in RRMS, compared with controls, with or without a history of ON. However, the difference is small, in the no-ON RRMS, the estimated mean difference (MD)= -0.03, 95% CI [-0.040, -0.014], p=0.0004.

The main influence on this AVR difference appears to be the CRVE, which is also significantly different (higher) in RRMS, with MD=1.19, 95% CI [0.653, 1.741], p=0.008. In other words, the AVR is lower, due to a higher CRVE - implying thicker venules.

In RRMS +ON, the AVR MD= -0.05, 95% CI [-0.063, -0.028], p=0.0002, with a CRVE MD=1.92, 95% CI [1.180, 2.665], p=0.0004.

The small differences between RRMS and controls indicates that this should be viewed with caution. Despite the significant difference in means, the standard deviations overlap, thereby affecting discrimination.

ROC curve analysis reveals for RRMS vs controls, CRVE has an AUC=0.680, 95% CI [0.610, 0.751], p<0.0001, and AVR has an AUC=0.701, 95% CI [0.632, 0.769], p<0.0001.

Vessel tortuosity

There was no significant difference in vessel tortuosity in any MS subtype, when compared with healthy controls. (Table 4.11)

However, there was a significant difference in arteriolar tortuosity between RRMS with and without ON history, with a history of ON associated with reduced arteriolar tortuosity (MD= -0.29, 95% CI [-0.506, -0.074], p=0.009). The difference is small, and would not discriminate between groups with significant specificity or sensitivity (AUC=0.582, 95% CI [0.520, 0.644], p=0.007).

Table 4.11: Retinal vessel analysis: vessel tortuosity

	healthy controls	**RRMS - no ON**	**RRMS + ON**	**PPMS**	**SPMS**
aTort	-9.04 ± 0.92	-8.97 ± 0.94	-9.26 ± 1.05	-9.01 ± 1.30	-9.17 ± 0.84
vTort	-9.54 ± 0.66	-9.49 ± 0.66	-9.43 ± 0.63	-9.32 ± 0.59	-9.48 ± 0.78

Abbreviations: aTort, arteriolar tortuosity; vTort, venular tortuosity
NOTE. Right eye analysis only. Data are shown as natural log transformed, from the raw tortuosity measurement calculation, and as mean ± SD
*P < 0.05, **P < 0.01, ***P < 0.001.

Vessel fractal dimension

Fractal dimension was significantly reduced for some D_f calculations in all MS subtypes. The greatest reductions were seen in arteriolar D_f. (Table 4.12)

Mono-fractal analysis (box-counting method) revealed a reduced arteriolar D_f in PPMS (MD= -0.014, 95% CI [-0.025, -0.002], p=0.021), SPMS (MD= -0.014, 95% CI [-0.021, -0.007], p=0.023), and RRMS +ON (MD= -0.013, 95% CI [-0.019, -0.006], p<0.001).

It also found a reduced venular D_f in SPMS (MD= -0.012, 95% CI [-0.018, -0.005], p=0.011), RRMS no-ON (MD= -0.008, 95% CI [-0.013, -0.003], p=0.003), and RRMS +ON (MD= -0.008, 95% CI [-0.014, -0.002], p=0.01).

Combined arteriolar and venular mono-fractal D_f was also reduced for SPMS and RRMS.

Table 4.12: Retinal vessel analysis: fractal dimension

	healthy controls	RRMS - no ON	RRMS + ON	PPMS	SPMS
aD_0	1.63 ± 0.03	1.62 ± 0.12	1.61 ± 0.03*	1.61 ± 0.03*	1.61 ± 0.04*
aD_1	1.62 ± 0.03	1.61 ± 0.12	1.60 ± 0.03**	1.60 ± 0.03*	1.60 ± 0.04*
aD_2	1.61 ± 0.03	1.59 ± 0.12	1.59 ± 0.03*	1.59 ± 0.03*	1.59 ± 0.04*
aD_{BOX}	1.13 ± 0.02	1.12 ± 0.03	1.11 ± 0.02**	1.11 ± 0.02*	1.11 ± 0.03*
vD_0	1.62 ± 0.03	1.60 ± 0.12	1.60 ± 0.03*	1.62 ± 0.02	1.60 ± 0.04**
vD_1	1.60 ± 0.03	1.58 ± 0.12	1.60 ± 0.03	1.60 ± 0.02	1.59 ± 0.04
vD_2	1.60 ± 0.03	1.58 ± 0.12	1.59 ± 0.03	1.59 ± 0.02	1.58 ± 0.04
vD_{BOX}	1.12 ± 0.02	1.11 ± 0.03**	1.11 ± 0.02**	1.12 ± 0.01	1.11 ± 0.03*
cD_0	1.80 ± 0.02	1.78 ± 0.13	1.79 ± 0.02*	1.79 ± 0.02	1.78 ± 0.03*
cD_1	1.79 ± 0.02	1.77 ± 0.13	1.78 ± 0.03	1.78 ± 0.02	1.77 ± 0.03*
cD_2	1.78 ± 0.02	1.76 ± 0.13	1.76 ± 0.02*	1.77 ± 0.02	1.76 ± 0.03*
cD_{BOX}	1.26 ± 0.02	1.25 ± 0.02**	1.25 ± 0.02**	1.25 ± 0.01	1.25 ± 0.02*

Abbreviations: $aD_{0\text{-}BOX}$, arteriolar fractal dimension 0 - BOX; $vD_{0\text{-}BOX}$, venular fractal dimension 0 - BOX; $cD_{0\text{-}BOX}$, combined fractal dimension 0 - BOX
NOTE. Right eye analysis only. Data are shown mean ± SD (fractal units)
*P < 0.05, **P < 0.01, ***P < 0.001.

Superior multi-fractal analysis methods revealed similar results, and for all three algorithms - capacity dimension, entropy dimension and correlation dimension.

Arteriolar capacity D_f (aD_0) was significantly reduced in PPMS (MD= -0.017, 95% CI [-0.032, -0.003], p=0.021), SPMS (MD= -0.020, 95% CI [-0.029, -0.011], p=0.015), and RRMS +ON (MD= -0.017, 95% CI [-0.025, -0.008], p=0.02).

Arteriolar entropy D_f (aD_1) was significantly reduced in PPMS (MD= -0.017, 95% CI [-0.032, -0.002], p=0.02), SPMS (MD= -0.019, 95% CI [-0.028, -0.011], p=0.016), and RRMS +ON (MD= -0.0168, 95% CI [-0.026, -0.008], p=0.006).

Arteriolar correlation D_f (aD_2) was significantly reduced in PPMS (MD= -0.017, 95% CI [-0.031, -0.003], p=0.019), SPMS (MD= -0.019, 95% CI [-0.029, -0.011], p=0.015), and RRMS +ON (MD= -0.017, 95% CI [-0.026, -0.008], p<0.001).

Venular capacity D_f (vD_0) was significantly reduced in SPMS (MD= -0.017, 95% CI [-0.026, -0.009], p=0.007), and RRMS +ON (MD= -0.009, 95% CI [-0.017, -0.001], p=0.021).

Venular entropy D_f (vD_1) was not significantly reduced in any MS subtype.

Venular correlation D_f (vD_2) was not significantly reduced in any MS subtype.

Combined arteriolar and venular multi-fractal D_f was significantly reduced for only SPMS (cD_0, cD_1, cD_2) and RRMS +ON (cD_0, cD_2).

The predominant finding when taking all these results together is therefore a reduced fractal dimension in MS, mainly in SPMS and RRMS +ON, and mainly arteriolar.

These findings would not all survive Bonferroni-type correction for multiple statistical testing; although full Bonferroni correction was not carried out here, as the retinal measures are not independent. However, this correction can result in false negatives, and so it is worth highlighting these findings, within the context of this study, and with the caveats of the multiple testing performed.

Data Analysis

In summary, all MS subtypes were associated with some retinal vessel morphological changes. Some of these findings do distinguish between MS subtypes.

For vessel calibre, RRMS was associated with thicker venules, and therefore lower AVR. This differentiates between RRMS and SPMS with very good discrimination, AVR AUC=0.811, 95% CI [0.747, 0.775], p<0.0001.

Further investigation of the subgroups within MS reveal that AVR is lower in the non-treated/treatment-naïve RRMS patients than in those currently on disease-modifying treatment - non-treated RRMS AVR=0.73 ± 0.06, treated RRMS AVR=0.76 ± 0.05. MD = 0.04, 95% CI [0.011, 0.059], p=0.005. Although AUC=0.670, 95% CI [0.564, 0.777], p=0.0058, limiting its discriminatory potential.

There was no significant difference in vessel tortuosity in any MS subtype, and poor discrimination between subtypes.

Fractal dimension analysis however revealed significant findings. Reduced arteriolar D_f was observed in PPMS, SPMS and RRMS +ON with both mono-fractal and multi-fractal analysis. Some reduction in venular D_f was also seen, but really only with mono-fractal analysis. There were no significant differences between subtypes.

GCL vs RNFL in MS

Much of the existing work on retinal biomarkers in MS involves measurement of the RNFL thickness. This measure of axonal integrity is a good choice of surrogate marker in MS for white matter damage, although its popularity is partly a result of being the first retinal layer for which automated segmentation and measurement became available on commercial systems.

New software updates permit the automated measurement of other retinal layers, including the ganglion cell body layer (GCL). This provides an alternative method for measuring the impact of MS on the RGC, by looking for cell body atrophy/loss, rather than axonal loss. It's not perfectly comparable with the grey/white matter distinction in the brain, but it draws parallels.

I therefore utilised measurements of macular GCL volume in comparisons with RNFL measures, focussing first on their sensitivity and specificity in identifying MS.

Diagnostic discrimination

Using ROC curve analysis, I have identified the best cutoff for diagnostic discrimination of RNFL and GCL measures. I have used all subtypes of MS patients as the patient group.

For global RNFL, the AUC=0.785, 95% CI [0.744, 0.826], p<0.0001. The best cutoff comes at 94.5μm, with specificity 78.3%, sensitivity 67.8% for identifying MS.

For temporal RNFL, AUC=0.819, 95% CI [0.786, 0.853], p<0.0001. Best cutoff comes at 63.5μm, with specificity 86.8%, sensitivity 64.7%.

Finally, for macular GCLV, AUC=0.853, 95% CI [0.823, 0.883], p<0.0001. Best cutoff comes at 1.035mm^3, with specificity 85.9%, sensitivity 70.8%.

Therefore, using GCL volume to diagnose MS improves sensitivity over both RNFL measures, whilst retaining high specificity. The discrimination is very good for both tRNFL and GCLV. For diagnostic discrimination, GCL > tRNFL > gRNFL. (Fig. 4.6)

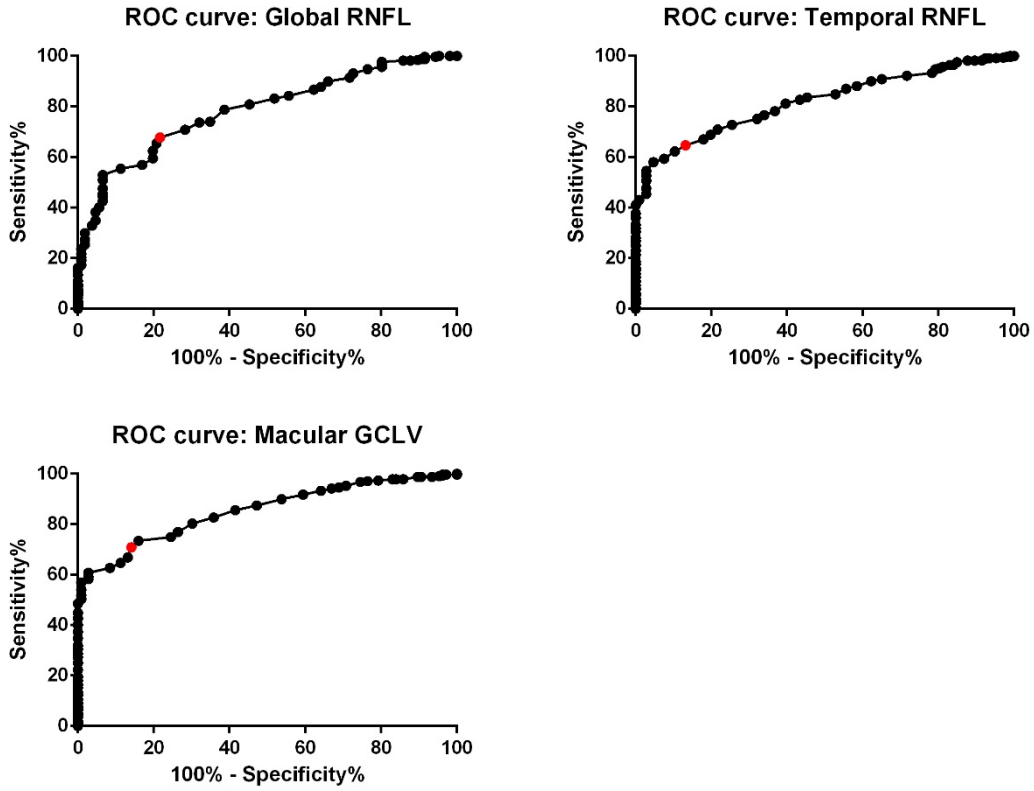

Figure 4.6: ROC curves for diagnostic discrimination of MS, using gRNFL, tRNFL and mGCLV

By comparison, measures of full macular volume (MV) and choroidal thickness (sfCT) are less useful in discriminating MS. For MV, AUC=0.766, 95% CI [0.725, 0.807], p<0.0001, with a cutoff of 8.545mm^3 giving specificity of 74.5%, sensitivity 66.8%. For sfCT, AUC=0.585, 95% CI [0.530, 0.640], p=0.0048.

Stability of measures

A key attribute of a reliable biomarker is repeatability, both within-session and visit-to-visit over the short-term. The degree of variance of physiological systems, from diurnal variations to fluctuations with other physiological parameters such as hydration or blood pressure, can influence the reliability and therefore clinical use of a biomarker.

The within-session repeatability of OCT-derived markers including RNFL thickness and GCL volume have been established, and are excellent.

What is more uncertain in MS is how they might vary in the short-term - over a few weeks to months.

With the hypothesis that RNFL may be more susceptible to small amounts of variation, due to proximity to the optic nerve, and fluid ingress as observed in asymptomatic microcystic macular oedema, or in optic neuritis, I asked a small sample of patients (and healthy controls) to return for repeated measures over a short time interval.

I imaged 3 RRMS (not on treatment) patients, and 3 healthy controls, 3 times over a six week period. I utilised the TruTrack™ active eye tracking to ensure the scans were repeated in the same exact location, to eliminate inter-scan variability related to position change of the OCT image.

I quantified variability of the metric using the coefficient of variation (CV) across the visits. (CV was chosen as a measure of variation because it is more independent of the mean than SD.)

The results showed that RNFL is vulnerable to short-term variability, when compared with GCLV. (Table 4.13)

Table 4.13: Inter-visit repeatability of OCT metrics using coefficient of variation

		First visit average	Across all visits average	CV
RRMS patients	tRNFL	64.2 ± 8.3	64.6 ± 8.3	12.8
	GCLV	75.2 ± 3.4	74.7 ± 2.3	3.1
Healthy controls	tRNFL	0.95 ± 0.08	0.94 ± 0.02	2.1
	GCLV	1.14 ± 0.04	1.14 ± 0.02	1.8

Abbreviations: tRNFL, temporal RNFL thickness; GCLV, macular GCL volume; CV, coefficient of variation
NOTE. Right eye analysis only. Data are shown mean ± SD
*P < 0.05, **P < 0.01, ***P < 0.001.

In addition, review of the individual patients' measures over the three visits confirmed that the RNFL measures occasionally varied by 1μm, whereas the GCLV measures did not vary.

The differences in CV for tRNFL between patients and controls refutes the possibility that the RNFL measure varies as a result of segmentation or measurement error, and so

supports the hypothesis that the RNFL can indeed vary in the short-term in MS patients, more than it does in healthy controls. Whereas the GCLV measure remains consistent and therefore a more reliable measure.

This was a very small study, but it is consistent with the knowledge of how the RNFL is susceptible to fluid ingress, resulting in minor variation in thickness measures.

Which first? Chronological relationship of tRNFL and GCLV thinning in MS

The ideal experiment for determining the natural history of change in each retinal layer is clearly a long prospective study. This is clearly very challenging in time and cost.

Cross-sectional data can provide some guide as to the relative timing of RNFL and GCL loss in MS, if we have sufficient recruitment across different disease duration periods.

My first thought was to look at early disease (up to 3 years duration) in treatment-naïve RRMS patients. However, I found there was too much variability in the thickness measures to draw any conclusions from this small group. Even dividing the sample into those with or without any optic neuritis history did not provide a workable comparison. (Fig. 4.7)

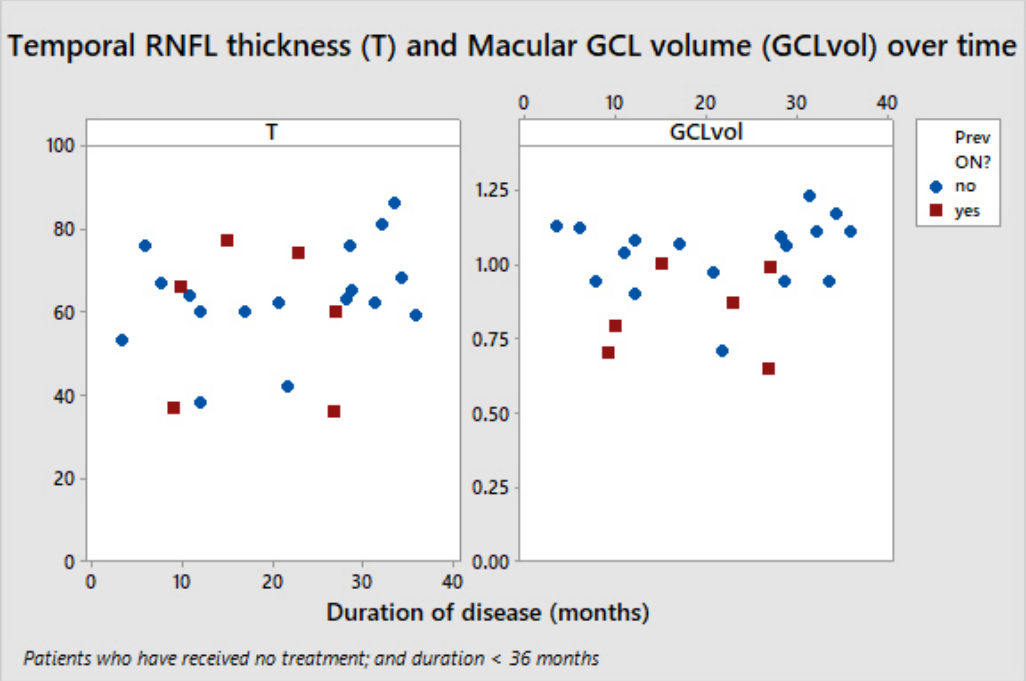

Figure 4.7: RGC measures with duration of disease in RRMS: early disease <36 months

I therefore looked at a longer duration of disease (up to 320 months), again in treatment-naive RRMS patients, and only those with no ON history. This was a larger sample size (n=202) and provided best-fit regression lines - (with the assumption that the regression lines are best fit for mean value at each duration; as duration is a continuous variable, it would lose precision if we switched to numerical discrete variable, as duration categories). (Fig. 4.8)

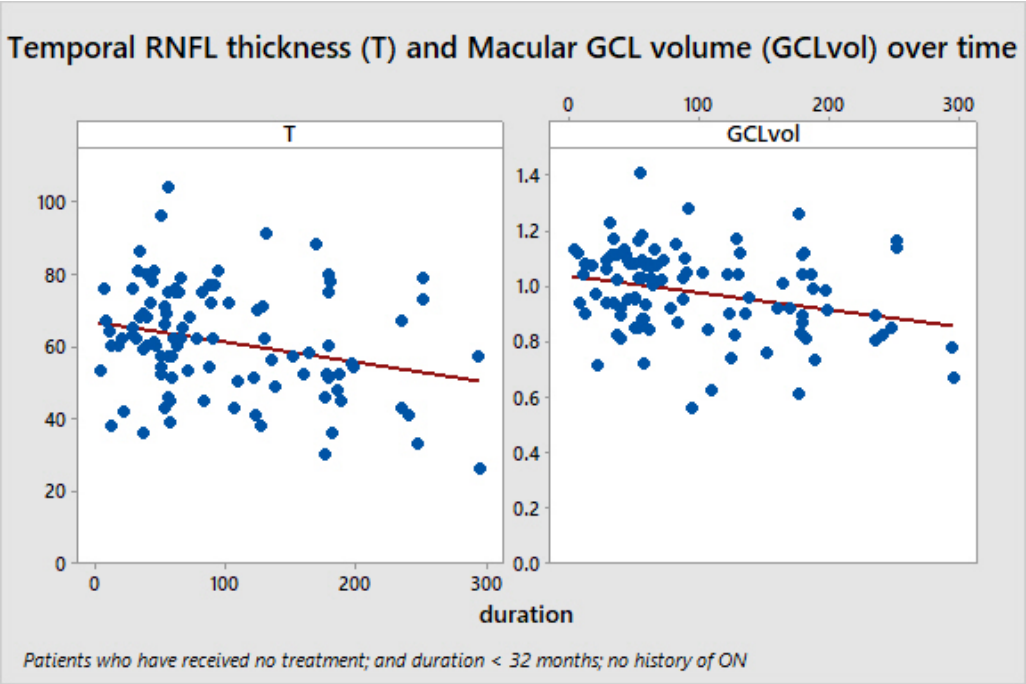

Figure 4.8: RGC measures with duration of disease in RRMS: duration of disease <320 months

From this analysis, we have sufficient sample size to enable us to calculate at what duration of disease do mean GCL and mean tRNFL in these RRMS patients fall below the corresponding control mean minus 2SD.

By comparison with healthy controls, we account for age-adjustment, and the natural history of RNFL and GCL layers over time.

From earlier data, we can extract the mean values for this the controls. (Tables 4.5, 4.7)

For tRNFL, control mean=74.9 ± 10.8 (μm). Therefore, mean minus 2SD = 53.3.

For GCLV, control mean=1.12 ± 0.08 (mm^3). Therefore, mean minus 2SD = 0.96.

From the graph data above we extracted the regression line formulae:

tRNFL regression line is T=66.78 - 0.05529 duration

GCLV regression line is GCL=1.038 - 0.000602duration

tRNFL falls to 53.3 at duration= (66.78 - 53.3)/0.05529 = 244 months.

And GCLV falls to 0.96 at duration= (1.038 - 0.96)/0.000602 = 130 months.

The gradient of GCLV decline is less than tRNFL and so this represents earlier rather than faster decline of the GCLV.

Therefore, this is tentative evidence that GCLV falls earlier in RRMS than RNFL.

This would support the hypothesis that involvement of the RGC in MS is via direct insult to the cell, causing cell-body atrophy and consequent axonal atrophy, rather than mere retrograde degeneration of brain white matter tracts.

In summary, GCL is superior to RNFL in diagnostic discrimination of MS, and is affected earlier in the disease course than RNFL. It is also a more stable measure than RNFL.

In addition, using the GCL overcomes an important weakness of the RNFL - that the layer contains not just RGC axons, but also vessels and glial tissue, and its thickness can be altered in MS by non-neuronal factors, such as inflammation, or even metabolic factors, such as cholesterol levels.[297]

Relationship with visual acuity

Visual acuity is the widest used measure of visual function. In this study, I measured VA in a sub-group of SPMS patients (n=80) - measuring full-contrast ETDRS VA, and also low-contrast 'Sloan' VA at contrast levels of 5%, 2.5% and 1.25%.

The aim was to look at how the structural measures of the neuroretina and retinal vasculature might correlate with visual function in MS, and also which of the low-contrast percentages were most clinically useful in MS patients, for longitudinal monitoring of visual function.

Visual acuity in SPMS

By choosing SPMS as the subgroup for this question, I benefit from a broad range of acuity across the patients, who may have had MS for some time, may have had multiple optic neuritis episodes, resulting in poorer subjective as well as objective acuity.

This hypothesis was shown to be accurate, as there was measurable variation of acuity even within the full-contrast chart. Across the low contrast 'Sloan' charts, VA measures were predictably poorer, with a 'floor effect' quickly apparent especially in the lowest contrast percentages. (Fig. 4.9)

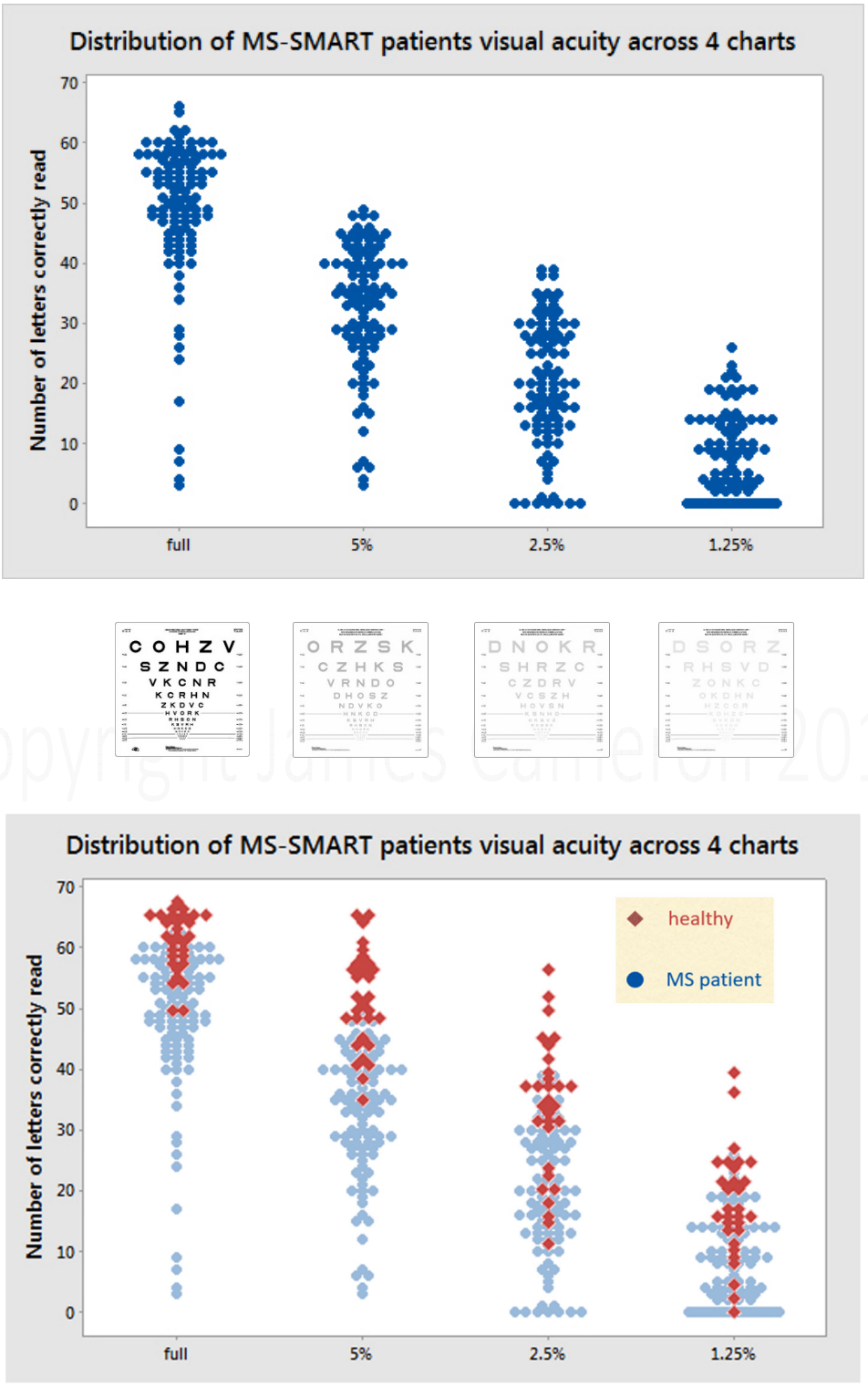

Figure 4.9: Visual acuity in SPMS: range of acuity levels. a) dot plot of SPMS patients for each VA chart type b) same data with healthy controls superimposed

If we desire a low contrast VA chart that can best encompass the range of acuity encountered within this patient population, and retain some ability to measure decline, then the 2.5% and 1.25% charts become too difficult to read, and too many patients will score zero letters.

Therefore, the 5% low contrast VA chart is the best low contrast chart for monitoring VA in SPMS.

The full contrast chart also maintains useful information in SPMS (but less so in RRMS), and so it is also recommended as a supplementary test.

I haven't reported the figures and graphs in PPMS and RRMS, due to incomplete data, but they also show a trend that the 5% low contrast chart is the most appropriate chart for visual assessment in these MS subgroups also, with the exception of early RRMS, where there is an approaching 'ceiling effect' in the 5% chart, and so the 2.5% chart becomes more useful in longitudinal studies.

Visual acuity and the RNFL

The relationship between structure and function within the retina is an important one, and often overlooked. It is clear that axonal damage and atrophy within the optic nerve - and the RNFL - can affect vision, but the association between the two has not been explored in detail.

With this same group of SPMS patients, I have examined the correlations between visual acuity (on the full contrast, 5% and 2.5% charts) and RNFL thickness (global, and temporal). (Fig. 4.10)

a)

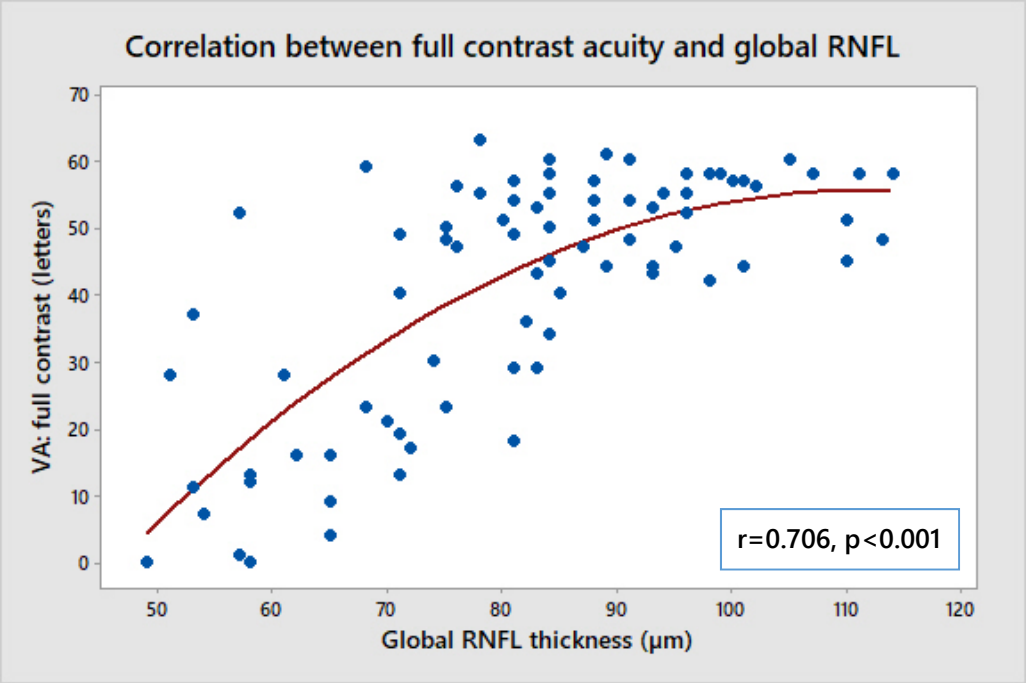

b)

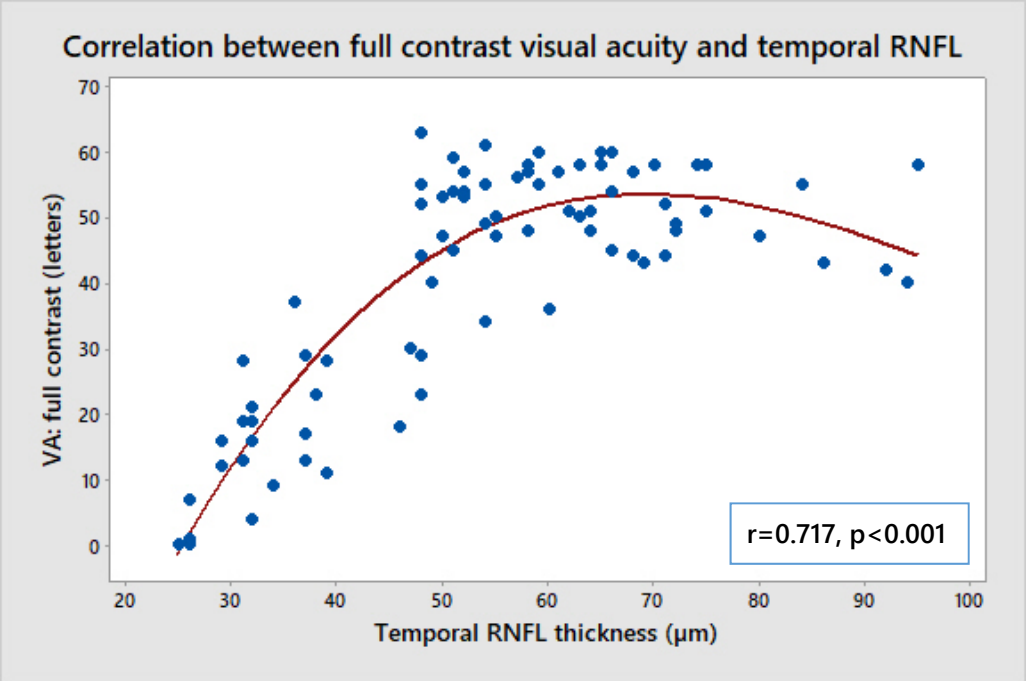

Figure 4.10: Visual acuity in SPMS: relationship with RNFL thickness. a) full contrast acuity and global RNFL b) full contrast acuity and temporal RNFL c) 5% low contrast acuity and global RNFL d) 5% low contrast acuity and temporal RNFL e) 2.5% low contrast acuity and global RNFL f) 2.5% low contrast acuity and temporal RNFL

c)

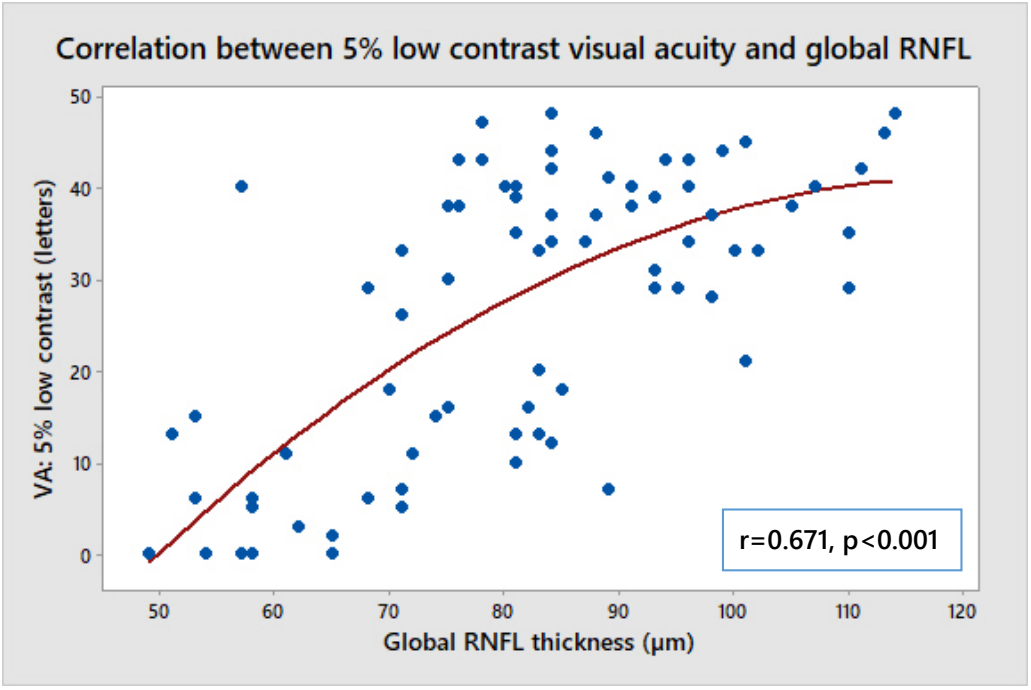

d)

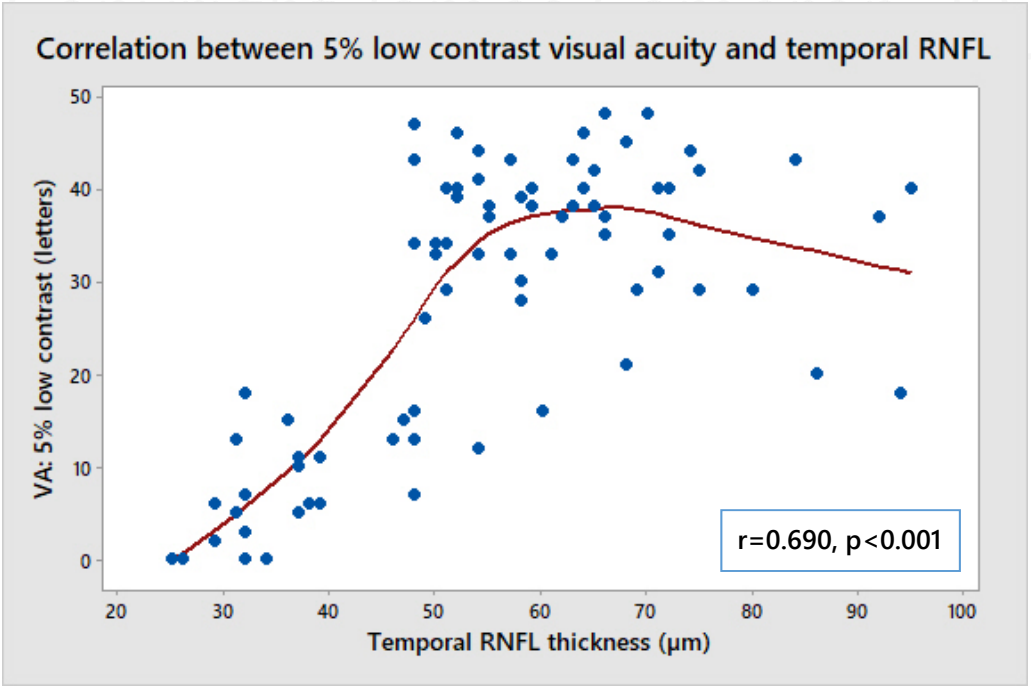

Figure 4.10: continued

e)

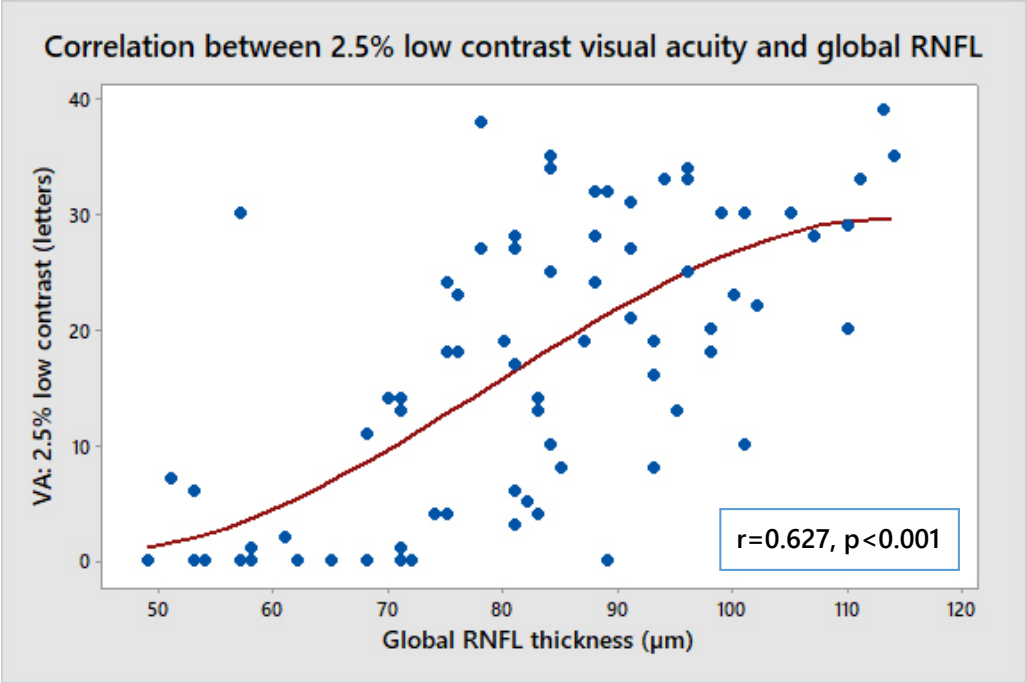

f)

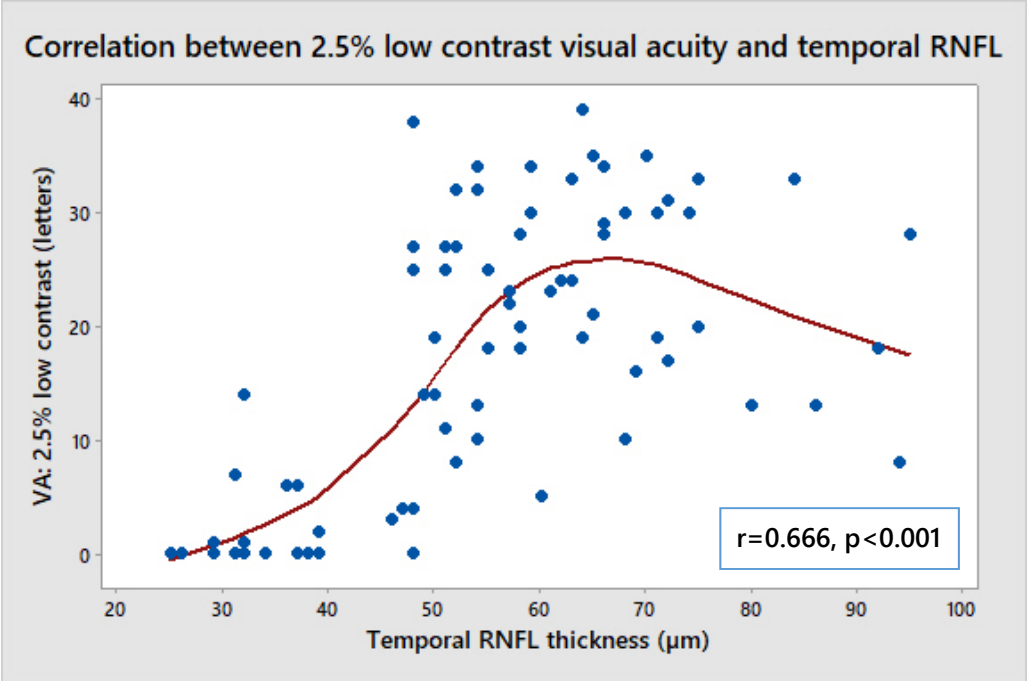

Figure 4.10: continued

It is apparent from these graphs that whilst there is a trend for reduced vision with reduced RNFL thickness, there remains a great variability in how much vision these patients have with different levels of axonopathy. Of course, acuity is only one component of vision, and we have not examined colour vision or reading acuity. Nevertheless, some interesting findings are evident.

Firstly, there is a strong correlation between visual acuity at all contrast levels and RNFL thickness. The Pearson correlation coefficients vary from 0.627 to 0.717, with temporal RNFL thickness showing a higher correlation at each acuity contrast.

Secondly, there is a much clearer threshold of axonal loss impacting visual acuity in the temporal RNFL graphs. Below around 48μm temporal RNFL thickness, visual acuity drops off significantly. Above 48μm, visual acuity is relatively well preserved. This appears true in both full contrast and low contrast measures of acuity. Even in the 2.5% low contrast chart, where the 'floor effect' has reduced the strength of the correlation with RNFL thickness, there is still a visible drop-off in vision below 48μm.

Whilst this is cross-sectional data, this suggestion of a threshold level above which vision is relatively reserved, and below which vision takes a significant hit, certainly has biological plausibility, and could be an important figure to use in clinical situations where patients may be asking about visual prognosis. Further evaluation of this finding would require a longitudinal study of individual patients, perhaps with added patient-reported quality of vision metrics, perhaps in different environmental domains, and recorded on a Likert scale, for correlation with objective VA and RNFL thickness.

Thirdly, the regression curves generated reported narrower confidence intervals for the temporal RNFL correlations. This further suggests temporal RNFL may be the better model of fit for visual acuity measures.

To further determine which model best fits the visual acuity data, we can perform a residuals (regression) analysis. The best tool is a 'residuals versus fits' plot. This shows the spread of points, and is usually used to check for non-linearity, unequal error variances, and outliers.

Plotting 'residuals versus fits' plots for gRNFL and tRNFL, we see that there is good randomness in the residuals of both RNFL measures, but the residuals are smaller and more symmetrical in the temporal RNFL, suggesting it is the better model. (Fig. 4.11)

a)

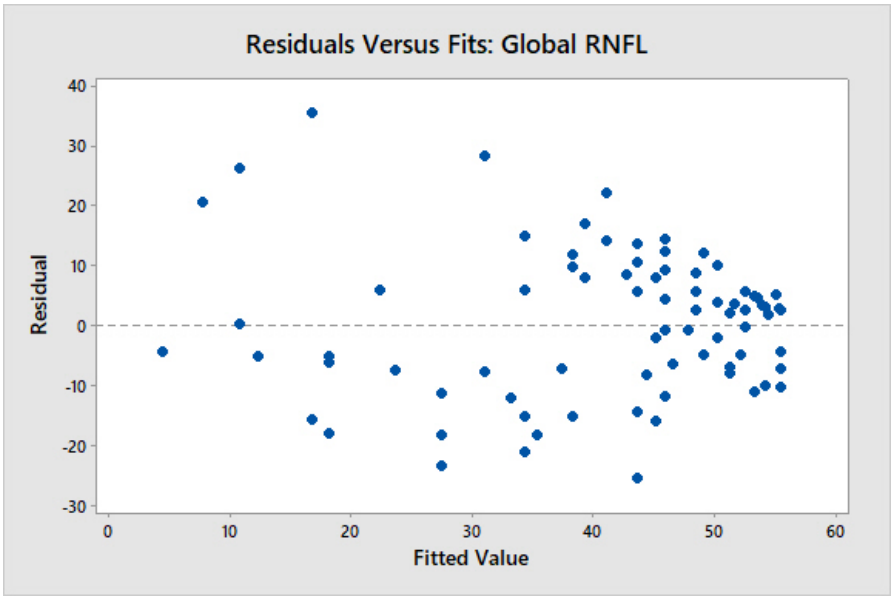

b)

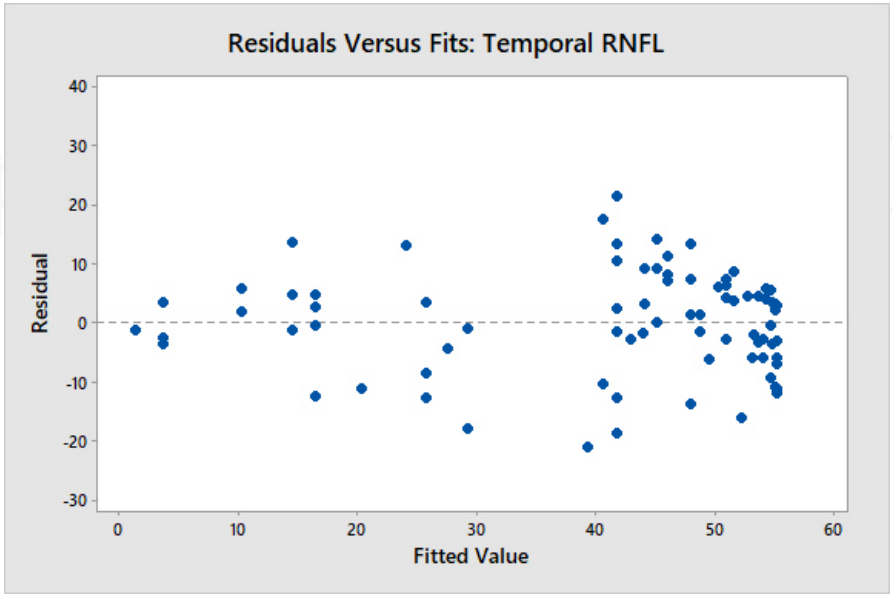

Figure 4.11: Visual acuity in SPMS: regression analysis. Residuals versus fits plots for full contrast acuity and a) global RNFL b) temporal RNFL

This makes sense, as visual acuity relies on macular neuroretinal function, which corresponds with the temporal RNFL and temporal optic nerve. With MS having a predilection for the temporal RGCs, and increasing importance of structure/function comparators, this provides further evidence for the superiority of temporal RNFL measures over global RNFL as a marker of MS disease.

Visual acuity and the GCL

The ability to now measure the GCL volume in the macula offers an opportunity for another measure of RGC integrity. It could be expected that macular GCL volume results will closely match temporal RNFL thickness measures, as the macular GCL is the direct connection of the temporal RNFL. However, there is not always a direct correlation between RGC measures and RNFL measures of the same region, in MS patients. This may be due to the timing of atrophy, or gliosis, or vascular changes.

A correlation graph of macular GCL volume and full contrast visual acuity actually shows a high level of correlation (r=0.746, p<0.001), which is superior to the temporal RNFL. (Fig. 4.12)

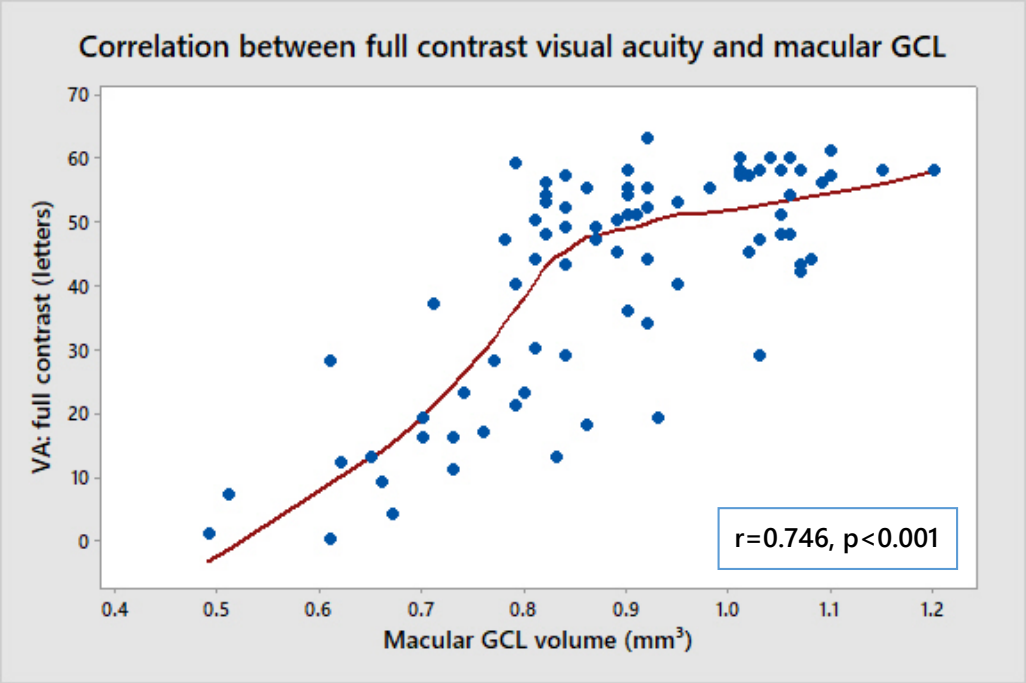

Figure 4.12: Visual acuity in SPMS: relationship with macular GCL volume

Although a 'residuals versus fits' plot reveals an asymmetric distribution, with clustering below the regression line. (Fig 4.13) This corresponds to the macular GCL volume of around 0.8 to 0.9 where there is a wider variation of acuity than expected. Similar results were seen with the low contrast visual acuity data.

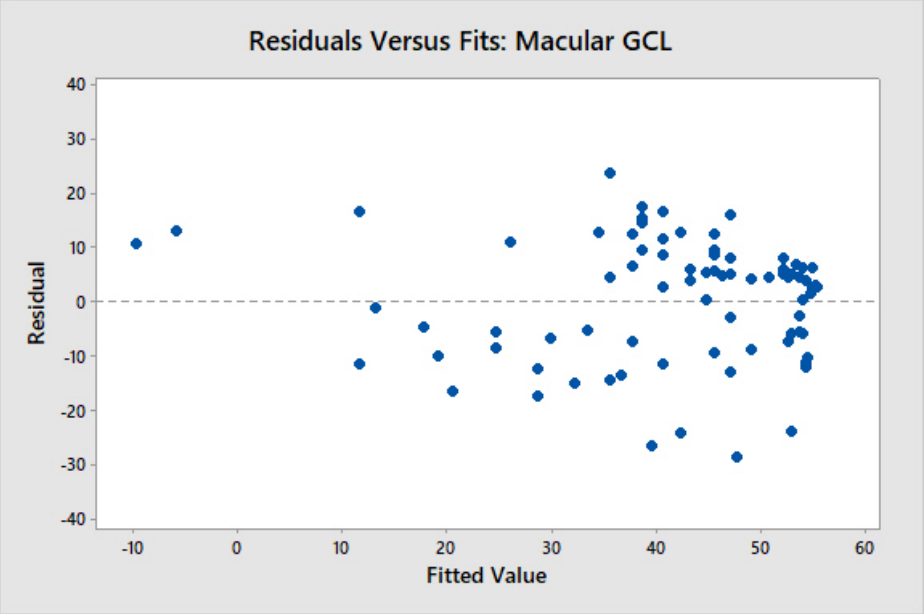

Figure 4.13: Visual acuity in SPMS: regression analysis. Residuals versus fits plots for full contrast acuity and macular GCL volume

Therefore, whilst macular GCLV has the highest correlation with visual function, variation persists and temporal RNFL is perhaps more reliable.

Similar trends were seen for PPMS, and RRMS.

Visual acuity and other outcome measures

There was poor correlation between visual acuity at all contrast levels and EDSS - full contrast (Spearman's rho= -0.171, p=0.130), 5% low contrast (rho= -0.090, p=0.429), 2.5% low contrast (rho= -0.139, p=0.219).

This is unsurprising given how motor-focussed the EDSS is.

Predicting clinical course

An important clinical measure in assessing disease activity in RRMS is the frequency of relapses, which can be averaged as the annualised relapse rate (ARR). Whilst this measure can be used to guide treatment plans, by highlighting patients with high disease activity, a far preferable marker would predict those relapses, and therefore enable treatment to commence earlier.

The hypothesis for this sub-study is that examination of the retina - and the retinal vessels in particular - could indicate higher inflammatory activity, and this may be predictive of future relapses.

Accurate recording of relapses generally requires an intensive prospective trial. Within my cohort of study patients, one neurologist judiciously records relapse events. I therefore selected only RRMS patients from that one neurologist, and that received retinal imaging in the first year of this study, permitting 18 months of follow-up.

The sample size was 44 RRMS patients, with a range of ARR of <1, 1-2, and 3-4.

Graphing the association between six measured retinal parameters and ARR reveals potential predictors. (Fig. 4.14)

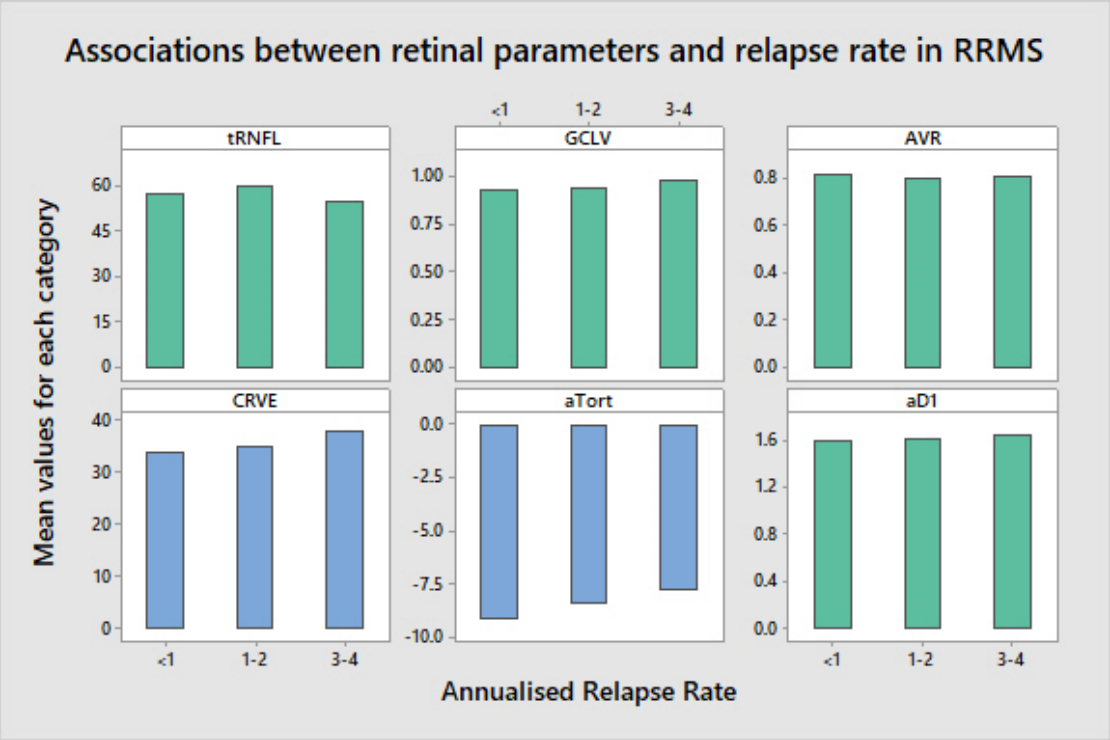

Figure 4.14: Relapse rate in RRMS: associations with baseline retinal parameters

Two measures of retinal vascular morphology - CRVE and arteriolar tortuosity - demonstrate an association with ARR.

Using logistic regression, higher CRVE is predictive of greater ARR (adjusted-OR=1.82, 95% CI [1.56, 2.09]) and higher arteriolar tortuosity is also predictive of greater ARR (adjusted-OR=1.66, 95% CI [1.61, 1.71]).

Whilst tRNFL thinning is not independently predictive of greater ARR (OR=1.02, 95% CI [0.96, 1.08]), adding it to the model with a threshold of tRNFL < 56 increases the predictive OR of CRVE to 2.22 (95% CI [1.98, 2.42]) of a rise in the ARR to 1-2 or 3-4.

In other words, if temporal RNFL is less than 56μm, a higher CRVE (above 35px) is associated with a 2x higher risk of at least one relapse in the next year.

Differentiating MS and NMO

A not uncommon clinical scenario is the presentation of a patient who may have an NMO-spectrum disorder, rather than MS. The presence of AQP4 antibodies enables the diagnosis in many cases, but with a far lower sensitivity than specificity, not all cases will be picked up this way.

The clinical presentation in NMO often features a more severe optic neuritis, and a higher chance of more permanent effect on vision. This suggests that examination of the neuroretina may aid discrimination of this condition.

RNFL, GCL and vessels in NMO and MS

To investigate the utility of neuroretinal markers in NMO, I recruited patients with NMO (n=17) from the specialist NMO clinic at the ARRNC.

This cohort were all AQP4-positive, and had sustained an optic neuritis in their right eye. This enabled a comparison with RRMS patients with an ON history.

The NMO sample group had a mean age of 48.7 years (SD 15.8, range 18-83), a male:female ratio of 7:10, and a mean refraction of -0.1 (SD 1.01, range -2 to 1.75).

All NMO patients had the full OCT imaging protocol as outlined in Chapter 3. SLO images were processed with VAMPIRE, and the standard vessel morphology parameters calculated.

Results

The mean age of the NMO group was slightly higher than the RRMS, and disease duration shorter. Therefore, the NMO mean data provided has been adjusted for age and disease duration, in line with the RRMS group. (Table 4.14)

Table 4.14: NMO and MS: comparison of selected OCT and vessel metrics, with controls

	healthy controls	**RRMS + ON**	**NMO †**
pRNFL thickness: global	101.0 ± 10.9	76.3 ± 15.5***	63.4 ± 9.5***
T	74.9 ± 10.8	48.5 ± 13.8***	42.9 ±7.5***
N/T	1.045 ± 0.23	1.254 ± 0.34**	1.115 ± 0.24*
Macular full thickness volume MV	8.74 ± 0.33	8.21 ± 0.41***	8.39 ± 0.51**
Macular GCLV	1.12 ± 0.08	0.88 ± 0.13***	0.92 ± 0.21***
sfCT	322.3 ± 92.5	294.7 ± 99.7*	333.8 ± 82.2
CRAE	28.08 ± 2.17	28.29 ± 2.30	29.06 ± 2.37
CRVE	35.37 ± 2.41	37.30 ± 3.15***	34.95 ± 2.63
AVR	0.80 ± 0.06	0.75 ± 0.07***	0.83 ± 0.05*
aTort	-9.04 ± 0.92	-9.26 ± 1.05	-8.86 ± 0.94
vTort	-9.54 ± 0.66	-9.43 ± 0.63	-9.08 ± 0.90
aD_1	1.62 ± 0.03	1.60 ± 0.03**	1.61 ± 0.03
vD_1	1.60 ± 0.03	1.60 ± 0.03	1.59 ± 0.05

Abbreviations: T, temporal; N, nasal; N/T, nasal-temporal ratio; MV, macular volume; GCLV, ganglion cell layer volume; sfCT, sub-foveal choroidal thickness; CRAE, central retinal arteriolar equivalent; CRVE, central retinal venular equivalent; AVR, arterio-venous ratio; aTort, arteriolar tortuosity; vTort, venular tortuosity; aD_1, arteriolar fractal dimension 1; vD_1, venular fractal dimension 1

NOTE. Right eye analysis only. Data are shown mean ± SD (μm)

† NMO data are age- and disease-duration-adjusted means

*P < 0.05, **P < 0.01, ***P < 0.001.

There is a fair degree of similarity between the NMO RGC data and RRMS. The global and temporal RNFL in NMO are significantly thinner than controls.

The MV and GCLV are also significantly reduced.

However, NMO is not associated with a thinner choroid, unlike RRMS.

Regarding the retinal vessel morphology, the only significant finding compared with controls was a raised mean AVR (MD=0.04, 95% CI [0.009, 0.066], p=0.013).

Diagnostic discrimination

To look for the strength of neuroretinal parameters in discriminating between MS and NMO, we need to compare the data from the two groups, and then use ROC curve AUC analysis to calculate specificity and sensitivity of each value.

Global RNFL was significantly thinner in NMO (MD= -12.9, 95% CI [-19.4, -6.2], p<0.001).

Temporal RNFL was significantly thinner in NMO (MD= -5.6, 95% CI [-7.3, -3.8], p=0.042)

N/T ratio was also significantly different between NMO and RRMS (MD= -0.133, 95% CI [-0.170, -0.095], p<0.001)

In addition, AVR was significantly different between RRMS and NMO (MD=-0.08, 95% CI [-0.11, 0.05], p<0.001) as was CRVE (MD=2.34, 95% CI [0.89, 3.80], p=0.003

We therefore have significant differences in the RNFL and the vessel calibre between MS and NMO.

For global RNFL, the AUC=0.735, 95% CI [0.626, 0.844], p<0.0001. The best cutoff comes at 66.5µm, with specificity 80.7%, sensitivity 65.5% for identifying NMO.

For temporal RNFL, AUC=0.629, 95% CI [0.513, 0.745], p=0.065. Best cutoff comes at 43.5µm, with specificity 59.7%, sensitivity 65.0%.

For the N/T ratio, AUC=0.612, 95% CI [0.507, 0.717], p=0.080. Best cutoff comes at 1.155, with specificity 56.1%, sensitivity 68.0%.

Finally, for macular GCLV, AUC=0.569, 95% CI [0.429, 0.708], p=0.386. Best cutoff comes at 0.905mm^3, with specificity 56.1%, sensitivity 60.0%. (Fig. 4.15)

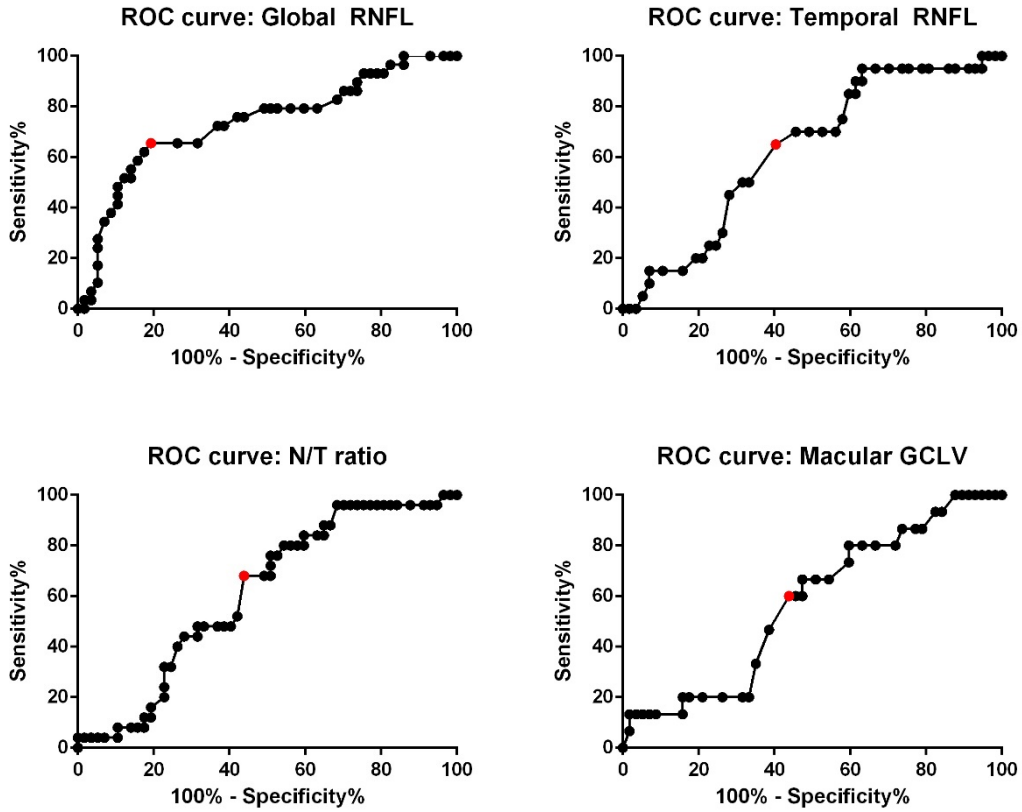

Figure 4.15: ROC curves for diagnostic discrimination of NMO from RRMS, using gRNFL, tRNFL, N/T ratio, and mGCLV

Generating ROC curves for multiple classes enables us to achieve a best cutoff for more than one variable.

With this further analysis, we can produce a compound cutoff score for discrimination. We find that for combined cutoffs of tRNFL<63.5µm + gRNFL <88µm + N/T ratio<1.24, the specificity for identifying NMO is 94.6%, with sensitivity 71.0%. Adjusting temporal RNFL upwards to a cutoff of 68µm improves sensitivity to 92%, but specificity drops to 81.5%.

Therefore, there is value in the N/T ratio, in demonstrating temporal loss is not out of proportion to global loss in NMO (whereas in MS, temporal RNFL loss predominates).

With integration of vessel data, we can refine this further.

Examining ROC curves for AVR and CRVE, we find for AVR, AUC=0.830, 95% CI [0.747, 0.913], p<0.0001. Best cutoff comes at 0.82, with specificity 79.8%, sensitivity 70.6%

And for CRVE, AUC=0.711, 95% CI [0.589, 0.833], p=0.005. Best cutoff comes at 35.56px, with specificity 71.9%, sensitivity 70.6%. (Fig. 4.16)

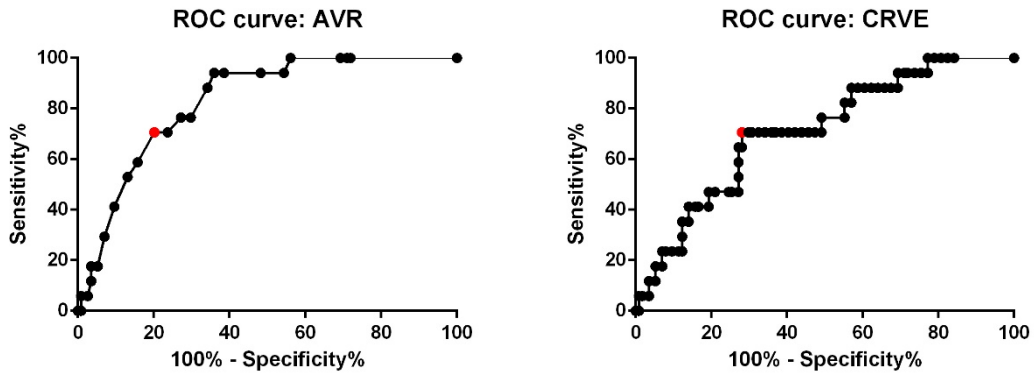

Figure 4.16: ROC curves for diagnostic discrimination of NMO from RRMS, using AVR, CRVE

It appears that AVR is the highest single discriminant of NMO versus RRMS. NMO is not associated with the wider venules as in MS.

So, in the clinical presentation of a profound optic neuritis, global RNFL loss (and a preserved N/T ratio<1.24) raises suspicion of NMO. However, evaluation of vessels could further assist with discrimination.

Whilst a molecular classification of demyelinating disorders is likely to form the basis of future diagnostic algorithms[298], the relatively high specificity and sensitivity of combination retinal metrics in discriminating NMO from MS, particularly after an early ON event, suggests it is likely to hold an important clinical role.

Discussion

This is the first study to look at neuroretinal markers in MS, in a Scottish population.

Having identified unanswered questions from the literature, I have investigated the utility of neuronal and vascular markers in the retina in association with all subtypes of MS in more detail, focussing on clinical utility and structure/function correlations.

I have studied diagnostic phenotyping, association with visual acuity, and discrimination with other similar diseases, and uncovered several novel findings.

Summary

I recruited 655 MS patients, across the subtypes RRMS, PPMS and SPMS.

RNFL, MV and GCLV

In agreement with the published results from the US, Germany and Spain, I found that all MS subtypes were associated with RNFL thinning, with a history of optic neuritis associated with the greatest degree of thinning.

In all MS subtypes, the temporal RNFL sector was affected the greatest. Temporal RNFL thickness was also the strongest in discriminating a history of optic neuritis.

Macular thickness and macular volume were significantly reduced in all MS subtypes, but with SPMS most affected, closely followed by RRMS with ON history. This includes macular GCL volume, which again was most significantly affected in RRMS +ON and SPMS.

No clear pattern of neuroretinal change emerged to distinguish between MS subtypes with high specificity. However, several measures discriminated NMO from RRMS. Combining measures of tRNFL, gRNFL, and N/T ratio provided very high discrimination with 94.6% specificity.

Correlation between these measures and EDSS was generally poor, except for RNFL thinning and EDSS in the RRMS +ON group, which showed moderate correlation.

Choroid

No previous studies have investigated choroidal thickness in MS.

The subfoveal choroid is thinner in MS, with or without ON history. It is thinner in all MS subtypes, and thinnest in SPMS. The degree of thinning does not correlate with duration of disease, visual acuity, EDSS or central macular thickness.

However, further analysis revealed that in RRMS, the choroid is thinner in patients currently on treatment, versus treatment-naïve patients. So rather than it being MS itself affecting the choroid, is it perhaps the disease-modifying treatment, with a direct effect on the choroidal blood vessels?

This would not explain why sfCT is thinnest in SPMS, but we can speculate that these patients may have been on treatment previously, or had multiple courses of steroids in the past. In non-MS patients, the effect of steroids on the choroid is unclear.[299]

Retinal vessel calibre, tortuosity and fractal dimension

RRMS was associated with significantly thicker venules, and corresponding lower AVR. PPMS and SPMS were not associated with any difference in vessel calibre. AVR differentiates between RRMS and SPMS with very good discrimination

Further investigation of the subgroups within MS reveal that AVR is lower in the non-treated/treatment-naïve RRMS patients than in those currently on disease-modifying treatment. Whilst this association cannot be causally linked, as this was not a randomised trial, it nevertheless adds some support to the working hypothesis that the inflammation associated with MS can perhaps be identified in the retinal vessels, and that in patients on anti-inflammatory treatment, those vessel changes may reverse. The findings in patients with or without a history of ocular involvement of their MS also adds weight to this subclinical involvement of the retina in MS.

There was no significant difference in vessel tortuosity in any MS subtype, when compared with healthy controls. However, there was a significant difference in arteriolar tortuosity in patients with and without a history of ON, with ON associated with reduced arteriolar tortuosity.

Fractal dimension was significantly lower in all MS subtypes, mainly arteriolar, and predominantly in RRMS +ON and SPMS.

AVR and CRVE discriminated between NMO and RRMS with high specificity, AVR being the highest single discriminant of NMO versus RRMS.

GCL vs RNFL

With global RNFL, temporal RNFL and macular GCL volume all showing significant reductions in MS, it is tempting to enquire as to which is best. The answer is that it depends on the purpose for using the measure.

For diagnostic discrimination of MS, GCL volume is superior to RNFL measures, with high specificity and sensitivity. And temporal RNFL is superior to global RNFL, again with very good discrimination, and high specificity.

An important quality of a reliable biomarker is stability over the short-term. here, GCL volume is superior to RNFL measures, as the RNFL is vulnerable to short-term variability. This is due to the nature of the RNFL - fluid can ingress into the layer during periods of inflammation, artificially thickening it. The larger retinal vessels also pass through the RNFL, and so their activity can influence the RNFL tissues.

The temporal relationship between RNFL and GCLV change in MS has not been investigated, but I have shown some tentative evidence that GCLV falls earlier in RRMS than RNFL. This supports the hypothesis that RGC involvement in MS is direct and specific, rather than retrograde and non-specific.

Therefore, for diagnostic discrimination of MS, GCLV appears superior to RNFL. It is also affected earlier in the disease course than RNFL, and is a more stable measure.

Future work could also examine the intra-retinal neurones, such as the inner nuclear layer, to see if it too is impacted by inflammatory insults to the neuroretina. Measurable impact and change could also be predictive of future treatment response. Though it is unknown if inflammation to mid-retinal layers causes atrophy and therefore thinning, or scarring and therefore thickening.

Visual acuity in MS

Visual acuity assessment is an important clinical test for patients with MS, and is highly correlated with quality-of-life metrics in this population. In this sub-study, I looked at a sample of SPMS patients, and performed visual acuity testing across four acuity charts - one full contrast, and three low-contrast (LCVA) charts. A ‘floor’ effect was immediately apparent in the lowest contrast charts.

The choice of LCVA chart in clinical use, as well as in research trials, is an important one. The importance of recognising the potential for 'floor effect' and 'ceiling effect' in assessing LCVA in MS has been expressed by L Balcer, one of the most important authors in this area of MS neuro-ophthalmic research.[300] My study suggests the 5% 'Sloan' LCVA as the best low contrast chart for clinical use in SPMS, and probably also in PPMS and RRMS, with perhaps the 2.5% chart for additional benefit in early RRMS.

Investigating the relationship between visual acuity and RNFL thickness revealed a strong correlation at all contrast levels, with temporal RNFL thickness showing the highest level of correlation. In addition, a threshold tRNFL thickness of 48μm corresponded to a level above which visual acuity remained relatively well preserved, but below which acuity dropped off significantly.

Temporal RNFL thickness was superior to global RNFL thickness in all correlations and residuals plots. This makes sense, as visual acuity relies on macular neuroretinal function, which corresponds with the temporal RNFL and temporal optic nerve. This then provides further evidence for the superiority of temporal RNFL measures over global RNFL as a marker of MS disease.

Macular GCL volume correlated very well with full contrast visual acuity in SPMS, but actually revealed a higher level of variation and wider confidence intervals than temporal RNFL. Therefore, tRNFL remains the best comparator with visual function.

Predicting clinical course

Relapses in MS represent a key indicator of disease activity and severity, and measures of relapse rate guide clinical care and treatment plans.

With a goal to treat patients earlier and in a stratified, personalised way, there is a need for markers that predict those with a higher risk of future relapses. The hypothesis for this sub-study was that observing the retinal vasculature could provide an indicator of inflammatory activity, and earlier than the occurrence of symptomatic relapses.

I analysed a sample of 44 RRMS patients with detailed relapse data for the 18 months following retinal imaging, and found that wider venules were predictive of a greater relapse rate, especially in patients with a lower tRNFL thickness. If temporal RNFL is less than 56μm, a higher CRVE (above 35px) is associated with a 2x higher risk of at least one relapse in the next year.

Utility as a biomarker

- *Detection method should be precise, reliable and transferrable*
  True for all OCT imaging derived measures: RNFL, MV, GCL, sfCT
  True for all VAMPIRE retinal vessel measures: calibre, tortuosity, fractal dimension

- *Distinguish between healthy and disease*
  True for RNFL; MV; GCL; sfCT; calibre; fractal dimension
  Not true for tortuosity

- *Differentiate between diseases that are clinical similar*
  True for tRNFL, gRNFL, N/T ratio, AVR, and CRVE (NMO and RRMS); arteriolar tortuosity (optic neuritis history in RRMS)
  Not true for fractal dimension

- *Value as a prognostic marker*
  True for CRVE, arteriolar tortuosity (predictive of relapse rate)
  No other prognostic endpoints assessed in this study.

- *Use in monitoring disease progression*
  True for RNFL, GCL (correlation with visual function), RNFL (EDSS)
  No other disease progression indicators assessed in this study.

- *Use as a pre-clinical screening test*
  Not assessed in this research study

Contributions to knowledge

- Relapsing-remitting multiple sclerosis with a history of optic neuritis, was associated with the greatest reduction in RNFL thickness, in all sectors, in macular GCL volume. It was also associated with thicker venules, and lower arterio-venous ratio. AVR discriminated between RRMS and SPMS with very good discrimination. In addition, treatment-naïve RRMS patients were associated with a lower AVR.

- Secondary-progressive MS was associated with the greatest reductions in macular thickness, macular volume and sub-foveal choroidal thickness.

- The choroidal thinning seen in all MS subtypes did not correlate with duration of disease or visual acuity, but was thinner in RRMS patients on treatment, versus treatment-naïve.

- Retinal vessel tortuosity was not associated with any MS subtype, but was associated with optic neuritis history in RRMS (reduced arteriolar tortuosity with ON history).

- Reduced retinal vessel fractal dimension was found in all MS subtypes, mainly of the arteriolar tree, and to the greatest degree in SPMS and RRMS +ON.

- GCL volume measures were superior to RNFL measures in diagnosing MS, although GCL and tRNFL both discriminated MS with high specificity. Macular volume and choroidal thickness were much less useful in discriminating MS. GCL volume measures were also more stable than RNFL over the short-term, reflecting the vulnerability of the RNFL to fluid changes and variation. Finally, GCL volume falls earlier in RRMS disease course than RNFL

- Visual acuity in SPMS was strongly correlated with RNFL thickness (particularly temporal RNFL) and macular GCLV, at all contrast levels. GCLV showed the best correlation, but tRNFL proved the more reliable comparator.

- ❖ Thicker retinal venules and higher arteriolar tortuosity were both predictive of greater relapse rate in RRMS. This was elevated further in patients with tRNFL less than 56μm, a higher CRVE (above 35px) was associated with a 2x higher risk of at least one relapse in the next year.

- ❖ Regarding discrimination between RRMS and NMO, temporal RNFL, global RNFL, N/T ratio, GCLV, AVR and CRVE were all significantly different between RRMS +ON and NMO. AVR was the highest single discriminant, but a combined score using cutoffs in tRNFL, gRNFL and N/T ratio discriminated NMO from RRMS +ON with 94.6% specificity.

Conclusion

Retinal markers of neuronal and vascular integrity do have excellent clinical utility in diagnostic phenotyping and predicting disease course in MS.

These neuroretinal measures can diagnostically discriminate MS from healthy controls, and from NMO. There is also potential for predicting disease progression.

The relative value of each marker depends upon the MS subtype, and disease-related question.

5 EARLY-ONSET DEMENTIA

Introduction

There have been several studies exploring the neuroretina in patients with Alzheimer's disease (AD), but unlike MS, there has been little progress beyond this in exploring how these metrics may correlate with existing clinical markers, or how they may be clinically useful with the individual patient.

There are several challenges to exploring this in the field of dementia. There are no 'gold standard' diagnostic or monitoring markers, and diagnostic classifications in dementia are syndromic rather than pathology based. However, these challenges do actually invite the study of new markers that could potentially improve diagnostic and phenotypic classification of patients, as well as the potential for individual patient monitoring.

Clinical diagnostic criteria in recent use for AD often fail to robustly differentiate accurately between AD and non-AD pathology with up to 40% of patients diagnosed with non-AD dementias identified as having pathology consistent with AD at post mortem in some series. Clinical diagnosis either provides good diagnostic sensitivity at expense of specificity or vice versa (pooled averages 81% sensitive and 70% specific).

The earlier systematic review also identified a lack of studies of both neuronal and vascular measures in non-AD dementias, and therefore any new findings in these dementias will be novel.

In addition, there has been no focus on younger patients, with early-onset dementia.

This study then aimed to investigate the diagnostic utility of optical coherence tomography in early onset dementia in a clinic based population. Specifically, I aimed to investigate changes in RNFL and the retinal vasculature in patients presenting with heterogenous causes of early onset dementia, the sensitivity of OCT in the differential diagnosis of early onset dementia and the relationship of OCT findings with clinic based cognitive performance on Addenbrooke's Cognitive Examination (ACE).

Subjects & Methods

The setting for the study was the ARRNC, with patients recruited from the specialist cognitive-disorders clinic. The patient case mix within each clinic list is mixed across dementia subtype, and severity. With the assistance of the neurologists, I could therefore be assured of recruiting sufficient numbers across the subtypes of dementia I am interested in, whilst remaining blinded to the diagnosis at the time of imaging.

Healthy control patients were recruited from family members and friends attending the clinic, and staff colleagues. (See Chapter 3 for more detail on recruitment methods)

Patient population

A challenge in phenotypic studies of dementia is the lack of a clear diagnostic tree, and a taxonomy essentially built around syndromic presentations with perceived brain localisation. Therefore, for this analysis, I will look for phentotypic associations with the syndromes as presented, rather than with the probable pathological mechanisms underlying them.

Frontotemporal dementia (FTD)

Frontotemporal dementias are characterised by involvement of the frontal and temporal lobes of the brain. The clinical presentation can vary, and sometimes overlap with other disorders. Whilst less common than Alzheimer's disease, FTD is increasingly recognised and with increasing diagnostic awareness, may account for a large proportion of younger onset dementia.

FTD is often sub-divided into behavioural variant FTD (bvFTD), primary progressive aphasia (PPA) and FTD-related movement disorders. Given the distinction between these sub-types, I will analyse them separately.

bvFTD presents with changes in personality and behaviour, sometimes inappropriate or disinhibited, sometimes impulsive behaviour with loss of insight.

There have been no studies of retinal imaging such as OCT, or retinal vessels, in FTD.

Primary progressive aphasia (PPA)

This typically affects language before behaviour. In the semantic dementia form of PPA, speech is easy, but language becomes less precise and comprehension also declines. Behaviour and cognition can otherwise remain unaffected.

There have been no studies of retinal imaging such as OCT, or retinal vessels, in PPA.

Corticobasal syndrome (CBD)

CBD is a movement disorder, with lack of coordination and trembling. Muscle spasms can be particularly troublesome.

There have been no studies of retinal imaging such as OCT, or retinal vessels, in CBD.

Posterior Cortical Atrophy (PCA)

PCA is thought to be a variant of AD, but affecting the visual and/or parietal cortex. The presentation is usually with visual impairment, such as inability to read, blind spots in the vision, impaired depth perception. As such, presentation is often first to an ophthalmologist, with assumed age-related eye disease such as cataract or glaucoma. Diagnosis is often delayed, as patients receive multiple and repeat visual testing that is often inconclusive. Eventually a patient may be referred for neuroimaging, at which point occipital cortex atrophy is seen and a diagnosis of PCA made.

Other symptoms can include difficulties with memory, simple calculations, driving, and spelling, reflecting wide parietal lobe involvement.

There are no validated standard diagnostic criteria for PCA, and clinical biomarkers are lacking. There have been no studies of retinal imaging such as OCT, or retinal vessels, in PCA.

Mild cognitive impairment (MCI)

I chose not to include mild cognitive impairment in this study, as on review, these were a heterogenous labelling of patients with subjective memory problems, drug and alcohol-related cognitive impairment, epilepsy-related impairment, and presumed vasculopaths. Therefore, there were many confounders that would compromise any potential analysis outcomes.

Clinical Assessment

Neurological history and examination

Neurological history-taking and examination is currently the mainstay of assessment in the dementia clinic. All participants in this study were seen in the specialist young-onset cognitive-disorders clinic, which includes multi-disciplinary assessment from neurologists, cognitive and behavioural neuropsychologists and psychiatrists.

Clinical diagnoses were made by specialist neurologists, using established diagnostic criteria including the NINCDS-ADRDA and DSM-IV criteria for Alzheimer's disease (AD), the Lund–Manchester criteria for frontotemporal dementia (FTD), and current international consensus for corticobasal syndrome (CBD) and posterior cortical atrophy (PCA).

Addenbrooke's Cognitive Examination

The Addenbrooke's Cognitive Examination (ACE) is an evolution of the Mini-Mental State Examination (MMSE) to assist diagnosis of early dementia, but is longer in order to provide clearer domains of cognitive testing, all still within a relatively quick to administer and patient acceptable test.[301, 302]

Developed in 2000, and revised in 2006[303] it is a 100-point neuropsychological test battery, across five cognitive domains. (Table 5.1) Taking around 15-20 minutes to perform, a cut-off score of < 88/100 shows high sensitivity and specificity for diagnosing dementia.[303] Although a lower cut-off of < 82/100 improves the test specificity and positive predictive value.[304] In a large meta-analysis, the revised ACE has been shown to be superior to the MMSE as a screening tool.[305]

Table 5.1: Domains of content of Addenbrooke's Cognitive Assessment (ACE-III)

Orientation / Attention	18
Memory	26
Verbal fluency	14
Language	26
Visuospatial	16

Total = 100

The third version (ACE-III) was released in 2012, and reflected some issues of copyright with certain tests, for example the overlapping pentagons.[306]

The test itself is available online and is offered freely for clinical and research use. (https://www.neura.edu.au/research-clinic/frontier/research/downloads/)

Since its release, the ACE-III has gained traction as a useful tool in both clinical and research environments, in the screening of early dementias, although some reports suggest it is less sensitive in diagnosing or discriminating frontotemporal dementia.[307] It also discriminates out affective disorders from early dementia, with a particular profile of low scoring in the memory and letter fluency sections.[308] The test has also been evaluated in the assessment and diagnosis of Parkinson's disease[309] and Huntington's disease.[310]

Retinal imaging and analysis

All participants had the full OCT imaging protocol as outlined in Chapter 3 (except for the patients with PCA, for whom only single images were possible, as a consequence of the disease-associated difficulties with visual awareness and fixation. Therefore, the macular volume scans were impossible.)

All images were of satisfactory quality for processing and analysis, as per the OSCAR-IB criteria.

Results

Participant characteristics

I recruited and imaged 140 dementia patients, and 40 healthy controls.

The mean ages of the dementia patients were AD 57.6 ± 6.6 years, bvFTD 60.8 ± 2.6 years, PPA 60.7 ± 3.5 years, CBD 61.6 ± 2.7 years and PCA 60.7 ± 4.2 years. The healthy controls were age- and sex-matched to the whole group of patients, with a mean age of 57.6 ± 6.6 years, and a range of 39-64 years.

Within each sample group, there were more male and female, and there was a moderate variation in disease duration. The mean refractive errors for each group were also comparable. (Table 5.2)

Table 5.2: Baseline participant characteristics

	Controls	AD	bvFTD	PPA	CBD	PCA
Number	40	58	30	17	11	24
Mean age (years)	57.6 ± 6.6	59.6 ± 4.6	60.8 ± 2.6	60.7 ± 3.5	61.6 ± 2.7	60.7 ± 4.2
Sex (male:female)	22:18	33:25	21:9	9:8	7:4	13:11
Refractive error (dioptres)	-0.24 ± 1.42	0.42 ± 1.28	-0.01 ± 0.89	0.55 ± 1.29	0.00 ± 1.75	-0.21 ± 1.40
Disease duration (months)	-	46 ± 32	39 ± 31	52 ± 28	43 ± 18	51 ± 30
Age of onset (years)	-	55.8 ± 4.7	57.6 ± 3.6	56.4 ± 3.4	58.0 ± 3.1	56.5 ± 4.5
ACE-III: total	-	65.5 ± 18.2	69.9 ± 13.6	70.4 ± 12.5	63.1 ± 18.5	64.8 ± 10.4

NOTE. Data are shown mean ± SD.

Of the 30 participants with bvFTD, five had genetic mutations isolated: four were C9ORF72 positive, and one had a progranulin gene mutation. Several patients were still awaiting testing at the time of this study.

OCT analysis

RNFL thickness

Peripapillary RNFL (pRNFL) was significantly thinner in just two dementia subtypes - AD and PCA. (Table 5.3)

Table 5.3: OCT analysis: peripapillary scan, RNFL thickness by sector

	healthy controls	**AD**	**bvFTD**	**PPA**	**CBD**	**PCA**
pRNFL thickness global	97.6±8.5	92.1±9.8**	96.1±9.6	97.1±6.3	98.5±12.2	94.4±8.2
PMB	57.1±7.5	51.6±9.1**	55.7±10.2	53.1±7.9	55.8±12.4	55.4±13.4
T	73.8±9.8	66.4±12.4**	68.9±11.0	68.2±7.4	69.4±16.9	71.5±14.4
TS	141.1±17.8	128.5±15.0***	134.8±20.0	140.4±13.4	133.1±20.2	134.4±16.5
NS	105.4±19.5	96.4±16.4**	102.6±16.9	99.7±13.9	101.8±21.4	104.9±24.4
N	77.4±14.3	79.0±15.1	77.0±13.6	80.3±11.1	77.1±11.4	67.6±13.3**
N/T	1.069 ±0.244	1.233 ±0.337**	1.103 ±0.357	1.189 ±0.209	1.213 ±0.474	0.997 ±0.312
NI	114.8±24.5	110.2±23.2	117.6±17.9	105.8±11.4	120.5±19.0	99.7±19.4**
TI	146.4±15.7	136.0±19.7**	138.4±17.5	133.8±27.4	139.0±21.6	136.7±15.6

Abbreviations: PMB, papillo-macular bundle; T, temporal; TS, temporal-superior; NS, nasal-superior, N, nasal; N/T, nasal-temporal ratio; NI, nasal-inferior; TI, temporal-inferior
NOTE. Right eye analysis only. Data are shown mean ± SD (μm)
*P < 0.05, **P < 0.01, ***P < 0.001.

Global pRNFL was significantly thinner in AD (= -5.51, 95% CI [-9.23, -1.79], p=0.004). There were also trends for thinning in bvFTD and PCA, but these were not significant. There was no difference in global pRNFL in PPA, or CBD.

This RNFL thinning in AD appears distributed across all the peripapillary sectors, but significantly most affecting superior and temporal sectors. Only the nasal and nasal-inferior sectors were unaffected.

For AD, the temporal RNFL was significantly thinner (MD= -7.35, 95% CI [-11.82, -9.8], p-0.002) as were the temporal-superior (MD= -12.61, 95% CI [-19.47, -5.75], p=0.0002), nasal-superior (MD= -9.06, 85% CI [-16.58, -1.55], p=0.009) and temporal-inferior sectors (MD= -10.42, 95% CI [-17.53, -3.30], p=0.005).

In PCA, the nasal sector was significantly thinner (MD= -9.73, 95% CI [-16.86, -2.60], p=0.008) as was the nasal-inferior sector (MD= -15.14, 95% CI [-26.25, -4.03], p=0.008).

For bvFTD, PPA and CBD, there was no significant RNFL thinning in any sector.

Macular thickness

Macular thickness averages were significantly reduced in all dementia subtypes, but only in certain macular sectors. The greatest mean reductions were seen in the outer nasal sector, and in bvFTD. (Table 5.4)

Table 5.4: OCT analysis: macular volume scan, macular average thickness by sector

	healthy controls	**AD**	**bvFTD**	**PPA**	**CBD**
Macular average thickness:					
central	276.9 ± 16.5	278.5 ± 18.6	275.7 ± 25.4	286.9 ± 19.2	271.9 ± 14.5
IN	347.9 ± 11.4	341.5 ± 15.7*	341.2 ± 19.5	346.8 ± 11.4	339.9 ± 6.7**
IS	346.3 ± 12.5	340.4 ± 15.1*	338.5 ± 15.5*	342.2 ± 11.1	340.4 ± 8.2
IT	332.6 ± 12.2	328.4 ± 16.9	327.9 ± 16.2	331.1 ± 9.7	327.4 ± 8.3
II	343.6 ± 12.3	336.1 ± 15.8*	335.9 ± 18.7	341.1 ± 11.3	336.4 ± 8.2*
ON	319.2 ± 12.4	311.5 ± 13.1**	307.7 ± 12.3***	310.2 ± 10.9*	313.3 ± 6.8*
OS	301.3 ± 11.8	295.3 ± 11.3*	292.4 ± 10.1**	293.3 ± 11.5*	295.4 ± 5.4*
OT	284.8 ± 12.9	283.1 ± 14.5	281.6 ± 10.7	278.4 ± 12.3	281.5 ± 9.7
OI	291.7 ± 12.0	286.3 ± 12.5*	280.8 ± 7.9***	284.4 ± 13.7	287.9 ± 7.0

Abbreviations: IN, inner nasal; IS, inner superior; IT, inner temporal; II, inner inferior; ON, outer nasal; OS, outer superior; OT, outer temporal; OI, outer inferior

NOTE. Right eye analysis only. Data are shown mean ± SD (μm)

*P < 0.05, **P < 0.01, ***P < 0.001.

Central macular thickness was not reduced in any dementia type.

Inner nasal sector was thinner in AD (MD= -6.40, 95% CI [-11.84, -0.95], p=0.022) and CBD (MD= -8.04, 95% CI [-13.59, -2.50], p=0.006).

Inner superior sector was thinner in AD (MD= -5.94, 95% CI [-11.51, -0.37], p=0.037), and bvFTD (MD= -7.85, 95% CI [-14.79, -0.91], p=0.027).

Inner inferior sector was thinner in AD (MD= -7.46, 95% CI [-13.10, -1.82], p=0.010) and CBD (MD= -7.15, 95% CI [-13.66, -0.63], p=0.033).

Outer nasal sector was thinner in AD (MD= -7.69, 95% CI [-12.86, -2.52], p=0.004), bvFTD (MD= -11.57, 95% CI [-17.52, -5.63], p<0.001), PPA (MD= -9.04, 95% CI [-15.75, -2.33], p=0.010) and CBD (MD= -5.91, 95% CI [-11.72, -0.10], p=0.046).

Outer superior sector was thinner in AD (MD= -6.07, 95% CI [-10.83, -1.32], p=0.013), bvFTD (MD= -8.92, 95% CI [-14.16, -3.68], p=0.001), PPA (MD= -8.00, 95% CI [-14.85, -1.14], p=0.024) and CBD (MD= -5.90, 95% CI [-10.93, -0.86], p=0.023).

Outer inferior sector was thinner in AD (MD= -5.43, 95% CI [-10.42, -0.44], p=0.033) and bvFTD (MD= -10.97, 95% CI [-15.75, -6.20], p<0.001).

Inner temporal and outer temporal sectors were not thinner in any dementia type.

Note: Volume scans were not possible for patients with PCA, as a result of their disease-associated difficulties with visual and spatial awareness, and instruction regarding gaze fixation. Whilst I was able to take single image scans, and select the highest quality image for analysis of RNFL thickness, etc., macular volume scans require fixation for several seconds as the serial scans are captured, and this proved impossible with these patients - despite many attempts.

Macular volume including GCL

Macular volume was significantly reduced in dementia types, apart from PPA where it did not reach significance. The greatest reduction was seen in bvFTD. (Table 5.5)

Macular volume was significantly reduced in AD (MD= -0.14, 95% CI [-0.27, -0.004], p=0.043), bvFTD (MD= -0.11, 95% CI [-0.37, -0.08], p=0.003) and CBD (MD= -0.14, 95% CI [-0.28, -0.01], p=0.044).

Macular GCL volume was significantly reduced in all dementia types. Again, the greatest reduction was seen in bvFTD.

Macular GCL volume was significantly reduced in AD (MD= -0.07, 95% CI [-0.09, -0.04], p<0.001), bvFTD (MD= -0.11, 95% CI [-0.14, -0.7], p<0.001), PPA (MD= -0.09, 95% CI [-0.13, -0.06], p=0<0.001) and CBD (MD= -0.04, 95% CI [-0.08, -0.01], p=0.036).

Table 5.5: OCT analysis: macular volume scan, macular volume of full 6mm circle

	healthy controls	AD	bvFTD	PPA	CBD
Macular full thickness volume MV	8.72 ± 0.31	8.58 ± 0.34*	8.49 ± 0.29**	8.55 ± 0.31	8.57 ± 0.16*
Macular GCLV	1.11 ± 0.06	1.05 ± 0.07***	1.00 ± 0.08***	1.02 ± 0.06***	1.08 ± 0.05*

Abbreviations: MV, macular volume; GCLV, ganglion cell layer volume
NOTE. Right eye analysis only. Data are shown mean ± SD (mm^3)
*P < 0.05, **P < 0.01, ***P < 0.001.

Choroidal thickness

The subfoveal choroid was significantly thinner in all dementia types. The greatest reductions were seen in bvFTD and PPA. (Table 5.6)

The sfCT was reduced in AD (MD= -44.8, 95% CI [-76.0, -13.6], p=0.006), bvFTD (MD= -80.1, 95% CI [-118.4, -41.7], p<0.001), PPA (MD= -76.9, 95% CI [-126.2, -27.7], p=0.003), CBD (MD= -48.1, 95% CI [-79.2, -17.1], p=0.003) and PCA (MD= -59.3, 95% CI [-108.6, -10.0], p=0.019).

Table 5.6: OCT analysis: horizontal EDI scan, choroidal thickness

	healthy controls	AD	bvFTD	PPA	CBD	PCA
sfCT	310.8 ± 88.2	265.9±53.0**	230.7±72.6***	233.8±81.5**	262.6±22.0**	251.4±98.4*

Abbreviations: sfCT, sub-foveal choroidal thickness
NOTE. Right eye analysis only. Data are shown mean ± SD (μm)
*P < 0.05, **P < 0.01, ***P < 0.001.

Data Analysis

In summary, all dementia subtypes were associated with some pattern of neuroretinal thinning.

AD was associated with RNFL thinning (especially superiorly), macular thinning in several sectors, a reduced macular volume and a reduced GCL volume.

bvFTD was associated with a normal RNFL, but significant macular thinning in the outer macular sectors, reduced macular volume and a reduced GCL volume.

PPA was associated with normal RNFL, and thinning of just two (outer) macular sectors. Macular volume was not reduced, but there was significant reduction of GCL volume.

CBD was associated with normal RNFL, and thinning of inner nasal and outer nasal macular sectors. Macular volume was also reduced, and so was GCL volume, though to a lesser extent than the reductions seen in the other dementias.

PCA was associated with nasal and nasal-inferior RNFL thinning. Macular parameters are unknown as the required scan protocol was not possible in this group of patients.

The finding of RNFL thinning in AD is not surprising, with the gRNFL mean difference found in this study (MD= -5.51, 95% CI [-9.23, -1.79], p=0.004) closely matching the mean difference from the pooled meta-analysis in Chapter 2.

The presence of nasal and nasal-inferior sector pRNFL thinning in PCA is a new finding, and is intriguing given that these are the only two sectors not thinned in AD. This provides an early glimpse at a potential discriminator between these two dementia types.

ROC curve analysis for distinguishing PCA from AD, for nasal RNFL reveals AUC=0.695, 95% CI [0.581, 0.810], p=0.005. Best cutoff comes at 72.5μm, with specificity 65.5%, sensitivity 62.5%.

For distinguishing bvFTD from AD, two candidates are global RNFL, and macular GCLV. For gRNFL, AUC=0.593, 95% CI [0.469, 0.718], p=0.154. For GCLV, AUC=0.625, 95% CI [0.493, 0.756], p0.056.

Therefore, none of these markers have very good discriminatory function.

Correlation between these measures and ACE-III was generally poor. (Table 5.7) There was a single good correlation between MV and ACE-III in the PPA group, but otherwise the correlations were weak.

Table 5.7: Correlation between neuroretinal parameters and ACE-III in dementia

	Spearman's rank correlation coefficient (p-value)				
	AD	**bvFTD**	**PPA**	**CBD**	**PCA**
gRNFL	-0.373 (0.004)	0.154 (0.417)	0.056 (0.832)	0.343 (0.301)	0.126 (0.556)
tRNFL	-0.137 (0.305)	0.109 (0.565)	-0.255 (0.322)	0.329 (0.324)	0.070 (0.744)
MV	-0.122 (0.362)	0.408 (0.025)	0.754 (<0.001)***	-0.374 (0.257)	-
mGCLV	-0.127 (0.340)	0.271 (0.148)	0.369 (0.145)	-0.491 (0.125)	-
sfCT	-0.011 (0.934)	0.343 (0.064)	-0.049 (0.851)	-0.388 (0.238)	-0.405 (0.050)

Abbreviations: gRNFL, global RNFL; tRNFL, temporal RNFL; MV, macular volume; GCLV, ganglion cell layer volume; sfCT, sub-foveal choroidal thickness

NOTE. Right eye analysis only. Data are shown Spearman's rho (p-value)

*P < 0.05, **P < 0.01, ***P < 0.001.

Regarding choroidal thickness, all dementia subtypes were associated with subfoveal choroidal thinning. The amount of thinning was also greater than that seen in RRMS in the previous chapter. Here, dementia was associated with an average thinning of 25%.

It is unclear why dementia would be associated with choroidal thinning. We can speculate that choroidal atrophy may occur because of unidentified circulating pro-inflammatory cytokines that also damage delicate small vessel endothelium. The overlap between dementia, small vessel disease, and inflammation suggests multiple converging hypotheses.

Much has been written about the association between dementia and age-related macular degeneration. It would be an interesting hypothesis to investigate the time sequence of these changes, and whether this choroidal thinning predisposes to the macular degenerative process, or is occurring simultaneously. Choroidal thinning is certainly implicated in the pathophysiology of several retinal diseases.

Retinal vessel analysis

Vessel calibre

CRVE was significantly higher in AD and CBD, but not in bvFTD, PPA or PCA. AVR was correspondingly lower in AD and bvFTD, but not reaching significance. There was no difference in CRAE in any of dementia types. (Table 5.8)

Table 5.8: Retinal vessel analysis: vessel calibre

	healthy controls	AD	bvFTD	PPA	CBD	PCA
CRAE	27.96 ± 1.99	28.42 ± 2.89	28.72 ± 2.64	29.50 ± 2.68	29.34 ± 2.49	28.78 ± 2.46
CRVE	34.95 ± 2.37	36.11 ± 2.71*	35.96 ± 2.75	36.17 ± 2.22	37.03 ± 2.13*	36.01 ± 3.28
AVR	0.80 ± 0.05	0.78 ± 0.07	0.80 ± 0.07	0.82 ± 0.05	0.79 ± 0.06	0.80 ± 0.07

Abbreviations: CRAE, central retinal arteriolar equivalent; CRVE, central retinal venular equivalent; AVR, arterio-venous ratio
NOTE. Right eye analysis only. Data are shown mean ± SD (pixels)
*P < 0.05, **P < 0.01, ***P < 0.001.

In AD, CRVE was significantly higher, though the difference was small (MD=1.15, 95% CI [0.12, 2.18], p=0.029).

In CBD, CRVE was also significantly higher, with a greater difference (MD=2.07, 95% CI [0.50, 3.64], p=0.013).

ROC curve analysis reveals for AD vs controls, CRVE has an AUC=0.627, 95% CI [0.515, 0.739], p=0.033. For bvFTD vs controls, CRVE has an AUC=0.609, 95% CI [0.474, 0.746], p=0.119. Therefore, the discrimination between these dementia types and healthy controls using CRVE is poor.

Vessel tortuosity

There was no significant difference in vessel tortuosity in any dementia type, when compared with healthy controls. (Table 5.9)

However, there was a significant difference in arteriolar tortuosity between PPA and PCA, and also CBD and PCA. PPA and CBD both had the lowest arteriolar tortuosity measurements.

Table 5.9: Retinal vessel analysis: vessel tortuosity

	healthy controls	AD	bvFTD	PPA	CBD	PCA
aTort	-9.06 ± 0.97	-9.01 ± 0.95	-9.11 ± 0.84	-9.24 ± 1.03	-9.24 ± 0.76	-8.90 ± 0.90
vTort	-9.65 ± 0.64	-9.42 ± 0.63	-9.57 ± 0.68	-9.20 ± 0.83	-9.23 ± 1.01	-9.45 ± 0.81

Abbreviations: aTort, arteriolar tortuosity; vTort, venular tortuosity
NOTE. Right eye analysis only. Data are shown as natural log transformed, from the raw tortuosity measurement calculation, and as mean ± SD
*P < 0.05, **P < 0.01, ***P < 0.001.

When compared with PCA, PPA was associated with reduced arteriolar tortuosity (MD= -0.34, 95% CI [-0.670, -0.014], p=0.023). The difference is small, and would not discriminate between groups with significant specificity or sensitivity (AUC=0.588, 95% CI [0.402, 0.774], p=0.341).

When compared with PCA, CBD was also associated with reduced arteriolar tortuosity (MD= -0.34, 95% CI [-0.650, -0.073], p=0.013). Again, the difference is small, and does not discriminate between the groups (AUC=0.636, 95% CI [0.435, 0.838], p=0.201).

Vessel fractal dimension

Fractal dimension

Fractal dimension was significantly reduced for some D_f calculations in all dementia types, with the exception of PPA. The greatest reductions were seen in arteriolar D_f, and in CBD. (Table 5.10)

Mono-fractal analysis (box-counting method) revealed a reduced arteriolar D_f in AD (MD= -0.019, 95% CI [-0.030, -0.009], p=0.001), bvFTD (MD= -0.021, 95% CI [-0.035, -0.008], p=0.003), CBD (MD= -0.037, 95% CI [-0.055, -0.019], p<0.001) and PCA (MD= -0.028, 95% CI [-0.042, -0.014], p<0.001).

It also found a reduced venular D_f in AD (MD= -0.013, 95% CI [-0.023, -0.002], p=0.016), bvFTD (MD= -0.016, 95% CI [-0.029, -0.003], p=0.016) and PCA (MD= -0.025, 95% CI [-0.037, -0.012], p<0.001).

Combined arteriolar and venular mono-fractal D_f was also reduced for AD, bvFTD, CBD and PCA.

Table 5.10: Retinal vessel analysis: fractal dimension

	healthy controls	AD	bvFTD	PPA	CBD	PCA
aD_0	1.63 ± 0.04	1.61 ± 0.04**	1.60 ± 0.04**	1.63 ± 0.04	1.58 ± 0.03***	1.59 ± 0.03***
aD_1	1.62 ± 0.04	1.59 ± 0.04**	1.59 ± 0.04**	1.61 ± 0.03	1.57 ± 0.03***	1.58 ± 0.03***
aD_2	1.61 ± 0.04	1.59 ± 0.04**	1.58 ± 0.04**	1.60 ± 0.03	1.56 ± 0.03***	1.57 ± 0.03***
aD_{BOX}	1.13 ± 0.03	1.11 ± 0.03**	1.11 ± 0.03**	1.12 ± 0.03	1.09 ± 0.02***	1.10 ± 0.03***
vD_0	1.62 ± 0.03	1.60 ± 0.04*	1.60 ± 0.04*	1.61 ± 0.04	1.61 ± 0.03	1.58 ± 0.04***
vD_1	1.60 ± 0.03	1.59 ± 0.04*	1.59 ± 0.04*	1.59 ± 0.03	1.59 ± 0.03	1.57 ± 0.04***
vD_2	1.59 ± 0.03	1.58 ± 0.04*	1.58 ± 0.04*	1.59 ± 0.03	1.58 ± 0.03	1.56 ± 0.04***
vD_{BOX}	1.12 ± 0.02	1.11 ± 0.03*	1.10 ± 0.03*	1.11 ± 0.02	1.11 ± 0.03	1.09 ± 0.03***
cD_0	1.80 ± 0.03	1.78 ± 0.03***	1.78 ± 0.04**	1.80 ± 0.03	1.77 ± 0.03**	1.77 ± 0.03***
cD_1	1.79 ± 0.03	1.77 ± 0.03***	1.76 ± 0.03**	1.78 ± 1.71	1.76 ± 0.03**	1.75 ± 0.03***
cD_2	1.78 ± 0.03	1.76 ± 0.03***	1.75 ± 0.03**	1.77 ± 0.02	1.75 ± 0.03*	1.74 ± 0.03***
cD_{BOX}	1.26 ± 0.02	1.24 ± 0.03***	1.24 ± 0.03**	1.26 ± 0.02	1.24 ± 0.02*	1.23 ± 0.02***

Abbreviations: $aD_{0\text{-}BOX}$, arteriolar fractal dimension 0 - BOX; $vD_{0\text{-}BOX}$, venular fractal dimension 0 - BOX; $cD_{0\text{-}BOX}$, combined fractal dimension 0 - BOX

NOTE. Right eye analysis only. Data are shown mean ± SD (fractal units)

*P < 0.05, **P < 0.01, ***P < 0.001.

Superior multi-fractal analysis methods revealed similar results, and for all three algorithms - capacity dimension, entropy dimension and correlation dimension.

Arteriolar capacity D_f (aD_0) was significantly reduced in AD (ad0 MD= -0.027, 95% CI [-0.043, -0.012], p=0.001), bvFTD (MD= -0.032, 95% CI [-0.051, -0.013], p=0.001), CBD (MD= -0.050, 95% CI [-0.075, -0.026], p<0.001) and PCA (MD= -0.039, 95% CI [-0.058, -0.022], p<0.001).

Arteriolar entropy D_f (aD_1) was significantly reduced in AD (MD= -0.027, 95% CI [-0.042, -0.012], p=0.001), bvFTD (MD= -0.032, 95% CI [-0.050, -0.013], p=0.001), CBD (MD= -0.050, 95% CI [-0.074, -0.026], p<0.001) and PCA (MD= -0.040, 95% CI [-0.058, -0.022], p<0.001).

Arteriolar correlation D_f (aD_2) was significantly reduced in AD (MD= -0.027, 95% CI [-0.041, -0.012], p=0.001), bvFTD (MD= -0.032, 95% CI [-0.049, -0.013], p=0.001), CBD (MD= -0.049, 95% CI [-0.074, -0.026], p<0.001) and PCA (MD= -0.040, 95% CI [-0.058, -0.022], p<0.001).

Venular capacity D_f (vD_0) was significantly reduced in AD (MD= -0.016, 95% CI [-0.029, -0.002], p=0.023), bvFTD (MD= -0.019, 95% CI [-0.037, -0.001], p=0.038) and PCA (MD= -0.034, 95% CI [-0.052, -0.016], p<0.001).

Venular entropy D_f (vD_1) was significantly reduced in AD (MD= -0.016, 95% CI [-0.029, -0.002], p=0.0), bvFTD (MD= -0.019, 95% CI [-0.037, -0.001], p=0.036) and PCA (MD= -0.033, 95% CI [-0.051, -0.016], p<0.001).

Venular correlation D_f (vD_2) was significantly reduced in AD (MD= -0.016, 95% CI [-0.029, -0.002], p=0.024), bvFTD (MD= -0.019, 95% CI [-0.037, -0.002], p=0.034) and PCA (MD= -0.033, 95% CI [-0.050, -0.015], p<0.001).

Combined arteriolar and venular multi-fractal D_f was significantly reduced for AD, bvFTD, CBD and PCA (cD_0, cD_1, cD_2).

The key finding when taking all these results together is that all dementia types are associated with reduced arteriolar fractal dimension, with the exception of PPA. The greatest reduction is seen in CBD.

Venular fractal dimension was also reduced in AD, bvFTD and PCA.

Data Analysis

In summary, all dementia types were associated with some retinal vessel morphological changes. Some of these findings do distinguish dementia types.

For vessel calibre, AD and CBD were associated with thicker venules.

Whilst mean AVR was not statistically different from controls, it does distinguish between AD and PPA (AUC=0.718, 95% CI [0.584, 0.852], p=0.014). This was partly due to a (non-significant) trend for thicker arterioles in PPA.

There was no significant difference in vessel tortuosity in any dementia type, when compared with healthy controls. However, there was a significant difference in arteriolar tortuosity between PPA and PCA, and also CBD and PCA. This was not highly discriminatory however.

Fractal dimension analysis however revealed significant findings. Reduced arteriolar D_f was observed in AD, bvFTD, CBD and PCA, with both mono-fractal and multi-fractal analysis. Some reduction in venular D_f was also seen, in AD, bvFTD and PCA. There were no significant differences between these dementia types.

However, PPA was not associated with any reduction in fractal dimension. This shows discriminatory potential using an arteriolar multi-fractal analysis.

Using arteriolar capacity D_f (aD_0), AD, bvFTD, CBD and PCA all have significantly reduced D_f compared with PPA. Mean differences are AD (MD= -0.021, 95% CI [-0.041, -0.004], p=0.045), bvFTD (MD= -0.025, 95% CI [-0.048, -0.014], p=0.039), CBD (MD= -0.043, 95% CI [-0.071, -0.016], p=0.004) and PCA (MD= -0.033, 95% CI [-0.056, -0.010] p=0.006).

ROC analysis of these relationship reveals for AD AUC=0.625, 95% CI [0.473, 0.777], p=0.119, bvFTD AUC=0.639, 95% CI [0.476, 0.802], p=0.116, CBD AUC=0.808, 95% CI [0.635, 0.980], p=0.007, PCA AUC=0.741, 95% CI [0.589, 0.894], p=0.009.

Therefore, arteriolar D_f has very good discriminating potential between CBD and PPA, and acceptable discrimination for PCA and PPA.

Relationship with CSF biomarkers

CSF analysis demonstrating decreased amyloid-beta 1-42 ($A\beta_{1-42}$) concentrations in combination with raised total-tau (t-tau) and phosphorylated-tau (*P*-tau) concentrations have been demonstrated as features characteristic of AD when evaluated against patients with MCI and healthy controls. The relative concentrations are thought to be proportional to the neuronal injury caused by the accumulation of these abnormal proteins in AD, though they lack ideal specificity and sensitivity.

The question for this sub-study is whether these CSF markers of disease severity in AD correlate with neuroretinal markers of axonal and neuronal loss.

Within the cognitive disorders clinic, a cohort of patients received a lumbar puncture and CSF analysis as diagnostic adjuncts. The CSF analysis included measures of $A\beta_{1-42}$ (>500pg/ml), t-tau (<500pg/ml), and *P*-tau (<75pg/ml), with centre specific references ranges as indicated.

Using this cohort, I investigated for any correlation between the CSF and retinal measures, using Pearson's correlation analysis.

Results

The sample size was 30 patients with AD. The mean global RNFL thickness was 93.9 ± 11.9µm, and mean macular GCL volume 1.033 ± 0.09mm^3.

Pearson's correlation analysis demonstrated no strong correlations between RNFL thickness or GCLV and the previously established pattern in AD patients of increased CSF *P*-tau/CSF t-tau and decreased CSF $A\beta_{1-42}$. (Table 5.11)

Table 5.11: Correlation between neuroretinal parameters and CSF biomarkers, in AD

	Pearson's correlation coefficient (p-value)	
	Global RNFL	**Macular GCLV**
CSF *P*-tau, pg/ml	0.558 (0.001)**	0.062 (0.772)
CSF $A\beta_{1-42}$, pg/ml	-0.112 (0.571)	0.333 (0.130)
CSF t-tau, pg/ml	0.288 (0.122)	-0.103 (0.634)

Abbreviations: *P*-tau, phosphorylated tau; Aβ, amyloid beta; t-tau, total tau
NOTE. Right eye analysis only. Data are shown Pearson's r (p-value)
*P < 0.05, **P < 0.01, ***P < 0.001.

The data did reveal a significant positive correlation between increasing RNFL thickness and elevation in CSF *P*-tau levels (r=0.558, p=0.001), although this contradicted the study hypothesis. The correlations generated between RNFL thickness and CSF t-tau (r=0.288, p=0.122) and RNFL thickness and CSF Aβ1-42 (r= -0.112, p=0.571) were both found to be statistically insignificant. Similarly, GCLV and all correlations with CSF *P*-tau (r=0.062, p=0.772), CSF t-tau (r= -0.103, p=0.634), and CSF $A\beta_{1\text{-}42}$ (r=0.333, p=0.130), were statistically insignificant.

In summary, there were no clear correlations between CSF markers of AD and neuroretinal markers of disease.

The single significant findings of a positive correlation between RNFL thickness and CSF *P*-tau is in contradiction with the proposed mechanism in the hypothesis. To further investigate this, the established cut-off value for CSF *P*-tau was adjusted to 60pg/ml, in line with other reports of AD. This reduced the AD sample size to 19, and with a multivariate regression, there was no longer a statistically significant relationship between CSF *P*-tau and RNFL thickness.

Ultimately, this shows that the two domains of testing, of CSF and retina, are complementary, rather than duplicatory.

Predicting clinical course

I have explored the diagnostic phenotyping potential of neuroretinal markers in some detail. However, an additional potential role for these markers is in their capacity for predicting the clinical course of the disease.

In dementia, an important question - and frequently an unanswerable one - is what to expect in terms of cognitive decline over coming months and years. The spectrum and gradient of disease is very wide, and information about the future can be very helpful in social planning for the patient, as well as family and carers.

Therefore, the question for this sub-study is do any of the measured neuroretinal parameters predict cognitive decline. I have chosen FTD for this study, as firstly a lot less is known about prognostic indicators of decline in this disease, and secondly I have the most complete longitudinal data on cognitive scoring for this dementia type.

Results

The sample size was 30 bvFTD patients, with data on ACE-III scores at baseline (at the same timepoint as OCT imaging) and 6 months later. Baseline mean RNFL was 95.2 ± 13.6. The 6-month change in ACE-III ranged from +5 to -10 points.

To determine if baseline RNFL thickness was predictive of cognitive decline, as measured by a fall in ACE-III score, I produced a scatterplot and regression line - known as a fitted line plot. (Fig. 5.1)

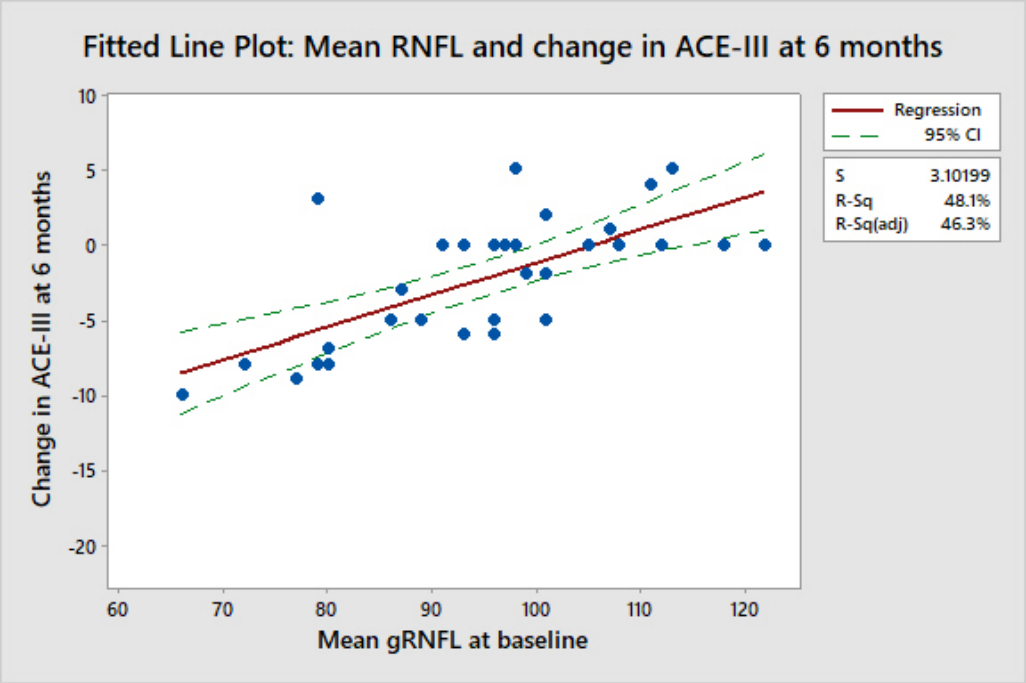

Figure 5.1: Cognitive decline in FTD: Fitted line plot, showing change in ACE-III score at 6 months, against baseline RNFL thickness

This figure shows a moderate R-squared response of 48.1%, suggesting that mean gRNFL is a potential predictor of cognitive decline. However, the model is incomplete, possibly due to variability in ACE-III scoring, which is known for normal fluctuation, but which regression models do not account for.

Therefore, I can improve the value of the model by transforming the continuous variable of ACE score into categorical grouping: no change in ACE (± 4), mild decline in ACE (-4 to -8), and moderate decline in ACE (-8 to -12). (Fig. 5.2)

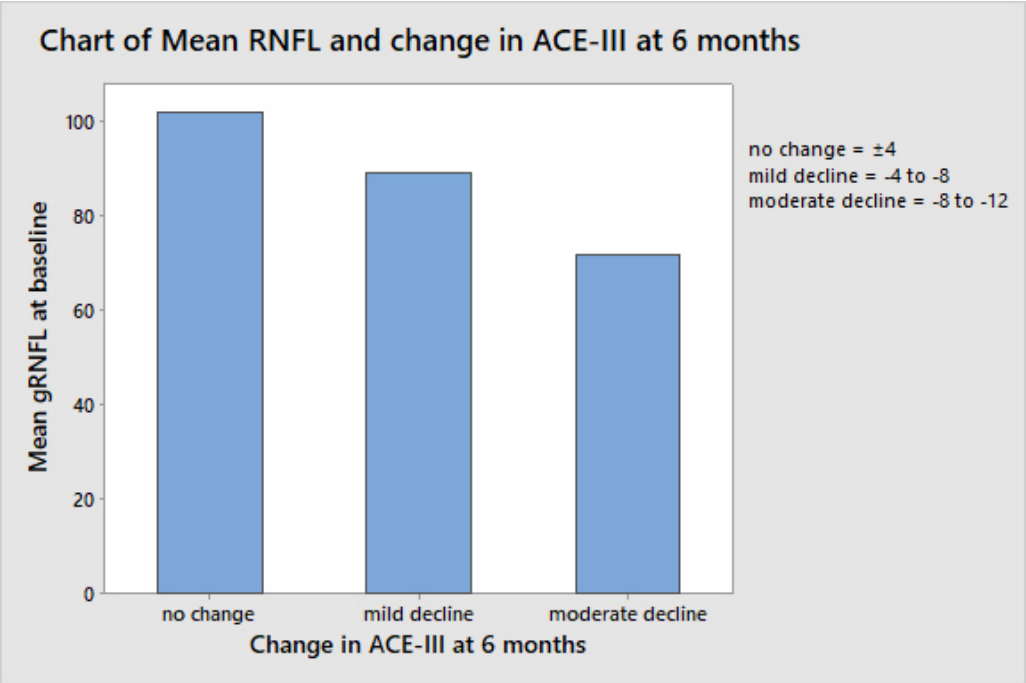

Figure 5.2: Cognitive decline in FTD: Chart of grouped categories of change in ACE-III scores at 6 months, against mean RNFL thickness

This graph reveals a significant difference in mean RNFL between the three categorical groupings of ACE-III change.

Therefore, by measuring RNFL at baseline, we can predict the likely cognitive decline in patients with FTD.

Using ACE-III scores as an indicator of disease severity and change in dementia is convenient as it is a numerical variable and therefore amenable to simple statistical analysis. However, cognitive decline is just one domain of deterioration in FTD. Symptoms of behavioural disinhibition, aggression (verbal and physical), apathy, gluttony and loss of sympathy are all common features that increase over time in FTD, and have a great impact on quality of life. A future study could attempt to include these behavioural manifestations in a broader investigation of predictors of decline in this disease.

Discussion

This is the first study to look at neuroretinal markers in dementia, in a Scottish population.

Having identified unanswered questions from the literature, I have investigated the utility of neuronal and vascular markers in the retina in association with early-onset AD, bvFTD, PPA, CBD and PCA.

I have studied diagnostic phenotyping, association with CSF biomarkers, and the potential for disease course prediction, and uncovered several novel findings.

Summary

I recruited 140 dementia patients, across the dementia types AD, bvFTD, PPA, CBD, PCA. All were early-onset with age < 65 years.

RNFL, MV and GCLV

In agreement with the pooled data from my meta-analysis of RNFL thinning in AD, I found that early-onset AD was also associated with RNFL thinning, and mostly in the superior and temporal sectors. AD was also associated with macular thinning, reduced macular volume, and reduced GCL volume.

The other dementia subtypes have never been studied for these neuroretinal markers.

I found that bvFTD was not associated with significant RNFL thinning, but did reveal significant macular thinning in the outer macular sectors, reduced macular volume and a reduced GCL volume.

PPA was also not associated with RNFL thinning, or reduced macular volume, but the GCL volume was significantly reduced.

CBD also had a normal RNFL, but thinning of the macular, reduced macular volume, and reduced GCL volume - though not to the same degree as the other dementias.

PCA was associated with nasal and nasal-inferior RNFL thinning. This was a surprising finding as PCA was previously assumed to have no effect on the RNFL, though this had

never been formally studied. Several PCA patients in this study had been under ophthalmological care for some time, prior to the diagnosis of PCA, having presented with vague visual symptoms, and been labelled as 'glaucoma suspects'. After OCT examination had demonstrated normal RNFL - and therefore ruling out glaucoma - neuroimaging was requested which ultimately led to the correct diagnosis.

This new finding of nasal thinning should therefore be added as an addendum to the thinking of RNFL assessment in 'glaucoma suspects', that nasal thinning can still be present in a diagnosis of PCA.

None of these neuroretinal markers discriminated between the dementia types with high specificity.

Correlation with ACE-III scores was also poor, with the exception of a positive correlation with MV in PPA.

It is interesting that there is macular GCL reduction in all dementia types, particularly bvFTD, but no corresponding loss of temporal RNFL (which represents the axons of the macular RGCs). This implies there is damage to the RGC cell bodies, but not yet causing axonal atrophy. As well as challenging the previous assumption that RGC involvement in dementia is via retrograde degeneration down the optic nerve, this also hints at a separate process involving the intra-retinal neurones. A future study could examine the other retinal layers containing fully intra-retinal neurones.

Choroid

No previous studies have investigated choroidal thickness in early-onset AD, or other dementia types.

I found that all early-onset dementia subtypes were associated with subfoveal choroidal thinning, of around 25% - greater than that seen in RRMS.

The cause of this is unknown, and adds to the growing list of diseases and environmental factors that can impact the choroid.

Retinal vessel calibre, tortuosity and fractal dimension

The meta-analysis of retinal vessel measures in AD suggested AD is associated with thinner arterioles (and possible venules), reduced fractal dimension, and conflicting reports on vessel tortuosity.

In this study, I have found that early-onset AD and CBD were both associated with wider venules, but normal arterioles. The difference was small, however, and poor at discriminating dementia types. Whilst mean AVR was not statistically different from controls, it did distinguish between AD and PPA, partly due to a (non-significant) trend for thicker arterioles in PPA.

Perhaps the arteriolar thinning reported in older AD populations is confounded by age, or other diseases such as hypertension, which are both associated with arteriolar attenuation.

I found no significant difference in vessel tortuosity when compared to healthy controls, in any dementia type. However, there were significant differences in arteriolar tortuosity when comparing PPA and PCA, and also CBD and PCA.

Fractal dimension was significantly reduced in all early-onset dementia types, with the exception of PPA. The greatest reductions were seen in arteriolar $D_{f,}$ and in CBD. Venular fractal dimension was also reduced in AD, bvFTD and PCA.

Arteriolar Df has very good discriminating potential between CBD and PPA, and acceptable discrimination for PCA and PPA.

Multi-fractal analysis provided more detailed analysis than mon-fractal techniques, although no significant differences were seen between the entropy, correlation and capacity algorithms.

Relationship with CSF biomarkers

There were no clear correlations between CSF markers of AD and neuroretinal markers of disease.

Predicting clinical course

In this longitudinal sub-study of cognitive change in bvFTD patients, I found that baseline RNFL thickness could predict the likely change in cognition - as measured by ACE-III assessment - in the following six months.

Utility as a biomarker

- *Detection method should be precise, reliable and transferrable*
  True for all OCT imaging derived measures: RNFL, MV, GCL, sfCT
  True for all VAMPIRE retinal vessel measures: calibre, tortuosity, fractal dimension

- *Distinguish between healthy and disease*
  True for RNFL in AD and PCA; MV in AD, bvFTD and CBD; GCL in AD, bvFTD, PPA and CBD; sfCT in AD, bvFTD, PPA, CBD, and PCA; calibre in AD and CBD; fractal dimension in AD, bvFTD, CBD and PCA.
  Not true for RNFL in bvFTD, PPA and CBD; MV in PPA; calibre in bvFTD, PPA and PCA; fractal dimension in PPA; tortuosity in all types

- *Differentiate between diseases that are clinical similar*
  True for AVR (AD and PPA), arteriolar fractal dimension (CBD and PPA, PCA and PPA)
  Not true for RNFL, MV, GCL, sfCT, calibre and tortuosity, when assessed independently. but combining values can reveal patterns that do correlate with dementia type

- *Value as a prognostic marker*
  True for RNFL in bvFTD
  Insufficient data to assess for other markers or in other dementia types

- *Use in monitoring disease progression*
  Not assessed in this research study

- *Use as a pre-clinical screening test*
  Not assessed in this research study

Contributions to knowledge

- Early-onset Alzheimer's disease is associated with global RNFL thinning (especially superiorly), macular thinning, reduced macular volume, reduced GCL volume, and reduced retinal arteriolar and venular fractal dimensions; but has normal retinal arterioles, and retinal vessel tortuosity.

  There was no correlation between RNFL or GCL volume and CSF biochemical markers of dementia in early-onset AD.

- Behavioural-variant frontotemporal dementia is associated with macular thinning, reduced macular volume, reduced GCL volume, choroidal thinning, and reduced retinal arteriolar and venular fractal dimension; but has normal RNFL, retinal arterioles, and retinal vessel tortuosity.

  However, the RNFL thickness measure predicts cognitive decline in bvFTD.

- Primary progressive aphasia is associated with partial macular thinning, reduced GCL volume, choroidal thinning, and wider retinal venules; but has normal RNFL, macular volume, retinal arterioles, retinal vessel tortuosity, and retinal vessel fractal dimension.

- Corticobasal degeneration is associated with partial macular thinning, reduced macular volume, reduced GCL volume, choroidal thinning, wider retinal venules, and reduced retinal arteriolar fractal dimension; but has normal RNFL, retinal arterioles, retinal vessel tortuosity, and retinal venular fractal dimension.

- Posterior cortical atrophy is associated with nasal RNFL thinning, choroidal thinning, and reduced retinal arteriolar and venular fractal dimension; but has normal retinal arterioles, and retinal vessel tortuosity. (Macular parameters of volume were not assessed.)

- None of these neuroretinal markers independently discriminated between all the dementia types with high specificity. Although arterio-venous ratio discriminated between AD and PPA, and arteriolar fractal dimension between CBD and PPA, and between PCA and PPA.

  However, in combination, the pattern of neuroretinal involvement across all the markers does discriminate between all the dementia types.

- Correlation with ACE-III scores was also poor, except for a positive correlation with macular volume in PPA.

Conclusion

Retinal markers of neuronal and vascular integrity do have clinical utility in diagnostic phenotyping and predicting disease course in early-onset dementias.

These neuroretinal measures can diagnostically discriminate dementia types from healthy controls, as well as differentiate between dementia types. There is also potential for predicting disease progression.

The relative value of each marker depends upon the dementia type.

6 AMYOTROPHIC LATERAL SCLEROSIS

Note: Excerpts of this section have been presented and published – in "Neuroretinal involvement of ALS, assessed with optical coherence tomography (OCT)", JR Cameron, S Pal, R Davenport, B Dhillon, S Chandran.
27th International Symposium on ALS/MND, Dublin; proceedings in Amyotrophic Lateral Sclerosis and Frontotemporal Degeneration, 2016; 17 (Suppl S1): 215-235.

Introduction

Amyotrophic lateral sclerosis (ALS) - often termed motor neurone disease (MND) in the UK - is a devastating neurodegenerative disease, with no current treatment.

Unlike MS, it is not thought to involve the visual pathways, and patients generally retain good vision. However, this does not exclude the potential for neuroretinal measures to offer an insight into the disease, from the patient perspective. In addition, if these retinal biomarkers are to ultimately provide a reliable discrimination between neurodegenerative diseases, then we need to fully understand the relationship in each disease, even those considered non-retinal involving.

What is clear from the dementias is that a deeper exploration of neuroretinal markers such as GCL volume and retinal vascular morphology can uncover some novel associations, and provide useful discriminating power in the clinical environment.

The three studies of RNFL in ALS presented in my systematic literature review were heterogenous in design, and in results. It therefore remains unclear if neuroretinal thinning is indeed a feature of ALS.

In addition, no studies of retinal vessel morphology or the choroid in ALS have been published.

Therefore, the aim of this pilot study was to recruit a well characterised sample of ALS patients, and analyse their retinal imaging in accordance with the rigorous methodology outlined in my methods chapter.

Subjects & Methods

The setting for the study was the ARRNC, with patients recruited from the specialist ALS clinic. Coordination with the specialist nurses within the clinic enabled recruitment of a board patient mix, with different duration of disease, and across the two subtypes of disease-onset pattern - bulbar and spinal-onset.

Healthy control patients were recruited from family members and friends attending the clinic, and staff colleagues. (See Chapter 3 for more detail on recruitment methods)

Patient population

The local prevalence of patients with ALS can vary considerably, due to the rapidity of the disease, and access to specialist services can bring patients from out with the area.

Revival of the 'Scottish MND Register' is enabling more reliable data on the incidence and prevalence of ALS across Scotland.[14] They determined a point prevalence of ALS in Scotland at 431 patients, as of 31 Dec 2015. Locally around 10-15% of these patients will attend ARRNC, so an approximate patient population pool of 40-60 patients for me to recruit from over the period of the study.

Clinical assessment

All patients are seen by a consultant neurologist with a specialist interest in ALS, along a multi-disciplinary team according to patient needs. This can include a respiratory specialist, speech & language therapy, neuropsychology, and specialist nurses.

For the purposes of this pilot study, only basic clinical data regarding their disease type, onset and duration, and treatment history was retrieved.

Retinal imaging and analysis

All participants had the full OCT imaging protocol as outlined in Chapter 3.

All images were of satisfactory quality for processing and analysis, as per the OSCAR-IB criteria.

Results

Participant characteristics

I recruited 20 patients with clinically definite ALS, from the specialist ALS clinic.

The age range was from 30-75 years, with a male-female ratio of 16:4. There were equal groups of limb/spinal and bulbar-onset of ALS, and 11 of the 20 patients were on riluzole treatment. (Table 6.1)

For healthy controls, I used 20 age- and sex-matched participants at random. They were also matched for refractive error.

Table 6.1: Baseline participant characteristics

	Controls	**ALS**	***p-value for difference***
Number	20	20	-
Mean age (years)	55.6 ± 13.5	57.9 ± 12.8	*0.59*
Sex (male:female)	16:4	16:4	-
Refractive error * (dioptres)	-0.60 ± 1.91	0.45 ± 2.43	*0.13*
Disease duration (months)	-	20.2 ± 14.5	-
Age of onset (years)	-	55.6 ± 12.7	-
Spinal-onset - n (%)	-	10 (50)	-
On riluzole - n (%)	-	11 (55)	-

NOTE. Data are shown mean ± SD
* in right eye, as image analysis data will be from right eye images only

OCT analysis

RNFL thickness

From the peripapillary RNFL thickness data, the only significant findings was a thinner PMB sector of the RNFL in bulbar-onset ALS, compared to controls, with a mean difference (MD)= -7.65, 95% CI [-13.73, -1.57], p=0.016.

Otherwise, whist there appeared to be a trend towards RNFL thinning in ALS, possibly more-so in the bulbar-onset group, this was not significant. (Table 6.2)

Table 6.2: OCT analysis: peripapillary scan, RNFL thickness by sector

	healthy controls	**ALS patients**	**spinal-onset group**	**bulbar-onset group**
pRNFL thickness: global	98.5 ± 5.8	98.4 ± 15.5	99.0 ± 13.7	97.8 ± 14.7
PMB	58.3 ± 10.2	52.5 ± 7.4	54.5 ± 8.5	50.6 ± 5.9*
T	76.4 ± 13.6	69.5 ± 10.4	70.2 ± 12.1	68.9 ± 8.9
TS	134.4 ± 23.2	125.8 ± 17.1	127.2 ± 16.3	124.4 ± 18.5
NS	99.7 ± 24.0	95.5 ± 21.1	101.2 ± 24.1	89.7 ± 17.1
N	75.2 ± 18.8	72.2 ± 13.1	73.0 ± 11.9	71.3 ± 14.8
N/T	1.019 ± 0.293	1.116 ± 0.280	1.112 ± 0.302	1.120 ± 0.273
NI	112.4 ± 31.8	111.8 ± 28.3	112.7 ± 27.8	110.9 ± 30.27
TI	148.9 ± 15.2	143.3 ± 16.2	144.5 ± 16.9	142.1 ± 16.34

Abbreviations: PMB, papillo-macular bundle; T, temporal; TS, temporal-superior; NS, nasal-superior, N, nasal; N/T, nasal-temporal ratio; NI, nasal-inferior; TI, temporal-inferior

NOTE. Right eye analysis only. Data are shown mean ± SD (μm)

*P < 0.05, **P < 0.01, ***P < 0.001.

Macular thickness

There were no significant differences in average thickness of any macular region in ALS compared with controls, in either group.

Table 6.3: OCT analysis: macular volume scan, macular average thickness by sector

	healthy controls	ALS patients	spinal-onset group	bulbar-onset group
Macular average thickness: central	269.0 ± 17.2	281.5 ± 24.0	286.3 ± 23.6	276.8 ± 24.7
IN	343.8 ± 12.5	342.7 ± 18.8	339.5 ± 20.6	345.9 ± 17.4
IS	342.6 ± 12.9	341.1 ± 18.1	336.8 ± 19.3	345.4 ± 16.7
IT	329.4 ± 12.5	330.0 ± 17.3	327.1 ± 19.3	333.0 ± 15.6
II	340.7 ± 13.3	338.5 ± 16.3	335.7 ± 17.9	341.3 ± 14.9
ON	314.9 ± 13.8	307.1 ± 13.3	304.1 ± 13.9	310.1 ± 12.6
OS	297.6 ± 12.2	293.5 ± 12.9	291.8 ± 13.4	295.2 ± 12.8
OT	281.6 ± 12.6	279.5 ± 13.5	276.5 ± 14.7	282.5 ± 12.3
OI	289.5 ± 15.2	282.4 ± 12.2	280.4 ± 12.6	284.4 ± 12.2

Abbreviations: IN, inner nasal; IS, inner superior; IT, inner temporal; II, inner inferior; ON, outer nasal; OS, outer superior; OT, outer temporal; OI, outer inferior

NOTE. Right eye analysis only. Data are shown mean ± SD (μm)

*P < 0.05, **P < 0.01, ***P < 0.001.

Macular volume

There were no significant differences in macular volume between ALS and controls, or when sub-divided into spinal-onset and bulbar-onset groups.

When segmented for just the ganglion cell layer of the macular, and the volume calculated, there was a trend for reduction in the bulbar-onset group, but this was not significant. (Table 6.4)

Table 6.4: OCT analysis: macular volume scan, macular volume of full 6mm circle

	healthy controls	ALS patients	spinal-onset group	bulbar-onset group
Macular full thickness volume MV	8.61 ± 0.34	8.50 ± 0.37	8.44 ± 0.40	8.57 ± 0.35
Macular GCLV	1.06 ± 0.07	1.02 ± 0.10	1.04 ± 0.09	0.99 ± 0.10

Abbreviations: MV, macular volume; GCLV, ganglion cell layer volume
NOTE. Right eye analysis only. Data are shown mean ± SD (mm^3)
*P < 0.05, **P < 0.01, ***P < 0.001.

Choroidal thickness

The subfoveal choroid was thinner in spinal-onset ALS, but this did not reach significance. (Table 6.5)

Table 6.5: OCT analysis: horizontal EDI scan, choroidal thickness

	healthy controls	ALS patients	spinal-onset group	bulbar-onset group
sfCT	292.8 ± 71.7	268.4 ± 99.6	246.0 ± 100.0	291.2 ± 98.4

Abbreviations: sfCT, sub-foveal choroidal thickness
NOTE. Right eye analysis only. Data are shown mean ± SD (μm)
*P < 0.05, **P < 0.01, ***P < 0.001.

Data analysis

In summary, there were no significant associations between ALS and retinal thinning.

All metrics were adjusted for duration of disease/time since onset of symptoms. This showed trends for RNFL thinning and reduced GCL volume in bulbar-onset ALS, but these did not reach significance. This could be a result of the relatively small sample size analysed. However, it is worth exploring in more detail.

In the global RNFL measurement (and macular GCL volume), the standard deviation was much higher for ALS than healthy controls (SD=15.5 for ALS, compared to SD=5.8 for the controls), and therefore it is worth looking at the raw data for any visual pattern clues. (Fig. 6.1)

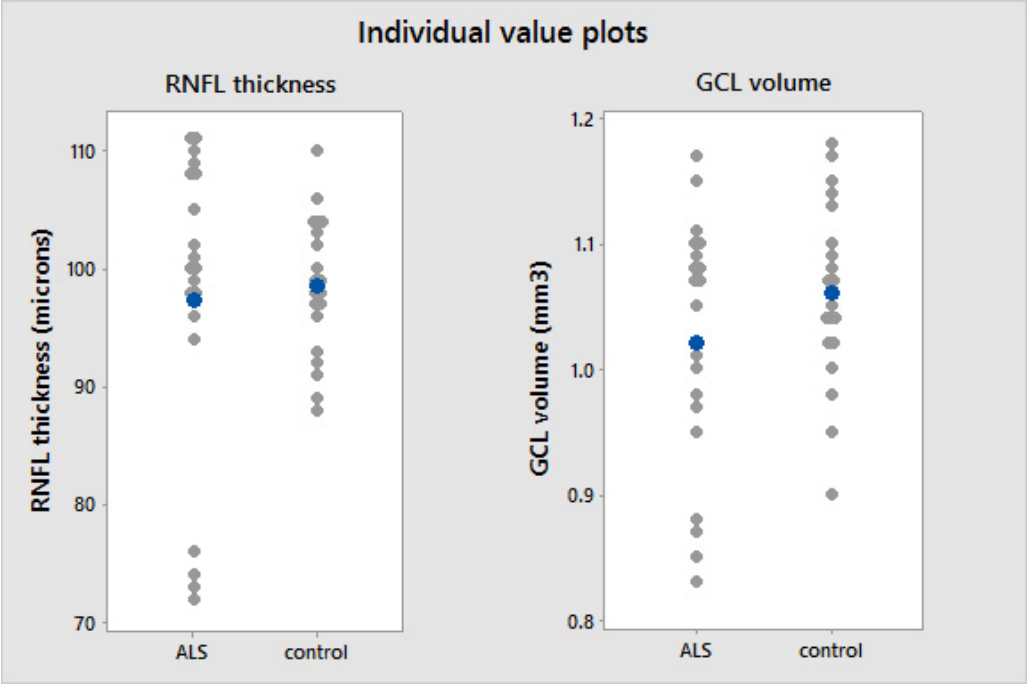

Figure 6.1: ALS: RNFL thickness and macular GCL volume individual value plots (blue dots indicate mean values)

From these plots, it is visually apparent that there appears to be a cluster of four ALS participants who are distinctly separate from the rest of the sample. These four have significantly thinner RNFL and reduced GCL volume, compared with controls.

Multivariate cluster analysis (agglomerative hierarchical) confirms two clusters, normal and those with thinning, $p<0.01$. (Fig. 6.2)

No clinical phenotype measure aligned to this sub-group, leaving it unclear why this specific group of patients demonstrated neuroretinal thinning.

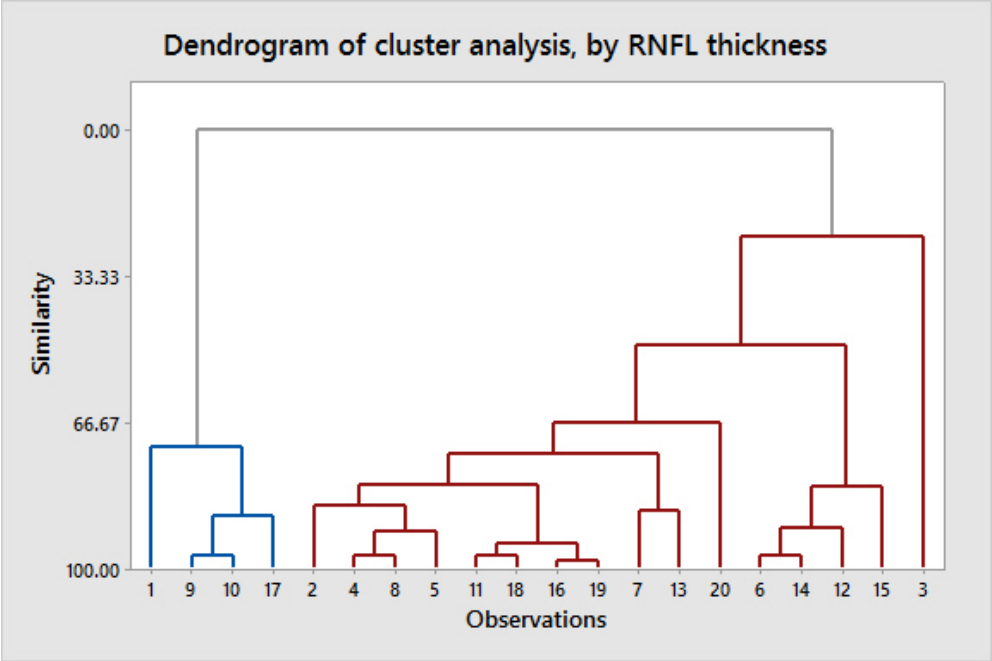

Figure 6.2: ALS: Dendrogram of RNFL thickness in ALS group, confirming clusters

Regarding other disease characteristics, there was no significant correlation between any of these neuroretinal parameters and disease duration. (Fig. 6.3)

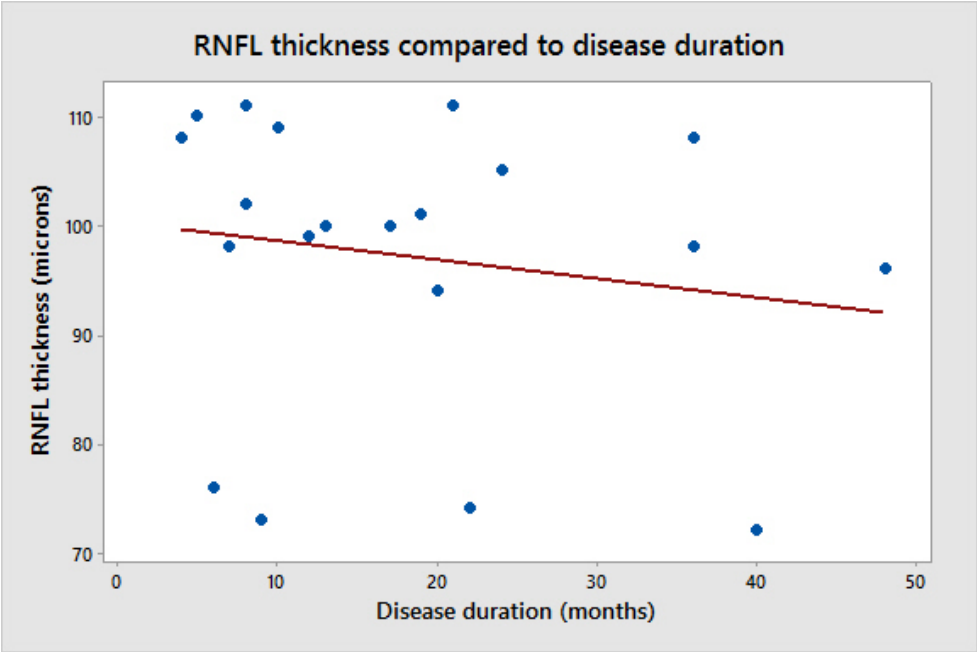

Figure 6.3: ALS: Scatterplot of RNFL thickness relationship with disease duration

However there does appear to be an association with choroidal thickness, for ALS patients on riluzole.

If just those 11 patients are used, their mean sfCT=216.5 ± 61 μm. When compared to healthy controls, there is a MD= -76.3, 95% CI [25.8, 126.8], p=0.005.

This suggests ALS patients on riluzole have significantly thinner choroid, compared with healthy controls, whereas ALS patients who are not on riluzole do not. Riluzole is not known to have any ocular effects. This observation in the choroid is of unclear mechanism.

Review of the images of those patients shows only relative thinning of the whole choroid, with no evidence of focal atrophy of any specific choroidal layer. Perhaps the treatment is causing local vasoconstriction in the choroid, but this is speculation.

Retinal vessel analysis

Vessel calibre

There were no significant differences in retinal vessel calibre in ALS compared with controls, or in either subgroup. (Table 6.6)

Table 6.6: Retinal vessel analysis: vessel calibre

	healthy controls	ALS patients	spinal-onset group	bulbar-onset group
CRAE	28.06 ± 2.30	28.44 ± 1.90	28.96 ± 1.54	27.92 ± 2.16
CRVE	35.51 ± 2.28	35.66 ± 2.91	36.02 ± 3.37	35.29 ± 2.50
AVR	0.79 ± 0.07	0.80 ± 0.06	0.81 ± 0.08	0.79 ± 0.04

Abbreviations: CRAE, central retinal arteriolar equivalent; CRVE, central retinal venular equivalent; AVR, arterio-venous ratio
NOTE. Right eye analysis only. Data are shown mean ± SD (pixels)
*P < 0.05, **P < 0.01, ***P < 0.001.

Vessel tortuosity

There was no significant difference in vessel tortuosity in either ALS group, when compared with healthy controls. (Table 6.7)

Table 6.7: Retinal vessel analysis: vessel tortuosity

	healthy controls	ALS patients	spinal-onset group	bulbar-onset group
aTort	-9.11 ± 1.02	-9.12 ± 0.78	-8.71 ± 0.78	-9.52 ± 0.56
vTort	-9.57 ± 0.65	-9.47 ± 0.70	-9.75 ± 0.80	-9.19 ± 0.46

Abbreviations: aTort, arteriolar tortuosity; vTort, venular tortuosity
NOTE. Right eye analysis only. Data are shown as natural log transformed, from the raw tortuosity measurement calculation, and as mean ± SD
*P < 0.05, **P < 0.01, ***P < 0.001.

Vessel fractal dimension

Fractal dimension was significantly reduced in ALS, for both arteriolar and venular trees. When divided into ALS subtypes, only bulbar-onset ALS showed significant reduction in D_f, and only for multi-fractal calculation of arteriolar D_f. (Table 6.8)

Table 6.8: Retinal vessel analysis: fractal dimension

	healthy controls	ALS patients	spinal-onset group	bulbar-onset group
aD_0	1.63 ± 0.03	1.60 ± 0.04*	1.62 ± 0.04	1.58 ± 0.04**
aD_1	1.61 ± 0.03	1.59 ± 0.04*	1.60 ± 0.04	1.57 ± 0.04**
aD_2	1.61 ± 0.03	1.58 ± 0.04*	1.59 ± 0.03	1.56 ± 0.04**
aD_{BOX}	1.13 ± 0.02	1.11 ± 0.03*	1.12 ± 0.02	1.09 ± 0.03**
vD_0	1.62 ± 0.03	1.60 ± 0.04*	1.61 ± 0.02	1.59 ± 0.05
vD_1	1.61 ± 0.03	1.59 ± 0.03*	1.59 ± 0.03	1.58 ± 0.05
vD_2	1.60 ± 0.03	1.58 ± 0.03*	1.58 ± 0.02	1.57 ± 0.05
vD_{BOX}	1.12 ± 0.02	1.11 ± 0.02*	1.11 ± 0.02	1.10 ± 0.03
cD_0	1.80 ± 0.02	1.78 ± 0.03**	1.79 ± 0.02	1.77 ± 0.04*
cD_1	1.79 ± 0.02	1.76 ± 0.03**	1.77 ± 0.02	1.75 ± 0.04*
cD_2	1.78 ± 0.02	1.75 ± 0.03**	1.77 ± 0.02	1.74 ± 0.04*
cD_{BOX}	1.26 ± 0.01	1.24 ± 0.02**	1.25 ± 0.02	1.23 ± 0.03*

Abbreviations: $aD_{0\text{-}BOX}$, arteriolar fractal dimension 0 to BOX; $vD_{0\text{-}BOX}$, venular fractal dimension 0 to BOX; $cD_{0\text{-}BOX}$, combined fractal dimension 0 to BOX

NOTE. Right eye analysis only. Data are shown mean ± SD (fractal units)

*P < 0.05, **P < 0.01, ***P < 0.001.

Mono-fractal analysis (box-counting method) revealed a reduced arteriolar D_f in ALS (MD= -0.019, 95% CI [-0.037, -0.003], p=0.021), and a reduced venular D_f (MD= -0.016, 95% CI [-0.031, -0.002], p=0.025), and a reduced combined mono-fractal D_f.

It also found a reduced arteriolar D_f in just the bulbar-onset ALS group (MD= -0.033, 95% CI [-0.057, -0.010], p=0.008), and a reduced combined mono-fractal D_f.

Superior multi-fractal analysis methods revealed similar results for ALS as whole group, and for all three algorithms - capacity dimension, entropy dimension and correlation dimension. In addition, venular D_f was found to be reduced in bulbar-onset ALS subgroup.

Arteriolar capacity D_f (aD_0) was significantly reduced in ALS (MD= -0.031, 95% CI [-0.053, -0.008], p=0.010), and in bulbar-onset only ALS (MD= -0.048, 95% CI [-0.080, -0.016], p=0.007).

Arteriolar entropy D_f (aD_1) was significantly reduced in ALS (MD= -0.029, 95% CI [-0.052, -0.007], p=0.010), and in bulbar-onset only ALS (MD= -0.047, 95% CI [-0.079, -0.016], p=0.007).

Arteriolar correlation D_f (aD_2) was significantly reduced in ALS (MD= -0.029, 95% CI [-0.051, -0.008], p=0.010), and in bulbar-onset only ALS (MD= -0.047, 95% CI [-0.078, -0.016], p=0.007).

Venular capacity D_f (vD_0) was significantly reduced in ALS (MD= -0.022, 95% CI [-0.043, -0.001], p=0.038).

Venular entropy D_f (vD_1) was significantly reduced in ALS (MD= -0.021, 95% CI [-0.041, -0.001], p=0.044).

Venular correlation D_f (vD_2) was significantly reduced in ALS (MD= -0.020, 95% CI [-0.040, -0.001], p=0.044).

Combined arteriolar and venular multi-fractal D_f was significantly reduced in ALS and in bulbar-onset ALS alone (cD_0, cD_1, cD_2).

The predominant finding when taking all these results together is therefore a reduced arteriolar fractal dimension in bulbar-onset ALS, and reduced arteriolar and venular fractal dimension in the whole ALS group.

Spinal-onset ALS as a group were not associated significantly with reduced fractal dimension.

As with the analysis in early-onset dementia, these findings would be unlikely to survive correction for multiple testing, however they are worth highlighting within this exploratory pilot study.

Data Analysis

In summary, ALS is not associated with retinal vessel morphological change, with the exception of reduced arteriolar (multi-fractal) fractal dimension in bulbar-onset ALS.

Vessel calibre and vessel tortuosity were not significantly different in ALS, when analysed as a whole group.

However, comparing spinal-onset and bulbar-onset ALS yields a significant difference in arteriolar tortuosity.

Arteriolar tortuosity was significantly lower in bulbar-onset ALS, compared with spinal-onset ALS (MD= -0.80, 95% CI [-1.446, -0.163], p=0.017). ROC curve analysis of this relationship reveals AUC=0.770, 95% CI [0.558, 0.982], p=0.041. Best cutoff comes at -9.323, with specificity 90%, sensitivity 60%.

Therefore, arteriolar tortuosity has acceptable discrimination for bulbar-onset and spinal-onset ALS.

Fractal dimension was also reduced in bulbar-onset ALS, compared with spinal-onset ALS. For example, using arteriolar capacity D_f (aD_0), bulbar-onset ALS has significantly reduced Df compared with spinal-onset ALS (MD= -0.3, 95% CI [-0.073, -0.005], p=0.028). ROC curve analysis of the ability of aD_0 to distinguish between bulbar-onset and spinal-onset ALS reveals AUC=0.750, 95% CI [0.529, 0.972], p=0.038. Best cutoff comes at 1.585, with specificity 80.0%, sensitivity 70.0%.

Therefore, arteriolar D_f has acceptable discrimination for bulbar-onset and spinal-onset ALS.

There were no significant differences in these vessel parameters between patients on riluzole treatment, and patients who were not on treatment.

Differentiating ALS and MS

A clinical situation that arose more than once during my research was uncertainty in the diagnosis of a patient. On each occasion, a patient with a previous diagnosis of ALS was being reconsidered as a result of the atypical clinical course of the disease. The diagnostic differential was between ALS and progressive MS.

With the well characterised RNFL findings in MS, OCT was thought to be a useful clinical imaging tool to discriminate between the two diseases.

However, it is of interest to evaluate this more thoroughly, and include other neuroretinal metrics, to determine the best measures for discriminating SPMS and ALS.

I therefore compared measures from each disease, with appropriate matching.

Results

There is a fair degree of similarity in the retinal vessel data between ALS and SPMS. However, the RNFL and macular measures appear different, with SPMS having significantly thinner RNFL, and reduced MV and GCL volume. (Table 6.9)

Diagnostic discrimination

To look for the strength of these differences, we can compare the data between ALS and SPMS, and use ROC curve AUC analysis to calculate specificity and sensitivity.

Global RNFL is significantly thinner in SPMS than ALS (MD= -17.3, 95% CI [-24.2, -10.4], $p<0.001$).

Temporal RNFL is significantly thinner in SPMS (MD= -14.1, 95% CI [-19.6, -8.6], $p<0.001$).

Macular volume is significantly reduced in SPMS (MD= -0.39, 95% CI [-0.58, -0.20], $p<0.001$).

Macular GCL volume is also significantly reduced in SPMS (MD= -0.15, 95% CI [-0.205, -0.098], $p<0.001$).

There is no difference in sfCT, or in any of the retinal vessel measures.

We therefore have significant differences in the RNFL and macular measures between ALS and SPMS.

For global RNFL, the AUC=0.806, 95% CI [0.692, 0.921], p<0.0001. The best cutoff comes at 95.5µm, with specificity 80.0%, sensitivity 81.1%.

For temporal RNFL, the AUC=0.872, 95% CI [0.789, 0.954], p<0.0001. The best cutoff comes at 57.5µm, with specificity 85.0%, sensitivity 82.2%.

For macular volume, the AUC=0.755, 95% CI [0.645, 0.864], p=0.0002. The best cutoff comes at 8.39mm^3, with specificity 70.0%, sensitivity 75.0%.

Finally, for macular GCL volume, the AUC=0.792, 95% CI [0.698, 0.886], p<0.0001. The best cutoff comes at 0.935mm^3, with specificity 80.0%, sensitivity 65.9%.

Table 6.9: ALS and SPMS: comparison of selected OCT and vessel metrics, with controls

	healthy controls	**ALS**	**SPMS**
pRNFL thickness: global	98.5 ± 5.8	98.4 ± 15.5	81.1 ± 14.8***
T	76.4 ± 13.6	69.5 ± 10.4	52.4 ± 15.8***
Macular full thickness volume MV	8.61 ± 0.34	8.50 ± 0.37	8.12 ± 0.42***
Macular GCLV	1.06 ± 0.07	1.02 ± 0.10	0.86 ± 0.15***
sfCT	292.8 ± 71.7	268.4 ± 99.6	275.0 ± 84.4
CRAE	28.06 ± 2.30	28.44 ± 1.90	28.20 ± 2.36
CRVE	35.51 ± 2.28	35.66 ± 2.91	34.93 ± 2.97
AVR	0.79 ± 0.07	0.80 ± 0.06	0.81 ± 0.09
aTort	-9.11 ± 1.02	-9.12 ± 0.78	-9.17 ± 0.84
vTort	-9.57 ± 0.65	-9.47 ± 0.70	-9.48 ± 0.78
aD_1	1.61 ± 0.03	1.59 ± 0.04*	1.60 ± 0.04*
vD_1	1.61 ± 0.03	1.59 ± 0.03*	1.59 ± 0.04*

Abbreviations: T, temporal; MV, macular volume; GCLV, ganglion cell layer volume; sfCT, sub-foveal choroidal thickness; CRAE, central retinal arteriolar equivalent; CRVE, central retinal venular equivalent; AVR, arterio-venous ratio; aTort, arteriolar tortuosity; vTort, venular tortuosity; aD_1, arteriolar fractal dimension 1; vD_1, venular fractal dimension 1

NOTE. Right eye analysis only. Data are shown mean ± SD (µm)

*P < 0.05, **P < 0.01, ***P < 0.001.

With global and temporal RNFL thickness measures both showing very good discrimination, there is therefore clinical value in using these measures to discriminate between ALS and SPMS. They both independently have very good specificity and sensitivity, but when combined, this improves further.

For global RNFL thickness less than 95.5μm, and temporal RNFL thickness less than 57.5μm, SPMS can be discriminated from ALS with 92.4% specificity, and 88.0% sensitivity.

Macular volume and macular GCL volume did also distinguish SPMS from ALS with acceptable discrimination, although not as well as RNFL.

So, in the clinical situation of an uncertain diagnosis, RNFL measures can be used to distinguish between ALS and SPMS.

Discussion

This is the first study to look at neuroretinal markers in ALS, in a Scottish population.

Having identified conflict and unanswered questions from the literature, I have investigated the utility of neuronal and vascular markers in the retina in association with spinal-onset and bulbar-onset ALS.

I have studied diagnostic phenotyping, and uncovered several novel findings.

Summary

I recruited 20 clinically definite ALS patients, 10 spinal-onset ALS and 10 bulbar-onset ALS. The male:female ratio was 16:4, and 11 of the patients were on riluzole treatment.

RNFL, MV and GCLV

I found that whilst there was trend towards RNFL thinning in ALS, this was not significant, apart from a thinner PMB sector of the RNFL in bulbar-onset ALS.

However, cluster analysis revealed that in fact there were two clusters of ALS patients, with one cluster (n=4) having significantly thinner global RNFL. No clinical phenotype aligned to this sub-group, they were not the oldest patients nor those with the longest disease duration. The mechanism of this RNFL thinning then is unclear.

ALS was not associated with macular thinning of any macular sector, or reduced macular volume.

Bulbar-onset ALS showed a trend for reduction in macular GCL volume, but this was not significant.

Global RNFL thickness and temporal RNFL thickness both discriminated very well between ALS and SPMS with high specificity and sensitivity.

Macular volume and macular GCL volume both discriminated acceptably between ALS and SPMS.

Choroid

No previous studies have investigated choroidal thickness in ALS.

I found that the subfoveal choroid was thinner in spinal-onset ALS, but this did not reach significance.

However, ALS patients on riluzole treatment had significantly thinner choroid, compared with healthy controls. The reason for this is unknown.

Retinal vessel calibre, tortuosity and fractal dimension

Retinal vessel parameters have not previously been studied in ALS.

In this study, I have found that ALS is not associated with retinal vessel morphological change, with the exception of reduced arteriolar (multi-fractal) fractal dimension in bulbar-onset ALS.

Vessel calibre and vessel tortuosity were not significantly different in ALS, when analysed as a whole group. However, arteriolar tortuosity was significantly lower in bulbar-onset ALS, compared with spinal-onset ALS, with acceptable discrimination, and 90% specificity.

Arteriolar fractal dimension was also significantly reduced in bulbar-onset ALS, compared with spinal-onset ALS, again with acceptable discrimination, and 80% specificity.

There were no significant differences in these vessel parameters between patients on riluzole treatment, and patients who were not on treatment.

Utility as a biomarker

- *Detection method should be precise, reliable and transferrable*
  True for all OCT imaging derived measures: RNFL, MV, GCL, sfCT
  True for all VAMPIRE retinal vessel measures: calibre, tortuosity, fractal dimension

- *Distinguish between healthy and disease*
  True for RNFL in a small cluster of ALS patients; sfCT for ALS patients on riluzole treatment
  Not true for RNFL in the majority of patients; MV in ALS; GCLV in ALS; sfCT for ALS patients not on riluzole treatment; calibre in ALS; tortuosity in ALS

- *Differentiate between diseases that are clinical similar*
  True for tRNFL (ALS and SPMS); tRNFL (ALS and SPMS); MV (ALS and SPMS), GCLV (ALS and SPMA); arteriolar tortuosity (spinal-onset and bulbar-onset ALS); arteriolar fractal dimension (spinal-onset and bulbar-onset ALS)
  Other markers not assessed

- *Value as a prognostic marker*
  Not assessed in this research study

- *Use in monitoring disease progression*
  Not assessed in this research study

- *Use as a pre-clinical screening test*
  Not assessed in this research study

Contributions to knowledge

- Amyotrophic lateral sclerosis is associated with a thinner RNFL in a small cluster of patients, thinner choroid when on riluzole treatment, and a reduced arteriolar and venular fractal dimension; but has normal RNFL (in most patients), macular thickness, macular volume, macular GCL volume, retinal vessel calibre and retinal vessel tortuosity.

- Bulbar-onset amyotrophic lateral sclerosis is associated with a thinner PMB sector of RNFL, and reduced arteriolar fractal dimension; but has normal macular thickness, macular volume, macular GCL volume, retinal vessel calibre and retinal vessel tortuosity

- Spinal-onset amyotrophic lateral sclerosis is not associated with any neuroretinal marker, with no value significantly different from controls.

- Regarding discrimination between ALS subtypes, arteriolar tortuosity and arteriolar fractal dimension both discriminated between bulbar-onset and spinal-onset ALS.

Conclusion

Despite some significant findings, it is unlikely that retinal markers of neuronal and vascular integrity will have clinical utility in diagnostic phenotyping of ALS.

There was discrimination between ALS subtypes using retinal vessel morphological parameters, but the clinical value in this is low.

The cluster analysis of RNFL thickness in ALS that revealed a small cluster of ALS patients with significant RNFL thinning is intriguing, but probably more relevant to the pathology of ALS than any potential as a future biomarker of this disease.

7 CONCLUSIONS

Research findings

In this research study, I have explored the clinical utility of retinal imaging derived biomarkers of neuroretinal and neurovascular metrics in the diagnosis and monitoring of MS, early-onset dementia and ALS.

Overview

The three phases of my research have been:

1. systematic reviews of the literature for different retinal biomarkers of neurodegenerative disease, including meta-analyses of the most studied markers

2. detailed description and expansion on the required methodology for reliable retinal imaging and image analysis, including a novel modulation of image analysis software to extend the utility of single-episode patient retinal imaging

3. In depth analysis of the clinical utility of both neuronal and vascular metrics in the phenotyping of multiple sclerosis, early-onset dementia syndromes and amyotrophic lateral sclerosis.

Systematic reviews

In these reviews, I started with a systematic review for the use of OCT technology in informing on neurological disease. This showed a sizable presence of work on MS, and several studies in dementia and Parkinson's disease, but only a scattering of other diseases. Notable absences were non-AD dementias, and early-onset dementia.

Reviewing the literature on MS, it was clear that the evidence for RNFL measures as a surrogate of brain atrophy was substantial, and accepted. What remained unclear however was the detail in RNFL and other neuroretinal measures, in regard to their discriminatory potential, and clinical utility in comparison with functional

characteristics, such as visual acuity. There were also no imaging studies on retinal or choroidal vasculature in MS.

In dementia, the focus has purely been on Alzheimer's disease, and mild cognitive impairment. A meta-analysis of these studies of RNFL change in AD (and MCI) revealed a significant finding of moderate RNFL thinning in AD. A second meta-analysis of retinal vessel metrics in AD showed an extremely heterogenous group of studies, with variable methodology and varied results.

There were no studies on either neuroretinal or retinal vascular markers in early-onset dementia, or in any non-AD dementia, such as FTD, PPA, CBD or PCA. And no studies of correlation with other AD markers, such as CSF biomarkers.

ALS had just three published studies relating to neuroretinal associations, with methodological weaknesses and conflicting results. There were no studies of retinal vascular markers or the choroid in ALS.

Therefore, there were clear unanswered questions regarding the utility of OCT imaging (including retinal vascular morphology assessment) in these diseases.

Methodology

The rapid evolution of retinal imaging devices has now delivered us devices with extraordinary capability. However, it is essential for reliable data that the devices are operated by informed and trained users, supported by good analysis tools, and underpinned by a thorough understanding of ocular anatomy, physiology, pathology and imaging.

In this thesis, I have detailed some of the most important steps in retinal imaging acquisition, review, processing and analysis. This includes a novel methodological innovation, of analysing the retinal vessel morphology from the OCT SLO images, using bespoke modulated semi-automated software. Therefore, this is the first ever study to analyse and calculate vessel metrics such as fractal dimension from SPECTRALIS SLO images.

Analysis studies

The three clinical diseases of MS, early-onset dementia (including non-AD dementia types), and ALS were highlighted and chosen from my literature review.

I recruited almost a thousand participants to this research study, performed all the retinal imaging, processing and analysis, and have presented here my detailed findings, including many novel findings.

The breadth and depth of this research adds significant knowledge to the field.

Contributions to knowledge

MS

- Relapsing-remitting multiple sclerosis with a history of optic neuritis, was associated with the greatest reduction in RNFL thickness, in all sectors, and in macular GCL volume. It was also associated with thicker venules, and lower arterio-venous ratio. AVR discriminated between RRMS and SPMS with very good discrimination. In addition, treatment-naïve RRMS patients were associated with a lower AVR.

- Secondary-progressive MS was associated with the greatest reductions in macular thickness, macular volume and sub-foveal choroidal thickness.

- The choroidal thinning seen in all MS subtypes did not correlate with duration of disease or visual acuity, but was thinner in RRMS patients on treatment, versus treatment-naïve.

- Retinal vessel tortuosity was not associated with any MS subtype, but was associated with optic neuritis history in RRMS (reduced arteriolar tortuosity with ON history).

- Reduced retinal vessel fractal dimension was found in all MS subtypes, mainly of the arteriolar tree, and to the greatest degree in SPMS and RRMS +ON.

- GCL volume measures were superior to RNFL measures in diagnosing MS, although GCL and tRNFL both discriminated MS with high specificity. Macular volume and choroidal thickness were much less useful in discriminating MS. GCL volume measures were also more stable than RNFL over the short-term, reflecting the vulnerability of the RNFL to fluid changes and variation. Finally, GCL volume falls earlier in RRMS disease course than RNFL

- Visual acuity in SPMS was strongly correlated with RNFL thickness (particularly temporal RNFL) and macular GCLV, at all contrast levels. GCLV showed the best correlation, but tRNFL proved the more reliable comparator.

- Thicker retinal venules and higher arteriolar tortuosity were both predictive of greater relapse rate in RRMS. This was elevated further in patients with tRNFL less than 56μm, a higher CRVE (above 35px) was associated with a 2x higher risk of at least one relapse in the next year.

- Regarding discrimination between RRMS and NMO, temporal RNFL, global RNFL, N/T ratio, GCLV, AVR and CRVE were all significantly different between RRMS +ON and NMO. AVR was the highest single discriminant, but a combined score using cutoffs in tRNFL, gRNFL and N/T ratio discriminated NMO from RRMS +ON with 94.6% specificity.

Dementia

- Early-onset Alzheimer's disease is associated with global RNFL thinning (especially superiorly), macular thinning, reduced macular volume, reduced GCL volume, and reduced retinal arteriolar and venular fractal dimensions; but has normal retinal arterioles, and retinal vessel tortuosity. There was no correlation between RNFL or GCL volume and CSF biochemical markers of dementia in early-onset AD.

- Behavioural-variant frontotemporal dementia is associated with macular thinning, reduced macular volume, reduced GCL volume, choroidal thinning, and reduced retinal arteriolar and venular fractal dimension; but has normal RNFL, retinal arterioles, and retinal vessel tortuosity. However, the RNFL thickness measure predicts cognitive decline in bvFTD.

- Primary progressive aphasia is associated with partial macular thinning, reduced GCL volume, choroidal thinning, and wider retinal venules; but has normal RNFL, macular volume, retinal arterioles, retinal vessel tortuosity, and retinal vessel fractal dimension.

- Corticobasal degeneration is associated with partial macular thinning, reduced macular volume, reduced GCL volume, choroidal thinning, wider retinal venules, and reduced retinal arteriolar fractal dimension; but has normal RNFL, retinal arterioles, retinal vessel tortuosity, and retinal venular fractal dimension.

- Posterior cortical atrophy is associated with nasal RNFL thinning, choroidal thinning, and reduced retinal arteriolar and venular fractal dimension; but has normal retinal arterioles, and retinal vessel tortuosity. (Macular parameters of volume were not assessed.)

- None of these neuroretinal markers independently discriminated between all the dementia types with high specificity. Although arterio-venous ratio discriminated between AD and PPA, and arteriolar fractal dimension between CBD and PPA, and between PCA and PPA. However, in combination, the pattern of neuroretinal involvement across all the markers does discriminate between all the dementia types.

- Correlation with ACE-III scores was also poor, except for a positive correlation with macular volume in PPA.

ALS

- Amyotrophic lateral sclerosis is associated with a thinner RNFL in a small cluster of patients, thinner choroid when on riluzole treatment, and a reduced arteriolar and venular fractal dimension; but has normal RNFL (in most patients), macular thickness, macular volume, macular GCL volume, retinal vessel calibre and retinal vessel tortuosity.

- Bulbar-onset amyotrophic lateral sclerosis is associated with a thinner PMB sector of RNFL, and reduced arteriolar fractal dimension; but has normal macular thickness, macular volume, macular GCL volume, retinal vessel calibre and retinal vessel tortuosity

- ❖ Spinal-onset amyotrophic lateral sclerosis is not associated with any neuroretinal marker, with no value significantly different from controls.

- ❖ Regarding discrimination between ALS subtypes, arteriolar tortuosity and arteriolar fractal dimension both discriminated between bulbar-onset and spinal-onset ALS.

Methodological advancements

A substantial component of this thesis has been the detailed description of the methods of retinal imaging in relation to acquisition, processing and interpretation of the imaging, and how this underpins any research data output. This depth of study and scrutiny of the imaging procedure requires a solid understanding of retinal structure and function, as well as experience in the use of the retinal imaging devices.

In addition, the protocols established for this study, whilst sufficiently interoperable with comparable studies in the literature, contain a higher level of quality assurance and detailed procedure of image processing that is often missing from published work. In fact, the figures within some published papers occasionally 'red-flag' the study as without sufficient scientific rigor when basic image processing techniques are clearly absent. For example, ignoring the foveal location of RNFL scans. This appears a minor step to the inexperienced observer, but failure to account for this can generate garbage RNFL data that can lead to wrong conclusions.

The modulation of vessel analysis software to provide semi-automatic quantitative vessel metrics from the SPECTRALIS SLO images is a novel development, and one that should not be undervalued. The process and evaluation of this has already been published in a leading medical imaging journal.[97] In an industry that is led by large and well-resourced technical companies, with proprietary IT development teams and products, software developments such as this are rare from small research groups.

Pathology and mechanisms

GCL versus RNFL

There are weaknesses in the broad interpretation of RNFL thickness.

The RNFL consists of more than just axons. And RNFL thinning does not distinguish between axonal thinning, axonal loss, or other tissue atrophy within the layer. In addition, pRNFL scan is a single circular scan around the disc, giving thickness across a single position in the anterior pathway.

Measurement of GCL thickness - or volume - is potentially a superior marker of RGC integrity. It can be used to measure damage soon after an ON episode, unlike the RNFL where there may still be inflammation/swelling precluding its use for measuring axonal loss in the first few months after ON.[311]

In the study of MS biomarkers in this research, I have compared RNFL and GCL in many parts of the analysis, and concluded that the choice of measure depends upon the circumstances and clinical question, but that in general GCL measures are more sensitive and reliable than RNFL.

On the subject of RGC loss pathophysiology, I remain unconvinced that the observed RNFL and GCL thinning in neurodegeneration is simply the product of retrograde trans-synaptic degeneration, spreading towards the eye when the visual pathways become involved in the intracranial pathology. The evidence from MS (selective temporal loss) and Alzheimer's disease (no loss of neurones in LGN[209]) in conjunction with many observed findings in this research project suggests that RGCs are selectively and directly targeted in different diseases, and in different ways. In MS, to the RGC cell body first. In dementia, perhaps a toxic effect of amyloid-β in the RGC.[312]

In ALS, several mechanisms have been proposed to explain the relentless and progressive character of the disease, and how it 'spreads' through the motor system. Degenerative patterns of 'dying-forward' and 'dying-back' of the motor neurone have been demonstrated, and therefore both anterograde and retrograde degeneration processes of the neurone. With RGC involvement in only some cases of ALS, this pushes the hypothesis again to some specific pathologies targeting the RGC, with others

avoiding it, until perhaps very late stage disease, where retrograde trans-synaptic degeneration towards the eye may occur.

Genetics may ultimately answer this question in ALS. New genes in the pathogenesis of ALS are being discovered all the time. Three genes so far linked with ALS are also linked with glaucoma and optic neuropathy (ataxin-2, optineurin, tank-binding kinase 1).[313-315] Therefore it is possible that the observed impact on the RGC in some patients is a consequence of the root pathological cause.

In MS, the RGC is selectively targeted, as with the brain white matter tracts, and in terms of inflammation, and in demyelination. Therefore, are the oligodendrocytes of the anterior visual pathways similar to the brain oligodendrocytes? Are they functionally and structurally similar? Inflammation in the anterior visual pathway is perhaps IL-17 driven[316], unlike in the spinal cord.

I've looked in this research at RGC (GCL and RNFL) but there is some emerging suggestion for deeper retinal layers to be involved in MS, such as the inner plexiform layer.[317] Although these changes may be dynamic, rather than simply atrophic.[318]

Therefore, the hypothesis relating the eye to the brain, as simply an end extrusion, with retrograde degeneration perhaps needs modification. The eye is as much part of the brain as any other location, and as all brain disease preferentially affect specific parts of the brain - at least in their early stage - then the eye is included within this.

This makes the eye more powerful as a window to the brain, as the presence and pattern of involvement if the eye in brain disease is specific, rather than surrogate end marker of global brain atrophy. Ans therefore it is essential to know which diseases involve the eye, how they involve the eye, and how we can use that information to benefit patient care.

This study has developed this idea of specific patterns that we can observe in the eye, and attempted to quantify the degree of specificity and sensitivity of correlation with phenotype, with existing markers of disease and prognostic utility. Our evolving understanding of disease pathophysiology complements this research, and it is likely that we will see further evidence for the specific involvement of the eye in these diseases, confirming the findings from this and other studies on the subject.

Limitations and Cautions

Study limitations

The primary limitation of this study is that it is cross-sectional. This is satisfactory for diagnostic phenotyping and discrimination, but leaves some unanswered questions regarding the natural history of neuroretinal metrics, in relation to disease trajectory.

A longitudinal study would add value to determine the temporal relationship of neuroretinal changes, and particularly timing of any changes in relation to development of the syndromic symptoms, so do the changes happen before, early or during the disease. It would also enable prospective recording of ON episodes, which would better aid understanding of the impact of optic neuritis on the GCL.

I have also used only right eye data, to avoid confounding bias issues from units of analysis paired clustering. However, I have gone through the data and carried out identical comparisons of left eye data for the majority of the analyses presented here, and they matched without exception.

Ocular Disease

The growing number of studies providing evidence of abnormal retinal structural measurements in diseases viewed as predominantly non-ocular also has important implications for the management of ophthalmic disease. For example, RNFL thinning due to neurological diseases may complicate the management of glaucoma in which measurement of change in RNFL thickness over time is commonly used to detect progression. Particularly in the elderly population where comorbidity is common, a condition such as dementia, which appears to be associated with RNFL thinning, may introduce a potentially confounding factor to the assessment of glaucoma progression.[319]

On the other hand, the observation that diseases such as glaucoma and dementia have shared features raises the possibility that neuroprotective treatments effective for one disease may be utilised for another. For example, neuroprotective and neuroregenerative treatments that aim to protect existing and regenerate damaged cells respectively may be effective for a range of diseases with heterogeneous mechanisms from Alzheimer's disease to glaucoma.[320, 321]

The ability to identify ocular biomarkers of systemic disease is an attractive prospect as the optical properties of the eye permit visualisation of vascular and neural tissues that is not possible in any other part of the body. The identification of ocular biomarkers of systemic and predominantly non-ocular disease is not a new concept and it is clear that many ocular diseases, such as diabetic retinopathy and arteritic ischemic optic neuropathy are a direct consequence of systemic pathology. In fact, the diabetic retinopathy grading system is an excellent example of the use of ocular biomarkers for monitoring a systemic disease, with other useful diabetes biomarkers including HbA1c and blood pressure. The introduction of OCT has though, led to the realisation that an increasing number of conditions can have ocular manifestations, and it is possible to quantify these changes using imaging devices. This raises the possibility that OCT imaging might reduce the need for more invasive, time consuming or costly tests, for example reducing the need for MRI imaging of the brain to monitor for disease progression in multiple sclerosis. Measurements from OCT may be used for diagnoses, assessing disease progression, for predicting clinical outcomes, or for providing more acceptable and cost-effective ways to assess the effect of new treatments. In clinical trials, appropriately used biomarkers have the potential to replace or supplement conventional endpoints with something that can be measured earlier, more easily and more frequently.[322]

Utility as biomarkers

We should though exercise caution when considering introducing new biological markers, particularly if considering them for inclusion as endpoints in clinical trials or to base decision-making regarding effectiveness of treatment. Few biomarkers fully capture the full effect of treatment, and this is particularly likely to be true for ocular biomarkers of systemic diseases.[323] Nevertheless, there is great hope that quantification of retinal parameters using OCT may be a useful surrogate for the assessment of a wide range of predominantly non-ocular diseases.

The ultimate goal with neurodegenerative disease is of course prevention. This will require a combination of strategies, from early identification of individuals at risk, to modification of that risk. Until that becomes possible, then our strategy is to slow down the disease process, halt it, and eventually reverse the degenerative damage done. All these interventions will require reliable and well-researched biomarkers of the disease, both in diagnostic discrimination and also in disease monitoring.

There is increasing evidence that no single biomarker will in itself be sufficient to characterise an individual in term of their disease and likely trajectory. Stratified medicine identifies that the future of managing these difficult conditions is personalised diagnosing and treating, with multi-modal and combination investigations and tests, from genetic profiling to detailed clinical assessment, to imaging biomarkers.

In cancer treatment, for example, a personal workup of all these factors is pivotal in titrating the most appropriate treatment regime for the individual patients, as well as understanding their likely disease course. This is a great advance from when cancer diagnoses were only dichotomised based on the presence of metastases, and treated accordingly.

Across the diseases of multiple sclerosis, dementia and motor neurone disease, there is varying understanding of the disease pathophysiology, and where to target possible treatments, with MS perhaps the furthest ahead in disease modifying therapeutics. However, there is some commonality in how we might use biomarkers to diagnose and monitor these dissimilar diseases, with imaging markers such as retinal imaging a plausible candidate.

Ultimately, with no 'gold standards' of diagnosis or monitoring in dementia, it is hard to fully explore and determine the utility of neuroretinal biomarkers. Better disease genotyping may provide a useful comparator in the future, and allow us to realise the potential of the retina in informing on these complex diseases. In the meantime, we can continue to explore the utility of the retina in providing prognostic disease markers, in longitudinal studies of disease manifestations such as cognitive and psychological changes.

The emergence of retinal imaging derived markers of neurodegenerative disease is a very young field, with a surge of interest over the last few years - mainly a result of new ocular imaging technologies such as OCT providing the ability to provide incredible images, with resolutions suitable for precise measures of neuronal integrity.

Retinal imaging in neuroscience research

Optical coherence tomography

Retinal imaging is very much an ophthalmic sub-specialty in its own right, with most ophthalmology departments employing dedicated ophthalmic photographers with particular expertise in all aspects of ocular imaging, from external macro-photography to micron-level retinal analysis.

The emergence of OCT has transformed ophthalmic investigation and management, and created an exciting area within the world of retinal imaging. The rapid evolution of the technology, in conjunction with the inherent ease-of-use and patient-acceptability of the test, have made it not only an essential tool in clinical ophthalmology, but now an exciting research tool in new areas such as neurology.

The images created by the latest OCT machines are stunning. The micron-level resolution along with software refinements of image averaging and noise reduction facilitate clear and logical images, that easily visually represent the retina in health and in disease. The ability to also generate quantitative measures of retinal layer thicknesses and volumes automatically is a powerful capability, and one that enables drastically improved patient care in the management of diseases such as age-related macular degeneration (ARMD) and also aids the research use of OCT in defining and learning the sub-clinical retinal changes occurring in both ocular and systemic diseases.

The value of measuring neuroretinal alterations in brain diseases is a rapidly growing area of research, with exponential growth in published work and conference interest. The benefits of OCT as a clinical investigation are quite clear. The extent of superiority over traditional brain imaging technologies are becoming better understood, as are the aspects where OCT provides complementary information that is useful clinically.

It is of course essential to also have an experienced ophthalmologist to interpret the OCT images. Someone who understands the pathophysiology and natural history of retinal disease, the differential diagnosis of abnormalities or incidental findings, as well the correct decisions in relation to disease monitoring or treatment plans. As with any new imaging technology, the accessible visual image can result in the technology being

mistaken for simplicity, where in fact subtleties of image acquisition, processing, and interpretation, can be missed and erroneous conclusions made.

A final important consideration is whether patients included in OCT-device normative databases might have systemic diseases that affect the RNFL layer and thereby affect the ability of these databases to detect ophthalmic disease. Normative databases are often used to categorise patients with suspected glaucoma as within normal limits, borderline, or outside normal limits, and although the databases differ in size, eligibility criteria and ethnic makeup between manufacturers[324], all exclude patients with diseases known to affect the retina or optic nerve. It is however, apparent that a growing number of conditions may result in retinal changes, not previously appreciated, meaning the exclusion criteria may need to be refined.

Future developments in retinal imaging

Adaptive optics OCT

Adaptive optics (AO) is an optical system of real-time correction of motion or aberration. The system has previously been integrated into fundus cameras and scanning laser ophthalmoscopes, where it can improve image quality, although with the drawbacks of limited field of view and depth of focus.[325]

Its natural home is with integration into OCT systems, where it can not only reduce blur and image artefact, but also increase the resolution of the image, particularly in the lateral direction, where standard OCT is limited to around 20μm resolution, AO improves this to 3-4μm - identical to the axial resolution - enhancing the full 3D detail and precision.

One area of current interest is the (automated) measurement of 3D lamina cribrosa microstructure using AO-OCT. Posterior deformation of the lamina cribrosa is thought to be the cause and site of axonal injury in some patients with glaucoma, and therefore understanding this structure and the pores within it that support the RGC axons, could be an important tool in glaucoma diagnosis.[326]

Polarisation Sensitive OCT

Polarisation sensitive OCT (PS-OCT) is a hardware adaptation of a conventional OCT system, generating additional contrast in images, based upon the polarisation

properties of the tissue being examined. Its utility in the assessment of neuroretinal integrity is unclear, but it may offer a method of detecting axonal compromise earlier than existing OCT imaging, extrapolating from results of its performance in evaluating outer retinal pathology.[327]

OCT-angiography

OCT angiography (OCT-A) is an innovative evolution of OCT technology, generating remarkable depth-resolved images of the retinal micro-circulation, without the need for intravenous contrast. The microvascular vessel information is extracted from the standard OCT image data, with specialised - and intensive - processing to identify the vessels. The resulting angiographic image is remarkable, and enchanting many retinal researchers. (Fig. 7.1) Several variants of the technology are available, using one or both of Doppler shift (phase variance), and decorrelation (speckle variance) processes.

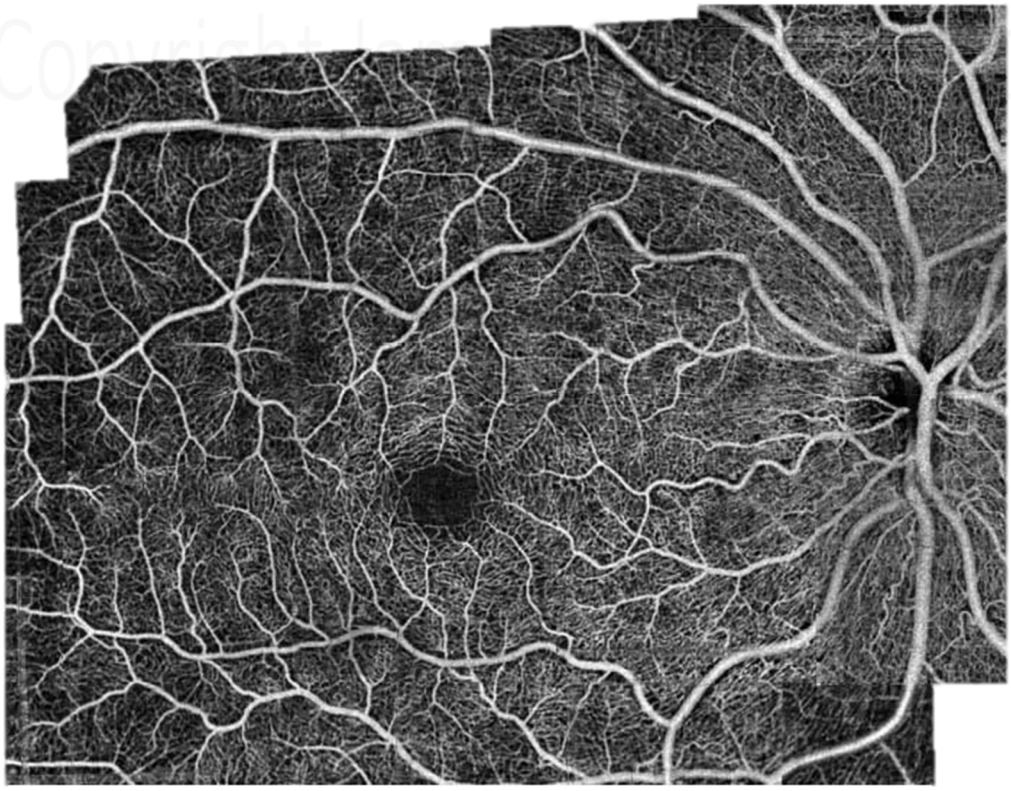

Figure 7.1: AngioMontage - overlaid single 3x3mm OCT-A images from the Heidelberg OCT-A device, to create a full optic nerve head and macular angiographic image

The standard OCT-A image provides no absolute flow or velocity information, only the presence of flow above a threshold low level. However, much work is being done to develop quantitative measures of flow from these images. Glaucoma is an area of particular relevance and interest for determining microvascular flow, in and around the optic nerve head, and work on this is progressing well.[328, 329] (Fig. 7.2)

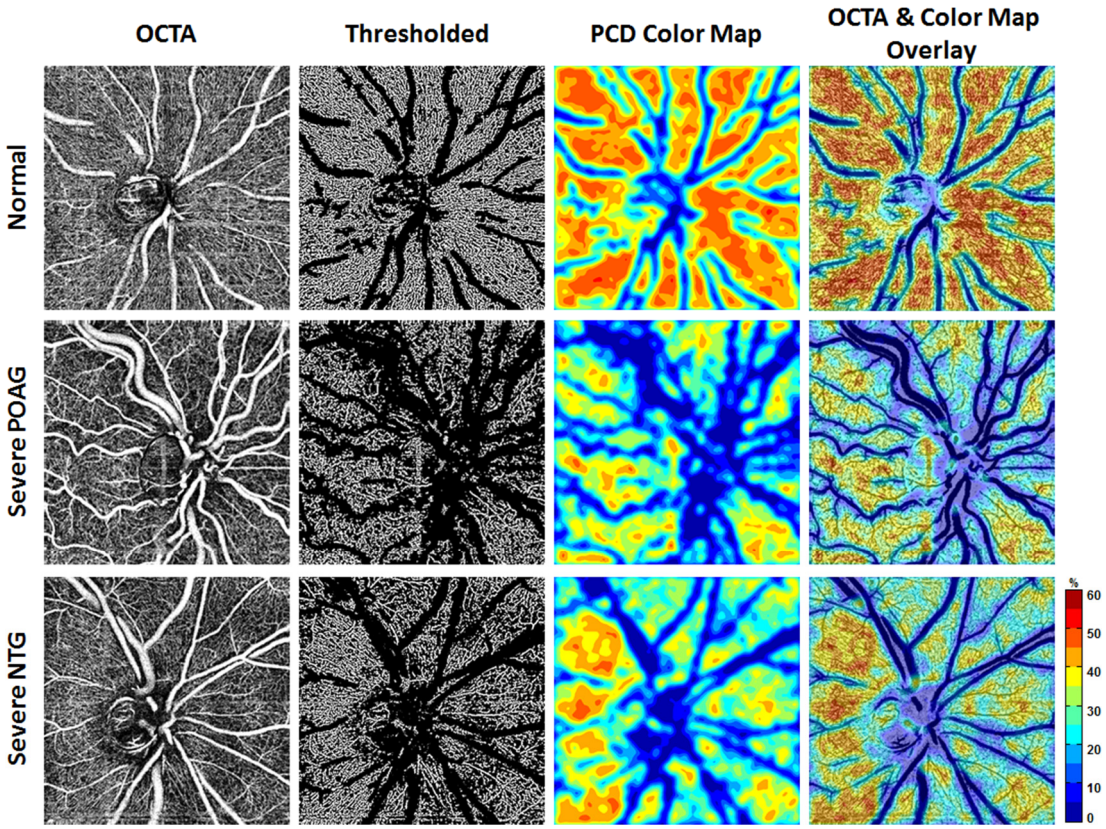

Figure 7.2: Comparisons of 4.5mm OCT-A images and color-coded perfused capillary density maps in a normal, a severe POAG, and a severe NTG patient. First column: grayscale OCT-A images generated using SSADA algorithm. Second column: thresholded binary images containing only the perfused capillaries after the removal of major blood vessels. Third column: corresponding colour-coded perfused capillary density maps. Last column: superimposed image of the colour maps and the inverted OCT-A images.

[Image from Scripsema et al. IOVS 2016 [329]]

Absolute measures of flow within the microvasculature remains a goal for OCT-A systems. Variable interscan time analysis (VISTA) is a step towards this, providing relative flow information. This is achieved by multiple imaging of the same location, but varying the cut-off threshold level for determining whether a vessel segment will

appear in the image (flow) or not appear (no or slow flow). By varying this threshold, and then applying a colour scale to the vessels per their presence at varied thresholds, a relative flow map is produced. (Fig. 7.3)

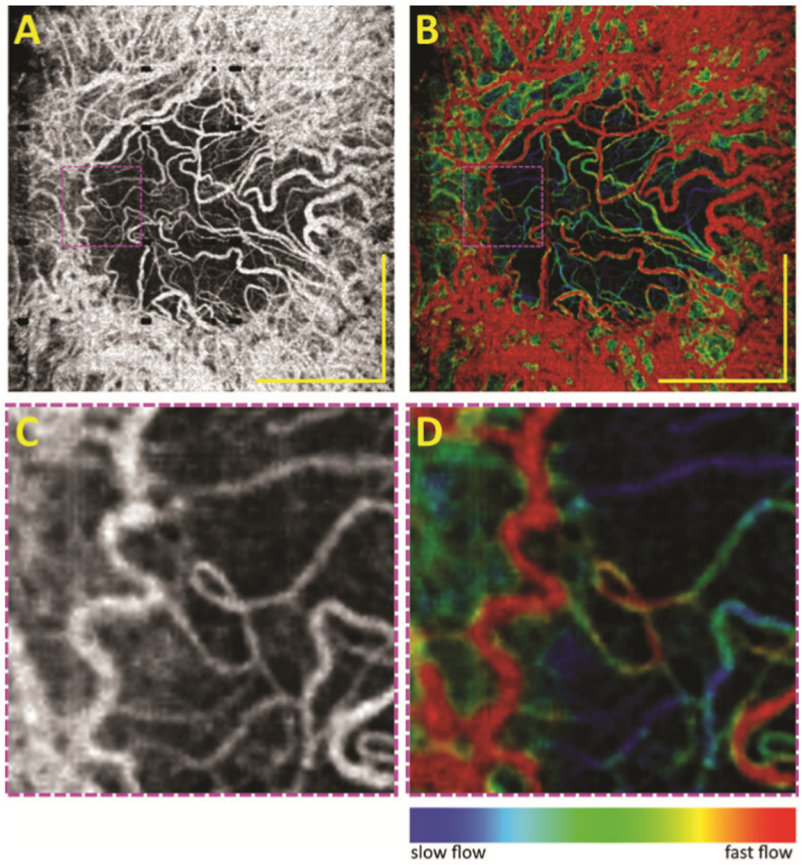

Figure 7.3: Variable interscan time analysis (VISTA) modification of OCT-A, to provide **relative** flow information on a colour scale; blue (slow) to red (fast)

The key strength of OCT-A imaging is the ability to visualise flow in the retinal microcirculation, without the need for an intravenous injection of fluorescent dye.

The limitation at present is that OCT-A is based on the motion of blood flow, but does not at this stage inform on the dynamic of that flow, nor any information regarding the vessel wall, its permeability, inflammatory changes or other manifestations of extra-luminal blood leakage.

OCT-A is therefore likely to be part of combination imaging over the next decade, rather than a single overarching imaging system.

OCT-Leakage

OCT-Leakage is a software innovation in OCT technology, that has recently been proposed as a potential new non-invasive method for identifying and mapping abnormal retinal oedema that is leaking from nearby vessels.[330] The chief limitation and complaint regarding OCT and OCT-A technologies has been the inability to identify leakage, in a way comparable with the fluorescein angiogram. However, this new development claims to have achieved this, and with even better sensitivity than fluorescein angiography.[331] It is too early to know if this technology matches up to the headlines, however it is the first to target this unmet need.

Future work

Widening the field

The SLO images I used in this research study - extracted from the SPECTRALIS OCT device - had a field of view of 35°. This is sufficient to view, and analyse, the first and second-order vessels, but we are only seeing a small part of the retinal vasculature.

This was sufficient to report wider venules in MS, perhaps associated with inflammation. However, we know clinically that visibly inflamed vessels are typically in the mid-to-far periphery, and therefore wide-angle vessel analysis may be more sensitive to changes, and more clinically useful.

Optos is a world leader in wide-field retinal imaging devices, such as the P200 Daytona. (Fig. 7.4) the wide-field retinal images are terrific (Fig. 7.5), and work has already been done on vessel morphological assessment in there SLO images.[280] Such a device is now located in the ARRNC where I performed my research study, and so could be used in future work to look at the peripheral blood vessels in patients with MS, and other neurodegenerative diseases.

Figure 7.4: Optos Daytona P200 wide-field SLO device

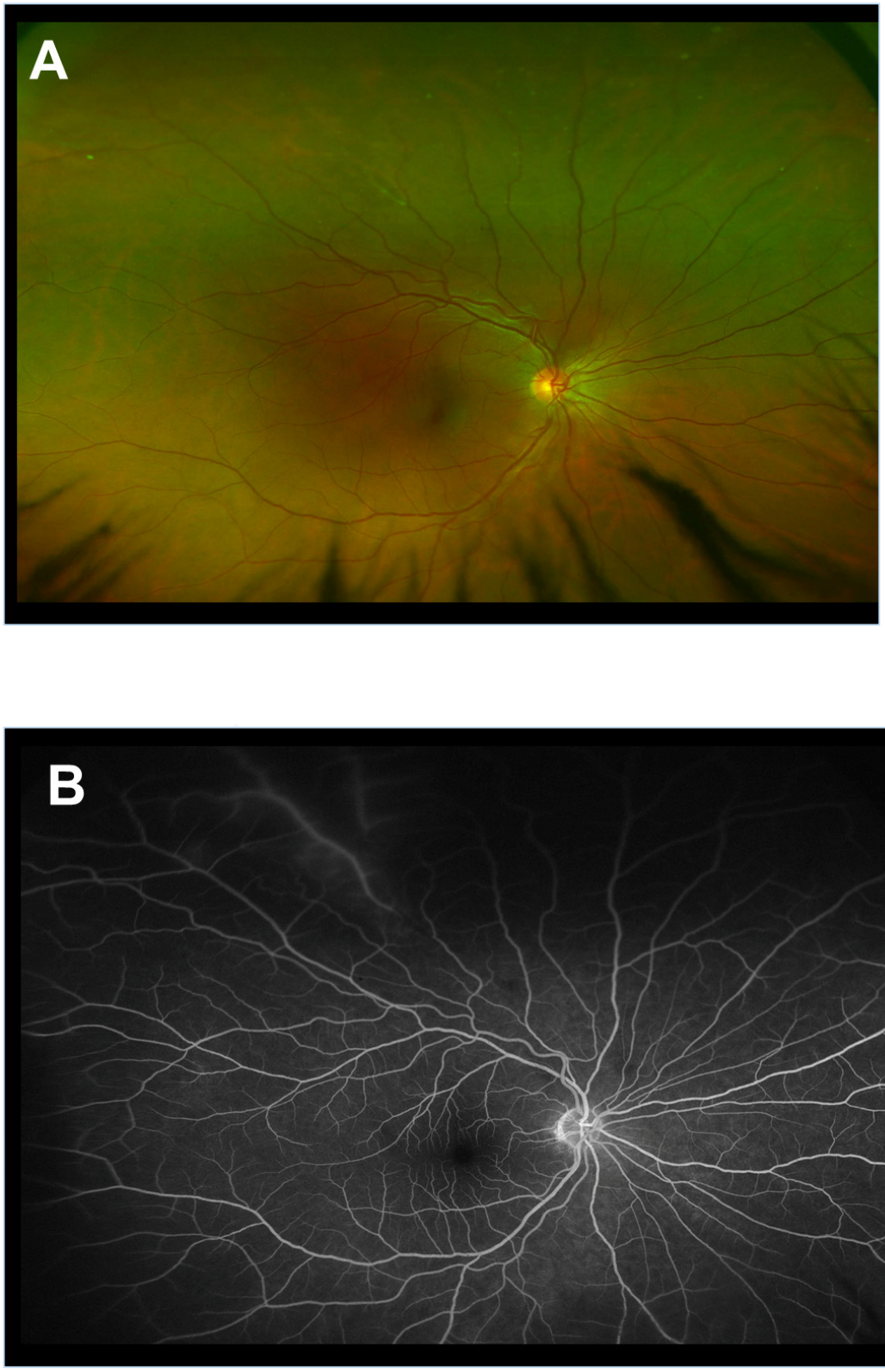

Figure 7.5: Sample images from Optos Daytona P200 wide-field SLO device

Big data

One of the biggest challenges during my research was manually collecting, and processing all the clinical and imaging data. With no master database or routine collection system, every phenotypic detail had to be retrieved individually. The benefits of an electronic system providing the infrastructure for a routine data collection culture within a research facility are immense. Providing not only routine clinical audit data for quality improvement activities in patient care, but a substantial resource for any clinical research projects that rely upon accurate and comprehensive phenotypic data. Modern data policies allow for anonymised data to be used in this way, provided consent is given at the point of entry.

In a world where 'big data" is becoming more of a cliché than actual use, it is time to embrace the benefits of systems that can collect and organise data in this way, and to operators who are trained in the handling and reporting of this complex data resource.

And indeed, for medical challenges such as neurodegenerative disease, where it is clear that complex multifactorial risks and genetics are at play, then it is only through large patient populations, deeply phenotyped and genotyped, that signals will emerge that point us towards clues, and ultimately treatment targets.

Imaging workload

In this research project, I recruited and imaged 961 participants (655 MS, 140 dementia, 20 ALS, and 166 total controls). Each imaging set required quality assurance, and image processing/correction as outlined in Chapter 3. In addition, the secondary processing of the SLO images with VAMPIRE software took around many hundreds of hours of work.

Whilst the tools I used were user-friendly, and I have extensive experience in using them, this makes the work different from those who use the imaging data from MRI etc where the process of capturing and transferring the images is performed by other staff.

There are benefits of being personally responsible for capturing the images: identifying patterns or trends in the images, that may result in testable hypotheses or new findings; real-time processing; and immediate clinical feedback to the patients/participants, which enhances their satisfaction with participating in research, as well as providing a clinic role, and being able to address any incidental findings as they occur.

Final thoughts

It is not certain which poet or philosopher first proclaimed the eye as a 'window to the soul', but many since have been fascinated and seduced by the extraordinary nature of our eyes and our visual sense. Over the centuries, metaphysical ideas on the nature of our ocular system have converged with scientific understanding of visual pathway anatomy and ocular physiology, to a point where we now have a detailed insight into how our eyes work, whilst maintaining a healthy respect for the preciousness of our sight, albeit with a less supernatural stance.

The eye as a 'window to the body' is a compelling concept. Studying the eye has benefited greatly from advances in technology, clinical medicine, and biomedical research, enabling new discoveries on the eye's role in systemic diseases such as hypertension and diabetes. Imaging of the eye fulfils many of the criteria to be an acceptable patient investigation and even a screening tool. This relies upon us identifying reliable biomarkers of pre-symptomatic disease at the same time as we uncover effective treatments or interventions.

The eye as an 'extension of the brain' provides us with an intriguing opportunity to complement the variety of tools we use in neuroscience to research the function and dysfunction of our brain, with the ability to directly visualise this forward projection of brain tissue, and examine its structure and function in extreme detail.

References

1. Chandran S. Can the damaged brain repair itself? : TED Talks : TED Global 2013; [cited 2017 2 Feb]. Available from: https://www.ted.com/talks/siddharthan_chandran_can_the_damaged_brain_repair_itself.

2. Solomon A, Bourdette D, Cross A, Applebee A, Skidd P, Howard D, et al. The spectrum of multiple sclerosis misdiagnosis in the era of McDonald criteria: A multicenter study (PL01.003). Neurology. 2016;86(16 Supplement).

3. Visser EM, Wilde K, Wilson JF, Yong KK, Counsell CE. A new prevalence study of multiple sclerosis in Orkney, Shetland and Aberdeen city. J Neurol Neurosurg Psychiatry. 2012;83(7):719-24.

4. Compston A, Coles A. Multiple sclerosis. Lancet. 2002;359(9313):1221-31.

5. Alzheimer Scotland. Number of people with dementia in Scotland 2017 [cited 2017 6 May]. Available from: http://www.alzscot.org/campaigning/statistics.

6. Wu YT, Fratiglioni L, Matthews FE, Lobo A, Breteler MM, Skoog I, et al. Dementia in western Europe: epidemiological evidence and implications for policy making. Lancet Neurol. 2016;15(1):116-24.

7. Langa KM, Larson EB, Crimmins EM, Faul JD, Levine DA, Kabeto MU, et al. A Comparison of the Prevalence of Dementia in the United States in 2000 and 2012. JAMA Intern Med. 2017;177(1):51-8.

8. Office for National Statistics. Deaths registered in England and Wales (Series DR): 2015;. 2016 14 November 2016.

9. National Records of Scotland. 2015 Births, Deaths and Other Vital Events - Preliminary Annual Figures;. 2016 9 March 2016.

10. Tomaskova H, Kuhnova J, Cimler R, Dolezal O, Kuca K. Prediction of population with Alzheimer's disease in the European Union using a system dynamics model. Neuropsychiatr Dis Treat. 2016;12:1589-98.

11. Marin B, Boumediene F, Logroscino G, Couratier P, Babron MC, Leutenegger AL, et al. Variation in worldwide incidence of amyotrophic lateral sclerosis: a meta-analysis. Int J Epidemiol. 2017;46(1):57-74.

12. Cronin S, Hardiman O, Traynor BJ. Ethnic variation in the incidence of ALS: a systematic review. Neurology. 2007;68(13):1002-7.

13. Forbes RB, Colville S, Parratt J, Swingler RJ. The incidence of motor nueron disease in Scotland. J Neurol. 2007;254(7):866-9.

14. Leighton D, Stephenson L, Colville S, Newton J, Davenport R, Gorrie G, et al., editors. Incidence of motor neurone disease in the Scottish population: a 25 year perspective. 27th International Symposium on ALS/MND; 2016; Dublin, Ireland: Taylor & Francis.

15. Katz Sand I. Classification, diagnosis, and differential diagnosis of multiple sclerosis. Curr Opin Neurol. 2015;28(3):193-205.

16. Lumley R, Davenport R, Williams A. Most Scottish neurologists do not apply the 2010 McDonald criteria when diagnosing multiple sclerosis. J R Coll Physicians Edinb. 2015;45(1):23-6.

17. Lublin FD, Reingold SC, Cohen JA, Cutter GR, Sorensen PS, Thompson AJ, et al. Defining the clinical course of multiple sclerosis: the 2013 revisions. Neurology. 2014;83(3):278-86.

18. Fox RJ, Cohen JA. Multiple sclerosis: the importance of early recognition and treatment. Cleve Clin J Med. 2001;68(2):157-71.

19. Brooks BR. El Escorial World Federation of Neurology criteria for the diagnosis of amyotrophic lateral sclerosis. Subcommittee on Motor Neuron Diseases/Amyotrophic Lateral Sclerosis of the World Federation of Neurology Research Group on Neuromuscular Diseases and the El Escorial "Clinical limits of amyotrophic lateral sclerosis" workshop contributors. J Neurol Sci. 1994;124 Suppl:96-107.

20. Wilbourn AJ. Clinical neurophysiology in the diagnosis of amyotrophic lateral sclerosis: the Lambert and the El Escorial criteria. J Neurol Sci. 1998;160 Suppl 1:S25-9.

21. Biomarkers Definitions Working Group. Biomarkers and surrogate endpoints: preferred definitions and conceptual framework. Clin Pharmacol Ther. 2001;69(3):89-95.

22. Strimbu K, Tavel JA. What are biomarkers? Curr Opin HIV AIDS. 2010;5(6):463-6.

23. Pletcher MJ, Pignone M. Evaluating the clinical utility of a biomarker: a review of methods for estimating health impact. Circulation. 2011;123(10):1116-24.

24. Agrawal M, Biswas A. Molecular diagnostics of neurodegenerative disorders. Front Mol Biosci. 2015;2:54.

25. Bergamaschi R. Prognostic factors in multiple sclerosis. Int Rev Neurobiol. 2007;79:423-47.

26. Kraft GH, Freal JE, Coryell JK, Hanan CL, Chitnis N. Multiple sclerosis: early prognostic guidelines. Arch Phys Med Rehabil. 1981;62(2):54-8.

27. Miller D, Barkhof F, Montalban X, Thompson A, Filippi M. Clinically isolated syndromes suggestive of multiple sclerosis, part I: natural history, pathogenesis, diagnosis, and prognosis. Lancet Neurol. 2005;4(5):281-8.

28. Tintore M, Rovira A, Rio J, Otero-Romero S, Arrambide G, Tur C, et al. Defining high, medium and low impact prognostic factors for developing multiple sclerosis. Brain. 2015;138(Pt 7):1863-74.

29. American Psychiatric Association. Diagnostic and Statistical Manual of Mental Disorders. 5 ed. Washington, DC2013.

30. Kawas CH. Clinical practice. Early Alzheimer's disease. N Engl J Med. 2003;349(11):1056-63.

31. Elamin M, Holloway G, Bak TH, Pal S. The Utility of the Addenbrooke's Cognitive Examination Version Three in Early-Onset Dementia. Dement Geriatr Cogn Disord. 2016;41(1-2):9-15.

32. Herrmann N, Harimoto T, Balshaw R, Lanctot KL, Canadian Outcomes Study in Dementia I. Risk Factors for Progression of Alzheimer Disease in a Canadian

Population: The Canadian Outcomes Study in Dementia (COSID). Can J Psychiatry. 2015;60(4):189-99.

33. Tokuchi R, Hishikawa N, Kurata T, Sato K, Kono S, Yamashita T, et al. Clinical and demographic predictors of mild cognitive impairment for converting to Alzheimer's disease and reverting to normal cognition. J Neurol Sci. 2014;346(1-2):288-92.

34. Lee SJ, Ritchie CS, Yaffe K, Stijacic Cenzer I, Barnes DE. A clinical index to predict progression from mild cognitive impairment to dementia due to Alzheimer's disease. PLoS One. 2014;9(12):e113535.

35. Gordon PH, Cheng B, Salachas F, Pradat PF, Bruneteau G, Corcia P, et al. Progression in ALS is not linear but is curvilinear. J Neurol. 2010;257(10):1713-7.

36. Ong ML, Tan PF, Holbrook JD. Predicting functional decline and survival in amyotrophic lateral sclerosis. PLoS One. 2017;12(4):e0174925.

37. Cedarbaum JM, Stambler N, Malta E, Fuller C, Hilt D, Thurmond B, et al. The ALSFRS-R: a revised ALS functional rating scale that incorporates assessments of respiratory function. BDNF ALS Study Group (Phase III). J Neurol Sci. 1999;169(1-2):13-21.

38. Rooney J, Burke T, Vajda A, Heverin M, Hardiman O. What does the ALSFRS-R really measure? A longitudinal and survival analysis of functional dimension subscores in amyotrophic lateral sclerosis. J Neurol Neurosurg Psychiatry. 2017;88(5):381-5.

39. De Stefano N, Giorgio A, Battaglini M, Rovaris M, Sormani MP, Barkhof F, et al. Assessing brain atrophy rates in a large population of untreated multiple sclerosis subtypes. Neurology. 2010;74(23):1868-76.

40. Fisher E, Rudick RA, Simon JH, Cutter G, Baier M, Lee JC, et al. Eight-year follow-up study of brain atrophy in patients with MS. Neurology. 2002;59(9):1412-20.

41. Shiee N, Bazin PL, Zackowski KM, Farrell SK, Harrison DM, Newsome SD, et al. Revisiting brain atrophy and its relationship to disability in multiple sclerosis. PLoS One. 2012;7(5):e37049.

42. Mollison D, Sellar R, Bastin M, Mollison D, Chandran S, Wardlaw J, et al. The clinico-radiological paradox of cognitive function and MRI burden of white matter lesions in people with multiple sclerosis: A systematic review and meta-analysis. PLoS One. 2017;12(5):e0177727.

43. Barkhof F. The clinico-radiological paradox in multiple sclerosis revisited. Curr Opin Neurol. 2002;15(3):239-45.

44. Wingerchuk DM, Weinshenker BG. Disease modifying therapies for relapsing multiple sclerosis. BMJ. 2016;354:i3518.

45. Ontaneda D, Fox RJ, Chataway J. Clinical trials in progressive multiple sclerosis: lessons learned and future perspectives. Lancet Neurol. 2015;14(2):208-23.

46. Scholl M, Lockhart SN, Schonhaut DR, O'Neil JP, Janabi M, Ossenkoppele R, et al. PET Imaging of Tau Deposition in the Aging Human Brain. Neuron. 2016;89(5):971-82.

47. Yeo JM, Waddell B, Khan Z, Pal S. A systematic review and meta-analysis of (18)F-labeled amyloid imaging in Alzheimer's disease. Alzheimers Dement (Amst). 2015;1(1):5-13.

48. Yeo JM, Lim X, Khan Z, Pal S. Systematic review of the diagnostic utility of SPECT imaging in dementia. Eur Arch Psychiatry Clin Neurosci. 2013;263(7):539-52.

49. Lopez ME, Turrero A, Cuesta P, Lopez-Sanz D, Bruna R, Marcos A, et al. Searching for Primary Predictors of Conversion from Mild Cognitive Impairment to Alzheimer's Disease: A Multivariate Follow-Up Study. J Alzheimers Dis. 2016;52(1):133-43.

50. Buratti L, Balestrini S, Altamura C, Viticchi G, Falsetti L, Luzzi S, et al. Markers for the risk of progression from mild cognitive impairment to Alzheimer's disease. J Alzheimers Dis. 2015;45(3):883-90.

51. Curiati PK, Magaldi RM, Suemoto CK, Bottino CM, Nitrini R, Farfel JM, et al. Vascular risk as a predictor of cognitive decline in a cohort of elderly patients with mild to moderate dementia. Dement Geriatr Cogn Dis Extra. 2014;4(3):402-9.

52. Schuster C, Hardiman O, Bede P. Survival prediction in Amyotrophic lateral sclerosis based on MRI measures and clinical characteristics. BMC Neurol. 2017;17(1):73.

53. McGuire LI, Poleggi A, Poggiolini I, Suardi S, Grznarova K, Shi S, et al. Cerebrospinal fluid real-time quaking-induced conversion is a robust and reliable test for sporadic creutzfeldt-jakob disease: An international study. Ann Neurol. 2016;80(1):160-5.

54. Quintana E, Ortega FJ, Robles-Cedeno R, Villar ML, Buxo M, Mercader JM, et al. miRNAs in cerebrospinal fluid identify patients with MS and specifically those with lipid-specific oligoclonal IgM bands. Mult Scler. 2017;23(13):1716-26.

55. Gastaldi M, Zardini E, Franciotta D. An update on the use of cerebrospinal fluid analysis as a diagnostic tool in multiple sclerosis. Expert Rev Mol Diagn. 2017;17(1):31-46.

56. Llorens F, Schmitz M, Ferrer I, Zerr I. CSF biomarkers in neurodegenerative and vascular dementias. Prog Neurobiol. 2016;138-140:36-53.

57. Tapiola T, Alafuzoff I, Herukka SK, Parkkinen L, Hartikainen P, Soininen H, et al. Cerebrospinal fluid {beta}-amyloid 42 and tau proteins as biomarkers of Alzheimer-type pathologic changes in the brain. Arch Neurol. 2009;66(3):382-9.

58. Rivero-Santana A, Ferreira D, Perestelo-Perez L, Westman E, Wahlund LO, Sarria A, et al. Cerebrospinal Fluid Biomarkers for the Differential Diagnosis between Alzheimer's Disease and Frontotemporal Lobar Degeneration: Systematic Review, HSROC Analysis, and Confounding Factors. J Alzheimers Dis. 2017;55(2):625-44.

59. Lim X, Yeo JM, Green A, Pal S. The diagnostic utility of cerebrospinal fluid alpha-synuclein analysis in dementia with Lewy bodies - a systematic review and meta-analysis. Parkinsonism Relat Disord. 2013;19(10):851-8.

60. Lu CH, Macdonald-Wallis C, Gray E, Pearce N, Petzold A, Norgren N, et al. Neurofilament light chain: A prognostic biomarker in amyotrophic lateral sclerosis. Neurology. 2015;84(22):2247-57.

61. Steinacker P, Feneberg E, Weishaupt J, Brettschneider J, Tumani H, Andersen PM, et al. Neurofilaments in the diagnosis of motoneuron diseases: a prospective study on 455 patients. J Neurol Neurosurg Psychiatry. 2016;87(1):12-20.

62. Li D, Shen D, Tai H, Cui L. Neurofilaments in CSF As Diagnostic Biomarkers in Motor Neuron Disease: A Meta-Analysis. Front Aging Neurosci. 2016;8:290.

63. Eftekharian MM, Noroozi R, Sayad A, Sarrafzadeh S, Toghi M, Azimi T, et al. RAR-related orphan receptor A (RORA): A new susceptibility gene for multiple sclerosis. J Neurol Sci. 2016;369:259-62.

64. Ruiz-Gaviria R, Baracaldo I, Castaneda C, Ruiz-Patino A, Acosta-Hernandez A, Rosselli D. Specificity and sensitivity of aquaporin 4 antibody detection tests in patients with neuromyelitis optica: A meta-analysis. Mult Scler Relat Disord. 2015;4(4):345-9.

65. Pereira W, Reiche EMV, Kallaur AP, Oliveira SR, Simao ANC, Lozovoy MAB, et al. Frequency of autoimmune disorders and autoantibodies in patients with neuromyelitis optica. Acta Neuropsychiatr. 2017;29(3):170-8.

66. Mahley RW, Weisgraber KH, Huang Y. Apolipoprotein E4: a causative factor and therapeutic target in neuropathology, including Alzheimer's disease. Proc Natl Acad Sci U S A. 2006;103(15):5644-51.

67. Corder EH, Saunders AM, Strittmatter WJ, Schmechel DE, Gaskell PC, Small GW, et al. Gene dose of apolipoprotein E type 4 allele and the risk of Alzheimer's disease in late onset families. Science. 1993;261(5123):921-3.

68. Tang MX, Maestre G, Tsai WY, Liu XH, Feng L, Chung WY, et al. Relative risk of Alzheimer disease and age-at-onset distributions, based on APOE genotypes among elderly African Americans, Caucasians, and Hispanics in New York City. Am J Hum Genet. 1996;58(3):574-84.

69. Mattsson N, Zetterberg H, Janelidze S, Insel PS, Andreasson U, Stomrud E, et al. Plasma tau in Alzheimer disease. Neurology. 2016;87(17):1827-35.

70. Ritchie CW, Ritchie K. The PREVENT study: a prospective cohort study to identify mid-life biomarkers of late-onset Alzheimer's disease. BMJ Open. 2012;2(6).

71. van Rheenen W, Shatunov A, Dekker AM, McLaughlin RL, Diekstra FP, Pulit SL, et al. Genome-wide association analyses identify new risk variants and the genetic architecture of amyotrophic lateral sclerosis. Nat Genet. 2016;48(9):1043-8.

72. Zufiria M, Gil-Bea FJ, Fernandez-Torron R, Poza JJ, Munoz-Blanco JL, Rojas-Garcia R, et al. ALS: A bucket of genes, environment, metabolism and unknown ingredients. Prog Neurobiol. 2016;142:104-29.

73. Renton AE, Chio A, Traynor BJ. State of play in amyotrophic lateral sclerosis genetics. Nat Neurosci. 2014;17(1):17-23.

74. Morello G, Spampinato AG, Cavallaro S. Molecular Taxonomy of Sporadic Amyotrophic Lateral Sclerosis Using Disease-Associated Genes. Front Neurol. 2017;8:152.

75. Ehrhart J, Smith AJ, Kuzmin-Nichols N, Zesiewicz TA, Jahan I, Shytle RD, et al. Humoral factors in ALS patients during disease progression. J Neuroinflammation. 2015;12:127.

76. Burns SB, Archive B. Ophthalmology: A Photographic History 1845-1945 : Selections from the Burns Archive. Disease & pathology: Burns Archive Press; 2009.

77. Bedell AJ. Photographs of the Fundus Oculi: A Photographic Study of Normal and Pathological Changes Seen with the Ophthalmoscope: FA Davis Company; 1929.

78. Trigt ACv. Dissertatio ophthalmologica inauguralis de speculo oculi: PW van de Weijer; 1853.

79. Huang D, Swanson EA, Lin CP, Schuman JS, Stinson WG, Chang W, et al. Optical coherence tomography. Science. 1991;254(5035):1178-81.

80. Lim SH. Clinical applications of anterior segment optical coherence tomography. J Ophthalmol. 2015;2015:605729.

81. Wang D, Lin S. New developments in anterior segment optical coherence tomography for glaucoma. Curr Opin Ophthalmol. 2016;27(2):111-7.

82. Hu CX, Mantravadi A, Zangalli C, Ali M, Faria BM, Richman J, et al. Comparing Gonioscopy With Visante and Cirrus Optical Coherence Tomography for Anterior Chamber Angle Assessment in Glaucoma Patients. J Glaucoma. 2016;25(2):177-83.

83. Werkmeister RM, Alex A, Kaya S, Unterhuber A, Hofer B, Riedl J, et al. Measurement of tear film thickness using ultrahigh-resolution optical coherence tomography. Invest Ophthalmol Vis Sci. 2013;54(8):5578-83.

84. Staurenghi G, Sadda S, Chakravarthy U, Spaide RF, International Nomenclature for Optical Coherence Tomography Panel. Proposed lexicon for anatomic landmarks in normal posterior segment spectral-domain optical coherence tomography: the IN•OCT consensus. Ophthalmology. 2014;121(8):1572-8.

85. Erskine L, Herrera E. Connecting the retina to the brain. ASN Neuro. 2014;6(6).

86. Amini N, Nowroozizadeh S, Cirineo N, Henry S, Chang T, Chou T, et al. Influence of the disc-fovea angle on limits of RNFL variability and glaucoma discrimination. Invest Ophthalmol Vis Sci. 2014;55(11):7332-42.

87. Chauhan BC, Sharpe GP, Hutchison DM. Imaging of the temporal raphe with optical coherence tomography. Ophthalmology. 2014;121(11):2287-8.

88. Curcio CA, Allen KA. Topography of ganglion cells in human retina. J Comp Neurol. 1990;300(1):5-25.

89. Huang D, Chopra V, Lu AT, Tan O, Francis B, Varma R, et al. Does optic nerve head size variation affect circumpapillary retinal nerve fiber layer thickness measurement by optical coherence tomography? Invest Ophthalmol Vis Sci. 2012;53(8):4990-7.

90. Lee JW, Morales E, Sharifipour F, Amini N, Yu F, Afifi AA, et al. The relationship between central visual field sensitivity and macular ganglion cell/inner plexiform layer thickness in glaucoma. Br J Ophthalmol. 2017;101(8):1052-8.

91. Nickla DL, Wallman J. The multifunctional choroid. Prog Retin Eye Res. 2010;29(2):144-68.

92. Vuong VS, Moisseiev E, Cunefare D, Farsiu S, Moshiri A, Yiu G. Repeatability of Choroidal Thickness Measurements on Enhanced Depth Imaging Optical Coherence Tomography Using Different Posterior Boundaries. Am J Ophthalmol. 2016;169:104-12.

93. Yiu G, Pecen P, Sarin N, Chiu SJ, Farsiu S, Mruthyunjaya P, et al. Characterization of the choroid-scleral junction and suprachoroidal layer in healthy individuals on enhanced-depth imaging optical coherence tomography. JAMA Ophthalmol. 2014;132(2):174-81.

94. Liew G, Wang JJ, Mitchell P, Wong TY. Retinal vascular imaging: a new tool in microvascular disease research. Circ Cardiovasc Imaging. 2008;1(2):156-61.

95. Garway-Heath DF, Rudnicka AR, Lowe T, Foster PJ, Fitzke FW, Hitchings RA. Measurement of optic disc size: equivalence of methods to correct for ocular magnification. Br J Ophthalmol. 1998;82(6):643-9.

96. Relan D, MacGillivray T, Ballerini L, Trucco E. Retinal vessel classification: sorting arteries and veins. Conf Proc IEEE Eng Med Biol Soc. 2013;2013:7396-9.

97. Cameron JR, Ballerini L, Langan C, Warren C, Denholm N, Smart K, et al. Modulation of retinal image vasculature analysis to extend utility and provide secondary value from optical coherence tomography imaging. J Med Imaging (Bellingham). 2016;3(2):020501.

98. Knudtson MD, Lee KE, Hubbard LD, Wong TY, Klein R, Klein BE. Revised formulas for summarizing retinal vessel diameters. Curr Eye Res. 2003;27(3):143-9.

99. Cederbaum LS, Haller E, Pfeifer P. Fractal dimension function for energy levels. Phys Rev A Gen Phys. 1985;31(3):1869-71.

100. Mandelbrot BB. Stochastic models for the Earth's relief, the shape and the fractal dimension of the coastlines, and the number-area rule for islands. Proc Natl Acad Sci U S A. 1975;72(10):3825-8.

101. Macgillivray TJ, Patton N, Doubal FN, Graham C, Wardlaw JM. Fractal analysis of the retinal vascular network in fundus images. Conf Proc IEEE Eng Med Biol Soc. 2007;2007:6456-9.

102. Stosic T, Stosic BD. Multifractal analysis of human retinal vessels. IEEE Trans Med Imaging. 2006;25(8):1101-7.

103. Taylor AM, MacGillivray TJ, Henderson RD, Ilzina L, Dhillon B, Starr JM, et al. Retinal vascular fractal dimension, childhood IQ, and cognitive ability in old age: the Lothian Birth Cohort Study 1936. PLoS One. 2015;10(3):e0121119.

104. Murray CD. The Physiological Principle of Minimum Work: I. The Vascular System and the Cost of Blood Volume. Proc Natl Acad Sci U S A. 1926;12(3):207-14.

105. Li H, Mitchell P, Liew G, Rochtchina E, Kifley A, Wong TY, et al. Lens opacity and refractive influences on the measurement of retinal vascular fractal dimension. Acta Ophthalmol. 2010;88(6):e234-40.

106. Cheung CY, Ong S, Ikram MK, Ong YT, Chen CP, Venketasubramanian N, et al. Retinal vascular fractal dimension is associated with cognitive dysfunction. J Stroke Cerebrovasc Dis. 2014;23(1):43-50.

107. Doubal FN, MacGillivray TJ, Patton N, Dhillon B, Dennis MS, Wardlaw JM. Fractal analysis of retinal vessels suggests that a distinct vasculopathy causes lacunar stroke. Neurology. 2010;74(14):1102-7.

108. Cheung CY, Thomas GN, Tay W, Ikram MK, Hsu W, Lee ML, et al. Retinal vascular fractal dimension and its relationship with cardiovascular and ocular risk factors. Am J Ophthalmol. 2012;154(4):663-74 e1.

109. Wong TY, Knudtson MD, Klein R, Klein BE, Meuer SM, Hubbard LD. Computer-assisted measurement of retinal vessel diameters in the Beaver Dam Eye Study: methodology, correlation between eyes, and effect of refractive errors. Ophthalmology. 2004;111(6):1183-90.

110. Lim LS, Cheung CY, Lin X, Mitchell P, Wong TY, Mei-Saw S. Influence of refractive error and axial length on retinal vessel geometric characteristics. Invest Ophthalmol Vis Sci. 2011;52(2):669-78.

111. Patton N, Maini R, MacGillivary T, Aslam TM, Deary IJ, Dhillon B. Effect of axial length on retinal vascular network geometry. Am J Ophthalmol. 2005;140(4):648-53.

112. Perez-Rovira A, MacGillivray T, Trucco E, Chin KS, Zutis K, Lupascu C, et al. VAMPIRE: Vessel assessment and measurement platform for images of the REtina. Conf Proc IEEE Eng Med Biol Soc. 2011;2011:3391-4.

113. Cheung CY, Tay WT, Mitchell P, Wang JJ, Hsu W, Lee ML, et al. Quantitative and qualitative retinal microvascular characteristics and blood pressure. J Hypertens. 2011;29(7):1380-91.

114. Cheung CY, Tay WT, Ikram MK, Ong YT, De Silva DA, Chow KY, et al. Retinal microvascular changes and risk of stroke: the Singapore Malay Eye Study. Stroke. 2013;44(9):2402-8.

115. Bankhead P, Scholfield CN, McGeown JG, Curtis TM. Fast retinal vessel detection and measurement using wavelets and edge location refinement. PLoS One. 2012;7(3):e32435.

116. Klein R, Myers CE, Knudtson MD, Lee KE, Gangnon R, Wong TY, et al. Relationship of blood pressure and other factors to serial retinal arteriolar diameter measurements over time: the beaver dam eye study. Arch Ophthalmol. 2012;130(8):1019-27.

117. de Jong FJ, Schrijvers EM, Ikram MK, Koudstaal PJ, de Jong PT, Hofman A, et al. Retinal vascular caliber and risk of dementia: the Rotterdam study. Neurology. 2011;76(9):816-21.

118. MacGillivray TJ, Trucco E, Cameron JR, Dhillon B, Houston JG, van Beek EJ. Retinal imaging as a source of biomarkers for diagnosis, characterization and prognosis of chronic illness or long-term conditions. Br J Radiol. 2014;87(1040):20130832.

119. Facey K, Cummins E, Macpherson K, Morris A, Reay L, Slattery J. Health technology assessment report 1: Organisations of services for diabetic retinopathy screening. Glasgow: Health Technology Board for Scotland. 2002.

120. Scotland GS, McNamee P, Philip S, Fleming AD, Goatman KA, Prescott GJ, et al. Cost-effectiveness of implementing automated grading within the national screening programme for diabetic retinopathy in Scotland. Br J Ophthalmol. 2007;91(11):1518-23.

121. Goh JK, Cheung CY, Sim SS, Tan PC, Tan GS, Wong TY. Retinal Imaging Techniques for Diabetic Retinopathy Screening. J Diabetes Sci Technol. 2016;10(2):282-94.

122. Patton N, Aslam T, Macgillivray T, Pattie A, Deary IJ, Dhillon B. Retinal vascular image analysis as a potential screening tool for cerebrovascular disease: a rationale based on homology between cerebral and retinal microvasculatures. J Anat. 2005;206(4):319-48.

123. Doubal FN, Hokke PE, Wardlaw JM. Retinal microvascular abnormalities and stroke: a systematic review. J Neurol Neurosurg Psychiatry. 2009;80(2):158-65.

124. Doubal FN, MacGillivray TJ, Hokke PE, Dhillon B, Dennis MS, Wardlaw JM. Differences in retinal vessels support a distinct vasculopathy causing lacunar stroke. Neurology. 2009;72(20):1773-8.

125. Balmforth C, van Bragt JJ, Ruijs T, Cameron JR, Kimmitt R, Moorhouse R, et al. Chorioretinal thinning in chronic kidney disease links to inflammation and endothelial dysfunction. JCI Insight. 2016;1(20):e89173.

126. Klein R, Klein BE, Moss SE, Cruickshanks KJ. The Wisconsin Epidemiologic Study of Diabetic Retinopathy: XVII. The 14-year incidence and progression of diabetic retinopathy and associated risk factors in type 1 diabetes. Ophthalmology. 1998;105(10):1801-15.

127. Wong TY, Klein R, Sharrett AR, Duncan BB, Couper DJ, Tielsch JM, et al. Retinal arteriolar narrowing and risk of coronary heart disease in men and women. The Atherosclerosis Risk in Communities Study. JAMA. 2002;287(9):1153-9.

128. Liew G, Wang JJ. [Retinal vascular signs: a window to the heart?]. Rev Esp Cardiol. 2011;64(6):515-21.

129. Wang JJ, Liew G, Klein R, Rochtchina E, Knudtson MD, Klein BE, et al. Retinal vessel diameter and cardiovascular mortality: pooled data analysis from two older populations. Eur Heart J. 2007;28(16):1984-92.

130. Wang JJ, Mitchell P, Leung H, Rochtchina E, Wong TY, Klein R. Hypertensive retinal vessel wall signs in a general older population: the Blue Mountains Eye Study. Hypertension. 2003;42(4):534-41.

131. Ikram MK, Witteman JC, Vingerling JR, Breteler MM, Hofman A, de Jong PT. Retinal vessel diameters and risk of hypertension: the Rotterdam Study. Hypertension. 2006;47(2):189-94.

132. Ikram MK, de Jong FJ, Bos MJ, Vingerling JR, Hofman A, Koudstaal PJ, et al. Retinal vessel diameters and risk of stroke: the Rotterdam Study. Neurology. 2006;66(9):1339-43.

133. Wong TY, Islam FM, Klein R, Klein BE, Cotch MF, Castro C, et al. Retinal vascular caliber, cardiovascular risk factors, and inflammation: the multi-ethnic study of atherosclerosis (MESA). Invest Ophthalmol Vis Sci. 2006;47(6):2341-50.

134. Kawasaki R, Xie J, Cheung N, Lamoureux E, Klein R, Klein BE, et al. Retinal microvascular signs and risk of stroke: the Multi-Ethnic Study of Atherosclerosis (MESA). Stroke. 2012;43(12):3245-51.

135. Patel PJ, Foster PJ, Grossi CM, Keane PA, Ko F, Lotery A, et al. Spectral-Domain Optical Coherence Tomography Imaging in 67 321 Adults: Associations with Macular Thickness in the UK Biobank Study. Ophthalmology. 2016;123(4):829-40.

136. Ko F, Foster PJ, Strouthidis NG, Shweikh Y, Yang Q, Reisman CA, et al. Associations with Retinal Pigment Epithelium Thickness Measures in a Large Cohort: Results from the UK Biobank. Ophthalmology. 2017;124(1):105-17.

137. Cameron JR, Tatham AJ. A window to beyond the orbit: the value of optical coherence tomography in non-ocular disease. Acta Ophthalmol. 2016;94(6):533-9.

138. Krebs W, Krebs I. Primate retina and choroid: atlas of fine structure in man and monkey: Springer Science & Business Media; 2012.

139. Remington LA. Clinical Anatomy of the Visual System E-Book: Elsevier Health Sciences; 2011.

140. Isenmann S, Kretz A, Cellerino A. Molecular determinants of retinal ganglion cell development, survival, and regeneration. Prog Retin Eye Res. 2003;22(4):483-543.

141. Oster SF, Sretavan DW. Connecting the eye to the brain: the molecular basis of ganglion cell axon guidance. Br J Ophthalmol. 2003;87(5):639-45.

142. Provis JM. Development of the primate retinal vasculature. Prog Retin Eye Res. 2001;20(6):799-821.

143. Wichmann W, Muller-Forell W. Anatomy of the visual system. Eur J Radiol. 2004;49(1):8-30.

144. MacCormick IJ, Beare NA, Taylor TE, Barrera V, White VA, Hiscott P, et al. Cerebral malaria in children: using the retina to study the brain. Brain. 2014;137(Pt 8):2119-42.

145. Wong-Riley MT. Energy metabolism of the visual system. Eye Brain. 2010;2:99-116.

146. Klaassen I, Van Noorden CJ, Schlingemann RO. Molecular basis of the inner blood-retinal barrier and its breakdown in diabetic macular edema and other pathological conditions. Prog Retin Eye Res. 2013;34:19-48.

147. Campbell M, Humphries P. The blood-retina barrier: tight junctions and barrier modulation. Adv Exp Med Biol. 2012;763:70-84.

148. Rucker CW. Sheathing of the retinal veins in multiple sclerosis. Review of pertinent literature. Mayo Clin Proc. 1972;47(5):335-40.

149. Birch MK, Barbosa S, Blumhardt LD, O'Brien C, Harding SP. Retinal venous sheathing and the blood-retinal barrier in multiple sclerosis. Arch Ophthalmol. 1996;114(1):34-9.

150. Engell T, Andersen PK. The frequency of periphlebitis retinae in multiple sclerosis. Acta Neurol Scand. 1982;65(6):601-8.

151. Arnold AC, Pepose JS, Hepler RS, Foos RY. Retinal periphlebitis and retinitis in multiple sclerosis. I. Pathologic characteristics. Ophthalmology. 1984;91(3):255-62.

152. Prineas JW, Wright RG. Macrophages, lymphocytes, and plasma cells in the perivascular compartment in chronic multiple sclerosis. Lab Invest. 1978;38(4):409-21.

153. Morse PH. Retinal venous sheathing and neovascularization in disseminated sclerosis. Ann Ophthalmol. 1975;7(7):949-52.

154. Vine AK. Severe periphlebitis, peripheral retinal ischemia, and preretinal neovascularization in patients with multiple sclerosis. Am J Ophthalmol. 1992;113(1):28-32.

155. Carmeliet P. Blood vessels and nerves: common signals, pathways and diseases. Nat Rev Genet. 2003;4(9):710-20.

156. Mukouyama YS, Shin D, Britsch S, Taniguchi M, Anderson DJ. Sensory nerves determine the pattern of arterial differentiation and blood vessel branching in the skin. Cell. 2002;109(6):693-705.

157. Mwanza JC, Durbin MK, Budenz DL, Sayyad FE, Chang RT, Neelakantan A, et al. Glaucoma diagnostic accuracy of ganglion cell-inner plexiform layer thickness: comparison with nerve fiber layer and optic nerve head. Ophthalmology. 2012;119(6):1151-8.

158. Fisher JB, Jacobs DA, Markowitz CE, Galetta SL, Volpe NJ, Nano-Schiavi ML, et al. Relation of visual function to retinal nerve fiber layer thickness in multiple sclerosis. Ophthalmology. 2006;113(2):324-32.

159. Pulicken M, Gordon-Lipkin E, Balcer LJ, Frohman E, Cutter G, Calabresi PA. Optical coherence tomography and disease subtype in multiple sclerosis. Neurology. 2007;69(22):2085-92.

160. Henderson AP, Trip SA, Schlottmann PG, Altmann DR, Garway-Heath DF, Plant GT, et al. An investigation of the retinal nerve fibre layer in progressive multiple sclerosis using optical coherence tomography. Brain. 2008;131(Pt 1):277-87.

161. Cettomai D, Pulicken M, Gordon-Lipkin E, Salter A, Frohman TC, Conger A, et al. Reproducibility of optical coherence tomography in multiple sclerosis. Arch Neurol. 2008;65(9):1218-22.

162. Petzold A, de Boer JF, Schippling S, Vermersch P, Kardon R, Green A, et al. Optical coherence tomography in multiple sclerosis: a systematic review and meta-analysis. Lancet Neurol. 2010;9(9):921-32.

163. Syc SB, Warner CV, Hiremath GS, Farrell SK, Ratchford JN, Conger A, et al. Reproducibility of high-resolution optical coherence tomography in multiple sclerosis. Mult Scler. 2010;16(7):829-39.

164. Khanifar AA, Parlitsis GJ, Ehrlich JR, Aaker GD, D'Amico DJ, Gauthier SA, et al. Retinal nerve fiber layer evaluation in multiple sclerosis with spectral domain optical coherence tomography. Clin Ophthalmol. 2010;4:1007-13.

165. Oberwahrenbrock T, Schippling S, Ringelstein M, Kaufhold F, Zimmermann H, Keser N, et al. Retinal damage in multiple sclerosis disease subtypes measured by high-resolution optical coherence tomography. Mult Scler Int. 2012;2012:530305.

166. Lange AP, Sadjadi R, Saeedi J, Lindley J, Costello F, Traboulsee AL. Time-Domain and Spectral-Domain Optical Coherence Tomography of Retinal Nerve Fiber Layer in MS Patients and Healthy Controls. J Ophthalmol. 2012;2012:564627.

167. Garcia-Martin E, Pablo LE, Herrero R, Satue M, Polo V, Larrosa JM, et al. Diagnostic ability of a linear discriminant function for spectral-domain optical coherence tomography in patients with multiple sclerosis. Ophthalmology. 2012;119(8):1705-11.

168. Merle H, Olindo S, Donnio A, Richer R, Smadja D, Cabre P. Retinal peripapillary nerve fiber layer thickness in neuromyelitis optica. Invest Ophthalmol Vis Sci. 2008;49(10):4412-7.

169. Fernandes DB, Raza AS, Nogueira RG, Wang D, Callegaro D, Hood DC, et al. Evaluation of inner retinal layers in patients with multiple sclerosis or neuromyelitis optica using optical coherence tomography. Ophthalmology. 2013;120(2):387-94.

170. Naismith RT, Tutlam NT, Xu J, Klawiter EC, Shepherd J, Trinkaus K, et al. Optical coherence tomography differs in neuromyelitis optica compared with multiple sclerosis. Neurology. 2009;72(12):1077-82.

171. Gelfand JM, Nolan R, Schwartz DM, Graves J, Green AJ. Microcystic macular oedema in multiple sclerosis is associated with disease severity. Brain. 2012;135(Pt 6):1786-93.

172. Monteiro ML, Fernandes DB, Apostolos-Pereira SL, Callegaro D. Quantification of retinal neural loss in patients with neuromyelitis optica and multiple sclerosis with or without optic neuritis using Fourier-domain optical coherence tomography. Invest Ophthalmol Vis Sci. 2012;53(7):3959-66.

173. Young KL, Brandt AU, Petzold A, Reitz LY, Lintze F, Paul F, et al. Loss of retinal nerve fibre layer axons indicates white but not grey matter damage in early multiple sclerosis. Eur J Neurol. 2013;20(5):803-11.

174. Serbecic N, Aboul-Enein F, Beutelspacher SC, Khan A, Vass C, Kristoferitsch W, et al. High-Resolution Spectral Domain-Optical Coherence Tomography in Multiple Sclerosis, Part II - the Total Macular Volume. The First Follow-Up Study over 2 Years. Front Neurol. 2014;5:20.

175. Petzold A. Optical Coherence Tomography to Assess Neurodegeneration in Multiple Sclerosis. Methods Mol Biol. 2016;1304:131-41.

176. Gordon-Lipkin E, Chodkowski B, Reich DS, Smith SA, Pulicken M, Balcer LJ, et al. Retinal nerve fiber layer is associated with brain atrophy in multiple sclerosis. Neurology. 2007;69(16):1603-9.

177. Grazioli E, Zivadinov R, Weinstock-Guttman B, Lincoff N, Baier M, Wong JR, et al. Retinal nerve fiber layer thickness is associated with brain MRI outcomes in multiple sclerosis. J Neurol Sci. 2008;268(1-2):12-7.

178. Siger M, Dziegielewski K, Jasek L, Bieniek M, Nicpan A, Nawrocki J, et al. Optical coherence tomography in multiple sclerosis: thickness of the retinal nerve fiber layer as a potential measure of axonal loss and brain atrophy. J Neurol. 2008;255(10):1555-60.

179. Abalo-Lojo JM, Limeres CC, Gomez MA, Baleato-Gonzalez S, Cadarso-Suarez C, Capeans-Tome C, et al. Retinal nerve fiber layer thickness, brain atrophy, and disability in multiple sclerosis patients. J Neuroophthalmol. 2014;34(1):23-8.

180. Saidha S, Sotirchos ES, Oh J, Syc SB, Seigo MA, Shiee N, et al. Relationships between retinal axonal and neuronal measures and global central nervous system pathology in multiple sclerosis. JAMA Neurol. 2013;70(1):34-43.

181. Scheel M, Finke C, Oberwahrenbrock T, Freing A, Pech LM, Schlichting J, et al. Retinal nerve fibre layer thickness correlates with brain white matter damage in multiple sclerosis: a combined optical coherence tomography and diffusion tensor imaging study. Mult Scler. 2014;20(14):1904-7.

182. Balk LJ, Steenwijk MD, Tewarie P, Daams M, Killestein J, Wattjes MP, et al. Bidirectional trans-synaptic axonal degeneration in the visual pathway in multiple sclerosis. J Neurol Neurosurg Psychiatry. 2015;86(4):419-24.

183. Saidha S, Al-Louzi O, Ratchford JN, Bhargava P, Oh J, Newsome SD, et al. Optical coherence tomography reflects brain atrophy in multiple sclerosis: A four-year study. Ann Neurol. 2015;78(5):801-13.

184. Oh J, Sotirchos ES, Saidha S, Whetstone A, Chen M, Newsome SD, et al. Relationships between quantitative spinal cord MRI and retinal layers in multiple sclerosis. Neurology. 2015;84(7):720-8.

185. Sepulcre J, Murie-Fernandez M, Salinas-Alaman A, Garcia-Layana A, Bejarano B, Villoslada P. Diagnostic accuracy of retinal abnormalities in predicting disease activity in MS. Neurology. 2007;68(18):1488-94.

186. Toledo J, Sepulcre J, Salinas-Alaman A, Garcia-Layana A, Murie-Fernandez M, Bejarano B, et al. Retinal nerve fiber layer atrophy is associated with physical and cognitive disability in multiple sclerosis. Mult Scler. 2008;14(7):906-12.

187. Spain RI, Maltenfort M, Sergott RC, Leist TP. Thickness of retinal nerve fiber layer correlates with disease duration in parallel with corticospinal tract dysfunction in untreated multiple sclerosis. J Rehabil Res Dev. 2009;46(5):633-42.

188. Costello F, Hodge W, Pan YI, Metz L, Kardon RH. Retinal nerve fiber layer and future risk of multiple sclerosis. Can J Neurol Sci. 2008;35(4):482-7.

189. Talman LS, Bisker ER, Sackel DJ, Long DA, Jr., Galetta KM, Ratchford JN, et al. Longitudinal study of vision and retinal nerve fiber layer thickness in multiple sclerosis. Ann Neurol. 2010;67(6):749-60.

190. Serbecic N, Aboul-Enein F, Beutelspacher SC, Vass C, Kristoferitsch W, Lassmann H, et al. High resolution spectral domain optical coherence tomography (SD-OCT) in multiple sclerosis: the first follow up study over two years. PLoS One. 2011;6(5):e19843.

191. Garcia-Martin E, Pueyo V, Ara JR, Almarcegui C, Martin J, Pablo L, et al. Effect of optic neuritis on progressive axonal damage in multiple sclerosis patients. Mult Scler. 2011;17(7):830-7.

192. Garcia-Martin E, Pueyo V, Almarcegui C, Martin J, Ara JR, Sancho E, et al. Risk factors for progressive axonal degeneration of the retinal nerve fibre layer in multiple sclerosis patients. Br J Ophthalmol. 2011;95(11):1577-82.

193. Galetta KM, Graves J, Talman LS, Lile DJ, Frohman EM, Calabresi PA, et al. Visual pathway axonal loss in benign multiple sclerosis: a longitudinal study. J Neuroophthalmol. 2012;32(2):116-23.

194. Oreja-Guevara C, Noval S, Alvarez-Linera J, Gabaldon L, Manzano B, Chamorro B, et al. Clinically isolated syndromes suggestive of multiple sclerosis: an optical coherence tomography study. PLoS One. 2012;7(3):e33907.

195. Warner CV, Syc SB, Stankiewicz AM, Hiremath G, Farrell SK, Crainiceanu CM, et al. The impact of utilizing different optical coherence tomography devices for clinical purposes and in multiple sclerosis trials. PLoS One. 2011;6(8):e22947.

196. Herrero R, Garcia-Martin E, Almarcegui C, Ara JR, Rodriguez-Mena D, Martin J, et al. Progressive degeneration of the retinal nerve fiber layer in patients with multiple sclerosis. Invest Ophthalmol Vis Sci. 2012;53(13):8344-9.

197. De Angelis F, Cameron J, Connick P, Miller D, Pavitt S, Giovannoni G, et al. Optical coherence tomography in secondary progressive mutiple sclerosis: a baseline data report from the MS-SMART trial. 32nd Congress of the European Committee for Treatment and Research in Multiple Sclerosis (ECTRIMS) London, UK;2016.

198. Davies EC, Galetta KM, Sackel DJ, Talman LS, Frohman EM, Calabresi PA, et al. Retinal ganglion cell layer volumetric assessment by spectral-domain optical coherence tomography in multiple sclerosis: application of a high-precision manual estimation technique. J Neuroophthalmol. 2011;31(3):260-4.

199. Saidha S, Syc SB, Durbin MK, Eckstein C, Oakley JD, Meyer SA, et al. Visual dysfunction in multiple sclerosis correlates better with optical coherence tomography derived estimates of macular ganglion cell layer thickness than peripapillary retinal nerve fiber layer thickness. Mult Scler. 2011;17(12):1449-63.

200. Walter SD, Ishikawa H, Galetta KM, Sakai RE, Feller DJ, Henderson SB, et al. Ganglion cell loss in relation to visual disability in multiple sclerosis. Ophthalmology. 2012;119(6):1250-7.

201. Syc SB, Saidha S, Newsome SD, Ratchford JN, Levy M, Ford E, et al. Optical coherence tomography segmentation reveals ganglion cell layer pathology after optic neuritis. Brain. 2012;135(Pt 2):521-33.

202. Ratchford JN, Saidha S, Sotirchos ES, Oh JA, Seigo MA, Eckstein C, et al. Active MS is associated with accelerated retinal ganglion cell/inner plexiform layer thinning. Neurology. 2013;80(1):47-54.

203. Albrecht P, Ringelstein M, Muller AK, Keser N, Dietlein T, Lappas A, et al. Degeneration of retinal layers in multiple sclerosis subtypes quantified by optical coherence tomography. Mult Scler. 2012;18(10):1422-9.

204. Seigo MA, Sotirchos ES, Newsome S, Babiarz A, Eckstein C, Ford E, et al. In vivo assessment of retinal neuronal layers in multiple sclerosis with manual and automated optical coherence tomography segmentation techniques. J Neurol. 2012;259(10):2119-30.

205. Oberwahrenbrock T, Ringelstein M, Jentschke S, Deuschle K, Klumbies K, Bellmann-Strobl J, et al. Retinal ganglion cell and inner plexiform layer thinning in clinically isolated syndrome. Mult Scler. 2013;19(14):1887-95.

206. Kochkorov A, Gugleta K, Kavroulaki D, Katamay R, Weier K, Mehling M, et al. Rigidity of retinal vessels in patients with multiple sclerosis. Klin Monbl Augenheilkd. 2009;226(4):276-9.

207. Gugleta K, Kochkorov A, Kavroulaki D, Katamay R, Weier K, Mehling M, et al. Retinal vessels in patients with multiple sclerosis: baseline diameter and response to flicker light stimulation. Klin Monbl Augenheilkd. 2009;226(4):272-5.

208. Hinton DR, Sadun AA, Blanks JC, Miller CA. Optic-nerve degeneration in Alzheimer's disease. N Engl J Med. 1986;315(8):485-7.

209. Blanks JC, Hinton DR, Sadun AA, Miller CA. Retinal ganglion cell degeneration in Alzheimer's disease. Brain Res. 1989;501(2):364-72.

210. Parisi V, Restuccia R, Fattapposta F, Mina C, Bucci MG, Pierelli F. Morphological and functional retinal impairment in Alzheimer's disease patients. Clin Neurophysiol. 2001;112(10):1860-7.

211. Jindahra P, Hedges TR, Mendoza-Santiesteban CE, Plant GT. Optical coherence tomography of the retina: applications in neurology. Curr Opin Neurol. 2010;23(1):16-23.

212. Gunes A, Demirci S, Tok L, Tok O, Demirci S. Evaluation of retinal nerve fiber layer thickness in Alzheimer disease using spectral-domain optical coherence tomography. Turk J Med Sci. 2015;45(5):1094-7.

213. Polo V, Garcia-Martin E, Bambo MP, Pinilla J, Larrosa JM, Satue M, et al. Reliability and validity of Cirrus and Spectralis optical coherence tomography for detecting retinal atrophy in Alzheimer's disease. Eye (Lond). 2014;28(6):680-90.

214. Kirbas S, Turkyilmaz K, Anlar O, Tufekci A, Durmus M. Retinal nerve fiber layer thickness in patients with Alzheimer disease. J Neuroophthalmol. 2013;33(1):58-61.

215. Kang BH, Kim JI. Decreased retinal thickness in patients with Alzheimer's disease. Journal of the Korean Neurological Association. 2013;31(3):173-7.

216. Ascaso FJ, Cruz N, Modrego PJ, Lopez-Anton R, Santabarbara J, Pascual LF, et al. Retinal alterations in mild cognitive impairment and Alzheimer's disease: an optical coherence tomography study. J Neurol. 2014;261(8):1522-30.

217. Kesler A, Vakhapova V, Korczyn AD, Naftaliev E, Neudorfer M. Retinal thickness in patients with mild cognitive impairment and Alzheimer's disease. Clin Neurol Neurosurg. 2011;113(7):523-6.

218. Paquet C, Boissonnot M, Roger F, Dighiero P, Gil R, Hugon J. Abnormal retinal thickness in patients with mild cognitive impairment and Alzheimer's disease. Neurosci Lett. 2007;420(2):97-9.

219. Iseri PK, Altinas O, Tokay T, Yuksel N. Relationship between cognitive impairment and retinal morphological and visual functional abnormalities in Alzheimer disease. J Neuroophthalmol. 2006;26(1):18-24.

220. Whiting P, Rutjes AW, Reitsma JB, Bossuyt PM, Kleijnen J. The development of QUADAS: a tool for the quality assessment of studies of diagnostic accuracy included in systematic reviews. BMC Med Res Methodol. 2003;3:25.

221. Berisha F, Feke GT, Trempe CL, McMeel JW, Schepens CL. Retinal abnormalities in early Alzheimer's disease. Invest Ophthalmol Vis Sci. 2007;48(5):2285-9.

222. Garcia-Martin ES, Rojas B, Ramirez AI, de Hoz R, Salazar JJ, Yubero R, et al. Macular thickness as a potential biomarker of mild Alzheimer's disease. Ophthalmology. 2014;121(5):1149-51 e3.

223. Chi Y, Wang YH, Yang L. [The investigation of retinal nerve fiber loss in Alzheimer's disease]. Zhonghua Yan Ke Za Zhi. 2010;46(2):134-9.

224. Gharbiya M, Trebbastoni A, Parisi F, Manganiello S, Cruciani F, D'Antonio F, et al. Choroidal thinning as a new finding in Alzheimer's disease: evidence from enhanced depth imaging spectral domain optical coherence tomography. J Alzheimers Dis. 2014;40(4):907-17.

225. Kromer R, Serbecic N, Hausner L, Froelich L, Aboul-Enein F, Beutelspacher SC. Detection of Retinal Nerve Fiber Layer Defects in Alzheimer's Disease Using SD-OCT. Front Psychiatry. 2014;5:22.

226. Larrosa JM, Garcia-Martin E, Bambo MP, Pinilla J, Polo V, Otin S, et al. Potential new diagnostic tool for Alzheimer's disease using a linear discriminant function for

Fourier domain optical coherence tomography. Invest Ophthalmol Vis Sci. 2014;55(5):3043-51.

227. Moreno-Ramos T, Benito-Leon J, Villarejo A, Bermejo-Pareja F. Retinal nerve fiber layer thinning in dementia associated with Parkinson's disease, dementia with Lewy bodies, and Alzheimer's disease. J Alzheimers Dis. 2013;34(3):659-64.

228. Zhu LP, Ren XL, Wang YX, Xu L, Zhang XJ. Retinal nerve fiber layer thickness in the patients with mild cognitive impairment or Alzheimer’s disease. Ophthalmol CHN. 2014;23:231-4.

229. Shen Y, Liu L, Cheng Y, Feng W, Shi Z, Zhu Y, et al. Retinal nerve fiber layer thickness is associated with episodic memory deficit in mild cognitive impairment patients. Curr Alzheimer Res. 2014;11(3):259-66.

230. Gramer E, Dirmeyer M. Optical coherence tomography (OCT) to measure nerve fiber layer thickness in normal eyes. Invest Ophthalmol Vis Sci. 1998;39(4):S933.

231. Coppola G, Di Renzo A, Ziccardi L, Martelli F, Fadda A, Manni G, et al. Optical Coherence Tomography in Alzheimer's Disease: A Meta-Analysis. PLoS One. 2015;10(8):e0134750.

232. den Haan J, Verbraak FD, Visser PJ, Bouwman FH. Retinal thickness in Alzheimer's disease: A systematic review and meta-analysis. Alzheimers Dement (Amst). 2017;6:162-70.

233. Wang M, Zhu Y, Shi Z, Li C, Shen Y. Meta-analysis of the relationship of peripheral retinal nerve fiber layer thickness to Alzheimer's disease and mild cognitive impairment. Shanghai Arch Psychiatry. 2015;27(5):263-79.

234. Knoll B, Simonett J, Volpe NJ, Farsiu S, Ward M, Rademaker A, et al. Retinal nerve fiber layer thickness in amnestic mild cognitive impairment: Case-control study and meta-analysis. Alzheimers Dement (Amst). 2016;4:85-93.

235. Kromer R, Serbecic N, Hausner L, Froelich L, Beutelspacher SC. Comparison of visual evoked potentials and retinal nerve fiber layer thickness in Alzheimer's disease. Front Neurol. 2013;4:203.

236. Heringa SM, Bouvy WH, van den Berg E, Moll AC, Kappelle LJ, Biessels GJ. Associations between retinal microvascular changes and dementia, cognitive functioning, and brain imaging abnormalities: a systematic review. J Cereb Blood Flow Metab. 2013;33(7):983-95.

237. Cheung CY, Chen C, Wong TY. Ocular Fundus Photography as a Tool to Study Stroke and Dementia. Semin Neurol. 2015;35(5):481-90.

238. Ding J, Strachan MW, Reynolds RM, Frier BM, Deary IJ, Fowkes FG, et al. Diabetic retinopathy and cognitive decline in older people with type 2 diabetes: the Edinburgh Type 2 Diabetes Study. Diabetes. 2010;59(11):2883-9.

239. Klaver CC, Ott A, Hofman A, Assink JJ, Breteler MM, de Jong PT. Is age-related maculopathy associated with Alzheimer's Disease? The Rotterdam Study. Am J Epidemiol. 1999;150(9):963-8.

240. Schrijvers EM, Buitendijk GH, Ikram MK, Koudstaal PJ, Hofman A, Vingerling JR, et al. Retinopathy and risk of dementia: the Rotterdam Study. Neurology. 2012;79(4):365-70.

241. Baker ML, Marino Larsen EK, Kuller LH, Klein R, Klein BE, Siscovick DS, et al. Retinal microvascular signs, cognitive function, and dementia in older persons: the Cardiovascular Health Study. Stroke. 2007;38(7):2041-7.

242. Baker ML, Wang JJ, Rogers S, Klein R, Kuller LH, Larsen EK, et al. Early age-related macular degeneration, cognitive function, and dementia: the Cardiovascular Health Study. Arch Ophthalmol. 2009;127(5):667-73.

243. Qiu C, Cotch MF, Sigurdsson S, Jonsson PV, Jonsdottir MK, Sveinbjrnsdottir S, et al. Cerebral microbleeds, retinopathy, and dementia: the AGES-Reykjavik Study. Neurology. 2010;75(24):2221-8.

244. Cheung CY, Ong YT, Ikram MK, Ong SY, Li X, Hilal S, et al. Microvascular network alterations in the retina of patients with Alzheimer's disease. Alzheimers Dement. 2014;10(2):135-42.

245. Frost S, Kanagasingam Y, Sohrabi H, Vignarajan J, Bourgeat P, Salvado O, et al. Retinal vascular biomarkers for early detection and monitoring of Alzheimer's disease. Transl Psychiatry. 2013;3:e233.

246. Williams MA, Silvestri V, Craig D, Passmore AP, Silvestri G. The prevalence of age-related macular degeneration in Alzheimer's disease. J Alzheimers Dis. 2014;42(3):909-14.

247. Williams MA, McGowan AJ, Cardwell CR, Cheung CY, Craig D, Passmore P, et al. Retinal microvascular network attenuation in Alzheimer's disease. Alzheimers Dement (Amst). 2015;1(2):229-35.

248. McGrory S, Cameron JR, Pellegrini E, Warren C, Doubal FN, Deary IJ, et al. The application of retinal fundus camera imaging in dementia: A systematic review. Alzheimers Dement (Amst). 2017;6:91-107.

249. Kawasaki R, Che Azemin MZ, Kumar DK, Tan AG, Liew G, Wong TY, et al. Fractal dimension of the retinal vasculature and risk of stroke: a nested case-control study. Neurology. 2011;76(20):1766-7.

250. Hammes HP, Feng Y, Pfister F, Brownlee M. Diabetic retinopathy: targeting vasoregression. Diabetes. 2011;60(1):9-16.

251. Cheung CY, Ikram MK, Sabanayagam C, Wong TY. Retinal microvasculature as a model to study the manifestations of hypertension. Hypertension. 2012;60(5):1094-103.

252. Ding J, Wai KL, McGeechan K, Ikram MK, Kawasaki R, Xie J, et al. Retinal vascular caliber and the development of hypertension: a meta-analysis of individual participant data. J Hypertens. 2014;32(2):207-15.

253. Yang K, Zhan SY, Liang YB, Duan X, Wang F, Wong TY, et al. Association of dilated retinal arteriolar caliber with early age-related macular degeneration: the Handan Eye Study. Graefes Arch Clin Exp Ophthalmol. 2012;250(5):741-9.

254. MacCormick IJ, Somner J, Morris DS, MacGillivray TJ, Bourne RR, Huang SS, et al. Retinal vessel tortuosity in response to hypobaric hypoxia. High Alt Med Biol. 2012;13(4):263-8.

255. Bulut M, Yaman A, Erol MK, Kurtulus F, Toslak D, Dogan B, et al. Choroidal Thickness in Patients with Mild Cognitive Impairment and Alzheimer's Type Dementia. J Ophthalmol. 2016;2016:7291257.

256. Roth NM, Saidha S, Zimmermann H, Brandt AU, Oberwahrenbrock T, Maragakis NJ, et al. Optical coherence tomography does not support optic nerve involvement in amyotrophic lateral sclerosis. Eur J Neurol. 2013;20(8):1170-6.

257. Ringelstein M, Albrecht P, Sudmeyer M, Harmel J, Muller AK, Keser N, et al. Subtle retinal pathology in amyotrophic lateral sclerosis. Ann Clin Transl Neurol. 2014;1(4):290-7.

258. Hubers A, Muller HP, Dreyhaupt J, Bohm K, Lauda F, Tumani H, et al. Retinal involvement in amyotrophic lateral sclerosis: a study with optical coherence tomography and diffusion tensor imaging. J Neural Transm (Vienna). 2016;123(3):281-7.

259. Chio A, Pagani M, Agosta F, Calvo A, Cistaro A, Filippi M. Neuroimaging in amyotrophic lateral sclerosis: insights into structural and functional changes. Lancet Neurol. 2014;13(12):1228-40.

260. Fairless R, Williams SK, Hoffmann DB, Stojic A, Hochmeister S, Schmitz F, et al. Preclinical retinal neurodegeneration in a model of multiple sclerosis. J Neurosci. 2012;32(16):5585-97.

261. Gold R, Linington C, Lassmann H. Understanding pathogenesis and therapy of multiple sclerosis via animal models: 70 years of merits and culprits in experimental autoimmune encephalomyelitis research. Brain. 2006;129(Pt 8):1953-71.

262. Kardon RH. Role of the macular optical coherence tomography scan in neuro-ophthalmology. J Neuroophthalmol. 2011;31(4):353-61.

263. Grinton ME, Laude A, MacGillivray T, Henderson R, Starr JM, Deary IJ, et al. The association between retinal vessel morphology and retinal nerve fiber layer thickness in an elderly population. Ophthalmic Surg Lasers Imaging. 2012;43(6 Suppl):S61-6.

264. Yamada M. Cerebral amyloid angiopathy: emerging concepts. J Stroke. 2015;17(1):17-30.

265. Chhablani J, Wong IY, Kozak I. Choroidal imaging: A review. Saudi J Ophthalmol. 2014;28(2):123-8.

266. Chung SE, Kang SW, Lee JH, Kim YT. Choroidal thickness in polypoidal choroidal vasculopathy and exudative age-related macular degeneration. Ophthalmology. 2011;118(5):840-5.

267. Kuroda S, Ikuno Y, Yasuno Y, Nakai K, Usui S, Sawa M, et al. Choroidal thickness in central serous chorioretinopathy. Retina. 2013;33(2):302-8.

268. Carpineto P, Toto L, Aloia R, Ciciarelli V, Borrelli E, Vitacolonna E, et al. Neuroretinal alterations in the early stages of diabetic retinopathy in patients with type 2 diabetes mellitus. Eye (Lond). 2016;30(5):673-9.

269. Wu H, de Boer JF, Chen TC. Reproducibility of retinal nerve fiber layer thickness measurements using spectral domain optical coherence tomography. J Glaucoma. 2011;20(8):470-6.

270. Early Treatment Diabetic Retinopathy Study research group. Photocoagulation for diabetic macular edema. Early Treatment Diabetic Retinopathy Study report number 1. Arch Ophthalmol. 1985;103(12):1796-806.

271. Tewarie P, Balk L, Costello F, Green A, Martin R, Schippling S, et al. The OSCAR-IB consensus criteria for retinal OCT quality assessment. PLoS One. 2012;7(4):e34823.

272. Gardiner SK, Ren R, Yang H, Fortune B, Burgoyne CF, Demirel S. A method to estimate the amount of neuroretinal rim tissue in glaucoma: comparison with current methods for measuring rim area. Am J Ophthalmol. 2014;157(3):540-9 e1-2.

273. Chauhan BC, O'Leary N, Almobarak FA, Reis AS, Yang H, Sharpe GP, et al. Enhanced detection of open-angle glaucoma with an anatomically accurate optical coherence tomography-derived neuroretinal rim parameter. Ophthalmology. 2013;120(3):535-43.

274. Trucco E, Ballerini L, Relan D, Giachetti A, MacGillivray T, Zutis K, et al., editors. Novel VAMPIRE algorithms for quantitative analysis of the retinal vasculature. Biosignals and Biorobotics Conference (BRC), 2013 ISSNIP; 2013 18-20 Feb. 2013.

275. MacGillivray TJ, Cameron JR, Zhang Q, El-Medany A, Mulholland C, Sheng Z, et al. Suitability of UK Biobank Retinal Images for Automatic Analysis of Morphometric Properties of the Vasculature. PLoS One. 2015;10(5):e0127914.

276. Trucco E, Ruggeri A, Karnowski T, Giancardo L, Chaum E, Hubschman JP, et al. Validating retinal fundus image analysis algorithms: issues and a proposal. Invest Ophthalmol Vis Sci. 2013;54(5):3546-59.

277. Giachetti A, Ballerini L, Trucco E. Accurate and reliable segmentation of the optic disc in digital fundus images. J Med Imaging (Bellingham). 2014;1(2):024001.

278. Giachetti A, Ballerini L, Trucco E, Wilson PJ. The use of radial symmetry to localize retinal landmarks. Comput Med Imaging Graph. 2013;37(5-6):369-76.

279. Relan D, MacGillivray T, Ballerini L, Trucco E. Automatic retinal vessel classification using a Least Square-Support Vector Machine in VAMPIRE. Conf Proc IEEE Eng Med Biol Soc. 2014;2014:142-5.

280. Pellegrini E, Robertson G, Trucco E, MacGillivray TJ, Lupascu C, van Hemert J, et al. Blood vessel segmentation and width estimation in ultra-wide field scanning laser ophthalmoscopy. Biomed Opt Express. 2014;5(12):4329-37.

281. Lupascu CA, Tegolo D, Trucco E. Accurate estimation of retinal vessel width using bagged decision trees and an extended multiresolution Hermite model. Med Image Anal. 2013;17(8):1164-80.

282. Soares JV, Leandro JJ, Cesar RM, Jelinek HF, Cree MJ. Retinal vessel segmentation using the 2-D Gabor wavelet and supervised classification. Medical Imaging, IEEE Transactions on. 2006;25(9):1214-22.

283. Cavinato A, Ballerini L, Trucco E, Grisan E, editors. Spline-based refinement of vessel contours in fundus retinal images for width estimation. 2013 IEEE 10th International Symposium on Biomedical Imaging; 2013 7-11 April 2013.

284. Lisowska A, Annunziata R, Loh GK, Karl D, Trucco E, editors. An experimental assessment of five indices of retinal vessel tortuosity with the RET-TORT public dataset. 2014 36th Annual International Conference of the IEEE Engineering in Medicine and Biology Society; 2014 26-30 Aug. 2014.

285. Hubbard LD, Brothers RJ, King WN, Clegg LX, Klein R, Cooper LS, et al. Methods for evaluation of retinal microvascular abnormalities associated with hypertension/sclerosis in the Atherosclerosis Risk in Communities Study. Ophthalmology. 1999;106(12):2269-80.

286. Patton N, Aslam T, Macgillivray T, Dhillon B, Constable I. Asymmetry of retinal arteriolar branch widths at junctions affects ability of formulae to predict trunk arteriolar widths. Invest Ophthalmol Vis Sci. 2006;47(4):1329-33.

287. Altman DG, Bland JM. Statistics notes. Units of analysis. BMJ. 1997;314(7098):1874.

288. Bunce C, Patel KV, Xing W, Freemantle N, Dore CJ, Ophthalmic Statistics G. Ophthalmic statistics note 1: unit of analysis. Br J Ophthalmol. 2014;98(3):408-12.

289. Cameron JR, Megaw RD, Tatham AJ, McGrory S, MacGillivray TJ, Doubal FN, et al. Lateral thinking - Interocular symmetry and asymmetry in neurovascular patterning, in health and disease. Prog Retin Eye Res. 2017;59:131-57.

290. Health CfDaR. 510(k) Premarket Notification K121993. U.S. Food and Drug Administration; 2012.

291. Margolis R, Spaide RF. A pilot study of enhanced depth imaging optical coherence tomography of the choroid in normal eyes. Am J Ophthalmol. 2009;147(5):811-5.

292. Lavery AM, Verhey LH, Waldman AT. Outcome measures in relapsing-remitting multiple sclerosis: capturing disability and disease progression in clinical trials. Mult Scler Int. 2014;2014:262350.

293. Kurtzke JF. Rating neurologic impairment in multiple sclerosis: an expanded disability status scale (EDSS). Neurology. 1983;33(11):1444-52.

294. Holladay JT. Proper method for calculating average visual acuity. J Refract Surg. 1997;13(4):388-91.

295. Balcer LJ, Frohman EM. Evaluating loss of visual function in multiple sclerosis as measured by low-contrast letter acuity. Neurology. 2010;74 Suppl 3:S16-23.

296. Gross HJ, Watson C. Characteristics, burden of illness, and physical functioning of patients with relapsing-remitting and secondary progressive multiple sclerosis: a cross-sectional US survey. Neuropsychiatr Dis Treat. 2017;13:1349-57.

297. Kardys A, Weinstock-Guttman B, Dillon M, Masud MW, Weinstock N, Mahfooz N, et al. Cholesterol affects retinal nerve fiber layer thickness in patients with multiple sclerosis with optic neuritis. Eur J Neurol. 2013;20(9):1264-71.

298. Bennett JL. Finding NMO: The Evolving Diagnostic Criteria of Neuromyelitis Optica. J Neuroophthalmol. 2016;36(3):238-45.

299. Han JM, Hwang JM, Kim JS, Park KH, Woo SJ. Changes in choroidal thickness after systemic administration of high-dose corticosteroids: a pilot study. Invest Ophthalmol Vis Sci. 2014;55(1):440-5.

300. Balcer LJ, Miller DH, Reingold SC, Cohen JA. Vision and vision-related outcome measures in multiple sclerosis. Brain. 2015;138(Pt 1):11-27.

301. Larner AJ. Addenbrooke's Cognitive Examination (ACE) for the diagnosis and differential diagnosis of dementia. Clin Neurol Neurosurg. 2007;109(6):491-4.

302. Mathuranath PS, Nestor PJ, Berrios GE, Rakowicz W, Hodges JR. A brief cognitive test battery to differentiate Alzheimer's disease and frontotemporal dementia. Neurology. 2000;55(11):1613-20.

303. Mioshi E, Dawson K, Mitchell J, Arnold R, Hodges JR. The Addenbrooke's Cognitive Examination Revised (ACE-R): a brief cognitive test battery for dementia screening. Int J Geriatr Psychiatry. 2006;21(11):1078-85.

304. Larner AJ. Addenbrooke's Cognitive Examination-Revised (ACE-R) in day-to-day clinical practice. Age Ageing. 2007;36(6):685-6.

305. Larner AJ, Mitchell AJ. A meta-analysis of the accuracy of the Addenbrooke's Cognitive Examination (ACE) and the Addenbrooke's Cognitive Examination-Revised (ACE-R) in the detection of dementia. Int Psychogeriatr. 2014;26(4):555-63.

306. Hsieh S, Schubert S, Hoon C, Mioshi E, Hodges JR. Validation of the Addenbrooke's Cognitive Examination III in frontotemporal dementia and Alzheimer's disease. Dement Geriatr Cogn Disord. 2013;36(3-4):242-50.

307. Bier JC, Ventura M, Donckels V, Van Eyll E, Claes T, Slama H, et al. Is the Addenbrooke's cognitive examination effective to detect frontotemporal dementia? J Neurol. 2004;251(4):428-31.

308. Dudas RB, Berrios GE, Hodges JR. The Addenbrooke's cognitive examination (ACE) in the differential diagnosis of early dementias versus affective disorder. Am J Geriatr Psychiatry. 2005;13(3):218-26.

309. Berankova D, Janousova E, Mrackova M, Eliasova I, Kostalova M, Skutilova S, et al. Addenbrooke's Cognitive Examination and Individual Domain Cut-Off Scores for Discriminating between Different Cognitive Subtypes of Parkinson's Disease. Parkinsons Dis. 2015;2015:579417.

310. Begeti F, Tan AY, Cummins GA, Collins LM, Guzman NV, Mason SL, et al. The Addenbrooke's Cognitive Examination-Revised accurately detects cognitive decline in Huntington's disease. J Neurol. 2013;260(11):2777-85.

311. Huang-Link YM, Al-Hawasi A, Lindehammar H. Acute optic neuritis: retinal ganglion cell loss precedes retinal nerve fiber thinning. Neurol Sci. 2015;36(4):617-20.

312. Cordeiro MF, Guo L, Coxon KM, Duggan J, Nizari S, Normando EM, et al. Imaging multiple phases of neurodegeneration: a novel approach to assessing cell death in vivo. Cell Death Dis. 2010;1:e3.

313. Bailey JN, Loomis SJ, Kang JH, Allingham RR, Gharahkhani P, Khor CC, et al. Genome-wide association analysis identifies TXNRD2, ATXN2 and FOXC1 as susceptibility loci for primary open-angle glaucoma. Nat Genet. 2016;48(2):189-94.

314. Maruyama H, Morino H, Ito H, Izumi Y, Kato H, Watanabe Y, et al. Mutations of optineurin in amyotrophic lateral sclerosis. Nature. 2010;465(7295):223-6.

315. Freischmidt A, Wieland T, Richter B, Ruf W, Schaeffer V, Muller K, et al. Haploinsufficiency of TBK1 causes familial ALS and fronto-temporal dementia. Nat Neurosci. 2015;18(5):631-6.

316. Knier B, Rothhammer V, Heink S, Puk O, Graw J, Hemmer B, et al. Neutralizing IL-17 protects the optic nerve from autoimmune pathology and prevents retinal nerve fiber layer atrophy during experimental autoimmune encephalomyelitis. J Autoimmun. 2015;56:34-44.

317. Garcia-Martin E, Polo V, Larrosa JM, Marques ML, Herrero R, Martin J, et al. Retinal layer segmentation in patients with multiple sclerosis using spectral domain optical coherence tomography. Ophthalmology. 2014;121(2):573-9.

318. Al-Louzi OA, Bhargava P, Newsome SD, Balcer LJ, Frohman EM, Crainiceanu C, et al. Outer retinal changes following acute optic neuritis. Mult Scler. 2016;22(3):362-72.

319. Chang EE, Goldberg JL. Glaucoma 2.0: neuroprotection, neuroregeneration, neuroenhancement. Ophthalmology. 2012;119(5):979-86.

320. Gupta N, Yucel YH. Glaucoma as a neurodegenerative disease. Curr Opin Ophthalmol. 2007;18(2):110-4.

321. Johnson TV, Bull ND, Martin KR. Neurotrophic factor delivery as a protective treatment for glaucoma. Exp Eye Res. 2011;93(2):196-203.

322. Medeiros FA. Biomarkers and surrogate endpoints in glaucoma clinical trials. Br J Ophthalmol. 2015;99(5):599-603.

323. Lesko LJ, Atkinson AJ, Jr. Use of biomarkers and surrogate endpoints in drug development and regulatory decision making: criteria, validation, strategies. Annu Rev Pharmacol Toxicol. 2001;41:347-66.

324. Realini T, Zangwill LM, Flanagan JG, Garway-Heath D, Patella VM, Johnson CA, et al. Normative Databases for Imaging Instrumentation. J Glaucoma. 2015;24(6):480-3.

325. Dong ZM, Wollstein G, Wang B, Schuman JS. Adaptive optics optical coherence tomography in glaucoma. Prog Retin Eye Res. 2017;57:76-88.

326. Nadler Z, Wang B, Wollstein G, Nevins JE, Ishikawa H, Bilonick R, et al. Repeatability of in vivo 3D lamina cribrosa microarchitecture using adaptive optics spectral domain optical coherence tomography. Biomed Opt Express. 2014;5(4):1114-23.

327. Schutze C, Teleky K, Baumann B, Pircher M, Gotzinger E, Hitzenberger CK, et al. Polarisation-sensitive OCT is useful for evaluating retinal pigment epithelial lesions in patients with neovascular AMD. Br J Ophthalmol. 2016;100(3):371-7.

328. Jia Y, Morrison JC, Tokayer J, Tan O, Lombardi L, Baumann B, et al. Quantitative OCT angiography of optic nerve head blood flow. Biomed Opt Express. 2012;3(12):3127-37.

329. Scripsema NK, Garcia PM, Bavier RD, Chui TY, Krawitz BD, Mo S, et al. Optical Coherence Tomography Angiography Analysis of Perfused Peripapillary Capillaries in Primary Open-Angle Glaucoma and Normal-Tension Glaucoma. Invest Ophthalmol Vis Sci. 2016;57(9):OCT611-OCT20.

330. Farinha C, Santos T, Marques IP, Marques JP, Ribeiro L, Figueira J, et al. OCT-Leakage Mapping: A New Automated Method of OCT Data Analysis to Identify and Locate Abnormal Fluid in Retinal Edema. Ophthalmology Retina. 2017;In Press.

331. Cunha-Vaz J, Santos T, Alves D, Marques I, Neves C, Soares M, et al. Agreement between OCT Leakage and Fluorescein Angiography to Identify Sites of Alteration of the Blood–Retinal Barrier in Diabetes. Ophthalmology Retina. 2017;1(5):395-403.